Study of wear behavior of zircon sand reinforced aluminium matrix composites

A

Thesis

Submitted for the award of degree of

Doctor of Philosophy

By

Ranvir Singh Panwar
(Reg. No. 901112002)

Under the supervision of

Dr. O. P. Pandey
(Senior Professor)

School of Physics and Materials Science

Thapar University, Patiala- 147004.

December, 2013

CERTIFICATE

This is to certify that the thesis entitled **"Study of wear behavior of zircon sand reinforced aluminium matrix composites"** which is being submitted by Ranvir Singh Panwar in fulfillment of the requirements for the award of the degree of Doctor of Philosophy in the School of Physics and Materials Science, Thapar University, Patiala (Punjab), India is an exclusive record of candidate's own research work under my supervision. The thesis in part or in full has not been submitted in any other university or institute for the award of any degree. The thesis is fit to be considered for the award of degree of Doctor of Philosophy.

Dr. O.P. Pandey
Senior Professor
School of Physics and Materials Science
Thapar University
Patiala-147004 (INDIA)

ACKNOWLEDGEMENT

Completing my PhD degree is probably the most ambitious activity of my first 29 years of my life. The best and worst moments of my doctoral journey have been shared with many people. It has been a great privilege to spend several years in the School of Physics and Materials Science at Thapar University. I would have never been able to finish my dissertation without the guidance of my committee members, help from friends, and support from my family and wife.

I would like to express my deepest gratitude to my advisor **Dr. Om Prakash Pandey**, for his excellent guidance, care, patience and providing me with an excellent atmosphere for doing research. Throughout my thesis-writing period, he provided me encouragement, sound advice, good teaching, good company, and lots of good ideas. The good advice and support from him, has been invaluable on both an academic and a personal level, for which I am extremely grateful.

Besides my supervisor, I would like to thank the rest of my thesis committee members: **Dr. Tarun Nanda, Dr. Puneet Sharma and Dr. Poonam Uniyal** for their encouragement, insightful comments and useful criticism.

I am profoundly obliged to **Prof. K.K. Raina**, Deputy Director, Thapar University, Patiala, for his constant encouragement and needful help during various stages of the work.

I am thankful to **Dr. Kulvir Singh**, Head, School of Physics and Materials Science for constant encouragement and support.

I am very thankful all faculty of School of Physics and Materials Science, **Dr. Manoj Sharma, Dr. Suneel Kumar, Dr. Bhupendra Chudasama** for their valuable suggestions during my PhD work.

My special thanks to my colleague-cum-friend **Mr. Suresh Kumar** for his help and valuable suggestions during my PhD work. Without him, it would not have been possible to finish the work on time.

I am very thankful to **Mr. Purshottam Kumar Singh** for the help and valuables suggestions for the characterization of the samples. I would like to acknowledge **Mr. Jant Singh, Mr. Indermani mishra, Mrs. Parveen** and **Mr. Vijay** for their help and support during various stages of administrative formalities.

Words are enough in expressing my sincere thanks to my friends and lab-mates **Mr. Gaurav Singla, Ms. Jagdeep Kaur, Mr. Paramjyot Jha, Mr. Pradeep Teotia, Mrs.**

Amrita Singh, Mr. Umesh Gaur, Mr. Dushyant Tomar, Mrs. Shivani Rajpoot, Mrs. Sonia verma, Dr. Neeti Pathak, Dr. Gurbinder Chaudhary, Dr. Vishal Chaudhary, Dr. Kamalpreet Kaur, Ms. Samita Thakur and Ms. Mani Mahajan for their support in every moment of difficulty.

I am also grateful to **Dr. Sanjeev Das, Dr. Ravi Shukla and Dr. Akshay Kumar** for their kind help and valuable suggestions.

I am also indebted to **Mrs. Sushila Pandey, Mr. Pritam Singh** and **Mrs. Joginder Kaur** for providing me healthy home like environment for complete moral support.

My family especially my wife **Mrs. Rama Panwar** deserve the special thanks and great appreciation for her patience, persistent moral support and capability to revitalize me during the course of the PhD work at each step.

Last but not the least my parents **Mr. Sukhvir Singh** and **Mrs. Usha Devi** and my brother **Dr. Mahavir Singh Panwar** are the guiding pillars of my success. The constant motivation of my family has been the sole source of inspiration and strength to carry out my work. Finally, I would like to thank everybody who was important to the successful realization of thesis as well as expressing my apology that I could not mention personally one by one.

Above all, hidden force by **Almighty God** steered me in the right direction to achieve the goal.

(Ranvir Singh Panwar)

LIST OF PUBLICATIONS

RESEARCH PUBLICATIONS

1. **Ranvir Singh Panwar,** O.P. Pandey; Analysis of wear track and debris of stir cast LM13/Zr composite at elevated temperatures. Materials Charaterization; (2013) 75: 200-213.
2. **Ranvir Singh Panwar** and O.P. Pandey; Study of wear behavior of zircon sand-reinforced LM13 alloy composites at elevated temperatures. Journal of Materials Engineering and Performance. (2013) 22: 1765–1775.
3. **Ranvir Singh Panwar**, Suresh Kumar, and O. P. Pandey; Study of wear mechanism for LM13/Zr composite under dry sliding conditions at different loads. AIP Conf. Proc., (2013) 1536: 1143- 1144.
4. Suresh Kumar, Vipin Sharma, **Ranvir Singh Panwar**, O. P. Pandey ; Wear Behavior of Dual Particle Size (DPS) Zircon Sand Reinforced Aluminum Alloy. Tribology Letters (2012) 47: 231–251.
5. Suresh Kumar, **Ranvir Singh Panwar**, O.P. Pandey; Tribological characteristics of Aluminium tri-reinforced particles (Al- TRP) composites developed by liquid metallurgy route. Advanced Materials Research, (2012) 585: 574-578.
6. Vipin Sharma, Suresh Kumar, **Ranvir Singh Panwar**, O. P. Pandey; Microstructural and wear behavior of dual reinforced particle (DRP) aluminum alloy composite. Journal of Materials Science (2012) 47:6633–6646.
7. Suresh kumar, **Ranvir Singh Panwar**, O. P.Pandey; Effect of dual reinforced ceramic particles on high temperature tribological properties of aluminum composites. Ceramics International (2013) 39(6):6333–6342.
8. Suresh Kumar, **Ranvir Singh Panwar**, O. P. Pandey; Effect of particle size on wear of particulate reinforced aluminium alloy composites at elevated temperatures. Journal of Materials Engineering and Perofrmance (2013) 22(11): 3550-3560.
9. Suresh Kumar, **Ranvir Singh Panwar**, O.P. Pandey; Wear behavior at high temperature of dual-particle size zircon-sand-reinforced aluminum alloy composite. Metallurgical and Materials Transactions A, (2013) 44: 1548-1565.
10. Suresh Kumar, **Ranvir Singh Panwar**, and O. P. Pandey; Tribological properties of Zircon sand and Zirfloor reinforced LM13 alloy matrix composite-A comparative study. AIP Conf. Proc. (2013) 1536: 1286- 1287.

11. **Ranvir Singh Panwar**, Suresh Kumar, O.P. Pandey; Study of non lubricated wear behavior of the Al-Si alloy composite reinforced with different ratio of coarse and fine size zircon sand particles at different ambient temperatures. Tribology Letters **(In press)**.

12. **Ranvir Singh Panwar,** Suresh Kumar, O.P.Pandey; Wear and friction behavior of LM13 piston alloy reinforced with different size of zircon sand particles. Particulate Science and Technology. **(Communicated).**

List of Papers presented in the Conferences (International/ National)

1. **Ranvir Singh Panwar**, Suresh Kumar, O.P. Pandey; "Microstructural study and wear behavior of LM13/10%Zr composite at elevated temperature" in 4th National Symposium for Materials Research Scholars (MR-12) & Workshop on Advanced Characterization Techniques, May 2012 at IIT Bombay.
2. **Ranvir Singh Panwar**, Suresh Kumar, O.P. Pandey; "Effect of elevated temperature on wear behavior of LM13/Zr composite containing different size of zircon sand particles'' National Conference on Recent Trends in Material Science Research (RTMSR-2012)'' National Institute of Technology Srinagar, Hazratbal, Srinagar-190006, (J & K) during September 3-5, 2012.
3. Ranvir Singh Panwar, Suresh Kumar, O. P. Pandey; Effect of different ceramic particle on the sliding wear behavior of Al-Si alloy composites, International Conference on Powder, Granule and Bulk Solids: Innovations and Applications (PGBSIA 2013) November 28-30, 2013,India.
4. Suresh Kumar, **Ranvir Singh Panwar**, Vipin Sharma, O.P. Pandey; Effect of multi reinforced particles (MRP) and single reinforced particles (SRP) on the wear behavior of aluminum matrix composites" International Conference on Material Science and Technology (ICMST2012) held at St. Thomas College, Pala. Kottayam, Kerala during June 10-14 2012.
5. Ravi K. Shukla, **Ranvir Singh Panwar** and K.K. Raina "Controlled growth of ZnO via surfactant assisted complex sol-gel process in the basic medium" presented in International conferance on Electrocermaics 2009.

INDEX

LIST OF FIGURES

LIST OF TABLES

PREFACE

The present work deals with the development and characterization of zircon sand reinforced LM13 aluminum alloy composites. The entire work in this thesis is presented in **six chapters.**

In the **first chapter** general introduction to particle reinforced composite is given. A summary of discontinuous reinforced aluminum matrix composite along with different fabrication processes of aluminum matrix composites are also described in this chapter. The main factors affecting the mechanical properties of the composites along with brief introduction to different types of wear is also given at the end of the chapter.

Chapter 2 describes the development of discontinuous reinforced aluminum matrix composites (DRAMCs) by many researchers using different fabrication techniques and their study based on wear behavior is discussed in this chapter. As our work is based on the stir casting process, hence the main focus in this chapter is on the development of DRAMCs by stir casting process and study their physical properties especially wear resistance of the composites. The last section of this chapter presents the gaps in the study so far with aims and plan of the work of the thesis.

Chapter 3 describes about experimental procedure followed in the present work. Detailed procedure to develop the DRAMCs and their characterizations is given in this chapter. Different characterization techniques such as X- ray diffraction (XRD), Optical microscopy, Scanning electron microscopy (SEM), Energy dispersive spectroscopy (EDS), Rockwell hardness testing, Vickers hardness testing and wear testing with pin-on-disc machine along with their operating parameters are also discussed. A flow chart of the methodology used is also given in this chapter.

Chapter 4 deals with results and discussions on as developed composites reinforced with single size reinforcement. The effect of variation in amount and particle size of the reinforced zircon sand particles in the LM13 alloy matrix is discussed. On the basis of the results obtained by XRD, optical microscope, SEM, hardness testing and pin-on-disc wear test, a possible mechanism for wear is discussed. In this chapter, surface morphology of the single size particles reinforced composites were studied with the help of optical microscope to observe the distribution of the particles in the matrix. Both bulk and microhardness were measured for each composite with Rockwell and vicker's

hardness testing machine. All composites were tested with pin- on– disc machine for dry sliding wear test at different load and different temperature conditions. Wear tracks and wear debris were analyzed by using SEM.

In **Chapter 5,** results obtained from the composites reinforced with dual size particles (coarse and fine) are presented. The role of different ratios of the coarse and fine size particles in the matrix on the wear behavior have been studied with variation in the applied load and temperatures. However, on the basis of results, worn surfaces and wear debris of the DSR-15 composite (containing total 15 wt.% of dual particle size reinforcement) collected after the wear test at different conditions were analyzed under SEM.

Chapter 6 describes the conclusion of the entire work done in the present investigation along with the future scope. The present work shows a good distribution of the zircon sand particles in LM13 alloy matrix developed by stir casting process. XRD data shows the presence of zircon sand particles as well as new phase developed during the casting process. Uniform distribution and bonding of zircon sand particles with the matrix was observed. It was found that hardness of the base alloy was improved with increasing the amount of zircon sand particles in the matrix. However, with decreasing the particle size hardness of the composites was increased significantly. Ratios of the coarse and fine size particles in the matrix (dual size reinforced composites) shows better hardness in comparison to the single size reinforced composites.

Wear test of all the developed composites were done at different testing conditions with varying loads and temperatures. It was observed that wear resistance of the base alloy was improved with increasing the amount as well as decreasing the size of the reinforced particles. However, wear rate of the composites increases with increasing the applied load. Ambient temperature also plays an important role on the wear behavior of the composites. Formation of oxide layers at high temperature affects the wear rate significantly for all loading conditions. However, DSR composites shows better wear resistance in comparison to the SSR composites at all testing conditions.

CHAPTER 1
INTRODUCTION

Overview

Composite materials are existing in nature and are also man made. A brief history of composite materials and their classification on the basis of their constituents is given in this chapter. A summary of discontinuous reinforced aluminum matrix composite along with different fabrication processes of aluminum matrix composites are also described in this chapter. The main factors affecting the mechanical properties of the composites along with brief introduction of different types of wear is also given in the end of the chapter.

1.1 Brief history of composite materials:

Composite materials are in existence for many centuries [1]. However, as such no record exists as to when people first started using composites. Some of the earliest records of their use date back to the Egyptians, who are credited with the introduction of plywood and the use of straw in mud for strengthening bricks. Swords and armor were plated to add strength in medieval times. An example is the Samurai sword, which was produced by repeated folding and reshaping to form a multilayered composite (It is estimated that several million layers could have been used) [1]. Similarly, it is not uncommon to find horse hair in plaster for enhanced strength. All of these are examples of man-made composite materials. Bamboo, bone, and celery are examples of cellular composites that exist in nature. Muscles tissue is a multidirectional fibrous laminate. There are other numerous examples of both natural and man-made composite materials.

Numerous potential applications of composite materials over monolithic materials in different engineering fields such as in the automotive, military and aerospace industries make them of great interest to research community [2-4]. Tailoring the properties of the composites according to the industrial requirement with the reasonable cost is one of the key features of the materials. Right combination of metal, non-metal and ceramic materials in different ways give the opportunity to make composites for unlimited applications. Physical and chemical properties of the constituents used in fabrication of composites play an important role for the specified application.

1.2 Composite:

Composite material is a macroscopic combination of two or more constituent materials having significantly different physical or chemical properties. This combination produces a material exhibiting different properties from the individual components. However, the individual components remain separate and distinct within the finished structure. Most composites have two constituent materials: a binder or matrix, and a reinforcement. The reinforcement is usually much stronger and stiffer than the matrix which provides better mechanical (such as hardness, strength etc.) and chemical (such as oxidation state, flammability etc.) properties to composite.

1.2.1 Matrix:

The continuous phase in the composite or two phase alloy microstructure in which a second phase is dispersed is known as matrix. Selection of the matrix for the composite depends on the

required features of the desired material for the particular application, such as for the structural applications aluminum, titanium and magnesium are used as a matrix to develop light weight composite material. Similarly cobalt and cobalt-nickel alloys are used as matrix for high temperature applications. Main purpose of matrix in the composite is to transfer stress to other phases and to protect phases from environment.

1.2.2 Reinforcement:

The discontinuous phase present in the composite is known as reinforcement. In general the reinforcements are much stronger and stiffer than the matrix. The reinforcement materials exhibit excellent mechanical performance and are classified as continuous (monofilament/ multifilament) or discontinuous (particle/ whiskers/ short fiber/ other) reinforcement. Composites containing discontinuous reinforcement are usually less expensive than continuous reinforced composites.

1.3 Classifications of composite materials:

1.3.1 Classification of composite materials on the basis of matrix:

Generally composite materials are classified on the basis of the matrix used (e.g. metal matrix, polymer matrix, ceramic matrix). Figure 1.1 shows the allocation of the composite materials into groups of various types of materials presenting their main basic properties.

1.3.1.1 Metal matrix composite: Metal matrix composites (MMCs) possess significantly improved properties including high specific strength, specific modulus, damping capacity and good wear resistance as compared to unreinforced alloys and polymer matrices. These main properties of the MMCs make them suitable for vast applications in different engineering areas. Materials like cast iron having graphite flakes or steel with high carbide content, as well as tungsten carbides, consisting of carbides and metallic binders, also belong to this group of composite materials. But, they are heavier and more difficult to process. However, this limitation of the MMCs is improved when lightweight metals or alloys (e.g. aluminum, magnesium, titanium etc.) are used as a matrix for composites.

1.3.1.2 Polymer matrix composite: Polymer matrix composite materials use a polymer-based resin as matrix and a variety of fibers such as glass, carbon and aramid as the reinforcement. These are very popular due to their low cost and simple fabrication methods. Two types of polymers are used as matrix materials for fabrication of composites: Thermosets (epoxies,

phenolics) and Thermoplastics {Low Density Polyethylene (LDPE), High Density Polyethylene (HDPE), polypropylene, nylon, acrylics}. Polymer Matrix Composites (PMC) are used in manufacturing of secondary load-bearing aerospace structures, boat bodies, canoes, kayaks, automotive parts, radio controlled vehicles, sport goods, bullet-proof vests and other armor parts, brake and clutch linings.

1.3.1.3 Ceramic matrix composite: Ceramic matrix composite (CMC) is a material consisting of a ceramic matrix combined with a ceramic (oxides, carbides) as dispersed phase. Ceramic matrix composites are reinforced by either continuous (long) fibers or discontinuous (short) fibers. Most of CMCs are reinforced by silicon carbide fibers due to their high strength and stiffness (modulus of elasticity). The best strengthening effect is provided by dispersed phase in the form of continuous monofilament fibers, which are fabricated by chemical vapor deposition (CVD) of silicon carbide on a substrate made of tungsten (W) or carbon (C) fibers. High thermal shock resistance, high stiffness, high toughness, high thermal stability, low density, high corrosion resistance even at high temperatures make long-fiber CMCs a good choice for high temperature applications.

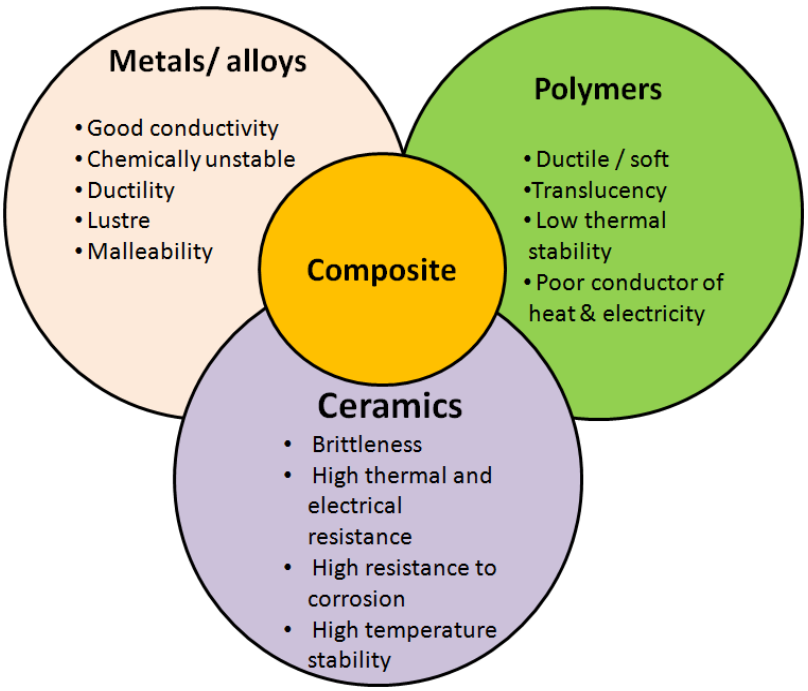

Figure 1.1: Classification of composite within the group of materials.

1.3.2 Classification of composite materials on the basis of reinforcement:

Most importantly, tailoring the properties of the matrix according to the application is done by reinforcing the appropriate material. In a continuous fiber-reinforced composite, the fibers provide virtually all of the strength and stiffness. However, discontinuous reinforcement materials (graphite, glass, SiC, alumina) may also provide thermal and electrical conductivity, controlled thermal expansion, and wear resistance in addition to structural properties. Again on the basis of type of reinforcement, composites can be classified mainly as particulate reinforced composite, fiber reinforced composite and structural reinforced composite. These composites can be further classified as shown in figure 1.2.

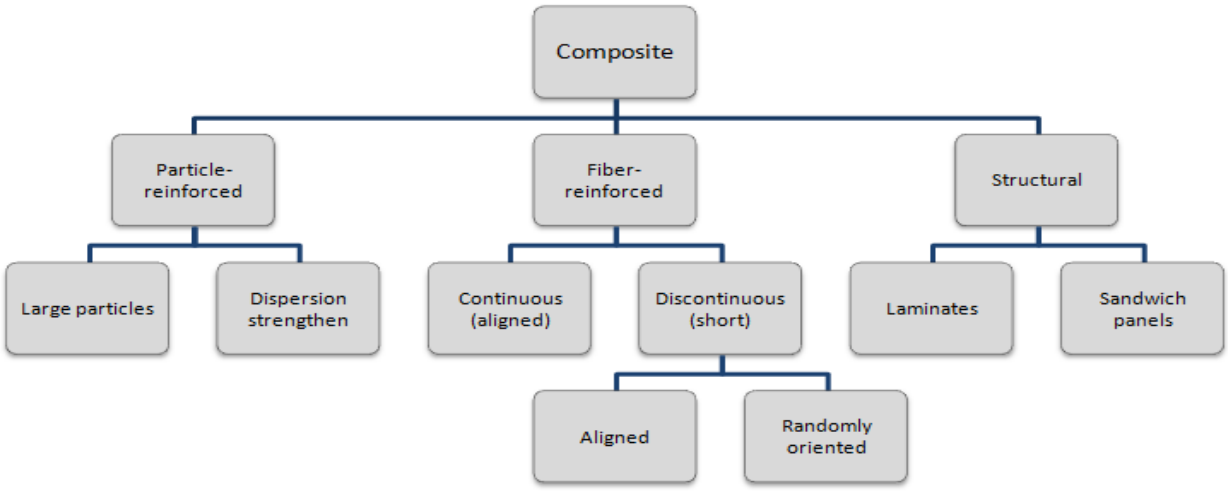

Figure 1.2: Classification of the composite on the basis of reinforcement [5].

1.3.2.1 Particulate reinforced composite: Particulate reinforced composites consist of a matrix reinforced by a dispersed phase in the form of particles. However, dispersion of particulates may be of random orientation or preferred orientation in the matrix. Dispersed phase in preferred orientation of materials consists of two-dimensional flat platelets (flakes), laid parallel to each other.

1.3.2.2 Fiber reinforced composite: Fiber reinforced composite on the basis of size of reinforcement can be divided in two main parts as short fiber reinforced and long fiber reinforced composite. However, orientation of the short/long fiber reinforcement in the matrix tailors the properties of the composites significantly.

1.3.2.3 Structural reinforced composite: When a fiber reinforced composite consists of several layers with different fiber orientations, it is called multilayer composite/structural reinforced

composite. This can be further divided on the basis of presence of reinforcement as laminated composite and sandwich panel composites.

Final properties of the composite depend on the type and amount of the reinforcement. Continuous reinforced composites are used where higher strength and stiffness are required (but at a higher cost), and discontinuous reinforced composites are used where cost is the main driver and strength and stiffness are less important. Particle reinforcement in the matrix offers a wide range of attractive material properties, both mechanical and physical, that cannot be achieved using conventional engineering alloys. Particle reinforced composites are commonly used in applications that require high specific materials properties, enhanced fatigue resistance, improved wear resistance and controlled expansion [6- 8]. The correct selection of reinforcement is very important in yielding desired materials properties.

1.4 Discontinuous reinforced aluminum matrix composite:

Performance of the composites depends more strongly on matrix properties. Composites having metal matrix offer high modulus of elasticity, ductility, and resistance to elevated temperature. A metal matrix is especially good for high-temperature use in oxidizing environments. The most commonly used metals are iron, nickel, tungsten, titanium, magnesium, and aluminum. Among MMCs, Al- alloy based composites are always on the forefront of research.

Discontinuous reinforced aluminum matrix composites are highly versatile class of material with an attractive balance of specific stiffness and strength and a host of other properties, including good wear resistance, thermal conductivity, and low thermal expansion, all of which makes them good multifunctional materials as well [2, 7- 10]. The correct selection of reinforcement is very important in yielding desired materials properties of composites. Hard ceramic particles are most common discontinuous reinforcement used for current aerospace structural applications. Particle size and shape are important factors in determining materials properties. Generally fatigue strength is greatly improved with the use of fine size ceramic particles[11].

Figure 1.3 shows the effect of particle size and shape on the properties and formability of materials. Typically, higher- purity ceramic powder yields higher composite performance, usually with higher raw material costs.

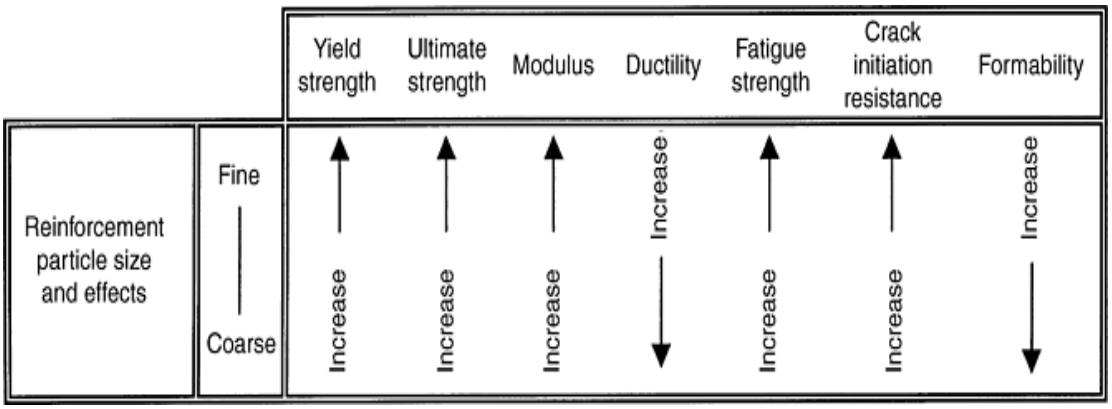

Figure 1.3: Materials properties and formability as a function of reinforcement particle size [10].

The major advantages of aluminium matrix composites (AMCs) compared to unreinforced materials are:

- Greater strength
- Improved stiffness
- Reduced density
- Improved high temperature properties
- Controlled thermal expansion coefficient
- Thermal/heat management
- Enhanced and tailored electrical performance
- Improved abrasion and wear resistance
- Improved damping capabilities.

1.5 Fabrication methods of AMCs:

Most of the present work is focused on discontinuously reinforced (particle or whisker) aluminum MMCs because of their greater ease of manufacture, lower production costs, and relatively isotropic properties. The combination of light weight, environmental resistance, and useful mechanical properties has made aluminum alloys very popular; these properties also make aluminum well suited for use as a matrix metal. The melting point of aluminum is high enough to satisfy many application requirements. Also, aluminum can accommodate a variety of reinforcing agents. Primary processes for manufacturing of AMCs at industrial scale can be classified into two main groups.

(i) Solid state processes (ii) Liquid state processes.

The selection of the processing route depends on many factors including type and level of reinforcement loading and the degree of microstructural integrity desired.

1.5.1 Solid state processing

1.5.1.1 Powder blending and consolidation (P/M processing): Blending of aluminium alloy powder with ceramic short fibre/whisker particle is versatile technique for the production of AMCs [11]. Blending can be carried out in dry or in liquid suspension. Blending is usually followed by cold compaction, canning, degassing and high temperature consolidation stage such as hot isostatic pressing (HIP) or extrusion. PM processed AMCs contain reinforced particles in the form of plate-like particles of few tens of nm thick and in volume fractions ranging from 0.05 to 0.5 depending on powder history and processing conditions. These fine reinforced particles tend to act as a dispersion-strengthening agent and often have strong influence on the matrix properties particularly during heat treatment.

1.5.1.2 Diffusion bonding: Mono filament-reinforced AMCs are mainly produced by the diffusion bonding (foil-fiber-foil) route or by the evaporation of relatively thick layers of aluminium on the surface of the fiber. 6061 Al-boron fiber composites have been produced by diffusion bonding via the foil-fiber-foil process. However, the process is more commonly used to produce Ti based fiber reinforced composites. The process is cumbersome and obtaining high fiber volume fraction and homogeneous fiber distribution is difficult. However, this process is not suitable to produce complex shapes components [12].

1.5.1.3 Physical vapour deposition (PVD): The process involves continuous passage of fiber through a region of high partial pressure of the metal to be deposited, where condensation takes place so as to produce a relatively thick coating on the fiber. The vapour is produced by directing a high power electron beam onto the end of a solid bar feed stock. Composites with uniform distribution of fiber and volume fraction as high as 80% can be produced by this technique [12].

1.5.2 Liquid state processing:

1.5.2.1 Stir casting: This involves incorporation of ceramic particulate into liquid aluminium melt and allowing the mixture to solidify. Here, the crucial thing is to create good wetting between the particulate reinforcement and the liquid aluminium alloy melt. The simplest and most commercially used technique is known as vortex technique or stir-casting technique. The vortex technique involves the introduction of pre-treated ceramic particles into the vortex of molten alloy created by the rotating impeller. Several aluminium companies further refined and modified the processes which are currently employed to manufacture a variety of AMCs on commercial scale [14]. Microstructural in-homogeneities can cause notably particle

agglomeration and sedimentation in the melt subsequently during solidification. Generally it is possible to incorporate upto 30% ceramic particles in the size range 5 to 100 μm in varieties of molten aluminium alloys [14]. The melt–ceramic particle slurry may be transferred directly to a shaped mould prior to complete solidification or it may be allowed to solidify in billet or rod shape so that it can be reheated to the slurry form for further processing by technique such as die casting and investment casting. However, this process is not suitable for the incorporation of sub-micron size ceramic particles or whiskers. Another variant of stir casting process is compo-casting.

1.5.2.2 Infiltration process: Liquid aluminium alloy is injected/infiltrated into the interstices of the porous pre-forms of continuous fibre/short fibre or whisker or particle to produce AMCs [15]. Depending on the nature of reinforcement and its volume fraction preform can be infiltrated, with or without the application of pressure or vacuum. AMCs having reinforcement volume fraction ranging from 10 to 70% can be produced using a variety of infiltration techniques. In order for the preform to retain its integrity and shape, it is often necessary to use silica and alumina based mixtures as binder. Some level of porosity and local variations in the volume fractions of the reinforcement are often noticed in the AMCs processed by infiltration technique. The process is widely used to produce aluminium matrix composites having article/whisker/short fiber/continuous fiber as reinforcement.

1.5.2.3 Spray deposition: Spray deposition techniques fall into two distinct classes, depending whether the droplet stream is produced from a molten bath (Osprey process) or by continuous feeding of cold metal into a zone of rapid heat injection (thermal spray process). The spray process has been extensively explored for the production of AMCs by injecting ceramic particle/whisker/short fiber into the spray [16]. AMCs produced in this way often exhibit inhomogeneous distribution of ceramic particles. Porosity in the as sprayed state is typically about 5–10%. AMCs processed by spray deposition technique are relatively inexpensive with cost that is usually intermediate between stir cast and PM processes.

1.5.2.4 In-situ processing: There are several different processes that would fall under this category including liquid-gas, liquid-solid, liquid-liquid and mixed salt reactions [11]. In these processes refractory reinforcement are created in the aluminium alloy matrix. One of the examples is directional oxidation of aluminium also known as direct metal oxidation (Dimox) process. In this process the alloy of Al–Mg is placed on the top of ceramic preform in a crucible.

The entire assembly is heated to a suitable temperature in the atmosphere of free flowing nitrogen bearing gas mixture. Al–Mg alloy soon after melting infiltrates into the preform and composite is formed. London and Scandinavian Metallurgical Company has developed an in-situ technique, which utilises reaction between mixed salts to produce a dispersion of fine TiB_2 particles in an aluminium matrix. A major limitation of in-situ technique is related to the thermodynamic restrictions on the composition and nature of the reinforcement phase that can form in a given system, and the kinetic restrictions on the shape, size and volume fraction of the reinforcement that can be achieved through chemical reactions under a given set of test conditions.

1.6 Factors affecting the mechanical properties of the MMCs:

Mechanical properties of the composite depend on the presence of reinforcement as well as the interaction of reinforcement with the matrix at micro-level. Factors like interface, solidification, microstructure, wettability, porosity and distribution of reinforcement in the matrix play an important role in tailoring the properties of the composites.

1.6.1 Microstructure: The characteristics of metal matrix composite materials are determined by their microstructure, which are affected by their production and thermal mechanical prehistory. The microstructure covers the structure of the matrix and the reinforced phase. The chemical composition, grain and/or sub-grain size, texture, precipitation behavior and lattice defects are of importance to the matrix. The second phase is characterized by its volume percentage, its kind, size, distribution and orientation.

1.6.2 Interface: Chemical interactions and reactions between the matrix and the reinforcement component determine the interface adhesion, which is responsible for the characteristics of the composite components that affect the mechanical characteristics significantly. In high temperature use of MMCs the microstructure has to remain stable for long service periods. The higher hardness value associated with near interface region and interface, caused by extensive weak interface bond, reduces the ductility of composites thereby limiting its applications. Generally the interface bond strength increases with increase in processing temperature due to increase in concentration of Si at the interface in AMCs. Interface bond strength was altered by the partially dissolved with uniform dispersion of reinforcement.

1.6.3 Wettability: Wettability is known as the ability of the liquid to maintain contact with a solid surface under the intermolecular interactions. Successful incorporation of solid ceramic particles in casting requires to wet the solid ceramic phase with melt. The wettability of reinforcement with a metal melt can be shown by the edge angle adjustment of a molten droplet on a solid base as the degree of wettability as given below:

$$\gamma_{SA} - \gamma_{LS} = \gamma_{LA} \cos\theta \quad (1)$$

Where γ_{LA} is the surface energy of the liquid phase, γ_{SA} the surface energy of the solid phase, γ_{LS} the interface energy between the liquid and solid phases and θ is the edge angle.

At an angle of > π/2 a nonwettable system is described and for an angle limit of < π/2 a wettable system. With decreasing angle the wettability improves [14].

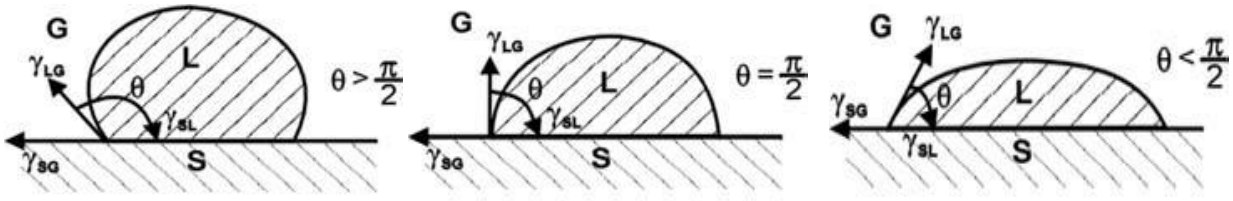

Figure 1.4: Edge angle adjustment of a melt drop on a solid base for various values of the interface energy [14].

1.6.4 Solidification: Phase transition of the material from liquid to solid phase by lowering the temperature below the melting point is known as solidification. Solidification affects the characteristics of the composite significantly. Solidification is most widely used for shaping of the materials to desired product, as it controls the microstructural and interfacial interaction of the matrix and reinforcement.

1.6.5 Porosity: The porosity of a composite material is determined by measuring the amount of void space inside, and determining what percentage of the total volume of the material is made up of void space. Porosity measurements can vary considerably, depending on the material and high or low porosity will impact the way in which the material performs. The property of porosity is actually slightly more complex than the simple percentage of void space inside a material. Another important consideration is the shape and size of the void spaces in the material.

1.6.6 Distribution of reinforcement: The major factor that significantly tailors the properties of the composite is presence of reinforcement in the matrix. However, shape and size of

reinforcement with the total amount in the matrix affects the characteristics of the composites greatly. Distributions of the reinforcement also play an important role to get desired property of the composite for particular application. Uniform distribution of particulate reinforcement in composite enhances the mechanical properties significantly. Particle-to-liquid density ratio is responsible for the distribution of reinforcement in the matrix. Segregation and clustering of the particles during casting process are major problems, which restrict the uniform distribution of particles in the matrix. Hence optimization condition for the uniform distribution of particles in matrix is necessary to get desired characteristics. Holding time, stirring, and solidification are some major factors to get uniform distribution of the particles in the matrix. Mixing of reinforcement without gas entrapment in the molten metal is also essential part of fabrication of good quality composite for particular application.

1.7 Wear:

A progressive loss of material from the operating surfaces as a result of relative motion is by mechanical and/or chemical processes known as wear [12]. Wear of material gives the idea about the durability of the material under different conditions like applied load, temperature, corrosion etc. Hence wear study of any material is very important part about the production and applications in different engineering fields.

On the basis of wear mechanism included, wear can be divided mainly in following types [17]:

(a) Abrasive wear (b) Adhesive wear (c) Impact wear

(d) Fretting wear (e) Erosive wear

1.7.1 Abrasive wear: Removal of the particular material from one surface, by another harder material known as abrasive wear. As a result hard particles of the debris between the two surfaces are formed [13]. There are two conditions in which abrasive wear occurs. The two body abrasion and three body abrasion. In the two body abrasion, the harder surface rubs the other. However, a third body is involved in three body abrasion. This third body is generally a small hard particle of abrasive between the two softer rubbing surfaces. Microscopically, abrasive wear causes asperities of the harder surface to press into the softer surface, with plastic flow of the softer surface formed around the harder asperities. These result in 'microploughing' and 'microcracking' where tangential motion is imposed.

1.7.2 Adhesive wear: Adhesive wear is general form of sliding wear, which is caused by relative motion, "direct contact" and plastic deformation. This plastic deformation creates wear debris and material transfer from one surface to another. Wearing occurs when interfaces in contact are made to slide and the locally adhered regions get separated. This separation may occur by one or two of the failure modes of solids, resulting in a very wide range of wear rate.

1.7.3 Impact wear: Impact wear can be defined as the wear of a solid surface that is due to percussion, which is a repetitive exposure to dynamic contact by another solid body. The various percussive wear mechanisms include adhesive, abrasive, surface fatigue, corrosive, and thermal wear.

1.7.4 Fretting wear: Small-amplitude oscillatory movement occurring between the contacting surfaces known as "Fretting". This fretting is responsible for the production of the oxide debris in normal atmospheric conditions, and this phenomenon is known as "Fretting wear".

1.7.5 Erosive wear: Loss of material from repeated impact of small, solid particles known as erosive wear**.** Erosive wear is observed as a serious problem in many engineering systems, including steam and jet turbines, pipelines and valves carrying particulate matter.

REFERENCES:

[1] MF Ashby; Technology in the 1990s: Advanced materials and predictive design, Philosophical Transactions of the Royal Society of London, A322 (1987) 393.

[2] A Banerji, SV Prasad, MK Surappa and PK Rohatgi; Abrasive wear of cast aluminium alloy-zircon particle composites. Wear, 82 (1982) 141–151.

[3] MK Surappa; Aluminium matrix composites: challenges and opportunities. Sadhana, 28 (2003) 319-334.

[4] J Clarke and AD Sarkar; Wear characteristics of as- cast binary aluminum silicon alloys. Wear, 54 (1979) 7-16.

[5] WD Callister; Materials Science and engineering: An introduction, Willey & sons 6th ed. (2006) p 529.

[6] YM Youssef, RJ Dashwood and PD Lee; Effect of clustering on particle pushing and solidification behavior in TiB_2 reinforced aluminium PMMCs. Composite A, 36 (2005) 747-763.

[7] S Das, S Das and K Das; Abrasive wear of zircon sand and alumina reinforced Al-4.5 wt% Cu alloy matrix composites- a comparative study. Composite Science and Technology, 67 (2007) 746-751.

[8] AW Fligier, LA Dobrzański and M Adamiak; Wear resistance of PM composite materials reinforced with the Ti(C, N) ceramic particles. Journal of Achievement in Materials Manufacturing Engineering, 30(2) (2008) 147-150.

[9] O Yilmaz and S Buytoz; Abrasive Wear of Al_2O_3-Reinforced Aluminum- Based MMCs. Composite Science and Technology, 61 (2001) 2381–2392.

[10] CL Hsieh and WH Tuan; Thermal Expansion Behavior of a Model Ceramic-Metal Composite. Materials Science and Engineering A, 460 (2007) 453– 458.

[11] ASM International Handbook Committee; Composites, 21 (2001); 134-135.

[12] KK Chawla; Composite Materials: Science and Engineering. Springer, (2012) 209- 210.

[13] Manufacturers of Discontinuously Reinforced Aluminum (DRA), DWA Composite. Specialties Inc., Chatsworth USA (1995).

[14] J Hashim, L Looney and MSJ Hashmi; Metal matrix composites: production by the stir casting method. Journal of Materials Processing and Technology, 92 (1999) 1–7.

[15] VC Srivastava, RK Mandal and SN Ojha; Microstructure and mechanical properties of Al–Si alloys produced by spray forming process. Materials Science and Engineering: A, 304–306, (2001), 555–558.

[16] Karl U. Kainer; Metal Matrix Composites: Custom-made Materials for Automotive and Aerospace Engineering, WILEY-VCH Verlag GmbH & Co. KGaA, Weinheim; 2006, 24-25.

[17] ASM International Handbook Committee; Friction, Lubrication, and Wear Technology, 21 (2001); 493- 494.

CHAPTER 2

LITERATURE REVIEW

Overview:

Development of discontinuous reinforced aluminum matrix composites (DRAMCs) by many researchers using different fabrication techniques and their study based on wear behavior is discussed in this chapter. As our work is based on the stir casting process, hence the main focus in this chapter is on the development of DRAMCs by stir casting process and study of their physical properties especially wear resistance of the composite. Different work describing the role of ceramic particles in the Al-alloy and their effect on the wear has been analyzed and discussed in this chapter.

Discontinuous reinforced aluminium matrix composites (DRAMCs) mainly contain the hard ceramic particles as reinforcement in the aluminum/aluminum alloy matrix. In the past, the presence of ceramic particles in metals and alloys were considered as undesirable inclusions impairing strength and ductility but now a days it is not so. Badia *et. al.* [1] in the mid-sixties, worked on particle reinforced metal matrix composite. They injected nickel-coated graphite powders in aluminium alloys in presence of argon gas into a molten bath of the alloy. S. Ray [2] in 1968 firstly used stir cast process to develop aluminium-alumina composites by incorporating alumina particles in aluminium metal matrix. For the MMCs, aluminium alloys are the most commonly utilized materials e.g. 2000, 5000, 6000 and 7000 alloy series. Silicon is an important alloying element, added to aluminium to improve its mechanical properties such as tensile strength, hardness and wear resistance. It also reduces thermal expansion and increases fluidity of the molten alloy which enables thin sections to be cast. Magnesium is used as a wetting agent in order to enhance wettability between the ceramic particles and matrix alloy. Other elements such as titanium, strontium and phosphorus could be added to refine the microstructure [3].

2.1 Al-Si alloy:

Excellent castability, high specific strength, excellent corrosion resistance and good wear properties of Al- Si alloys make them of wide industrial usage in the areas of automotive, aerospace and military applications [4, 5]. The silicon content in standardized commercial cast Al- Si alloys is in the range of 5 to 23 wt%. Depending on the Si concentration in weight percentage, the Al- Si alloy systems are divided into three major categories as hypoeutectic (Si < 12.6%), eutectic (Si = 12.6%) and hypereutectic (Si > 12.6%). Phase diagram of the Al-Si binary alloy is shown in figure 2.1. There is only one invariant reaction in this diagram, namely

$$L \rightarrow \alpha + \beta \text{ (eutectic)} \quad (1)$$

Where, L is the liquid phase, α is predominantly aluminum, and β is predominantly silicon. It is accepted that eutectic reaction takes place at 577°C and at a silicon level of 12.6%. Binary Al- Si alloys, near to the eutectic composition exhibit acicular or lamellar eutectic silicon which is in the form of large plates with sharp sides and edges. For Al-Si alloys, the eutectic composition is a structure of α + Si rather than α + β.

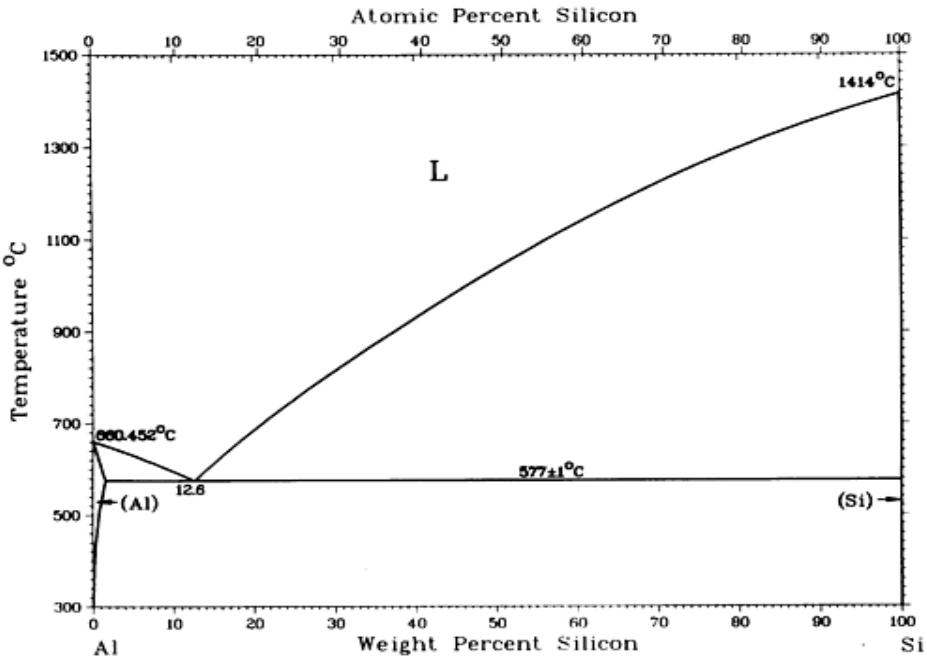

Figure 2.1: Al-Si binary phase diagram [6].

Cast eutectic alloys with coarse acicular silicon show low strength and ductility as these coarse flakes of Si in the eutectic promote brittleness within these alloys. During solidification, the primary aluminum grows in dendrites and silicon phase grows in angular primary particles. At the eutectic point, the eutectic Al-Si phases nucleate and grow until the end of solidification, while hypoeutectic alloys consist of a soft and ductile primary aluminum phase and a hard and brittle eutectic silicon phase. Hypereutectic alloys usually contain coarse, angular primary silicon particles as well as a eutectic silicon phase [7]. Most used Al- Si alloys have a near-eutectic composition since this gives a lower melting point and makes them cheaper to cast. However, dealing with the brittle Si flakes, properties of the Al-Si alloy can be modified according to the requirement.

Other alloying elements (e.g. Mg, Cu, Ni, Sn, Mn, etc.) are also added to the Al-Si alloy to fulfill the requirement of the material for the particular application. Each alloying elements in the particular composition change the physical or chemical properties of the Al- Si alloy. Copper affects the strength and hardness of aluminum casting alloys. Similarly magnesium combines with silicon to form Mg_2Si phase which provides good corrosion resistance and weldability or extremely high strength [8]. Hernández-Méndez *et al.* [9] suggested that presence of nickel (Ni) in Al- Si alloy makes an intermetallic compound named as Al_3Ni which is responsible for the

improvement in the hardness, compression and flexion resistances of Al-Si alloy. Tin (Sn) in Al-Si alloys provides short term liquid lubricant for rubbing surfaces which helps to reduce the friction in bearing and bushing applications [10]. Nam *et al.* [11] in their work found that addition of Mn improves the tensile strength, corrosion resistance as well as significantly improves the low-cycle fatigue resistance in the Al- Si alloys.

2.2 Reinforcement of ceramic particles:

Due to light weight, in comparison to other metals aluminum alloys get more and more interest in the architecture, transportation and packaging. However, inferior strength, rigidity and wear resistance compared with ferrous alloys motivate researchers to improve these properties of Al-Si alloys by using them as matrix in aluminum matrix composite [12]. Discontinuous reinforcement in Al-Si alloys is of great interest, due to large possibility to change the properties of materials with ease manufacturing process. The reinforcement phase in Al alloy matrix is generally hard ceramic particles such as SiC, Al_2O_3, B_4C, TiC and $ZrSiO_4$. The volume fraction of reinforced particles or whiskers is generally within the range of 10- 30%. Easy availability, low cost, independence of mechanical properties from particulate orientation and production via a wide range of manufacturing routes are the main features for the ceramic particles to be used as discontinuous reinforcement phase in MMCs [13- 15]. Addition of hard ceramic particles in the AMCs improves their hardness, Young's modulus and abrasion wear resistance; however, it also results in deterioration of their plastic properties.

2.3 Wear behavior of discontinuous reinforced AMCs:

As discussed above, ceramic particles modify the physical as well as mechanical properties of the Al alloys significantly. Hence their effect on the wear behavior of the materials is an interesting topic for the researchers to develop the much durable material for the particular application. The main factors controlling the sliding wear resistance of particle reinforced AMCs (PRAMCs) are the reinforcement volume fraction and their size [14, 16, 17]. Hosking *et al.* [14] have demonstrated an increase in wear resistance with increasing volume fraction of alumina particulates (at constant particle size) and also with increasing particle size (at constant volume fraction). The coefficients of friction of the composites, however, were lower than that of the aluminum alloy without reinforcement. Jokinen *et. al.* [18] evaluated the tribological properties

of an A1 6061 alloy reinforced with 20 vol.% SiC particulates prepared by the powder metallurgy (PM) route. They revealed a dramatic reduction in the wear rates of the composites when compared to unreinforced A1 6061 at light loads (contact stress: 3.2 MPa) but not at heavy loads (contact stress: 12.7 MPa). However, Roy *et al.* (1992) concluded that the wear rate of the aluminum matrix composites is not dependent on the type and size of the reinforcement but decreases with the increasing volume fraction of the particulates (up to 20 %) [19].

Apart from this there are some other parameters which affect the wear behavior of PRAMCs greatly and have been studied in detail by the researchers. Alpas and Zhang [17] in 1994 suggested that normal contact stress is a critical parameter which affects the wear resistance of PRAMCs. However, presence of ceramic particles improves the wear resistance of Al alloy at low contact stress. At low contact stresses, the ceramic particulates served as load-bearing elements, limiting the strains in the Al matrix. Zhang *et al.* [20] also introduced temperature as another very important parameter for the wear resistance property of the material. They suggested that at the critical temperature (0.4 T_m, where T_m is the melting temperature of the material), thermally activated deformation processes are expected to become active and lead to softening of the material adjacent to the contact surfaces. Matrin *et al.* [21] suggested that ambient temperature play an important role on the wear behavior of the materials. Critical transition temperature of the material improves with addition of ceramic particles in the metal matrix. They found that main effect of the SiC reinforcement on the sliding wear resistance at high temperature was to delay the transition from mild to severe wear by about 50 ^{o}C.

Hashim *et al.* [22] studied in detail about the factors which are responsible for a high quality particle reinforced MMCs fabricated by stir casting process. They suggested that uniform distribution of particles in matrix, wettability of particles with matrix, porosity in cast MMCs , chemical reactions between the metal matrix and ceramic particles are mainly responsible for the fabrication of high quality MMCs. In 2001, J. Hashim [23] proposed a modified stir casting route for the fabrication of the MMCs. Prabhu *et al.* in 2006 [24] studied the effect of stir speed and stirring time on distribution of particles in cast metal matrix composite. During their work, particle clustering in some places was observed with lower speed and lower stirring time. However, better homogeneous distribution of SiC in the Al matrix was observed by increasing the stirring speed and stirring time. Better distribution of SiC leading to higher hardness was observed at 600 rpm and 10 minutes stirring time condition. Aqida *et al.* [25] discussed about the

effect of porosity on the mechanical properties of the MMCs. They suggested that the reason of pore formation are air bubbles entering the melt matrix material, water vapour on the particles surfaces, gas entrapment during mixing process, evolution of hydrogen, and shrinkage during solidification. Generally, increasing content of porosity will decrease the mechanical properties of MMC such as tensile strength, Young's modulus, Poisson ratio, and damping capacity. They suggested that in tensile test, porosity tends to develop the strain of a particular region in MMC, when stress is applied. Consequently, the ultimate tensile strength as well as the Young's modulus of a cast MMC will decrease.

Chaudhary *et al.* [26] in 2005 studied the frictional and wear behavior of Al-2Mg-11TiO_2 composites prepared through spray forming and stir casting techniques. They demonstrated the operative wear mechanism through analysis of SEM images of the worn surfaces and wear debris collected after the wear test. Basavarajappa *et al.* [27] in 2007 used the pin on disc method with LVDT technique to study the effect of sliding velocity on the wear behavior of the composite materials. They used three different materials for the wear test and found the similar trend of wear behavior with the different sliding speeds.

Abdizadeh *et al.* [28] studied the effect of coefficient of thermal expansion of the ceramic particles on the mechanical properties. For this purpose they dispersed 5wt% of $ZrSiO_4$ and TiB_2 particles of 1 µm size in aluminum using stir casting process at different temperatures above pure aluminum melting point (750, 850 and 950 ºC). The best property for Al-5% $ZrSiO_4$ was achieved at 750 ºC and for Al-5% TiB_2 at 950 ºC. This may be related to the lower heat expansion coefficient of TiB_2 than of $ZrSiO_4$ that induces a larger dislocation density at boundaries between matrix metal and TiB_2 particulates. However, they also suggested that because of better wettability of TiB_2 by aluminum than of $ZrSiO_4$, a larger fraction of TiB_2 particulates can be incorporated in the matrix and may lead to the large value of hardness and tensile strength.

Yılmaz *et al.* [29] in their work studied the effect of Al_2O_3 particulate content, thermal properties and stir casting parameters on the dry sliding wear resistance of MMCs. They observed that the increase of Al_2O_3 vol% delayed the transition from mild to severe wear and increased the transition loads. The porosities in the structure increased wear rate. The wear rate of the Al alloy was significantly affected by the porosity while, the wear rate of the composite increased only slightly with increasing porosity. The increase in Al_2O_3 particulate concentration decreased

thermal conductivity, and increased friction coefficient. Jha *et al.* in 2009 [30] proposed that numerous porosities present in the casting of Al- Si alloy resulted in crack initiation. The crack propagated by interlinking of pores, and the casting failed. The acicular Si eutectic facilitated the cracking by debonding from the matrix.

Presence of alloying elements like Fe, Mn and Sr in the Al- alloy effectively changes the microstructure and mechanical properties of the MMCs. Addition of Fe causes precipitation of large β-Al_5FeSi. The addition of a modest level of Mn at the Mn:Fe ratio of 0.5 converts almost all β-phase plates to fine α-Chinese script phase, leading to improved tensile strength and elongation. Fracture micrographs revealed an apparently brittle fracture with large facets of β-phase plate in composites with higher Fe level, whereas Mn and Sr modified specimens and show fine dimples on the fractured faces [31].

Now a days, addition of nano-scale particles in Al alloys is also a new interesting area for the researchers to develop the aluminum matrix nanocomposites. Akio *et al.* [32] and Mussert *et al.* [33] found that nano-sized ceramic particles strengthen the metal matrix maintaining good ductility, high temperature creep resistance and better fatigue. Mazahery *et al.* [34] in 2008 developed the A356/nano-Al_2O_3 composites by stir casting process. For this purpose Al_2O_3 particles with average particle size of 50 nm were used as reinforcement. They found that the presence of nano-Al_2O_3 reinforcement led to significant improvement in hardness, 0.2% yield strength, UTS and ductility. Sajjadi *et al.* [35] in 2011, studied the effect on the microstructural and mechanical properties after reinforcing micro and nano size Al_2O_3 particles in the A356 aluminum alloy. They investigated the influence of various processing parameters such as heat treatment of particles, injection process, stirring speed, reinforcement particle size and weight percentage of reinforcement particles on the microstructure and mechanical properties of composites. They revealed that heat-treated particles, injection of particles and the stirring system improved the wettability and distribution of the nano particles within the aluminum melt. They also found that the amount of hardness, compressive strength and porosity increased as weight percentage of nano Al_2O_3 particles increased.

In addition to these, some other works pertaining to the field of particle reinforced aluminum matrix composite are tabulated in table 2.1. The summary of their research outcomes has also been given for a comparative study.

Table 2.1: Tabulated summary of outcomes of various investigators on the development and wear behavior study of ceramic particles reinforced AMCs.

Investigator [Year]	Materials [Matrix/Reinforcement]	Process	Parameter Investigated	Outcomes
Hashim *et al.* (1999) [36]	Particle reinforced metal matrix composite	Stir casting	Holding temperature, Stirring speed, Size of the impeller, Position of the impeller in the melt	• By controlling the processing conditions as well as the relative amount of the reinforcement material, it is possible to obtain a composite with a broad range of mechanical properties. • The method is potentially cost effective, but widespread adoption is dependent on a satisfactory resolution of the existing technical difficulties presented.
B.K. Prasad (2000) [37]	Zinc–aluminium alloy containing nickel under varying material	As cast/ Heat treatment	Microstructure, Wear beahviour study with Pin-on-disc method at different sliding velocity	• Heat treatment reduced the hardness and improved the extent of microhomogeneity in the alloy without practically affecting the morphology of the nickel containing microconstituents. • Heat-treated alloy pins showed better wear response in spite of reduced hardness over the as-cast ones due to reduced cracking tendency and better homogeneity of distribution of phases, the former owing to improved compatibility of the nickel containing phase with the softer matrix surrounding the phase. • Improved wear behaviour of the alloy pins agreed with mild surface damage and fine debris formation and vice versa.
Ho Jang *et al.* (2000) [38]	Non- asbestos organic (NAO) type materials containing different amounts of Sb_2S_3. and $ZrSiO_4$.	Brake dynamometer	Friction coefficient and Torque variation (friction force oscillation)	• The change of friction coefficient during light pressure drag showed that Sb_2S_3 improves the stability of the friction coefficient. • The amount of friction material wear during this dynamometer procedure shows that the relative amounts of Sb_2S_3 and $ZrSiO_4$ in the friction material plays a crucial role in determining the amount of friction material wear during the service. • Friction stability is improved by adding more Sb_2S_3 in the friction material.
L.N. Satapathy (2000) [39]	addition of zirconia in different proportions to	Compaction	Modulus of rapture (MOR), Modulus of elasticity (MOE), Hardness, Abrasion resistance , Microstructural	• There is an increase in trend in hardness and MOE and MOR upto some extent with increase in ZrO_2 in the flyash matrix. • As the ZrO_2 content increased in flyash, more and more Zircon are formed.

	flyash		investigation by SEM	
M. Singh *et al.* (2003) [40]	Aluminum alloy (LM 6) reinforced with sillimanite particles	Stir casting	High stress, Abrasive behavior	• The effect of load is more or less the same in the alloy and composite but the severity of the effect of abrasive size on wear of the composite is significantly higher than that in the alloy. • The critical abrasive size decreases with increase in applied load and vice versa. • The synergic effect of applied load and abrasive size is significantly higher than the synergic effects due to other factors like abrasive size and sliding distance, and applied load and sliding distance.
O. P. Modi *et al.* (2001) [41]	Zinc-based Al alloy with Al_2O_3 particles	Stir casting	Wear rate	• The wear rate of the specimens decreased with increasing sliding distance. • Factorial diagram is helpful to understand the individual and combined effects of the parameters on the wear response of the samples. • Mixed effects of the interaction of the variables were also noticed. Interaction of abrasive size and sliding distance caused more wear rate of the matrix alloy but helped to reduce the wear rate of the composite.
O. Yilmaz *et al.* (2001) [42]	Al- alloy reinforced with Al_2O_3	Stir casting	Porosity, Hardness, Wear behavior	• The wear rate of Al alloy increased drastically with increasing sintered porosity. • Although porosity existed in the compocasting composites, the effect of Al_2O_3 addition on the wear property far surpassed the existing porosity. • The effect of vol.% porosity increased when the Al_2O_3 particle content increased from 5 to 15 vol.%. • For the composites containing the same amount of Al_2O_3 reinforcements, the wear rates decreased with increasing Al_2O_3 size. • The strength of the composites that contain hard particles increases with the volume percentage of particles in the composite
P.N. Bindumadhavan *et al.* (2001) [43]	Al- alloy (A356) with dual particle size SiC particles	Stir casting	Hardness, Microstructure, Wear behavior	• The wear resistance of as-cast Al–Si–Mg alloy tested increases with increasing SiC reinforcement added. • Higher wear in the case of the unreinforced specimen was related to the higher thickness of the hardened layer, the formation of cracks and subsequent delamination of wear

				debris from the surface layer, which was confirmed by optical and scanning electron micrography. • For the same total volume fraction of SiC reinforcement, DPS composites containing both small (47 mm) and large (120 mm) SiC reinforcement particles showed higher wear resistance than composites having only small particles. • Thickness of the hardened layer varied between 10 and 30 mm in the case of reinforced specimens and between 30 and 60 mm in the case of unreinforced specimens.
J. Hasim (2001) [44]	Aluminium alloy A359 with SiC	Two step Stir Casting	Microstructure, Hardness, Tensile strength	• A new approach of fabricating cast aluminium matrix composite by using the stir casting method has proved to be successful. • During the initial stage of heating, any moisture in the ceramic particles and the matrix materials is burn off and thus reduces the level of porosity. • Microstructural observation suggests that the stirring action of the slurry produces cast MMC with smaller grain size compared to unstirred one. • The conditions of ceramic particle coupled with the smaller grain size are the factors that strengthen the alloy matrix.
M. Gui *et al.* (2003) [45]	Mg-Al9Zn & Mg-Zn5Zr alloys with SiC particles	Vacuum Stir casting	Microstructure, Yield strength, Tensile strength	• In this process no macrosegregation of SiC particles and gas bubbles were found in the composite ingots. • In the microstructure of the Mg-Al9Zn/15SiCp composite, SiC particles exhibit a reasonably homogenous distribution and SiC reinforcements are well bonded by magnesium. • 112% increase in yield strength and 33% increase in elastic modulus are obtained for this composite compared with the unreinforced magnesium alloy, while an increase of 24 and 21%, respectively, were observed for theMg-Zn5Zr/15SiCp composite.
Y. Sahin *et al.* (2003) [46]	Al–Si alloy with SiC particles	Vacuum infiltration process	Microstructure, Hardness, Density, Wear rate	• Al-9.42Si-0.36Mg alloy matrix composites containing up to 55 vol% SiC particles were successfully produced by this method. • The higher volume fraction composites could be achieved when vacuum between 400–500 mmHg pressure was applied while the lower volume fraction of composites was infiltrated at 200 mmHg pressure. The infiltration rate increased with increasing infiltration time. • The hardness and density of the composite increased linearly

				with increasing particulate content, however, porosity level decreased with increasing particulate content. • Dry sliding wear properties of the Al alloy improved significantly by the addition of SiC particles into the matrix alloy under all test conditions.
S. Naher *et al.* (2003) [47]	Water and transparent glycerol/water solutions with SiC particles MMCs	Stir casting	Stirring speed, Blade angle, Stirring depth	• A minimum stirring speed of 100 rpm for water and 200 rpm for glycerol/water–SiC mixtures is required for uniform dispersion to occur. • Higher blade angles and lower viscosity resulted in reduced particulate dispersion time. • A viscosity increase from 1mPa s (for liquid metal) to 300mPa s has a tremendous effect on the SiC dispersion and settling time. However, a further increase from 300 to 1000mPa s has negligible effect on this time.
D.K. Dwivedi *et al.* (2004) [48]	Al–18% Si–0.5% Mg alloy	Melting	Wear- friction behavior at different speeds and loads	• Increase in load increases the wear gradually in mild wear regime and beyond certain critical load (transition load) wear increases abruptly. • Transition load of hypereutectic alloy increases with the addition of copper. • Alloy with higher percentage of copper (3–5%) is subjected to increased wear rate especially at higher loads. • There is a critical sliding speed (at a given load) for each alloy at which transition from mild to severe wear takes place. This critical speed is not affected with the addition of copper in hypereutectic alloy.
K. Das *et al.* (2004) [49]	Fe_2O_3, $ZrSiO_4$, aluminum powder, carbon in the form of cast iron and graphite	Self-propagating high-temperature synthesis (SHS) reaction	Microstructure, Hardness, Abrasive wear rate	• The composite possesses attractive abrasive wear resistance property, which is better than a high-chromium iron. • The composite also possesses good high-temperature stability.
S.K. Chaudhury *et al.* (2005) [50]	Pure Al alloy and TiO_2	Spray casting, Stir casting	Friction and Wear behavior	• Wear properties of the spray formed composite are significantly improved with incorporation of TiO_2 particles. • The wear rate of the spray formed composite is lower than the base alloy and the stir cast composite. • The coefficients of friction of both as-spray and stir cast composites is lower than the base alloy and it decreases with increase in load.

D.P. Mondal *et al.* (2006) [51]	Al–Si alloy (ADC-12) with SiC	Stir casting	Microstructure, Wear behavior	• Addition of ceramic reinforcement such as SiC particles improves the wear resistance of the alloy. • Transition in wear mechanism from microcutting/plowing dominated to micro-cracking and -fracturing dominated wear took place when abrasive size increased from 100 to 120 μm. • The wear resistance increases linearly with increase in SiC content and decreases with increase in reinforcement size.
Han Jian-min *et al.* (2006) [52]	Al- alloy (A356) with SiC particles	Stir casting	Study of defects	• Black inclusions are SiC agglomerates, silver spots are Al-Fe-Si phase particles, white inclusions are SiC particles adhering to Al_2O_3 and the pores are caused by gas bubbles and agglomerated SiC particles. • An improved stir casting process is established for fabricating SiCp/A356 composites with good mechanical properties and less defects.
A. Vencl *et al.* (2006) [53]	Al- alloy (A356) with Al_2O_3	Compocasting technology	Hardness, Tribological behavior	• Improvement of wear resistance for the composite material with 3 wt. % Al_2O_3 reinforcement was significant for specific load up to 1 MPa. • Adhesive wear was a predominant mechanism of wear followed by plastic deformation with increase of specific load.
V.S. Aigbodiona *et al.* (2007) [54]	Al–Si–Fe alloy with SiC particle	Double stir-casting method	Microstructure, Porosity, Tensile strength, Impact strength	• Addition of silicon carbide particles using this method to Al–Si–Fe alloy increases both the yield strength, ultimate tensile strength and hardness values up to a maximum values of 79.98, 106.12Nmm^2 and 67.0HRB, respectively, at 20% SiC addition. • There is general slight increase in the apparent porosity of the composites with percentage SiC addition that is still lower than the recommended values. • For optimum service performances of this alloy, silicon carbide addition should be between 15 and 20% and not exceed 20% in order to develop better necessary properties.
H. Abdizadeha *et al.* (2008) [55]	Al-356 with $ZrSiO_4$ and TiB_2	Stir casting	Microstructure, Hardness, Tensile strength	• The improvement of hardness and tensile strength of aluminum by incorporation of $ZrSiO_4$ and TiB_2 particles is due to the high strengthening and work-hardening at low strain in the composite system. • It seems that because of better wettability of TiB_2 by aluminum than of $ZrSiO_4$, a larger fraction of TiB_2 particulates will be incorporated in the matrix and cause the large value of hardness and tensile strength. • The best property values for Al–5% $ZrSiO_4$are achieved at

				750ºC and for Al–5% TiB2at 950◦C.
T.V.S. Reddy *et al.* (2009) [56]	Cast Al–17%Si–0.3%Mg alloy	Conventional and Rheocasting processes	Microstructure, Hardness, Wear behavior	• Stir casting of hypereutectic cast Al–17%Si–0.3%Mg alloy results in finer and more uniformly distributed primary silicon particles compared to that of conventional cast alloy. • Stir cast alloy showed lower wear rate than conventional cast alloy under identical sliding conditions.
A. A. Yar (2009) [57]	Aluminum alloy (A356.1) with nano-particle MgO	Stir casting	Microhardness, Hardness Compressive, Tensile strength	• 356.1 aluminum alloy reinforced with nano-sized MgO was successfully fabricated via stir casting method. • Composite containing 1.5vol% MgO fabricated at 850 ˚C showed improved properties such as hardness, strength and toughness in comparison with other specimens. • Toughness of composites generally decreased by increasing the content of MgO.
A. Sharma *et al.* (2009) [58]	Al-4.5 wt% Cu with $ZrSiO_4$	Stir casting	Ageing behavior, Microhardness	• Under all the heat treatment conditions, the microhardness increased with the ageing time to a peak value and then decreased with a prolonged ageing time. • Thermal cycling of the composite revealed that the microhardness of the composite increases with the extent of solution heat treatment and attains a maximum and gradually drops with further number of heat treatment cycles. • For thin and complex aluminum castings, oil based quenching media can be a good option. The salt brine quenching is faster as compared to water quenching but suffers from distortion and cracking problems.
S. Ilo *et al.* (2010) [59]	Ni-based matrix embedded with WC/W_2C	Liquid-phase sintering	Microstructural study, Interface morphology	• Increasing process intensity (temperature and time) increased the extent of carbide dissolution. • The chemical composition and the micro-mechanical properties were almost constant within each of all the detected layers in the interface between matrix and carbides, indicating that the different microstructure gradients are dependent mainly on the interface growth kinetics. • The hardness of the carbide/matrix interface area is significantly lower than the hardness of the original primary tungsten carbides.
G. Rajaram *et al.* (2010) [60]	Al–Si alloy	Heating, Fluxing and Degassing	Microstructure, hardness, Tensile strength, Wear behavior	• The tensile strength and flow stress of Al–Si alloy is decreasing with the increase in temperature. • The % of elongation of Al–Si alloy is decreased till the temperature is 200 ˚C and then increased with increasing

				temperature. • The strain hardening exponent (n) value is decreasing with the increasing temperature due to thermal softening phenomenon. • Wear resistance of the alloy is increased linearly with increasing the operating temperature. • The alloy sustain under identical sliding condition up to 250 ˚C, beyond this temperature, the pin sample is squeezed out from the disc during test. • Wear mechanism of alloy at temperatures less than 100˚C is delamination followed by partial abrasive wear which leads to plastic deformation. The mechanism of oxidative wear dominates above 150 ˚C for alloy at high temperature.
A. Onat (2010) [61]	Al–4.5Cu–3Mg with SiC particles	Direct squeeze casting	Microstructure, Fracture surface, Wear and Friction behavior	• The microstructure of the SiCp-reinforced composite showed a reasonably uniform distribution of particles and good interfacial bonding of dispersed particles with the matrix alloy. • The amount of wear generally increases with increasing sliding speed and the extent of wear generally becomes greater with an increase in applied load. • The friction coefficient decreased with increasing applied load and sliding velocity.
S. Suresha (2010) [62]	LM25 with SiC and Gr particles	Stir casting	Wear behavior	• Interactions exist among sliding speed, load and sliding distance in Al–SiC–Gr hybrid composites and between load and sliding distance in Al–Gr composites. Such interactions do not exist in Al–SiC composites. • Increase of speed reduces wear by supporting mechanically mixed tribolayer and increase of load increases wear by reducing the role of tribolayer. • Al–SiC–Gr hybrid composites are better substitutes to Al–Gr and Al–SiC composites owing to improved wear resistance as a result of combined reinforcement of SiC and Gr particulates.
R.N. Rao *et al.* (2011) [63]	Al–Zn–Mg–Cu alloy with SiC particles	Stir casting	Microstructure, Wear behavior	• SiC content increases the wear rate and temperature decreases, but reverse trend can be observed for coefficient of friction. • The wear rate decreases linearly with increasing SiC content and increases with increasing sliding speed. • At higher sliding speeds the wear surface is characterized by the formation of deep continuous grooves, series of parallel

				transverse as well as longitudinal cracks, patches of damaged regions and pitting marks.
S.A. Sajjadi *et al.* (2011) [64]	A356 aluminum Alloy with Al_2O_3 particles of micro and nano size	Three step stir casting	Microstructure, Hardness, Density and Compressive strength	• The microstructure of the composites contained the primary α- Al dendrites and eutectic silicon. While Al_2O_3particles were separated at inter-dendritic regions and in the eutectic silicon. Also, another intermetallic compounds such as Mg_2Si, $FeSiAl_5$ and Al_4C_3 were observed at the eutectic phase. • It has been found that the three-step mixing method has only the ability to fabricate samples up to 5 wt.% of micron sized and 3 wt.% of nano sized Al_2O_3 reinforcement successfully. • The results also show that the compression strength of nanocomposites is greater than that of micro-composites.
Ali Mazahery *et al.* (2012) [65]	Al- alloy with Zircon sand	Powder metallurgy	Hardness, Density, Wear behavior	• The wear resistance of the composite was found to be considerably higher than that of the unreinforced alloy and increased with increasing particle content. • After the critical load there is a transition from smooth linear increase wear rate to sudden increase in wear rate. • The friction coefficient of the composite specimen is seen to be lower than that of the unreinforced alloy.
S. A Alidokht *et al.* (2012) [66]	A356 aluminum alloy,	Friction stir processes	Microstructure, Hardness, Wear behavior	• Friction stir processes (FSP) results in a significant breakup of acicular Si particles and Al dendrites, and subsequently creates a uniform distribution of small and near spherical Si particles throughout the A356 matrix with fine and recrystallized grains. • An increase in tool rotation rate causes a more refined microstructure, due to the more intense stirring effect. • The FS-Processed A356 displays higher hardness compared with the as-cast material. • Wear resistance of the FS-Processed samples was found to be superior to that of the as-cast A356. This is attributed to increased hardness value and a uniform distribution of fine and near spherical Si particles. • The magnitude of improvement in wear resistance of the FS processed samples over the as-cast A356 increases with increasing the rotation rates. In other words, the difference in wear rate is more pronounced at higher tool rotation rates.
Y. Mazaheri *et al.* (2013) [67]	Al, TiC, B_4C	Casting Techniques	Microstructure, Hardness, Tensile, Wear and Friction behavior	• Heat treatment of B_4C particles and addition of TiC particles with the flux can improve the wettability and incorporation of reinforcement particles in to melt.

				• Maximum hardness had belonged to Al–5%TiC–5%B_4C composite, maximum yield and tensile strength had belonged to Al–10%B_4C composite and maximum elongation had belonged to Al–10%TiC composite. • The fracture surfaces of composites revealed the mixture of ductile and brittle types of fracture. • Surface of composite Al–10%B_4C revealed low friction coefficients and wear rates, which were lower than those obtained for Al–5%TiC–5%B_4C andAl–10%TiC composites.
R. Yamanoglu *et al.* (2013) [68]	Al–Cu–Mg alloy, SiC	Casting Techniques	Heat treatment, Tribological properties	• For ageing temperatures of 200 and 225°C, an over ageing effect is reported and maximum hardness was obtained at 6 h. For 175°C, no over ageing is reported because of the lower ageing temperature. The hardness of the as-cast sample increased from 110 HV to 147.2 HV with heat treatment. • Addition of SiC to the alloy increases the hardness of the material but does not change the wear mechanism. • An increase in the hardness causes a decrease in the wear rate. • The specimen aged for 6 h at 225°C has the lowest wear rate for both counterfaces.
F. Grun *et al. (*2013) [69]	Al-Si alloy, Si, Cu	As cast	Tribological properties	• For the pure Al-matrix material high wear was detected and no gravimetric wear was measured for the hypereutectic AlSi material. Thereby, the wear resistance and also the load bearing capability of Al can be improved significantly by adding Si and Al_2Cu hardphases. • The tribological behavior of this hypereutectic Al-Si material is by formation of a load bearing particle structured surface. The initially coarser structure transforms itself into a finer morphology through the course of the test. • The loadability of tested AlSi system is predominantly limited • by the temperature stability of the Al-matrix.
M. Uthayakumar *et al.* (2013) [70]	Al, SiC, B_4C	Stir Casting route	Wear behavior	• The experimental results show that the hybrid composites retain the wear resistance properties up to 60 N and sliding speed ranges 1– 4 m/s. • The enhancement of wear resistance with small amount of SiC and B_4C is achieved by the cooperating effect of reinforcement particles. B_4C particles possibly produce boron oxide rich tribo layer which has reduced the progress of wear and coefficient of friction.

				• The operating wear mechanisms are plastic deformation driven by mild abrasion and severe abrasion at normal load ranges 20– 60 N and 80–100 N and sliding velocity ranges 1–4 m/s respectively. • The melt wear is also observed at higher load and high sliding speed due to high order of local stress prevailing at the condition.
A. Devaraju *et al.* (2013) [71]	Aluminum alloy 6061-T6, SiC, Al_2O_3	Casting process	Microstructure, Microhardness, Wear behavior, Tensile strength	• Microhardness at optimum condition increases due to presence and pining effect of hard SiC and Al_2O_3 particles. • Wear rate at optimum condition is decreased due to mechanically mixed layer generated between the composite pin and steel disk surfaces which contained fractured SiC and Al_2O_3 in which the presence of SiC particles serves as load bearing elements and Al_2O_3 particles acted as solid lubricant and also load bearing elements. • Tensile properties at optimum condition are less as compared to the base material due to presence of reinforcement particles which make the matrix brittle.

As discussed above many researchers have studied the wear behavior of particle reinforced Al-MMCs. However, some gaps in the study are also there which are as follows:

- Limited work is done with zircon sand particle as reinforcement in Al matrix.
- No data is available about the effect of size and amount of reinforcement in Al matrix to study the wear behavior of Al/$ZrSiO_4$ composite.
- Till date no work is available to find the effect of temperature on the wear behavior of Al/$ZrSiO_4$ composite

Plan of work:

Study of literature on the discontinuous reinforced aluminum matrix composites (DRAMCs) reveals that many researchers have worked in this area by using different reinforcement (e.g. SiC, Al_2O_3, Gr, TiO_2, $ZrSiO_4$, TiB_2 etc.) in Al alloy matrix. They studied the effect of amount, shape and size of reinforcements in the matrix on the microstructural and mechanical properties. Also, wear behavior of the DRAMCs has been studied at different conditions such as varying applied loads, sliding distances, sliding velocities etc. Moreover, the effect of ambient temperature on the wear behavior of the DRAMCs has not been studied in detail, which is a key factor for the wear mechanism of the materials.

Literature review brings out that zircon sand ($ZrSiO_4$) is a reliable reinforcement to develop the DRAMCs. However, a detailed study of the zircon sand reinforcement in the aluminum alloy matrix is not available. Moreover, high temperature wear behavior of zircon sand reinforced DRAMCs has not been studied so far.

Considering these facts, in the present work, we have planned to develop Al-Si/Zircon composites with following objectives:

a. To develop the cost effective zircon sand aluminum matrix composites by using stir casting technique.
b. To investigate the effect of particle size and compositions on microstructural and wear behavior of the composites.
c. To study the effect of ambient temperature on the wear behavior of the developed zircon sand reinforced aluminum matrix composites.

REFERENCES:

[1] FA Badia and PK Rohatgi; Dispersion of graphite particles in aluminium castings through injection of the melt. Trans. AFS, 79 (1969) 346.

[2] S Ray; M.Tech. Dissertation, Indian Institute of Technology, Kanpur (1969).

[3] C Subramanian; Some considerations towards the design of a wear resistant aluminium alloy. Wear, 155 (1992) 193-205.

[4] JR Davies; Editor. Aluminum and aluminium alloys. OH: ASM International; 1993.

[5] HR Kotadia, N Hari Babu, H Zhang and Z Fan; Microstructural refinement of Al- 10.2%Si alloy by intensitve shearing. Materials Letters, 64(6) (2010) 671-673.

[6] JL Murray and AJ McAlister; ASM Handbook Volume 3: Alloy Phase Diagrams, pp.312.

[7] Y Haizhi, An overview of the development of Al-Si-alloy based material for engine applications. Journal of Materials Engineering and Performance, 12 (2003) 288-297.

[8] JR Davis; Corrosion of Aluminum and Aluminum alloys. ASM International, 1999, Ohio.

[9] F Hernández-Méndez, A Altamirano-Torres, JG Miranda-Hernández, E Térres-Rojas and E Rocha-Rangel; Effect of Nickel Addition on Microstructure and Mechanical Properties of Aluminum-Based Alloys. Materials Science Forum, 691 (2011) 10-14.

[10] RS Rana, R Purohit and S Das; Reviews on the influences of alloying elements on the mircostructure and mechanical properties of Al alloys and aluminum alloy composites. International Journal of Scientific and Research Publications, 2(6) (2012), 1-7.

[11] SW Nam and DH Lee; The effect of Mn on the mechanical behavior of Al alloys. Metals and Materials, 6(1) (2000) 13-16.

[12] MA Tahaa; Industrialization of cast aluminum matrix composites (AMCCs). Materials and Manufacturing Processes, 16(5) (2001) 619- 641.

[13] C Milliere and M Suery; Fabrication and properties of metal matrix composites based on SiC fibre reinforced aluminium alloys. Material Science and Technology 4 (1988) 41- 51.

[14] FM Hosking, FF Portillo, R Wunderlin and R Mehrabian; Composites of aluminum alloys: fabrication and wear behavior. Journal of Materials Science, 17 (1982) 477- 498.

[15] RL Deuis, C Subramanian and JM Yellup; Abrasive wear of aluminium composites- a review; Wear, 201 (1996) 132-144.

[16] K Anand and Kishore; On the wear of aluminum-corundum composites. Wear, 85 (1983) 163-169.

[17] AT Alpas and J Zhang, Effect of microstructure (particulate size and volume fraction) and counterface material on the sliding wear resistance of particulate-reinforced aluminum matrix composites. Metallurgical and Materials Transactions, 25A (1994) 969- 983.

[18] A Jokinen and P. Anderson; Tribological properties of PM aluminum alloy matrix composites. Annual Powder Metallurgy Conf Proc., Metal Powder Industries Federation, American Powder Metallurgy Institute, Princeton, NJ (1990) 517–530.

[19] M Roy, B Venkataraman, VV Bhanuprasad, YR Mahajan and G Sundararajan; The effect of particulate reinforcement on the sliding wear behavior of aluminum matrix composites. Metallurgical and Materials Transactions A, 23A (1992) 2833-2847.

[20] J Zhang and AT Alpas; Transition between mild and severe wear in aluminum alloys. Acta Materialia, 45 (1997) 513- 28.

[21] A Martin, MA Martinez and J LLorca; Wear of Sic-reinforced Al-matrix composites in the temperature range 20-200 ºC. Wear, 193 (1996) 169-179.

[22] J Hashim, L Looney and MSJ Hashmi; Metal matrix composites: production by the stir casting method. Journal of Materials Processing Technology, 92-93 (1999) 1-7.

[23] J Hashmi; The production of cast metal matrix composite by a modified stir casting method. Jurnal Teknologi, 35(A) (2001) 9- 20.

[24] SB Prabu, L Karunamoorthy, S Kathiresan and B Mohan; Influence of stirring speed and stirring time on distribution of particles in cast metal matrix composite; Journal of Materials Processing Technology, 171 (2006) 268- 273.

[25] SN Aqida, MI Ghazali and J Hashim; Effects of porosity on mechanical properties of metal matrix composite: an overview. Jurnal Teknologi, 40(A) (2004) 17- 32.

[26] SK Chaudhury, AK Singh, CS Sivaramakrishnan and SC Panigrahi; Wear and friction behavior of spray formed and stir cast Al-2Mg-11TiO_2 composites. Wear, 258 (2005) 759-767.

[27] S Basavarajappa, G Chandramohan, A Mahadevan, M Thangavelu, R Subramanian and P Gopalakrishnan; Influence of sliding speed on the dry sliding wear behaviour and the subsurface deformation on hybrid metal matrix composite. Wear, 262 (2007) 1007-1012.

[28] H Abdizadeh, HR Baharvandi and KS Moghaddam; Comparing the effect of processing temperature on microstructure and mechanical behavior of ($ZrSiO_4$ or TiB_2)/aluminum composites. Materials Science and Engineering A, 498 (2008) 53-58.

[29] SO Yılmaz and S Buytoz; Relationship between thermal and sliding wear behavior of Al6061/Al_2O_3metal matrix composites; Journal of Materials Science, 42 (2007) 4485-4493.

[30] AK Jha and K Sreekumar; Effect of pores and acicular eutectic silicon particles on the performance of Al-Si-Mg (AS7G03) casting. Engineering Failure Analysis, 16 (2009) 2433-2439.

[31] K Abedi and M Emamy; The effect of Fe, Mn and Sr on the microstructure and tensile properties of A356–10% SiC composite. Materials Science and Engineering A, 527 (2010) 3733- 3740.

[32] K Akio, O Atsushi, K Toshiro and T Hiroyuki; Fabrication process of metal matrix composite with nano-size SiC particle produced by vortex method. Journal of Japan Institute of Light Metals, 49 (1999) 149-154.

[33] KM Mussert,WP Vellinga, A Bakker and S Van Der Zwaag; A nano-indentation study on the mechanical behaviour of the matrix material in an AA6061- Al_2O_3 MMC. Journal of Materials Science, 37 (2002) 789-794.

[34] A Mazahery, H Abdizadeh and HR Baharvandi; Development of high-performance A356/nano-Al_2O_3 composites. Materials Science and Engineering A, 518 (2009) 61-64.

[35] SA Sajjadi, HR Ezatpour and H Beygi; Microstructure and mechanical properties of Al-Al_2O_3 micro and nano composites fabricated by stir casting. Materials Science and Engineering A, 528 (2011) 8765- 8771.

[36] J Hashim, L Looney and MSJ Hashmi; Metal matrix composites: production by the stir casting method. Journal of Materials Processing Technology, 92-93 (1999) 1-7.

[37] BK Prasad; Effect of microstructure on the sliding wear performance of a Zn-Al-Ni alloy. Wear, 240 (2000) 100- 112.

[38] H Jang and SJ Kim; The effects of antimony tri-sulfide Sb_2S_3 / and zirconium silicate ($ZrSiO_4$) in the automotive brake friction material on friction characteristics. Wear, 239 (2000) 229- 236.

[39] LN Satapathy; A study on the mechanical, abrasion and microstructural properties of zirconia-flyash material; Ceramics International 26 (2000) 39- 45.

[40] M Singh, DP Mondal, AK Jha and AH Yegneswaran; High stress abrasive wear behavior of sillimanite-reinforced al-alloy matrix composite: a factorial design approach. Journal of Materials Engineering and Performance, 12 (2003) 331- 338.

[41] OP Modi, RP Yadav, DP Mondal, R Dasgupta, S Das and AH Yegneswaran; Abrasive wear behaviour of zinc- aluminium alloy - 10% Al_2O_3 composite through factorial design of experiment. Journal of Materials Science, 36 (2001) 1601- 1607.

[42] O Yilmaz and S Buytoz; Abrasive wear of Al_2O_3-reinforced aluminium- based MMCs. Composites Science and Technology, 61 (2001) 2381- 2392.

[43] PN Bindumadhavan, HK Wah and O Prabhakar; Dual particle size (DPS) composites: effect on wear and mechanical properties of particulate metal matrix composites. Wear, 248 (2001) 112-120.

[44] J Hashim; The Production of cast metal matrix composite by a modified stir casting method. Jurnal Teknologi, 35(A) (2001) 9- 20.

[45] M Gui, J Han and P Li; Fabrication and characterization of cast magnesium matrix composites by vacuum stir casting process. Journal of Materials Engineering and Performance, 12 (2003) 128-134.

[46] Y Sahina and M Acilar; Production and properties of SiCp- reinforced aluminium alloy composites. Composites: Part A, 34 (2003) 709- 718.

[47] S Naher, D Brabazon and L Looney; Simulation of the stir casting process. Journal of Materials Processing Technology, 143-144 (2003) 567- 571.

[48] DK Dwivedi, TS Arjun, P Thakur, H Vaidya and K Singh; Sliding wear and friction behaviour of Al–18% Si–0.5% Mg alloy. Journal of Materials Processing Technology, 152 (2004) 323- 328.

[49] K Das and TK Bandyopadhyay; Synthesis and characterization of zirconium carbide-reinforced iron-based composite. Materials Science and Engineering A, 379 (2004) 83- 91.

[50] SK Chaudhury, AK Singh, CS Sivaramakrishnan and SC Panigrahi; Wear and friction behavior of spray formed and stir cast Al-2Mg-11TiO_2 composites. Wear, 258 (2005) 759-767.

[51] DP Mondal and S Das; High stress abrasive wear behaviour of aluminium hard particle composites: Effect of experimental parameters, particle size and volume fraction. Tribology International, 39 (2006) 470- 478.

[52] H Jian-min, W Zhao-ling, C Shi-hai, L Wei-Jing and D Yong-ping; Investigation of defects in SiCp/A356 composites made by a stir casting method. Journal of Ceramic Processing Research, 8 (1) (2006) 74-77.

[53] A Vencl, A Rac, I Bobić and Z Mišković; Tribological properties of Al- Si alloy A356 reinforced with Al_2O_3 particles. Tribology in Industry, 28(1 & 2) (2006) 27- 31.

[54] VS Aigbodiona and SB Hassan; Effects of silicon carbide reinforcement on microstructure and properties of cast Al–Si–Fe/SiC particulate composites. Materials Science and Engineering A, 447 (2007) 355–360.

[55] H Abdizadeha, HR Baharvandib and KS Moghaddam; Comparing the effect of processing temperature on microstructure and mechanical behavior of ($ZrSiO_4$ or TiB_2)/aluminum composites; Materials Science and Engineering A, 498 (2008) 53- 58.

[56] TVS Reddy, DK Dwivedi and NK Jain; Adhesive wear of stir cast hypereutectic Al-Si-Mg alloy under reciprocating sliding conditions. Wear, 266 (2009) 1-5.

[57] AA Yar, M Montazerian, H Abdizadeh and HR Baharvandic; Microstructure and mechanical properties of aluminum alloy matrix composite reinforced with nano- particle MgO. Journal of Alloys and Compounds, 484 (2009) 400-404.

[58] A Sharma and S Das; Study of age hardening behavior of Al- 4.5 wt% Cu/zircon sand composite in different quenching media- A comparative study. Materials and Design, 30 (2009) 3900-3903.

[59] S Ilo, C Just, E Badisch, J Wosik and H Danninger; Effects of interface formation kinetics on the microstructural properties of wear-resistant metal-matrix composites. Materials Science and Engineering A, 527 (2010) 6378-6385.

[60] G Rajaram, S Kumaran and TS Rao; High temperature tensile and wear behaviour of aluminum silicon alloy. Materials Science and Engineering A, 528 (2010) 247- 253.

[61] A Onat; Mechanical and dry sliding wear properties of silicon carbide particulate reinforced aluminium- copper alloy matrix composites produced by direct squeeze casting method. Journal of Alloys and Compounds, 489 (2010) 119- 124.

[62] S Suresha and BK Sridhara; Wear characteristics of hybrid aluminium matrix composites reinforced with graphite and silicon carbide particulates. Composites Science and Technology, 70 (2010) 1652- 1659.

[63] RN Rao and S Das; Effect of SiC content and sliding speed on the wear behaviour of aluminium matrix composites. Materials and Design, 32 (2011) 1066- 1071.

[64] SA Sajjadi, HR Ezatpour and H Beygi; Microstructure and mechanical properties of Al-Al_2O_3 micro and nano composites fabricated by stir casting. Materials Science and Engineering A, 528 (2011) 8765- 8771.

[65] A Mazahery and MO Shabani; study on microstructure and abrasive wear behavior of sintered Al matrix composites. Ceramics International, 38 (2012) 4263- 4269.

[66] SA Alidokht, A Abdollah-zadeha, S Soleymani, T Saeid and H Assadi; Evaluation of microstructure and wear behavior of friction stir processed cast aluminum alloy. Materials Characterization, 63 (2012) 90- 97.

[67] Y Mazaheri, M Meratian, R Emadi and AR Najarian; Comparison of microstructural and mechanical properties of Al-TiC, Al-B_4C and Al-TiC-B_4C composites prepared by casting techniques. Materials Science & Engineering A, 560 (2013) 278- 287.

[68] R Yamanoglu, E Karakulak, A Zeren and M Zeren; Effect of heat treatment on the tribological properties of Al-Cu-Mg/nano SiC composites. Materials and Design, 49 (2013) 820- 825.

[69] F Grun, F Summer, KS Pondicherry, I Godor, M Offenbecher and E Lained; Tribological functionality of aluminium sliding materials with hard phases under lubricated conditions. Wear, 298-299(2013)127-134.

[70] M Uthayakumar, S Aravindan and K Rajkumar; Wear performance of Al-SiC-B_4C hybrid composites under dry sliding conditions. Materials and Design, 47 (2013) 456-464.

[71] A Devaraju, A Kumar, A Kumaraswamy and B Kotiveerachari; Influence of reinforcements (SiC and Al_2O_3) and rotational speed on wear and mechanical properties of aluminum alloy 6061-T6 based surface hybrid composites produced via friction stir processing. Materials and Design, 51 (2013) 331-341.

CHAPTER 3

EXPERIMENTAL DETAILS

Overview:

This chapter includes the details of the raw materials used for the development of the discontinuous reinforced aluminum matrix composite (DRAMCs). Detailed procedure of development of the DRAMCs and their characterizations is given in this chapter. Different characterization techniques such as X- ray diffraction (XRD), Optical microscopy, Scanning electron microscopy (SEM), Energy dispersive spectroscopy (EDS), Rockwell hardness testing, Vickers hardness testing and wear testing with pin-on-disc machine along with their operating parameters are also discussed. A flow chart of the methodology used is also given in this chapter.

3.1 Raw materials:

In the present work, for the fabrication of discontinuous reinforced aluminum matrix composites (DRAMCs), we choose LM13 alloy (an alloy of aluminum) as a matrix and zircon sand ($ZrSiO_4$) particles as reinforcement. LM13 alloy is selected due to light weight with good corrosion and wear resistance as well as good machinability. Apart from this the high hardness, high modulus of elasticity with good thermal stability are the reasons for the selection of zircon sand as reinforcement. Commercial grade LM13 alloy was purchased from Emmes Metals Private Limited, Mumbai (India) and zircon sand was supplied by Indian Rare Earths Limited, Orissa, India. The detailed chemical composition of the LM13 alloy and zircon sand is given in table 3.1 and 3.2 respectively.

Table 3.1: Chemical composition of the LM13 alloy

Elements	**Si**	**Fe**	**Cu**	**Mn**	**Mg**	**Zn**	**Ni**	**Al**
Chemical Analysis (Wt %)	12.0	0.4	1.2	0.4	1.00	0.2	1.0	Bal.

Table 3.2: Chemical composition of zircon sand ($ZrSiO_4$)

Elements	**ZrO_2 (+ HfO_2)**	**SiO_2**	**TiO_2**	**Fe_2O_3**
Wt% in Bulk	65.30	32.80	0.27	0.12

Effect of particle size of the reinforced zircon sand on the wear behavior of DRAMCs is monitored in the present work. For this purpose zircon sand was sieved in a range between 05-125 µm by using sieving machine AS-200 supplied by Retsch, Germany. Three ranges of size of the sieved particles were selected for the reinforcement: coarse size (106- 125 µm), medium size (50-75 µm) and fine size (20- 32 µm). However, to study the better effect of particle size we also developed composites with dual size particles (combination of fine and coarse size particles) as reinforcement.

3.2 Development of discontinuous reinforced aluminum matrix composite (DRAMCs):

In this work, we developed DRAMCs by stir casting process. For melting, a resistance furnace was used. The stirrer was attached at the top of the furnace. About 1500 gm of aluminum alloy (LM13) was melted at 800 °C in a graphite crucible of 2 kg capacity and held at 750 °C. The molten metal was stirred with graphite stirrer at 630 rpm to create the vortex in the melt. Before charging, zircon sand particles were heated at 400 ºC to remove the moisture and other volatile elements. These preheated zircon sand particles were added inside the vortex with the help of funnel kept on top of vortex during the stirring of the molten metal. After the incorporation of the reinforcement in the matrix, molten mass was further stirred for 5 minutes to get the uniform distribution of zircon sand particles. Then, the molten mass was poured into cast iron mold of dimension: 12×12×4 cm^3 and allowed to cool in air. Composites containing different amount and size of zircon sand particles were prepared by this procedure. From these stir cast composite materials, specimens were prepared for the characterization and testing. Figure 3.1 shows the flow chart of the methodology used for the development of the zircon sand reinforced aluminum matrix composite and their characterizations.

Table 3.3 and 3.4 shows the summary of developed composites with varying amount and size of zircon sand particles in aluminum alloy matrix.

Table 3.3: Composites on basis of reinforcement of different amount and size of particles.

Particle size (µm)	Amount of zircon sand particles (wt.%)			
	5%	10%	15%	20%
Coarse (106-125 µm)	✓	✓	✓	✓
Medium (50-75 µm)	✓	✓	✓	✓
Fine (20-32 µm)	✓	✓	✓	✓

Table 3.4: Composites on the basis reinforcement of dual size particles with different amount

Composite	Amount of reinforcement (wt.%)							
	5%		10%		15%		20%	
Ratio of (Fine + Coarse) particles in the matrix	1:4	2:3	1:4	2:3	1:4	2:3	1:4	2:3
	3:2	4:1	3:2	4:1	3:2	4:1	3:2	4:1

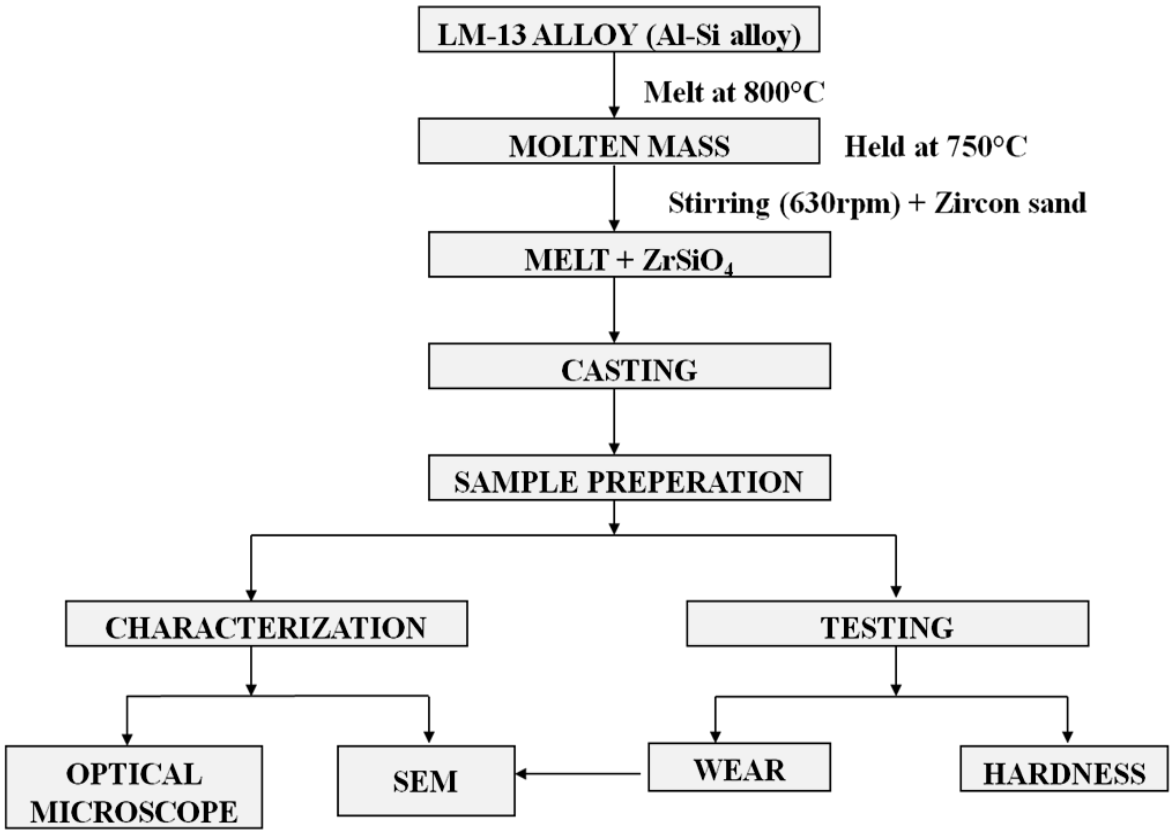

Figure 3.1: Flow chart of the methodology to develop the zircon sand reinforced aluminum matrix composite.

3.3 Materials characterization:

Composite samples along with the base LM13 alloy samples were characterized using different techniques. Morphological, mechanical and wear properties of the samples were observed by

using optical microscope, scanning electron microscope, Rockwell hardness, Vickers hardness and dry sliding wear test using pin-on-disc method.

3.3.1. X-ray analysis:

X-ray diffraction patterns of base alloy (LM13) and composites (LM13/Zr) were recorded by means of Panalytical X'pert PRO MPD, Netherland using Cu-Kα radiation (λ = 1.54 A˚) with scanning rate of 3° per minute. The collected data was matched with reference data for identification of different phases present in the base alloy and composites.

3.3.2. Morphological analysis:

For the morphological analysis of base alloy and composites, samples having dimensions 20mm × 20mm were cut from the different areas of the cast alloy and composites. These samples were mechanically polished and etched with Keller's reagent. The chemical composition of Keller's reagent is given in Table 3.5. The surface morphology of each sample was studied with the help of optical microscope (Eclipse MA-100, Nikon) and scanning electron microscope (JOEL, JSM-6510LV) at different magnifications. Elemental analysis of the composite at different phases was done with SEM-EDS (Oxford INCA).

Table 3.5: Chemical composition of Keller's reagent.

Composition	**Dist. Water**	**HNO_3**	**HCl**	**HF**
Vol.%	95ml	2.5ml	1.5ml	1ml

3.3.3 Hardness

Both the bulk and microhardness of the base alloy and composite samples have been measured by Rockwell and Vickers hardness test method respectively. Bulk hardness of all the samples were measured by digital Rockwell hardness tester (model TRSND, Fine manufacturing Industries, India) with 1/16 inch diameter steel ball indenter at 100 kg load at B scale. Microhardness values at different phases were measured using Vickers microhardness testing machine (model: MVK_HO, Mitutoyo, Japan). Each value of hardness is an average of the ten separate values taken from the different places of the samples at 100 gf load.

3.3.4 Wear testing

Dry sliding wear test using pin-on-disc method was done for the study of wear behavior of the materials. For wear tests a cylindrical pin of 8 mm in diameter was prepared from cast

composite. Wear testing was performed on wear testing machine (wear and friction monitor, TR-20 CH-400, Ducom Instruments, Bangalore India) under dry sliding conditions in ambient air at controlled temperature (Fig. 3.2).Wear tests were conducted at different temperatures (50, 100, 150, 200, 250 and 300 °C) and different loads (9.8 N, 19.6 N, 29.4 N, 39.2 N and 49 N). All the samples of base alloy (LM13) and LM13/Zr composites were tested against EN 32 steel disc having 65 HRC hardness. To get an average value of wear rate, each test was run three times. Before each test the track was cleaned with acetone. For each test a new track was used to get similar test conditions. Throughout the experiment a constant sliding velocity of 1.6 m s^{-1} was maintained. Sliding distance covered during the experiment was about 3000 meters. Wear rate was determined by measuring specimen height change using a linear variable displacement transducer (LVDT). In the entire study we have kept the worn out length of pin constant (2 mm) to have relative data. To study the wear behavior, wear rate was calculated by using the formula, [W (mm^3/m) = height change (mm) × pin area (mm^2) / sliding distance (m)]. Cylindrical shaped pins with flat end were used as samples for wear testing. Test pins were ground to a smooth finish on 600 grit SiC paper. The worn surface regions (wear tracks) and collected debris after the dry sliding wear tests were also examined under scanning electron microscope. All the wear tests were conducted at constant temperature. A programmable furnace consisting of three band heaters enclosing the rotating counterface with proper insulation, as shown in Fig. 3.2, was used for this purpose.

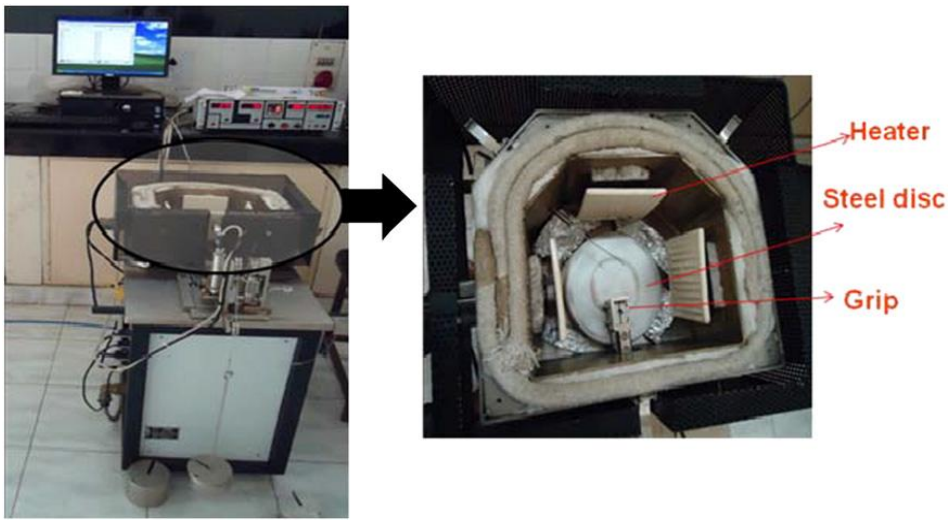

Figure 3.2: Images of pin on disc setup for wear test (Ducom-TR-20CH-400).

CHAPTER 4

RESULTS AND DISCUSSION

(Single size particle reinforced composites)

Overview:

In this present chapter, we have discussed the results obtained from as cast LM13 alloy and composites. It describes the results of single size reinforced particles for the development of composites. The composites so obtained have been tested for their wear behavior. The results show that wear characteristics of the 15wt.% zircon sand reinforced composite is better than other developed composites. The overall results of all the samples have also been discussed at the end of the chapter.

As describe in experimental section, LM13 alloy was used as matrix material for the reinforcement of zircon sand. In this chapter, the systematic study of alloy and composites is presented.

4.1 X-Ray diffraction analysis:

The X-ray diffraction (XRD) patterns of base alloy (LM13) and composite (LM13/15wt.%Zr) are shown in Fig. 4.1(a & b), respectively. Figure 4.1a shows the presence of Al and Si in base alloy. The presence of zircon sand particles ($ZrSiO_4$), along with Al and Si elements is observed in the XRD pattern of composite (Fig. 4.1b). Apart from these phases, Al_2SiO_5 (Sillimanite) was also observed in the composite. It is quite possible that Al_2SiO_5 has formed at the alloy-particle interface because of the reaction of zircon sand and LM13 alloy during casting.

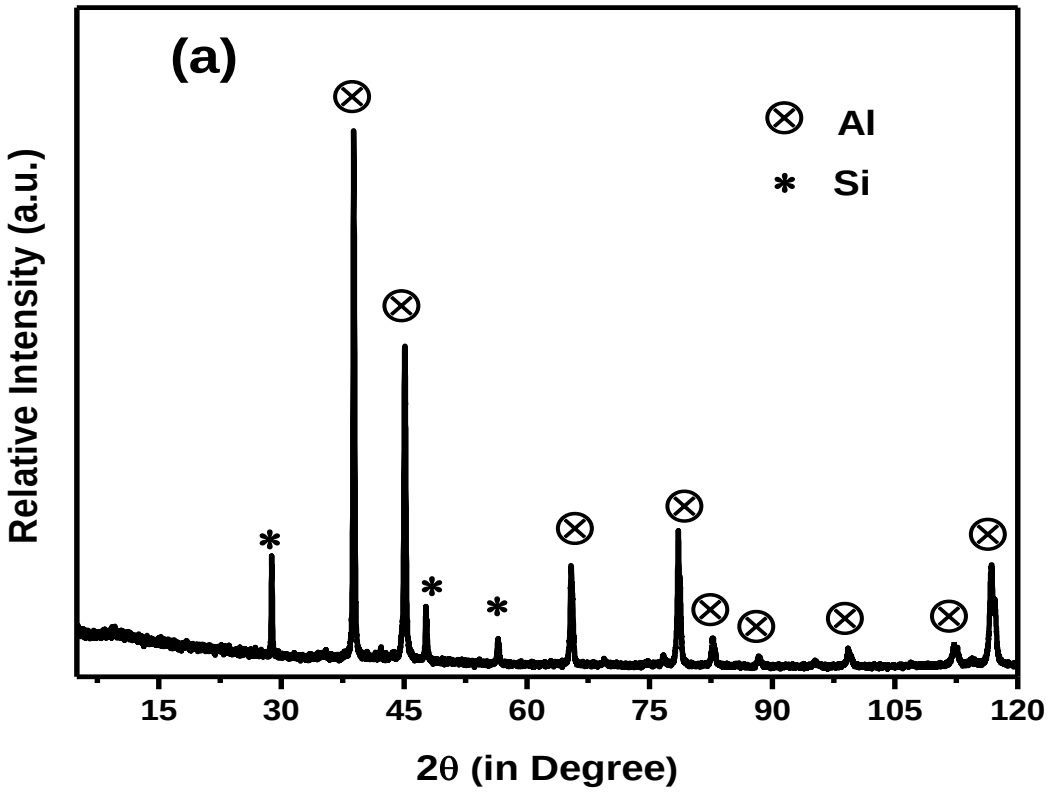

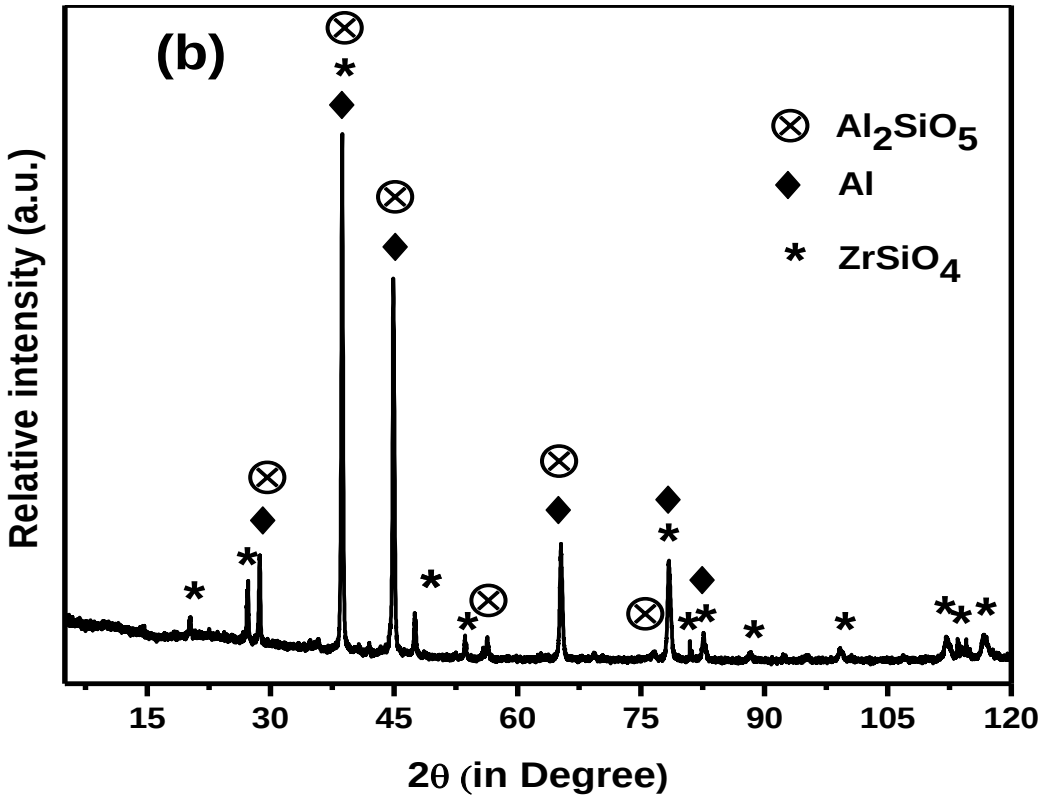

Figure 4.1: XRD patterns of (a) LM13 alloy and (b) LM13/15wt.%Zr composite showing the presence of different phases.

4.2 Morphological study:

Figure 4.2 (a & b) shows the micrographs of the LM13 alloy at low (100X) and high (500X) magnifications respectively. The dendritic growth of primary α-Al and eutectic phase in between the dendritic region (Fig. 4.2a) has been observed in LM13 base alloy which is more clear at higher magnification as shown in Fig. 4.2b. Presence of high silicon content in the LM13 alloy increases the corrosion and wear resistance along with the casting and machining characteristics of the alloy [1]. When Al-Si alloy solidifies, the primary aluminum forms and grows as dendrites, whereas silicon solidifies as needle like structure. The Al-Si alloy usually has some other coexisting elements such as copper, magnesium, manganese, zinc and iron. Alloying elements can also form intermetallic phases during solidification.

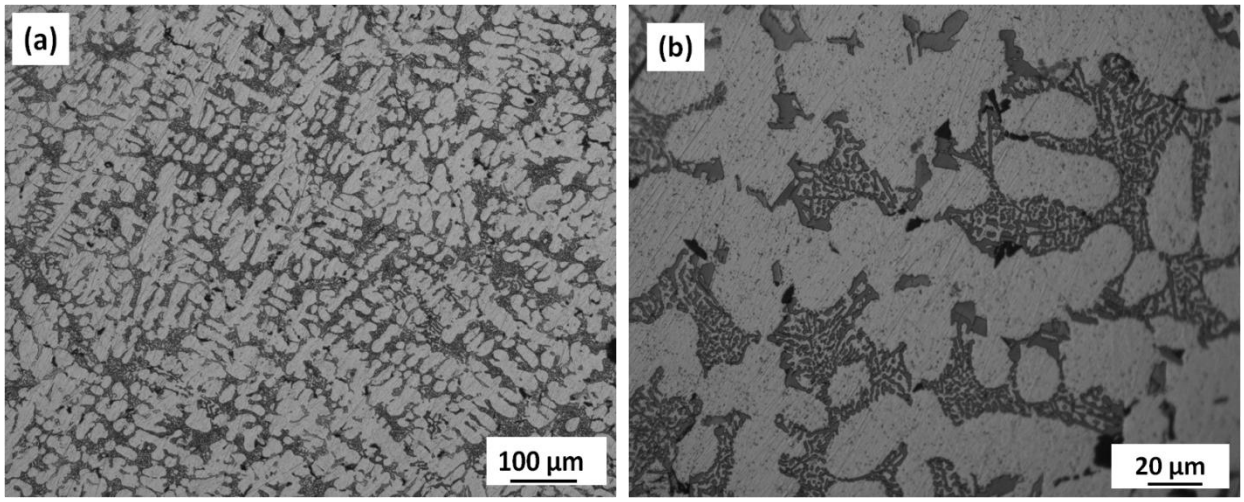

Figure 4.2: Optical micrographs of the LM13 alloy (a) showing dendritic structure and (b) showing inter dendritic region.

Size of the particles and their volume fraction influences the structure of composite to greater extent. Figure 4.3(a-d) shows the microstructure of composite reinforced with zircon sand particulates in the LM13 alloy matrix for 5, 10, 15 and 20 wt.% reinforcement respectively. In the present chapter, the results of composites reinforced with coarse particles (106-125 µm) are presented. It is observed that clustering tendency of reinforced particles increases with increase in reinforcement quantity. As the solid- liquid interface moves during solidification, coarse particles are easily engulfed by the moving interface (Fig. 4.3e). However, in certain areas, particles get segregated leading to clustering (Fig. 4.3 d & f). These segregated particles are loosely bonded with matrix as they overlap on each other at certain places (Fig. 4.3f) and are devoid of matrix area to bond them properly. However, in general the reinforced particles are observed to be randomly distributed in the entire mass. The strengthening zircon sand particles occupy the eutectic zone. They contribute to the restricted growth phenomenon. The presence of ceramic particulates in the melt slow down the velocity of solidification front, causing delay in solidification. As the solidification time increases, more nuclei form leading to grain refinement [2]. Microstructural examination of metal matrix composites reveals an interfacial zone between the metal matrix and the reinforcement material, as can be seen in higher magnification micrograph (Fig. 4.3e). This zone between these two phases is one of the essential part of MMCs.

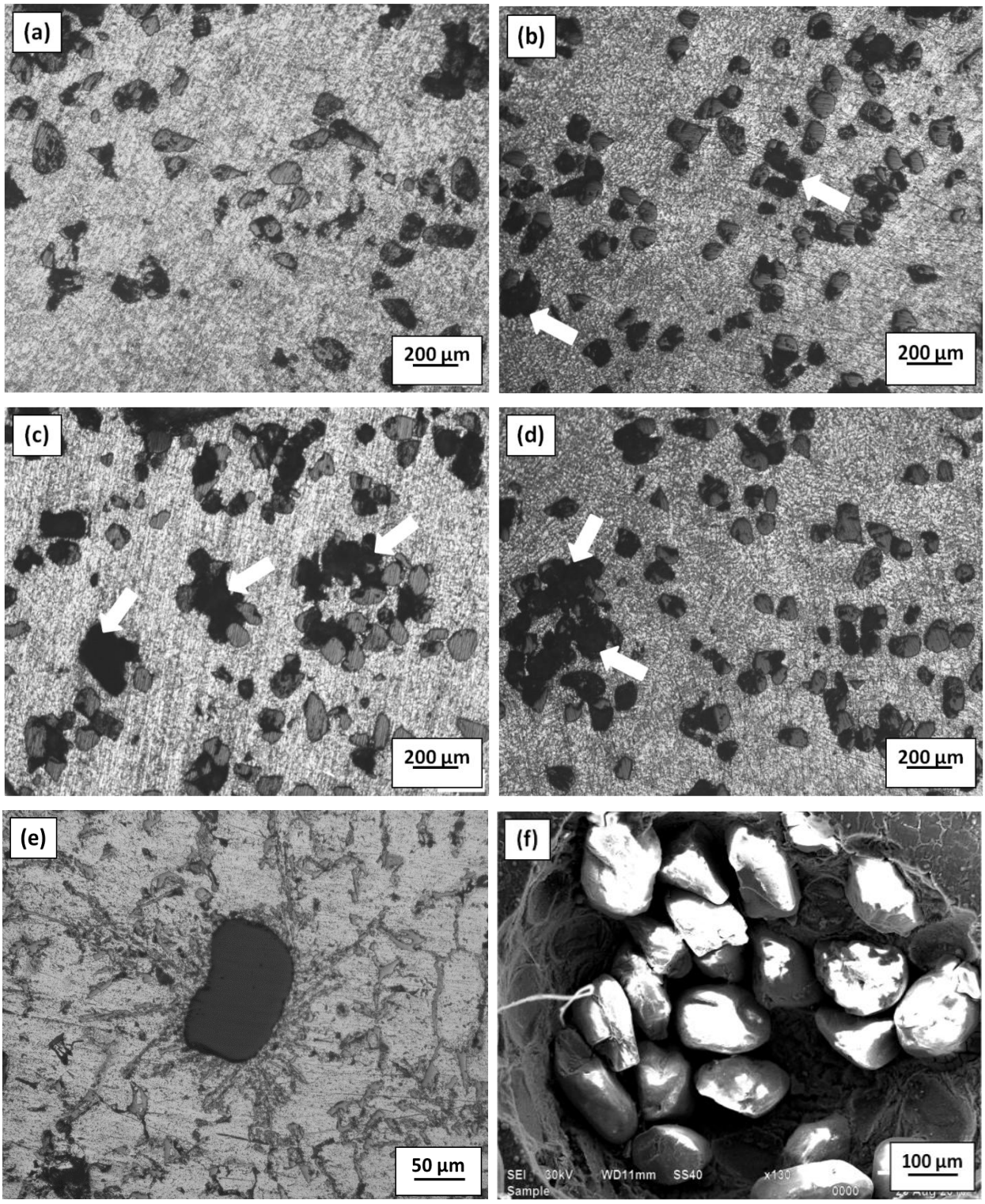

Figure 4.3: Optical micrographs of composites reinforced with coarse size (106-125 µm) zircon sand particles (a) LM13/5%Zr composite, (b) LM13/10%Zr composite, (c) LM13/15%Zr composite, (d) LM13/20%Zr composite, (e) LM13/10%Zr composite at higher magnification showing the interfacial bonding and (f) SEM image taken from black zone in LM13/20%Zr composite at higher magnification showing clustering of particles.

Interfacial bonds in the zone are developed from physical as well as chemical interaction of the particles with matrix. This causes interfacial frictional and thermal stresses due to difference between coefficient of thermal expansion of particulate and matrix [3]. The dendritic morphology changes to cellular one in composite as reinforced particles restrict the solute transport processes by diffusion and flow [4, 5]. However, dendrites are visible in areas away from the reinforced particles which can be seen in Fig. 4.3(a & b). The bigger black spots correspond to the area where clustering of particles has occurred due to relatively fast pushing up phenomenon at the interface (Fig. 4.3f). These particles have chipped out during grinding and polishing as they were loosely bonded as compared to single particle as has been marked by arrow in Fig. 4.3 (b- d). Moreover, the particles are distributed throughout the casting though their volume fraction is observed to vary in the entire casting.

Figure 4.4 shows the optical micrographs of the composites reinforced with medium size (50-75 µm) zircon sand particles in different amounts (5-20 wt.%). Figure 4.4 (a- d) shows the particle distribution in the matrix and Fig. 4.4e depicts the higher magnification micrograph of the LM13/20%Zr composite revealing the good interfacial bonding of particles with matrix. Figure 4.4(a- d) indicates nearly uniform distribution of the particles in the matrix which is essential to achieve better wear and mechanical properties with the composite materials.

Figure 4.4 shows the optical micrographs of the composites reinforced with medium size (50-75 µm) zircon sand particles in different amounts (5-20 wt.%). Figure 4.4 (a- d) shows the particle distribution in the matrix and Fig. 4.4e depicts the higher magnification micrograph of the LM13/20wt.%Zr composite revealing good interfacial bonding of particles with matrix. Figure 4.4(a- d) indicates nearly uniform distribution of the particles in the matrix which is essential to achieve better wear and mechanical properties with the composite materials. Figure 4.4e clearly shows some fractured particles. It is possible that these particles get fractured during preparing (grinding and polishing) the samples for the characterization. Due to the high shear rate during stirring, particles get distributed throughout the melt, which also minimizes the particles settling. During particle addition, local solidification of the melt occurs which is induced by the particles as there is a temperature difference between the particle and the melt. It was also found that the perturbation in the solute field due to the presence of particles can change the dendrite tip radius and the dendrite tip temperature.

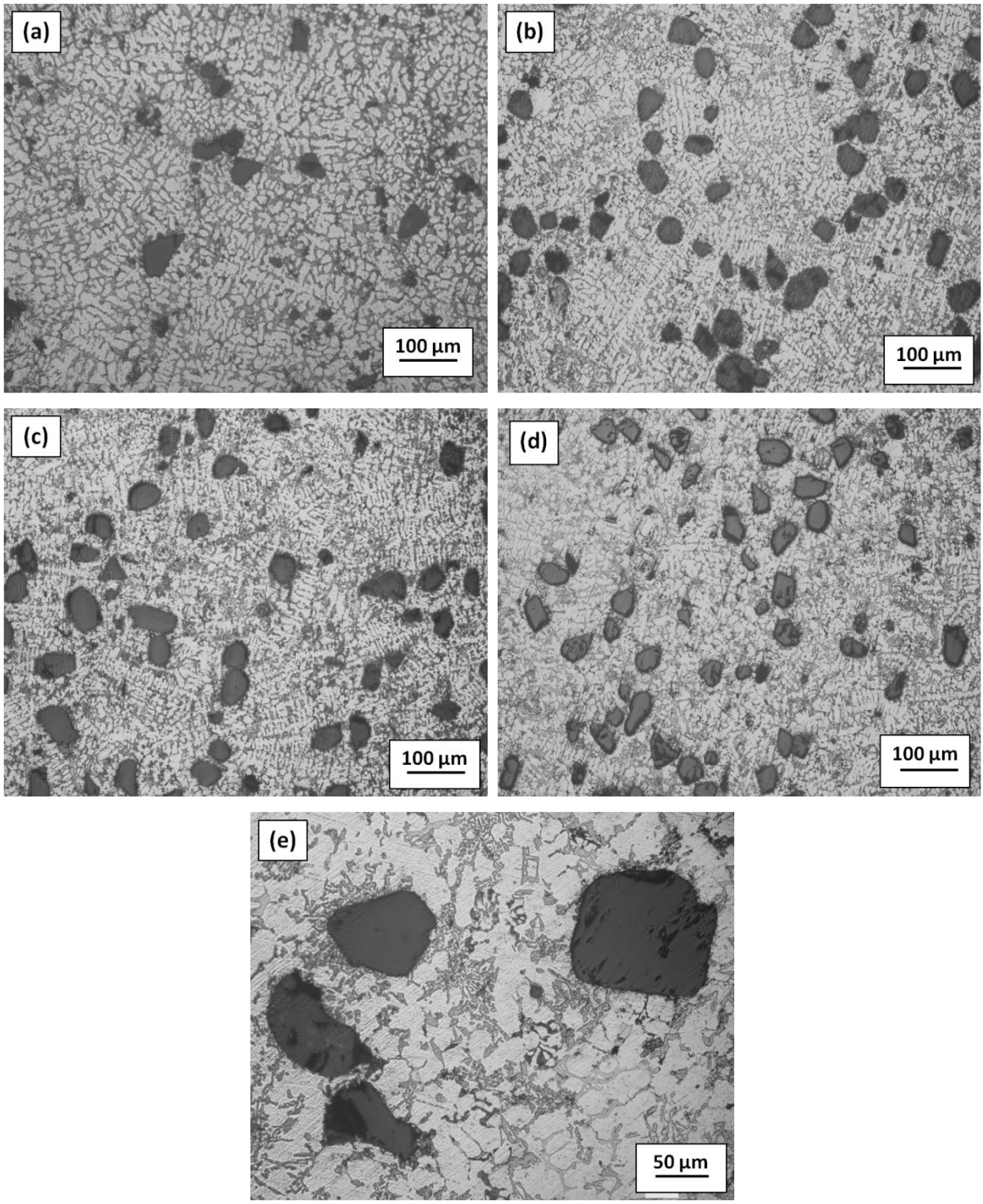

Figure 4.4: Optical micrographs of composites reinforced with medium size (50-75 µm) zircon sand particles (a) LM13/5%Zr composite, (b) LM13/10%Zr composite, (c) LM13/15%Zr composite, (d) LM13/20%Zr composite and (e) LM13/20%Zr composite at higher magnification.

These effects give rise to a dendrite to cell transition with increased density of particles in the melt. Also the length of the dendrite reduces in the presence of the particles [6]. During solidification the dendrite acquires cellular type of features on small under cooling which always exits ahead of solid–liquid interface. Second phase particles present in the melt also provide nucleation center. Since the system is continuously in the agitated state, where second phase particles are fairly distributed throughout the melt, it hinders the growth of long dendrites. Figure 4.4a shows the presence of long dendrite in areas where particle is not present. The second phase hard particle restricts the growth of dendrite and modifies the matrix with more refined structure leading to improvement in strength [7- 9]. It also contributes for refinement of silicon phase.

The silicon possessing acicular morphology in the matrix acquires globular form in vicinity to the particles. Similar modification in silicon morphology was also reported in earlier work by Kaur *et. al.* [10] and attributed this morphological transformation to the localized rapid cooling effect produced by zircon sand particles due to large temperature difference in the melt around its vicinity.

Figure 4.5 (a-d) shows the optical micrographs of the composites containing fine size (20-32 μm) zircon sand particles as reinforcement in the aluminum alloy matrix in different amounts 5, 10, 15 and 20wt% respectively. Figure 4.5e shows the higher magnification micrograph of the LM13/20wt.%Zr composite. It indicates a good interfacial bonding between the particle and matrix along with cellular structure of primary α- aluminum. Lower magnification micrograph of composites (Fig. 4.5 a- d) depicts fairly uniform distribution of reinforced particles in alloy matrix. However, agglomeration of particles is also observed which is visible at certain places in Fig. 4.5 (c & d). Figure 4.5e shows the micrograph of the composite where fragmented dendrites in the alloy matrix can be seen, though limited dendritic growth in the particle depleted region is also visible. This growth has occurred due to clustering of zircon sand. Fine size zircon sand particles are pushed or engulfed by advancing solid- liquid interface creating sufficient space inside the matrix, which leads to growth of dendrite [11]. Dendritic structure get modified during casting, which is influenced by many factors such as dendrite fragmentation, restriction of dendritic growth by the particles, and thermal conductivity mismatch between the particles and melt. Ceramic particle also act as a barrier for dendritic growth and this phenomena is more pronounced when cooling rate is high. Das *et. al.* [11] in their work reported that the particle can be assumed to act as a barrier for the dendritic growth.

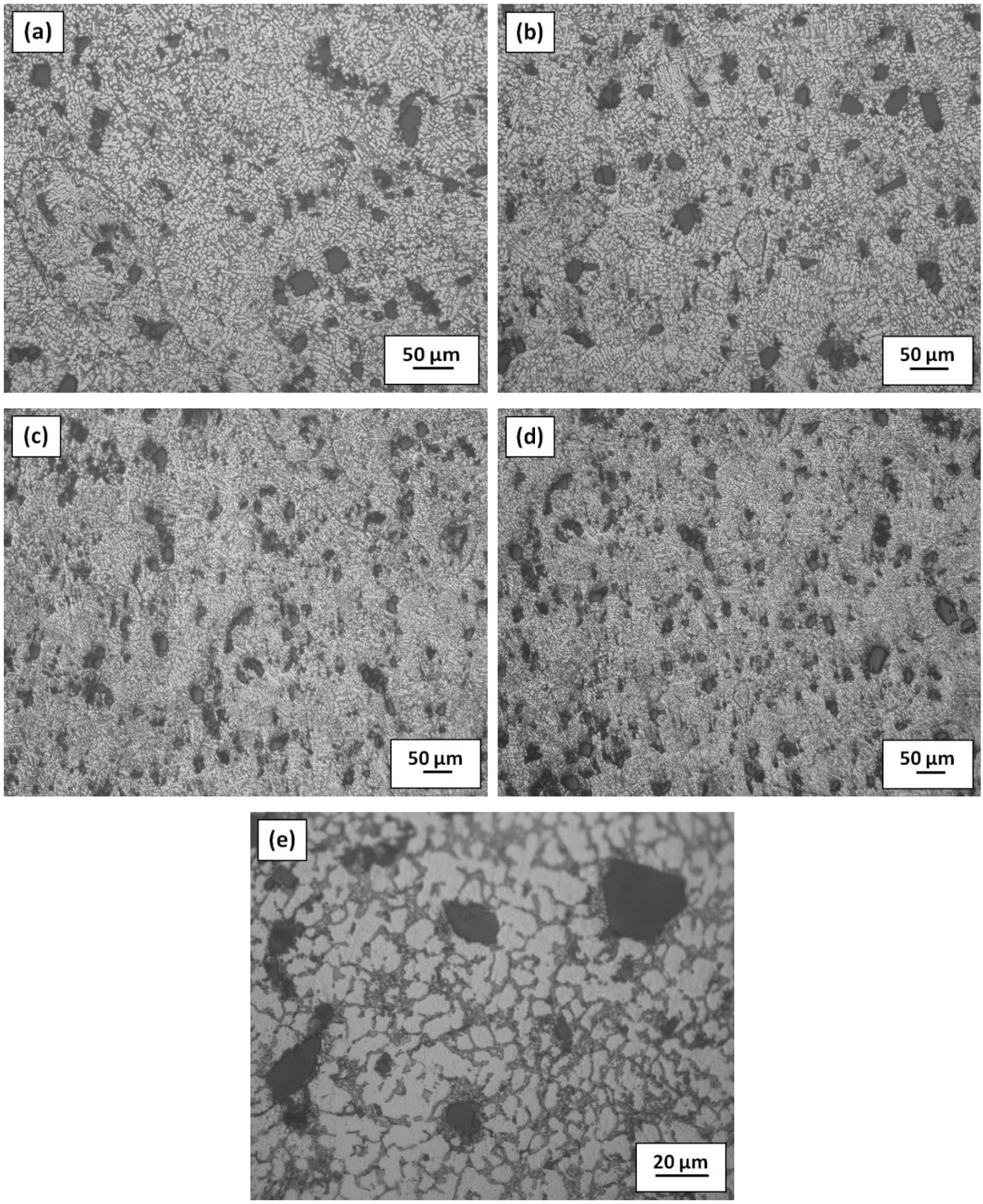

Figure 4.5: Optical micrographs of composites reinforced with fine size (20- 32 µm) zircon sand particles (a) LM13/5%Zr composite, (b) LM13/10%Zr composite, (c) LM13/15%Zr composite, (d) LM13/20%Zr composite and (e) LM13/20%Zr composite at higher magnification.

Clustering of the particles in the matrix is important phenomenon which affects the mechanical properties of the composites. Clustering of the particles increases with the decreasing the particle size, as smaller particles with the same amount of reinforcement in the matrix shows decrement between the particle and particle distances. This leads to improvement in the mechanical properties of the material as larger surface area of the particles in the matrix will affect the mechanical properties of the composite significantly.

Overall analysis of structure indicates that fine particles have tendency of clustering in the composite because these are pushed to a greater extent by solidification front as compared to coarse particles. Most of the fine particles are placed at grain boundaries and very limited particles are engulfed within the grains [12]. Particle pushing and engulfing phenomenon during solidification is also correlated with the mutual wetting behavior among the solid, liquid, and particle phases. If the contact angle at a solid–liquid interface of a particle is > 90°, the particle can be engulfed into the solid, and if the contact angle is <90°, the particle would be pushed ahead [13]. Coarse particles have greater tendency to settle as compared to fine particles. Composite reinforced with coarse particles in majority exhibit clustering due to settling of particles and fine particles form cluster by pushing action of solidification front [12, 13]. Moreover, most of these adverse phenomena are rectified in our prepared composites.

4.3 EDS analysis of the composite at different phases:

Figure 4.6 (a-c) shows the EDS analysis of the composite at different phases (particle, interface, and matrix). Figure 4.6 indicates the presence of Zr, Si, and O at particle and interface. Moreover, the matrix phase is rich in Al. However, Hf in very low quantity is also observed at the interface. The point analysis done on the particle (spectrum 1 in Fig. 4.6a) gives the chemical formula $Zr_{1.04}SiO_{4.47}Al_{0.032}$, which is very close to $ZrSiO_4$. When point analysis was done at the interface (spectrum 2 in Fig. 4.6b), it gives the chemical formula $Zr_{1.03}SiO_{2.93}Al_{0.04}Hf_{0.02}$ which is equivalent to $ZrSiO_3$. From X-ray analysis we could not observe $ZrSiO_3$ phase, so its presence can be ruled out. The interfacial reaction has led to the formation of Al_2SiO_5 phase, which is also present in the XRD pattern (Fig. 4.1b). Moreover, the matrix is rich in Al. As the EDS analysis gives the approximate composition, the above interpretation of data is only based on elemental composition given by EDS.

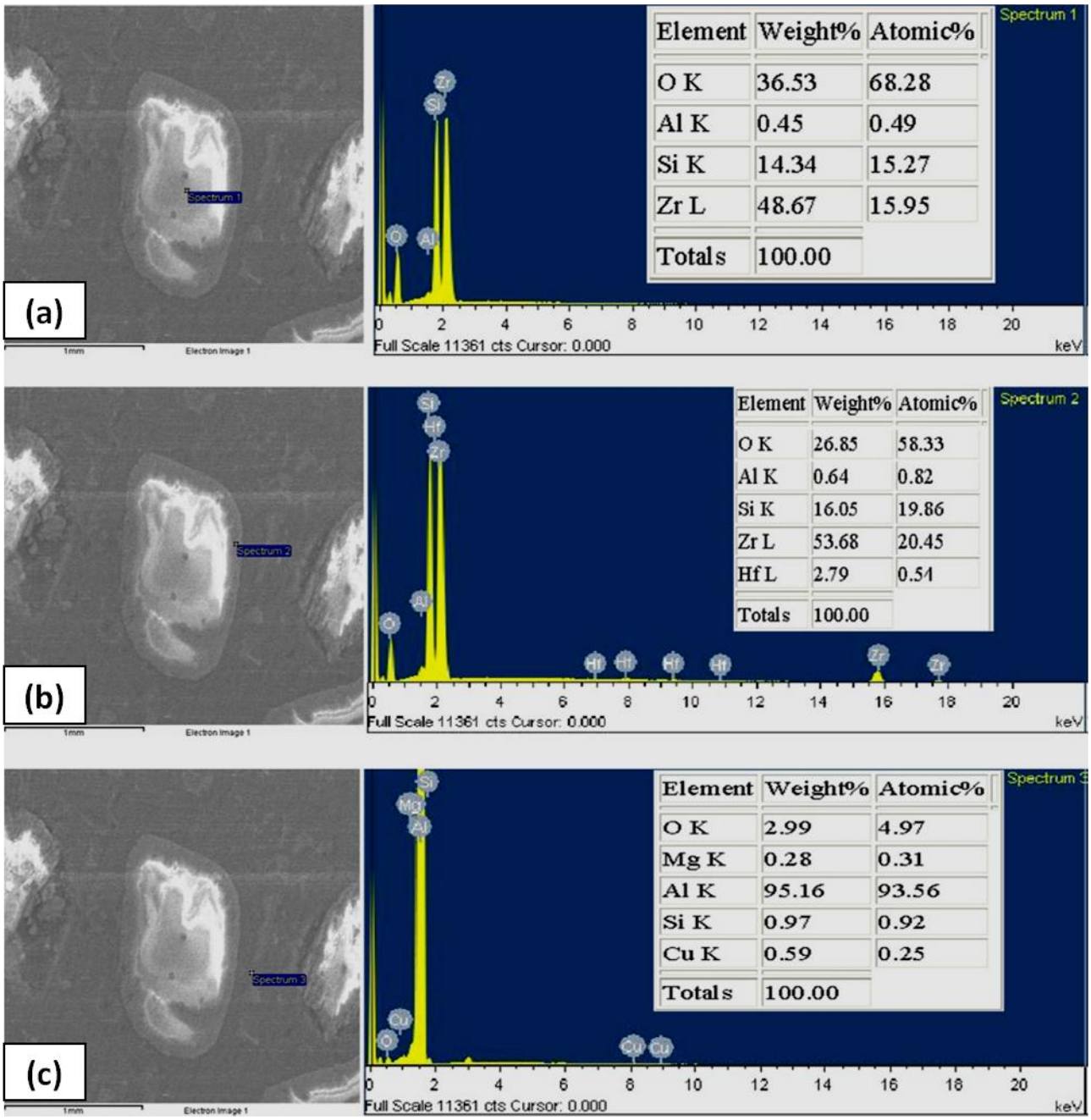

Figure 4.6: EDS analysis of the composite at different phases (a) particle, (b) interface and (c) matrix.

Line profile analysis shown in Fig. 4.7 (a & b) indicates the variation in the distribution of the elements around the particle. The important observation from line analysis is that the amount of Al decreases over an interfacial distance, whereas Zr increases along the interface. The sharp change occurring along the interface also confirms the interfacial reaction and the diffusion of

elements which enables the particle to have proper bonding with matrix. Moreover, it is also visible in the microstructure as variation in contrast at the interface is clearly observed (Fig. 4.7a)

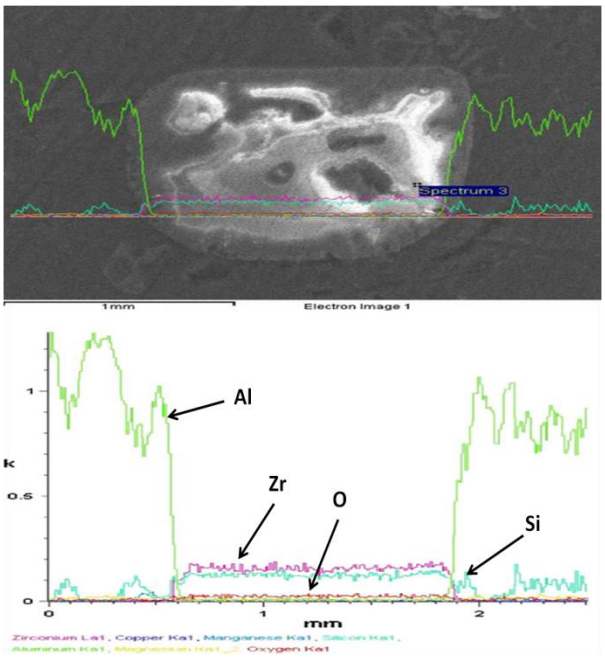

Figure 4.7: Line profile showing elemental distribution around the particle in the composite.

4.4 Hardness:

The microstructure of the LM13/zircon sand composite consists of three different regions: Al matrix, zircon sand particles, and the interface between Al matrix and zircon sand. Figure 4.8 shows the microhardness indentations taken from these regions. The variation in the size of the indentation in different zones was observed. Table 4.1 shows the variation in microhardness of composites observed at different areas. It reveals a decreasing trend of microhardness as we move away from particle to matrix. Size of indentation near interface indicates a good surface bonding of the particle with the matrix which is because of diffusion of elements at the interface and the formation of new phase sillimanite (Al_2SiO_5) at the interface as observed from EDS and XRD analysis.

Figure 4.9 shows the variation in the bulk hardness of the LM13 base alloy and composites reinforced with different amount and size of particles ranges. From the graph, it is observed that overall hardness of all the composites increases with increasing amounts of reinforcement.

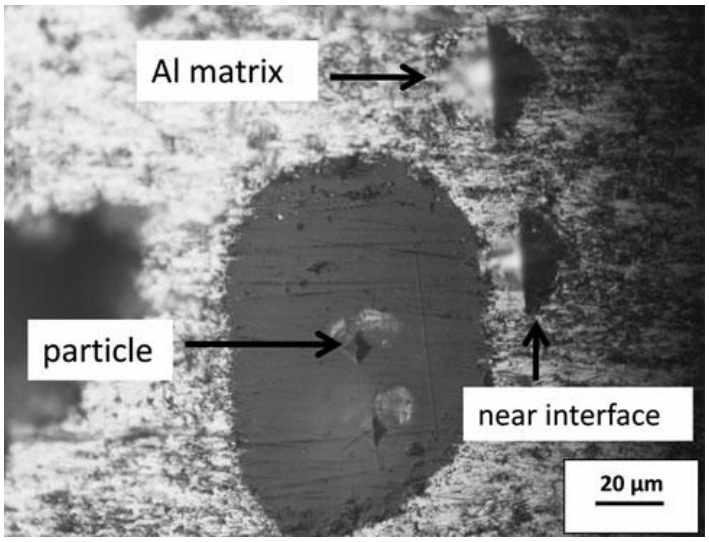

Figure 4.8: Optical micrograph of LM13/Zr composite showing variation in size of indentation marks on particle, interface and matrix.

However, at 20 wt.% reinforcement of coarse size particles in matrix, hardness of the composite decreased slightly. It may be due to agglomeration of the particles during stir casting as observed and shown in Fig. 4.3(f). These agglomerated particles are not strongly bonded with a matrix causing decrease in bulk hardness of the composite [10, 12].

Table 4.1: Variation of microhardness at different phases

Composite reinforced with different particle size	**Microhardness [Hv]**		
	At matrix	**At interface**	**At particle**
Coarse (106-125 µm)	89	102	709
Medium (50-75 µm)	85	108	712
Fine (20- 32 µm)	76	123	725

However, this variation is not significant as shown in Fig. 4.9. Increment in hardness of the composites was also observed with decreasing the particle size of the reinforced zircon sand in the matrix. This is due to larger surface area of the finer size particles in the matrix, which enhances the overall hardness of the composites. To get a better idea about the effect of particles on the hardness of the materials, standard errors have been incorporated for each composition of all values of hardness as shown in Fig. 4.9. Variation in standard error is maximum for the

composites containing higher amount of particles, which may be due to the non-homogeneous distribution of zircon sand particles in the matrix.

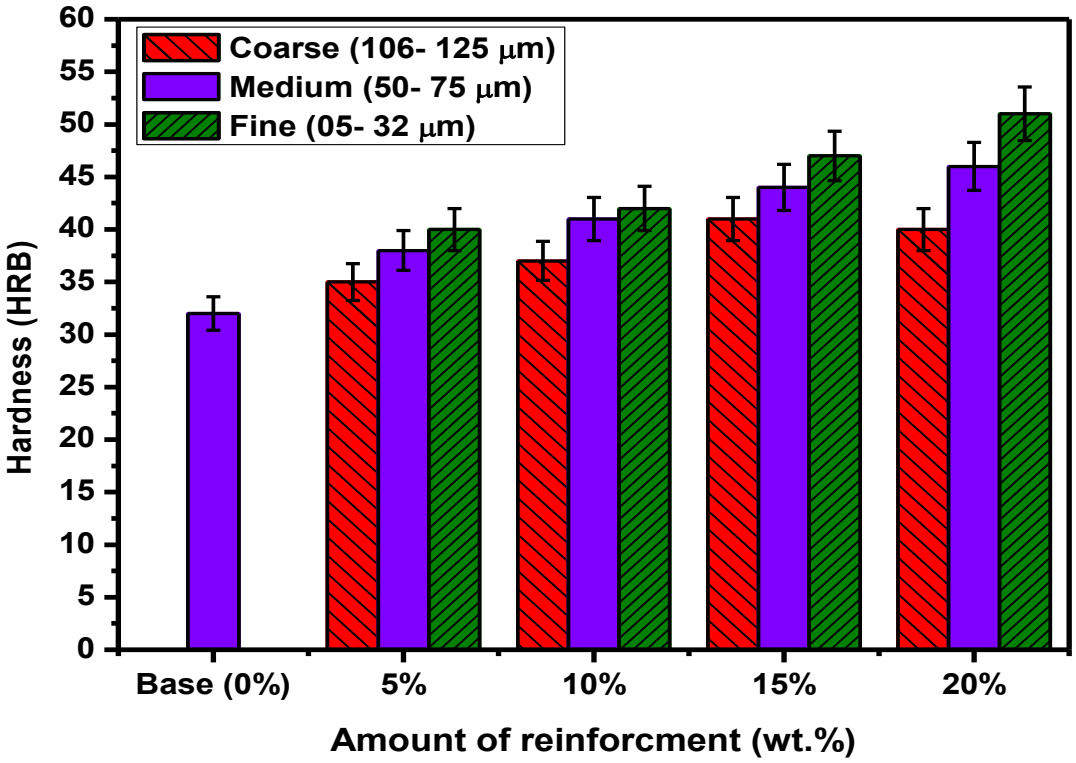

Figure 4.9: Showing variation in hardness of the base alloy and the composites containing different size and weight fraction of zircon sand reinforced particles.

4.5 Wear Behavior of the Base Alloy and Composites at Different Conditions:

A progressive loss of material from the operating surfaces as a result of relative motion is known as wear. In order to get idea about the durability of the materials under different conditions (particularly load and temperature), prepared samples were tested under dry sliding wear conditions. The effects of the applied load on the wear behaviors of LM13 alloy and the composites were studied at 9.8 N- 49 N loads.

4.5.1 Effect of applied loads on wear behavior:

The graphs of the wear rate versus sliding distance for the base LM13 alloy measured at room temperature with variation in applied loads are shown in Fig. 4.10. It is evident from the Fig.

4.10 that there is a rise in wear rate at the initial stage. This may be due to the abrasive nature of wear at the initial stage [14]. Once the initial transition period (run in wear) comes to end, the wear rate of the material falls, and a steady-state value of wear rate is attained. However, with the increase in the applied load from 9.8 N to 49 N, the wear rate of base alloy increased. There is a sharp change in wear rate at high load (49 N) with respect to low load (9.8 N). More material removal during the wear test at higher load is observed.

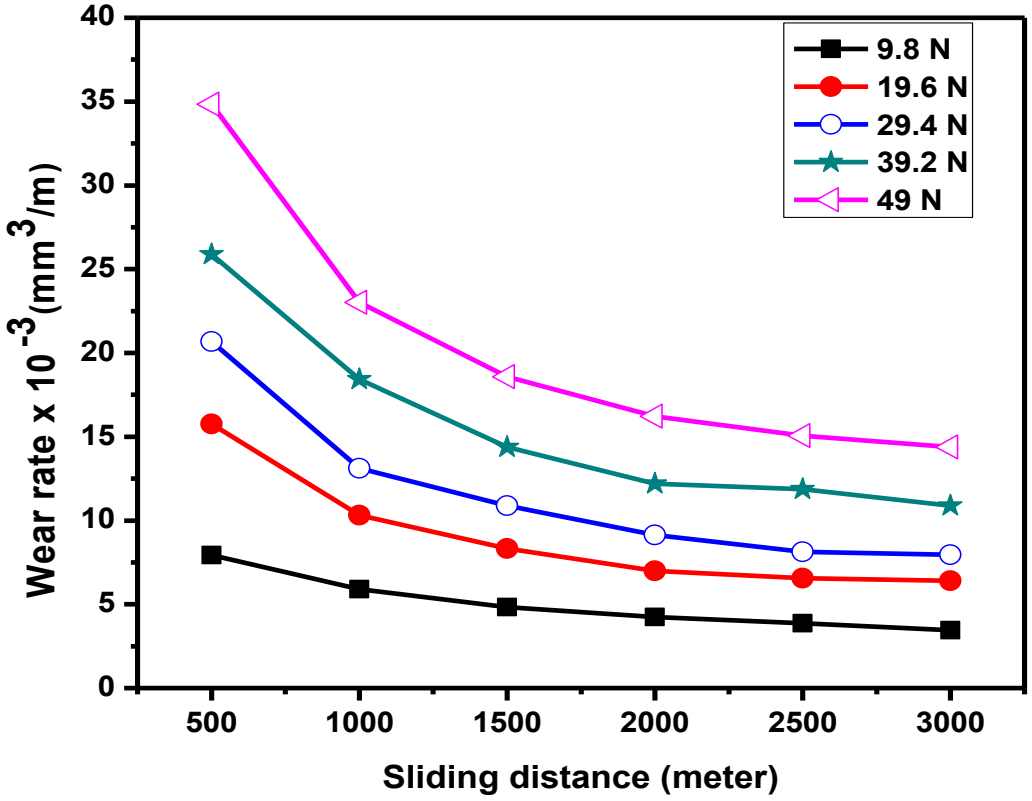

Figure 4.10: Wear rate against the sliding distance with variation in applied loads for LM13 base alloy.

Frey et al. [15] suggested that metals are usually covered with a film of oxide. When two such surfaces slide against each other, the oxide film breaks, producing contact between the solid layers. When contact pressure is high at higher load, the solid layer may fracture and expose the substrate material, particularly if the substrate beneath the solid layer deforms plastically. Small regions of both substrate materials may finally come into contact and weld together. After some sliding, there will be a layer of turbulently mixed substances, some of which will fall out as wear debris, but most of which will remain as a transfer film.

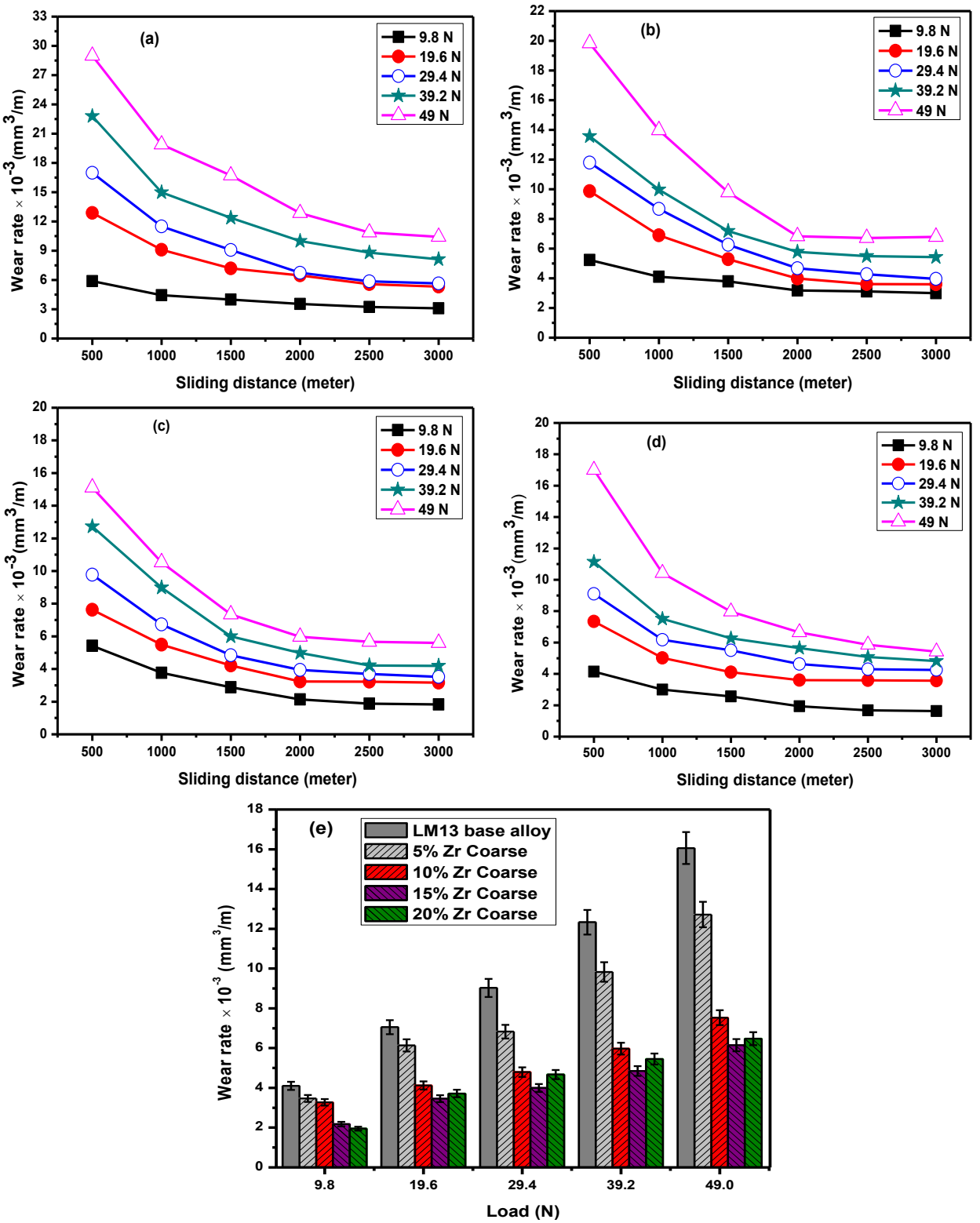

Figure 4.11: Wear rate against the sliding distance at different applied loads for the composite reinforced with coarse (106- 125 µm) size particle (a) LM13/5%Zr, (b) LM13/10%Zr, (c) LM13/15%Zr, (d) LM13/20%Zr and (e) comparison of wear rate of LM13 alloy and all the composites containing different weight fraction of zircon sand particles.

Figure 4.11 (a- d) shows the variation in wear rate with sliding distance at different applied loads for the composites having 5, 10, 15, and 20 wt.% of coarse size (106-125 µm) zircon sand particles, respectively. From Fig. 4.11e, it is observed that the presence of zircon sand particles in the matrix leads to reduction in the wear rate of the composite with respect to the base alloy. Moreover, wear rate in the composites is observed to increase with increasing load. As the amount of reinforced particles is increased in the base LM13 alloy, wear rate of the composites decreases significantly. It continue to decrease with increasing amount of the reinforcement up to 15wt.%. However, LM13/20wt.%Zr composite (Fig 4.11d) shows a slight increment in wear rate. As explained earlier, this may be because of fact that in composite containing 20wt.% zircon sand, the particles get agglomerated causing poor bonding with matrix. Owing to this agglomeration phenomenon, hardness of the LM13/ 20wt.%Zr composite decreases slightly as compared to LM13/15wt.%Zr composite. This decrease in hardness of the composite may also be one of the reasons for higher wear rate of LM13/20wt.%Zr in comparison with LM13/15 wt.%Zr (Fig. 4.9). Moreover, this segregation phenomenon is observed only in composite containing 20wt.% zircon sand even for repeated casting. There is a rapid increase in wear rate at higher load (49 N), indicating a transition phenomenon for both LM13 alloy and composites. At low load (9.8 N), wear is mild, and as the load is increased it becomes severe. However, when the amount of reinforced particles is increased above 10 wt.%, an improvement in mild-to-severe transition was observed.

Figure 4.12 represents the wear behavior of composites containing medium size (50- 75 µm) of reinforced zircon sand particles at different loading conditions. Figure 4.12 (a- d) shows the change in wear rate with respect to the sliding distance at different loads (9.8 N- 49 N) for the composites with 5, 10, 15 and 20 wt.% amount of medium size zircon sand particles respectively. Figure 4.12e represents a comparison of wear rate of the composites with medium size of reinforced particles at different loads. Almost similar wear behavior was observed for the composites having coarse and medium size particles as reinforcement. However, overall wear rate was improved for composite containing medium size of zircon sand particles. The improvement in the wear resistance was observed with increasing the amount of medium size zircon sand particles from 5 wt.% to 20 wt.% in the matrix for all loading conditions. However, wear rate also increased with the increasing the applied load from 9.8 N to 49 N. Wear behavior

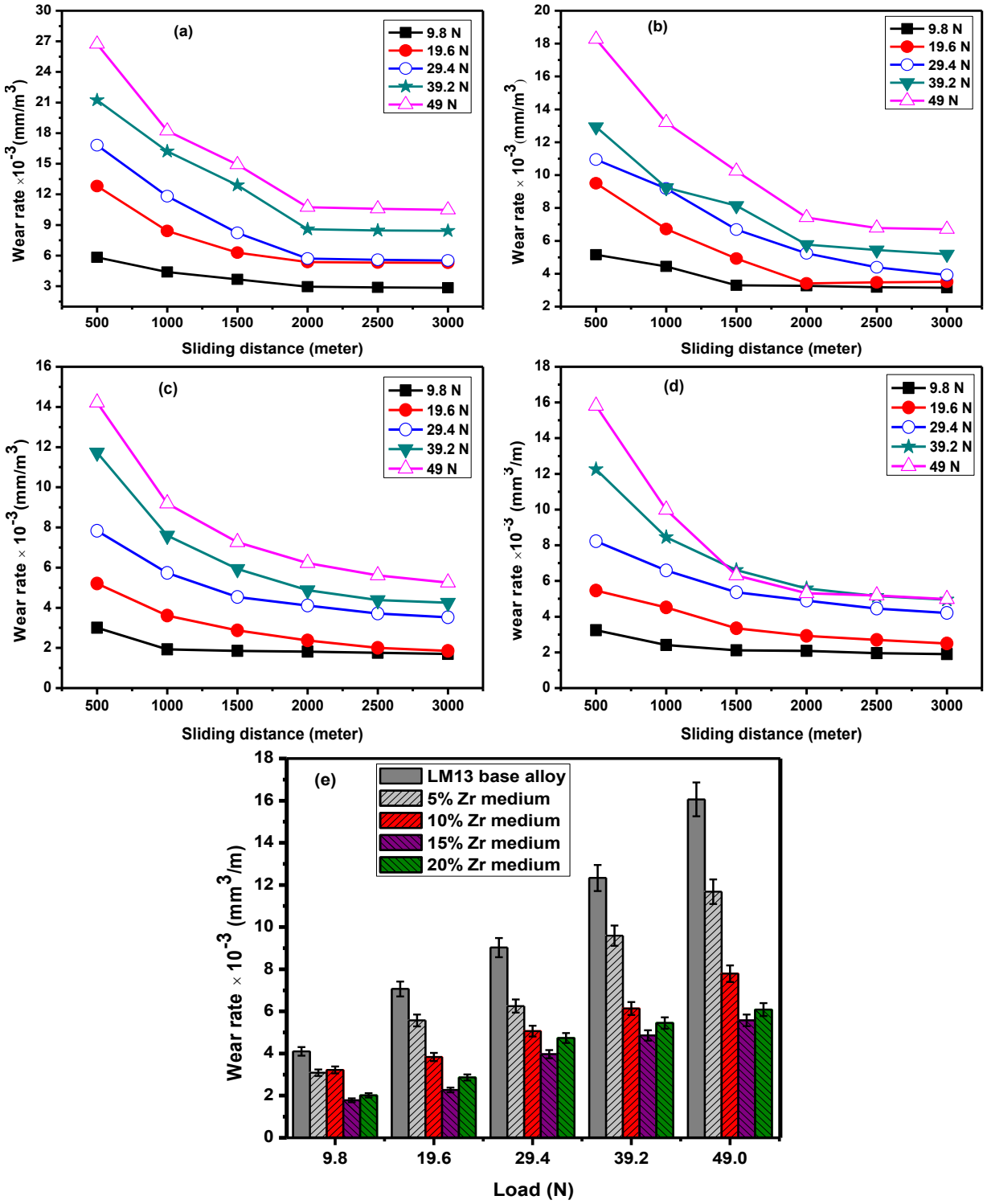

Figure 4.12: Wear rate against the sliding distance at different applied loads for the composite reinforced with medium (50-75 µm) size particles (a) LM13/5%Zr, (b) LM13/10%Zr, (c) LM13/15%Zr, (d) LM13/20%Zr and (e) comparison of wear rate of LM13 alloy and all the composites containing different weight fraction of zircon sand particles.

of LM13/20 wt.% shows steeper change in the wear rate in comparison to the other composites which may be due to agglomeration of the particles. However, at high load (49N) wear resistance was improved after addition of 20 wt.% zircon sand particles in comparison to others compositions for the composite.

Figure 4.13 shows the wear behavior of the composites containing 5, 10, 15 and 20 wt.% of fine size (20- 32 µm) zircon sand particles with variation in the applied loads from 9.8 N to 49 N respectively. An increment in wear rate was observed with increasing applied loads for all the composites (Fig. 4.13 a- d). Wear behavior of fine size reinforced composites (Fig. 4.13) is similar to that of medium (4.12) and coarse (4.11) size reinforced composites. However, composites containing fine size particles show an overall better wear resistance in comparison to other composites at all applied loads. Rate of agglomeration increases with the increasing the amount of reinforcement above 15 wt.% in the matrix. Composite with 15 wt.% of fine size zircon sand particles shows better wear behavior in comparison to the other compositions of composites having fine size particles (Fig. 4.13 e).

However, mild to severe transition in wear rate was observed at high load (49 N) condition. For the fine size particles chances of agglomeration increases which reduces the wear resistance of the composites at higher loads. Agglomeration of the reinforced particles also affects the wear behavior of the composites, which can be seen in Fig. 4.13d.

Wear rate of the base LM13 alloy and all the developed composites was observed to increase with increasing the applied load. However, decrement in wear rate was also observed with decreasing the particle size of the reinforced zircon sand in the matrix at all loads.

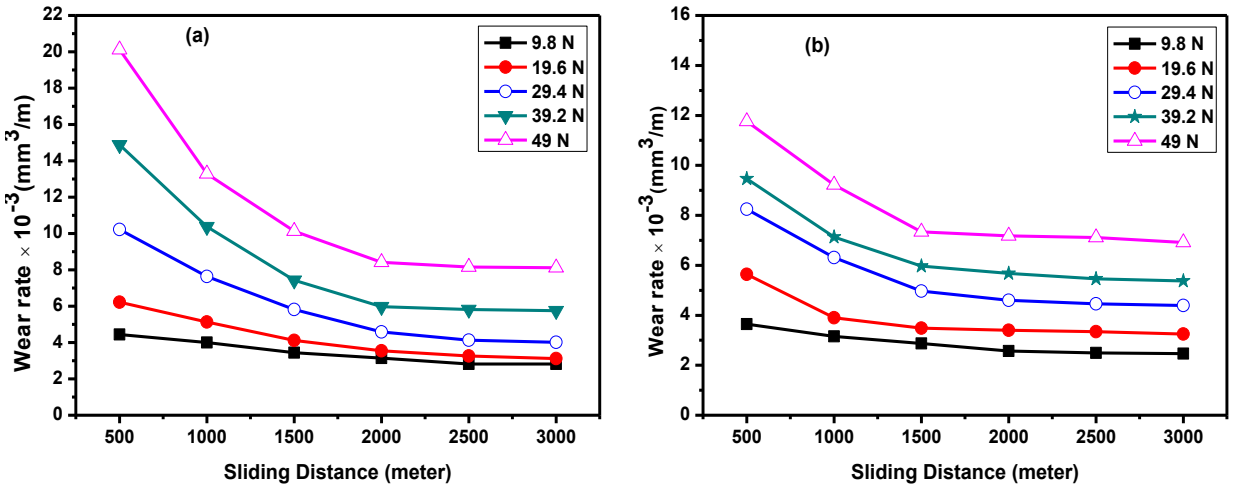

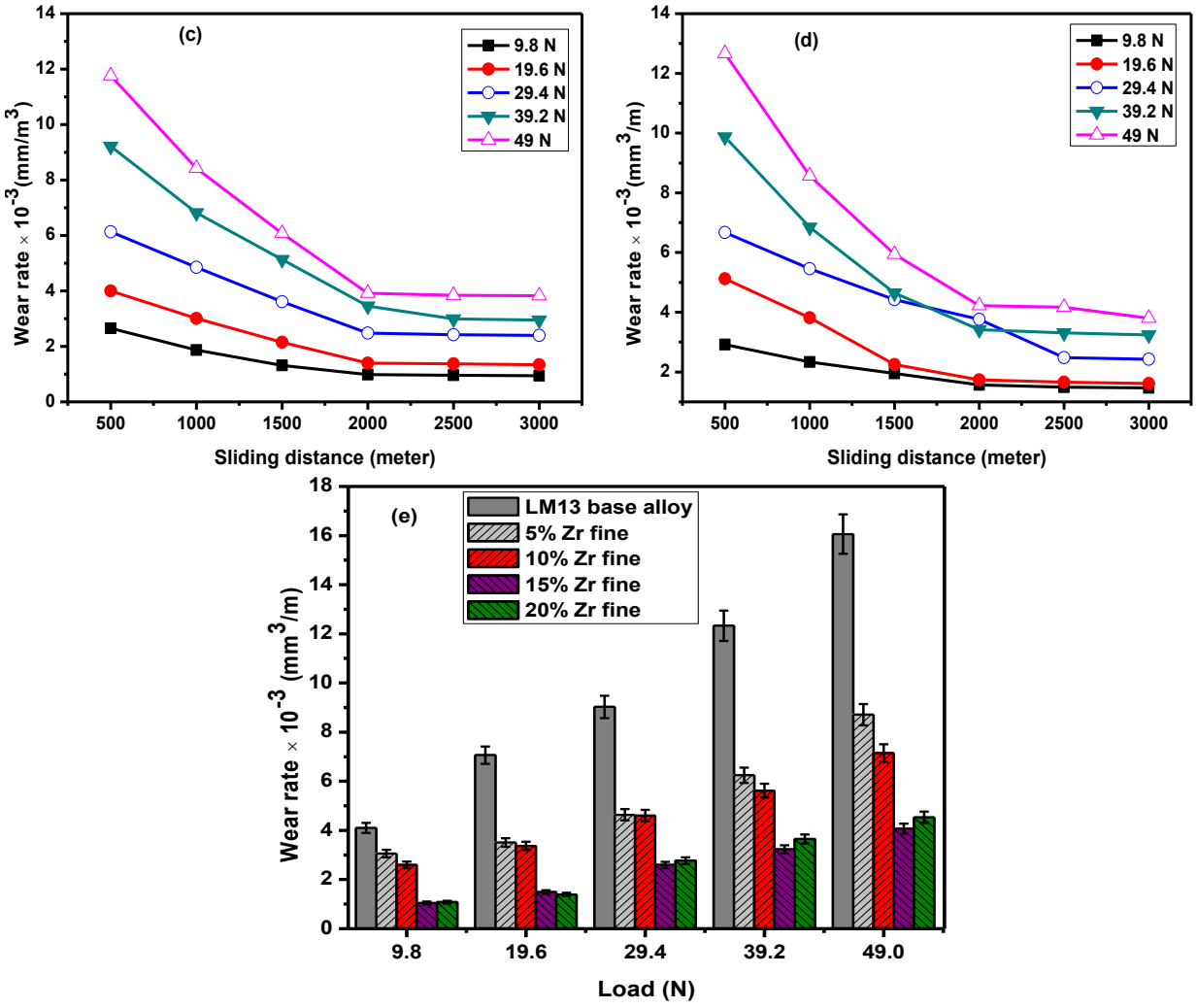

Figure 4.13: Wear rate against the sliding distance at different applied loads for the composite reinforced with fine size (20- 32 µm) particles (a) LM13/5%Zr, (b) LM13/10%Zr, (c) LM13/15%Zr, (d) LM13/20%Zr and (e) comparison of wear rate of LM13 alloy and all the composites containing different weight fraction of fine size zircon sand particles.

4.5.2 Effect of ambient temperature on the wear behavior:

LM13 alloy used as matrix for the development of composite material in this work is also known as piston alloy. In an engine, piston works at different conditions (e.g. friction, load, temperature etc.). Ambient temperature is also an important factor which affects the wear behavior of the materials. Hence to study the effect of ambient temperature on the wear behavior of the developed zircon sand particle reinforced LM13 alloy composite, wear test were done by varying the ambient temperature from 50- 300 °C. Though the study was carried out for the entire loads

as has been done for at room temperature but considering the fact that mild to severe transition in wear mode was observed at high load (49 N) test done at room temperature. So temperature dependent results of at low (9.8 N) and high (49 N) loads are presented here.

Bowden and Tabor [16] suggested that ‘‘strong adhesion’’ between two surfaces in contact occurs at a temperature which lies between $0.4T_m$- $0.5T_m$. Zhang and Alpas [17] suggested that the critical transition temperature in an alloy corresponds to $0.4T_m$. At this critical temperature, thermally activated deformation process is expected to become active and lead to softening of the material adjacent to the contact surfaces. Hence critical temperature of the material plays significant role on wear rate.

Presence of reinforced particles in the matrix affects the critical temperature of the alloy hence wear behavior of the materials is also affected. The low coefficient of thermal expansion (CTE) of zircon sand is attributed to lower CTE of the composite in comparison with the base alloy. As the amount of reinforced zircon sand is increased in matrix, composites behave as better thermal-resistant materials. Hence, owing to the addition of zircon sand, composites show better wear resistance as compared to the base alloy at high temperature.

Figure 4.14 shows the change in wear rate of base LM13 alloy at low (9.8 N) and high (49 N) load condition with variation in temperature from 50- 300 °C. Average wear rate of the materials

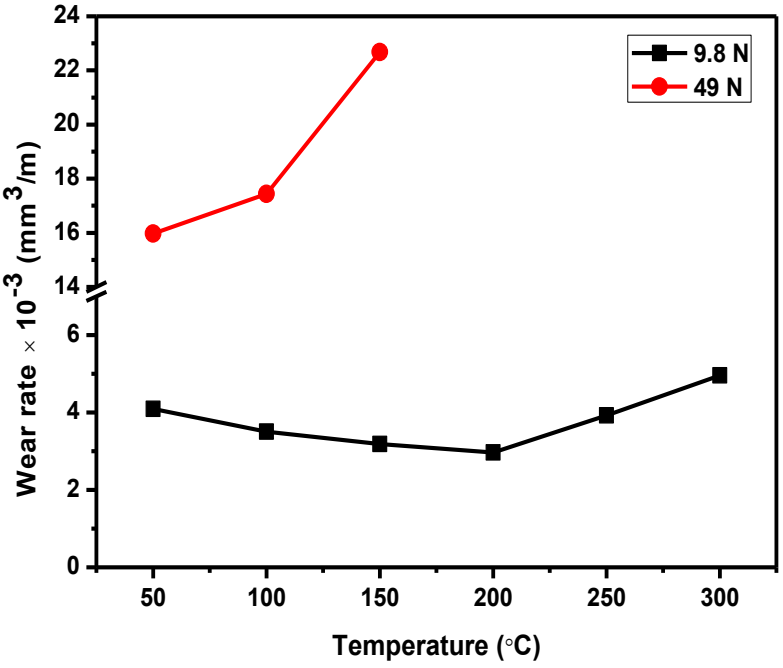

Figure 4.14: Wear rate against the temperature for the base LM13 alloy at 9.8 N and 49 N loads.

was taken during the sliding distance from 1500 to 3000 m, as in this range steady-state wear rate is observed (Fig. 4.10). It is evident from Fig. 4.14 that the wear rate of the material decreases slightly with increase in the temperature from 50 to 200 °C (near critical temperature) for base alloy. Wilson and Alpas [18] suggested that the formation of an oxide layer at high temperature (around 200 °C) reduces the wear rate by avoiding direct metal-to-metal contact. At higher temperature (above 200 °C), base alloy shows the transition from mild-to-severe wear, as at much higher temperature tearing of oxide layer occurs which expose new area for wear. However, at high load (49 N) condition wear rate of the base alloy increases sharply with increasing the temperature. At higher temperature (>150 °C), base alloy wears out early, and a transition from mild-to-severe wear is observed. There is a massive surface damage and large-scale material transfer to the counterface occurs. It was observed that 2 mm height (limit of the LVDT sensor) of the base alloy was worn out at 200, 250, and 300 °C at sliding distances of around 1,100, 150, and 50 m, respectively.

Presence of ceramic particles in the matrix introduces asperities on the surface of the composites during the wear test. Figure 4.15 shows a schematic diagram of real contact area between the surface of composite and counter surface of steel disc (Fig. 4.15a) and asperities (Fig. 4.15b). Figure 4.15 (c & d) shows the effect on asperities due to presence of fine and coarse size hard ceramic particles in matrix. Real contact area and asperities are key factors for the wear rate of any composite material at different loading conditions. The size of asperity and interasperity distance of the composites depends on the amount, the nature of distribution of reinforced particles, and their sizes in matrix with loads. The hardness is correlated very well with wear. Further, hardness determines the real area of contact between the rubbing partners. The real area of contact is only a fraction of the apparent area of contact. Kapoor and Johnson [19] have done the theoretical analysis of the steady-state wear of two sliding asperities.

Johnson and Shercliff [20] investigated the mechanics involved in the sliding contact of two rough surfaces (one hard and two soft as shown in Fig. 4.15a, although their analysis is restricted to the case when the roughness on the harder surface is regular (all asperities have the same height and curvature) and it is only the soft surface that is randomly rough.

Figure 4.16 (a & c) shows the wear rate of the composites containing 5, 10, 15 and 20 wt.% of coarse size zircon sand particles tested at 9.8 N and 49 N loads with variation in temperature from 50- 300 °C respectively.

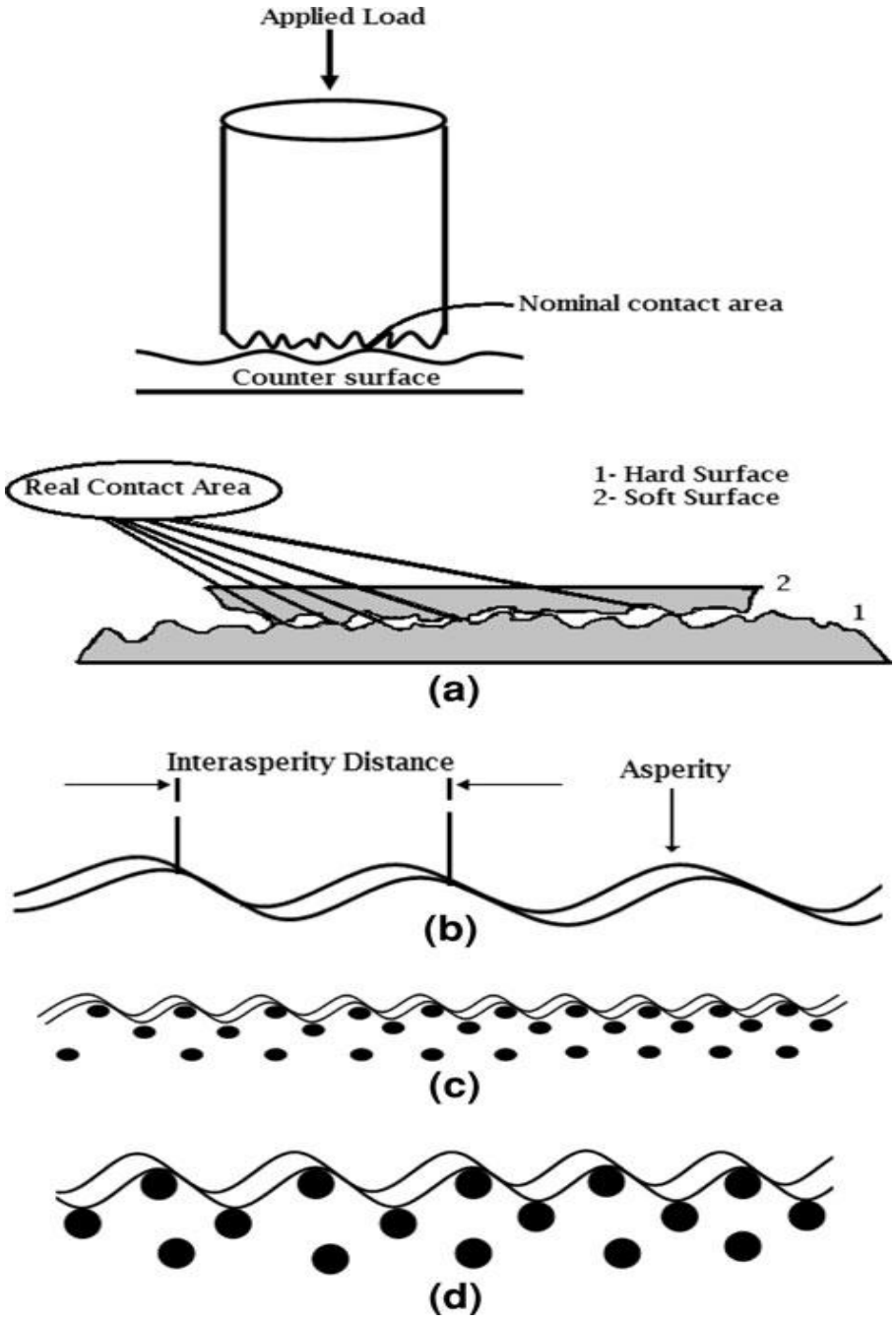

Figure 4.15: Schematic representation of (a) real contact area during wear testing, (b) size of an asperity and inter-asperity distance in a composite, (c) dispersion of zircon-sand-reinforced particles in composite (fine size) and (d) dispersion of zircon-sand reinforced particles in composite (coarse size particles)[20].

Figure 4.16a reveals that the wear rate of the composites slightly decreases with an increase in temperature from 50 to 150 ºC for both composites at 9.8 N load. Since at lower load, the asperities on the surface of composites undergo plastic deformation so, slight decrement is observed in wear rate. Under this condition, Al matrix expands and holds the particle more tightly, hence reinforced particles offer more resistance to wear causing a decrease in wear rate.

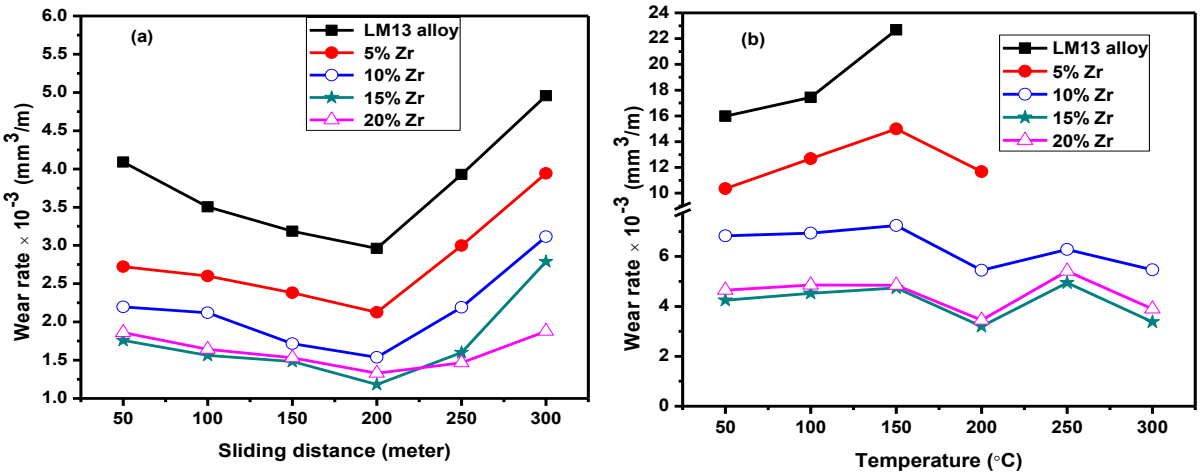

Figure 4.16: Wear rate against the temperature for LM13/Zr composite reinforced with coarse size (106-125 µm) particles at (a) 9.8 N and (b) 49 N loads.

At 200 °C wear rate is minimum, this may be due to the formation of oxide layers as suggested by Wilson and Alpas [18]. They proposed that the formation of an oxide layer at high temperature (around 200 °C) reduces the wear rate of the materials by avoiding direct metal-to-metal contact. At higher temperature (above 200 °C) all the composite materials show the transition from mild-to-severe wear. Severe wear is characterized by extensive plastic deformation and extrusion of material at the sliding contact zone.

Figure 4.16 reveal that all the composites having coarse size reinforcement show better wear resistance as compared to base alloy (Fig. 4.14). However, wear resistance was improved with increasing the amount of zircon sand particles in the matrix. The observed increase in hardness of the composite with increasing zircon content further supports to the better wear resistance offered by the composites.

Figure 4.16b shows the wear rate of the all the composites containing coarse size zircon particles tested at high (49 N) load with variation in temperature from 50- 300 °C. It indicates that the

wear rate of the composites increases slightly with an increase in temperature up to 150 °C at high load (49 N). Similar behavior of the wear was observed for the composite LM13/5wt.%Zr at 49 N load, with better wear resistance in comparison with base alloy. Figure 4.16b shows that the wear rate of LM13/5wt.%Zr composite decreased with increase in temperature up to 200 °C (near critical temperature). The composites worn out at 1,800 and 1,500 meter sliding distances at 250 and 300 °C respectively (maximum instrumental limit of 2 mm). However, composites containing more than 5wt.% zircon sand show better wear resistance at higher temperatures. This is because increased amount of zircon sand has improved the hardness and lowered CTE of the composite. With further increase in reinforcement content, composites show improvement in wear resistance at higher loads and temperatures as shown in Fig. 4.16b. The wear rate of the composite increased slowly with increasing temperature from 50 to 150 °C at higher loads. However, at higher temperatures (around 200 °C), the wear rates of composites containing 10, 15, and 20 wt.% zircon sand decreased sharply which may be due to the formation of oxide layer on sliding component. Rajaram et al. [21] have described that the formation of oxide films at higher temperature reduces the wear rate by avoiding direct metal-to-metal contact. Due to continuous sliding, the oxide film on the surface is removed which results in direct metal-to-metal contact and exposing new areas to environment. Tearing and formation of oxide layer is a continuous process which results in a decrement of wear rate when the temperature is increased. Beyond 200 ºC the matrix becomes soft causing plastic deformation on the surface. Some of the sharpest asperities also get fractured due to combined action of normal and shear stress causing increase in wear rate. As the temperature is increased to 250 °C, wear rate of the composites increased sharply. At this critical temperature (250 °C) composites show transition from mild to severe wear. Interesting behavior of wear rate at higher temperature (300 °C) and higher load is observed for composite having zircon sand more than 10 wt.%. Decrease in wear rate at 300 °C may be due to transfer of steel inclusion from the counterface surfaces to the composite wear surfaces which contributes to increase in wear resistance of the composites [9]. Wilson and Alpas [18] have observed similar behavior around 300 °C for Al matrix composite. They suggested that there is a transition from mild-to-severe wear in the counterface steel itself. Once severe wear and seizure effects arise within the steel during sliding contact, the steel debris generated by this process would be transferred to the opposing wear surface of the composite specimen leading to negative or minimum wear. However, LM13/15%Zr composites show better

wear resistance in comparison to all composites with coarse size zircon sand particles at higher load (49 N) condition. Figure 4.16 also indicates an improvement of around 100 °C in the critical transition temperature with the addition 10 wt.% or more.

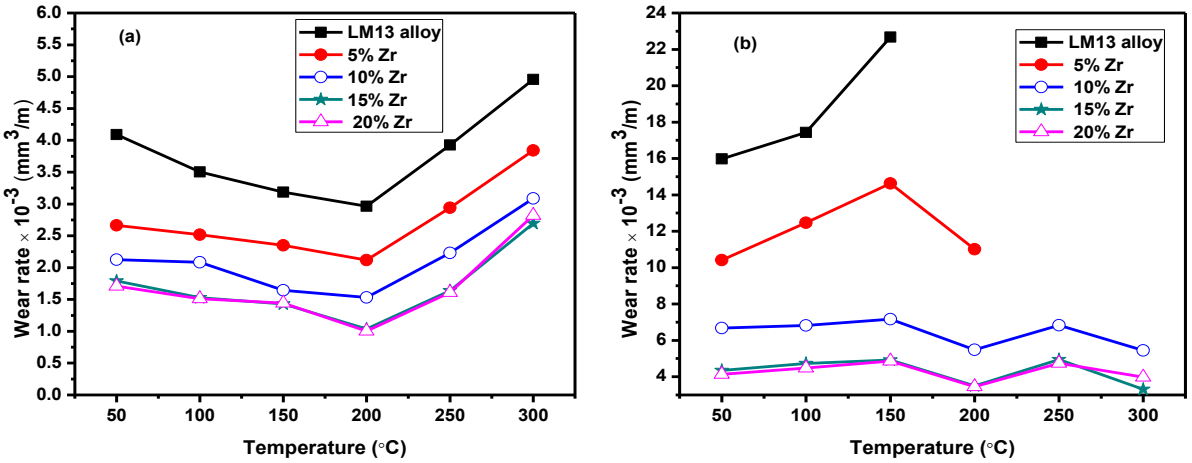

Figure 4.17: Wear rate against the temperature for LM13/Zr composite reinforced with medium size (50- 75 µm) particles at (a) 9.8 N and (b) 49 N loads.

Figure 4.17(a & b) shows the change in wear rate of the composite with respect to the temperature at low (9.8 N) and high (49 N) loads containing medium size of zircon sand particles respectively. Figure 4.17a reveals that wear rate for all the composites decreases with increasing the temperature from 50- 150 °C at low load (9.8 N) condition. This is due to good bonding of the particles with matrix. However, at much higher temperature (200 °C) wear rate decreases sharply, which is due to formation of oxide layers at this temperature as suggested by Wilson and Alpas [18]. At much higher temperature (250 and 300 °C) wear rate increases sharply due to the tearing of oxide layers which exposes new surface for the wear that leads to higher wear. However, it was observed that LM13/15wt.%Zr composite shows better wear resistance in comparison to the other composites as LM13/15wt.%Zr composite also shows better hardness. Agglomeration of zircon sand particles in LM13/20wt.%Zr composite is also responsible for the higher wear rate.

Figure 4.17b shows the wear rate of the composites containing medium size zircon sand particles with respect to the ambient temperature at high load (49 N). It was observed that wear rate of LM13/5%Zr composite increases sharply with increasing the temperature from 50- 150 °C at high load condition as applied load creates more contact stress which leads to higher wear rate. However, formation of oxide layer at 200 °C decreases the wear rate of the LM13/5%Zr

composite significantly. Higher temperature (250 and 300 °C) wear test at 49 N load leads to complete worn out of the surface of the sample after 1950 and 1600 meter of sliding distance (2 mm height). However, increased amount of reinforcement (> 5%Zr) in the matrix leads to improvement in wear resistance of the composite at high load and high temperature conditions. LM13/15wt.%Zr and LM13/20wt.%Zr composites show almost same wear behavior. However, it exhibits improved wear resistance as compared to the LM13/5wt.%Zr and LM13/20wt.%Zr composites. Higher wear rate of LM13/20wt.%Zr composite may be due to the agglomeration of the particles in the matrix.

Figure 4.18 (a & b) shows the wear rate of the composites reinforced with fine size (20- 32 μm) zircon sand particles tested at low (9.8 N) and high (49 N) loads with variation in temperature from 50- 300 °C. Due to larger surface area, fine size of reinforced particles affects the properties of the composites significantly in comparison with coarser one. Figure 4.18 shows almost similar behavior of change in wear rate at different temperatures for low and high loads. However, an improved wear resistance for higher amount of fine size zircon sand particles in matrix as compared to medium size zircon sand particles (shown in Fig. 4.16) is observed. Figure 4.18a shows that wear rate of the all composites reinforced with fine size zircon sand particles shows increment in wear rate with increasing the ambient temperature for low load condition. Minimum wear rate was observed at 200 °C that was due to formation of oxide layer. At much higher temperature (250 and 300 °C) wear rate again increases due to softening of matrix at high temperature which patronages plastic deformation as well as adhesive wear of the composite material. Presence of fine size particles in the matrix supports the formation of large number of asperities of small size, which provide the large real contact area during wear test. This large real contact area is responsible to the lower stress, hence wear rate decreases significantly in comparison to coarser size particles.

Figure 4.18b shows the variation in wear rate of the composites with varying the temperature from 50-300 °C at high (49 N) load. Figure 4.18b indicates that wear rate of LM13/5 wt.%Zr composite increases sharply with increasing the temperature from 50- 150 °C at high load. Increasing the temperature above 150 °C, composite was worn out at 2100, 1780 and 1350 meter in presence of high load. However, with increasing the amount of zircon sand particles in the matrix wear rate of the composite (LM13/10wt.%Zr, LM13/15wt.%Zr and LM13/20wt.%Zr) decreases significantly. Wear rate of these composites containing higher (> 5%) amount of

reinforced particles increases slightly with the increasing temperature. However, at 200 °C wear rate of the composites decreases sharply due to formation of oxide layers. At much higher temperature (250 °C), wear rate increases due to tearing of the oxide layers which provides new area to wear. But at 300 °C and high load condition wear rate decreases which may be due to transfer of steel inclusion from the counterface surfaces to the composite wear surfaces which contributes to increase in wear resistance of the composites.

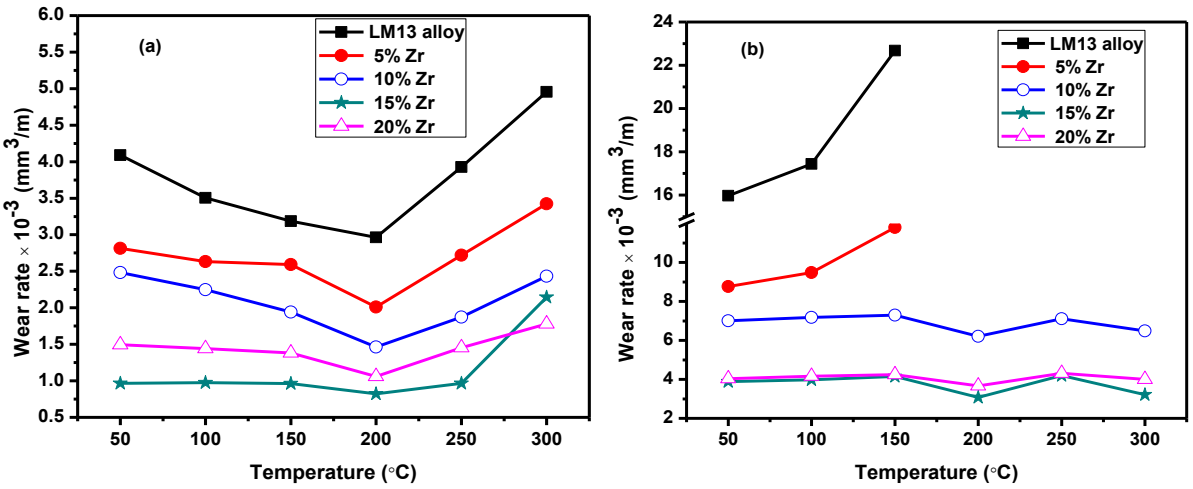

Figure 4.18: Wear rate against the temperature for LM13/Zr composite reinforced with fine size (20- 32 µm) particles at (a) 9.8 N and (b) 49 N loads.

It was observed that wear rate of base alloy and all developed composites increases with increasing the applied load. Wear behavior of the all developed composites indicates that wear rate decreases with increasing the amount of zircon sand in the matrix. However, among all the compositions 15wt.% amount of zircon sand shows better wear resistance in comparison to others. Wear rate of the composites also decreases with decreasing the particle size of reinforcement in the matrix. Hence, composite with 15wt.% amount of fine size particles in the matrix shows better wear resistance in comparison to the all other developed composites. Ambient temperature also plays important role on wear rate of the composites. Critical temperature of the base alloy is improved about 100 °C by addition of 10wt% and more amount of zircon sand particles. Due to good thermal stability and lower CTE, zircon sand particles provide good wear resistance to the composites at high temperature. However, due to good distribution and higher amount of zircon sand particles in matrix, LM13/15wt.%Zr composite

reinforced with fine size zircon sand particles shows better wear resistance at high load and high temperature conditions.

4.6 Topographical analysis of the worn surfaces and wear debris:

Wear is defined as the removal of material in contact with the counter surface when in motion [9]. Under dry sliding conditions, the loss of material from the sliding surfaces of alloys and composites takes place, which is classified as mild wear, severe wear, and seizure wear (on the basis of wear rate). The wear of materials was also classified on the basis of types of wear debris generated during sliding. Topographical analysis of the worn surfaces and collected wear debris is essential part to examine the nature of wear of any material under the exposed environmental conditions. It also helps to know the mechanism involved during the wear test at particular condition. For this purpose, worn surfaces and wear debris of the tested material were analyzed under the SEM. It was observed that all the developed composites show almost similar wear behavior at similar testing conditions. For the sake of simplicity, in this thesis we present the SEM images of wear tracks and wear debris for the base alloy and LM13/15wt.%Zr composites containing coarse and fine size particles, as composite containing 15wt.% of zircon sand particles shows better wear resistance in comparison to others.

4.6.1 Analysis of the worn surfaces and wear debris under different loading conditions

The effects of the applied load on the wear behaviors of LM13 alloy and the composites were studied at 9.8 N to 49 N loads. Figure 4.19 (a- e) shows the SEM images of wear tracks and wear debris of the base alloy collected at low (9.8 N) and high (49 N) loads. As shown in Fig. 4.10 almost similar wear behavior of the base alloy with respect to sliding distance at different applied loads is observed. However, the wear rate increases with increase in applied load. Transition in wear rate from mild to severe was observed at high (49 N) load. The SEM images of the wear track and wear debris of base alloy collected at low (9.8 N) and high (49 N) loads are presented. Figure 4.19a shows the wear tracks of the base alloy collected after the wear test at 9.8 N load. Presence of grooves on the worn surface was observed running parallel to the sliding direction. Figure 4.19b shows the deeper grooves with larger delaminated area on the worn surface collected at 49N load as compared to the Fig. 4.19a.

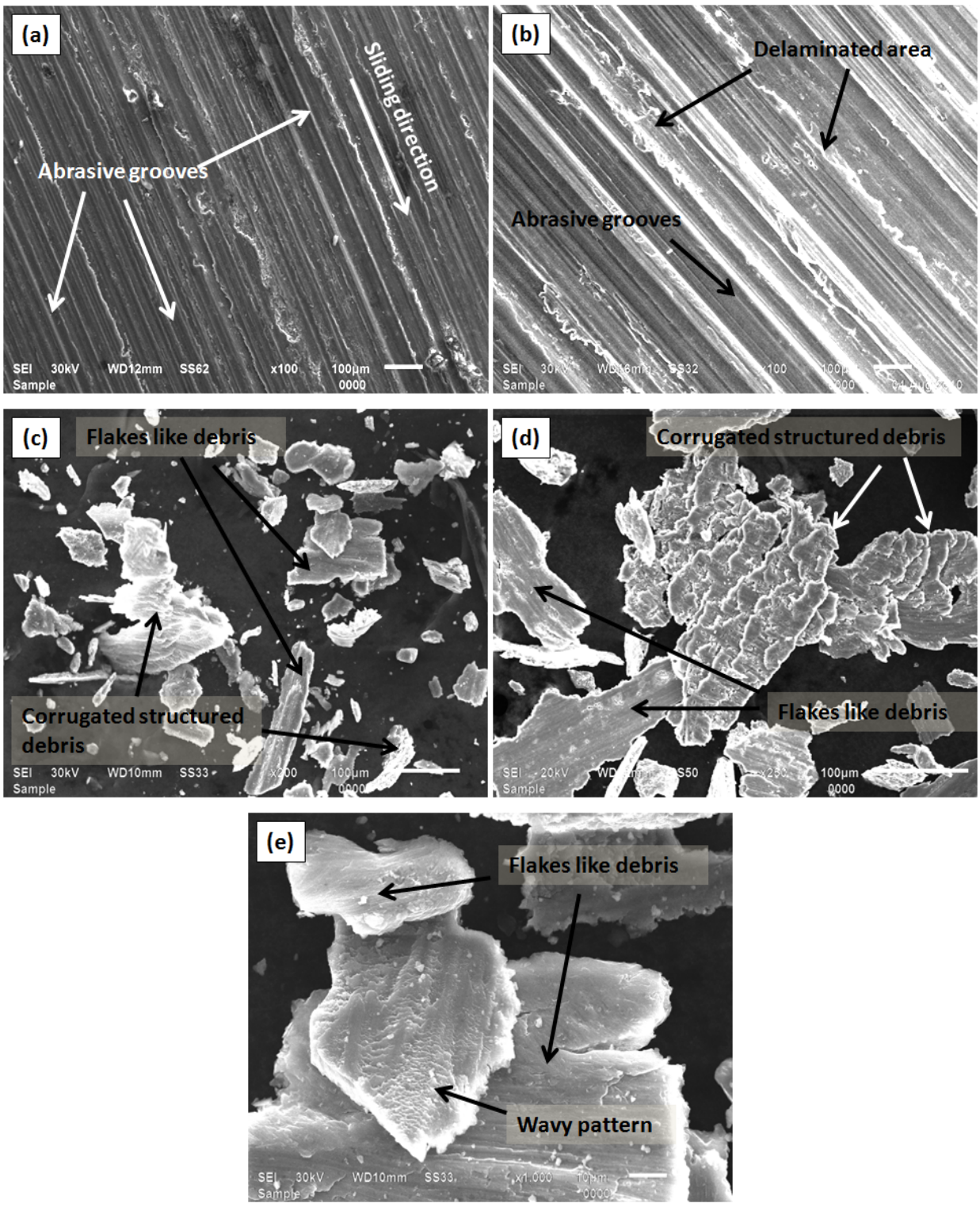

Figure 4.19: SEM images of base alloy (LM13) for (a) wear track at 9.8 N load, (b) wear track at 49 N load (c) wear debris at 9.8 N load, (d) wear debris at 49 N load and (e) higher magnification image of debris collected at 9.8 N.

Presence of abrasive wear during the sliding can be seen clearly in Fig. 4.19 (a & b) as material adheres along the sliding direction during the wear test. Figure 4.19c shows the debris collected after the wear test of base alloy with 9.8 N load. Formation of the debris is due to the removal of material during testing at different conditions. Flakes type debris in Fig. 4.19 (c & d) clearly indicates that adhesive wear occurs during wear test for the base alloy tested at low (9.8 N) and high (49 N) loads respectively. However, size and amount of debris increases at high load condition, which reveals higher wear rate of the material. Corrugated structure observed on the wear debris is due to the continuous rubbing of materials during the wear test. Higher magnified images of the debris collected at 9.8 N load also indicates the adhesive wear and delamination of plate like debris during the wear test. Wavy pattern observed on the debris indicates the delamination of material during continuous rubbing.

SEM micrographs of wear tracks of LM13/15wt.%Zr composites reinforced with coarse size particles taken after the test at 9.8 N– 49 N loads are presented in Fig. 4.20. One of the common features observed in both lower and higher loads is the formation of grooves and ridges running parallel to the sliding direction in composites. Flow of materials along the sliding direction, generation of cavities due to delamination of surface material, and tearing of the surface can be seen. Grooves are created because of the entrapment of hard particles between the sliding surfaces of sample and steel disk. The depth of microploughing is increased on increasing the load to 49 N where contact asperities change the shape. Consequently, the size and the depth of the grooves become higher at this stage. Figure 4.20a shows worn surface at 9.8 N load in which grooves and ridges running parallel to the sliding direction can be seen. Microploughing dominates the wear mechanism although local damaged spots are also observed on the surface. At 19.6 N load, the grooves are distinct and deeper, crater grow in size which exposes the reinforced particles, as shown in Fig. 4.20b.

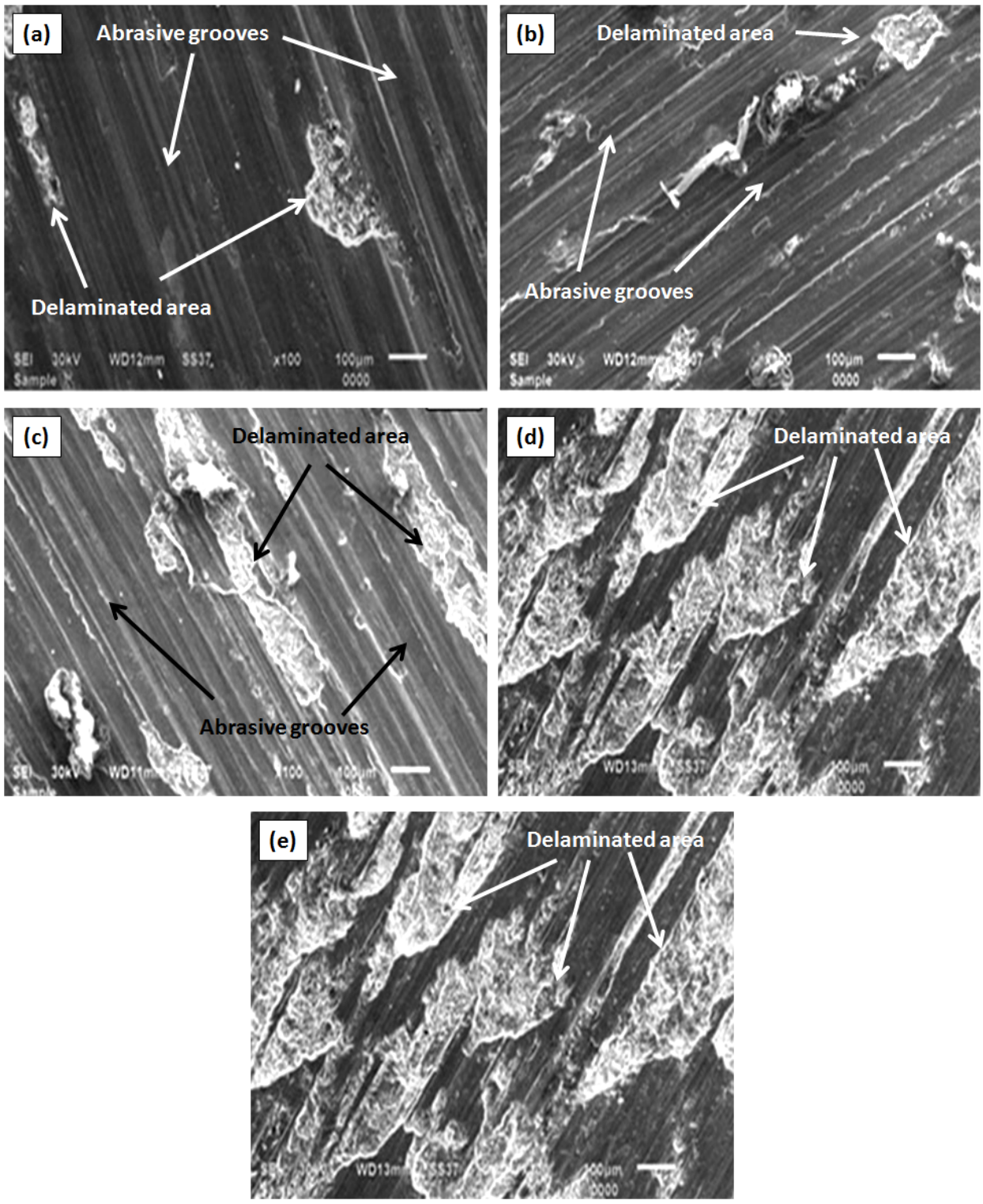

Figure 4.20: SEM images of the wear tracks for LM13/15%Zr composite reinforced with coarse size particles tested at (a) 9.8 N, (b) 19.6 N, (c) 29.4 N, (d) 39.2 N and (e) 49 N loads.

As load increases the adhesive wear mechanism operates and removes the ductile matrix material. Particles are protruding in the matrix depicting good bonding between particle and alloy matrix as observed in Fig. 4.20c. At higher load, the material removal is governed by adhesive wear and crack propagation resulting in delamination of matrix material. The protective layer of the reinforcing particles can no longer remains stable under the ploughing action at high load. The material removal is enhanced by adhesive wear mechanism and number of craters is increased between deep ploughing marks, as shown in Fig. 4.20 (d & e). Material removal during the process is in the form of small pieces resulting in the formation of flake-type debris. Higher magnified SEM image (Fig. 4.20f) of the composites tested at 49 N load shows that the craters are so large and distinct that the surface underneath is visible; presence of cracks indicates the delamination wear.

Wear debris of LM13/15wt.%Zr composite reinforced with coarse size particles collected after the wear test at different load is shown in Fig. 4.21. The debris obtained at low (9.8 N) load is of plate-like morphology and zircon sand particle is not observed, which indicates that the reinforced particles are bearing the load where plate like debris as shown in Fig. 4.21a is generated. As load increases the debonding of zircon sand particles occurs and long flakes of debris having different morphologies as shown in Fig. 4.21b are observed. In the collected wear debris, zircon sand particles are present in the form of mechanically mixed layer. The particle itself has cracked into further smaller fragments and after long run it makes an oxide-rich layer on the worn surface by picking iron oxide from the counterface which was confirmed by EDS analysis (discussed later). Several microcracks are visible in debris indicating delamination while zircon sand particle takes spherical shape by trapping during course of sliding. Twisted and layered debris reveal the repetitive nature of stress that occurred at high load sliding condition.

At 29.4 N load, as shown in Fig. 4.21c the debris having long flakes apart from the small metallic debris is also observed, which get fragmented during sliding action. Debris at 39.2 N load (Fig. 4.21d) presents mixed morphology with long flakes, small fragmented flakes, and layered flakes. Debris collected at 49 N after wear test, point out some flakes depicting microcutting behavior as shown in Fig.4.21e. Deep grooves along with the corrugated structure formed under high stress can be easily seen on the debris, which indicates about the high wear rate of the material.

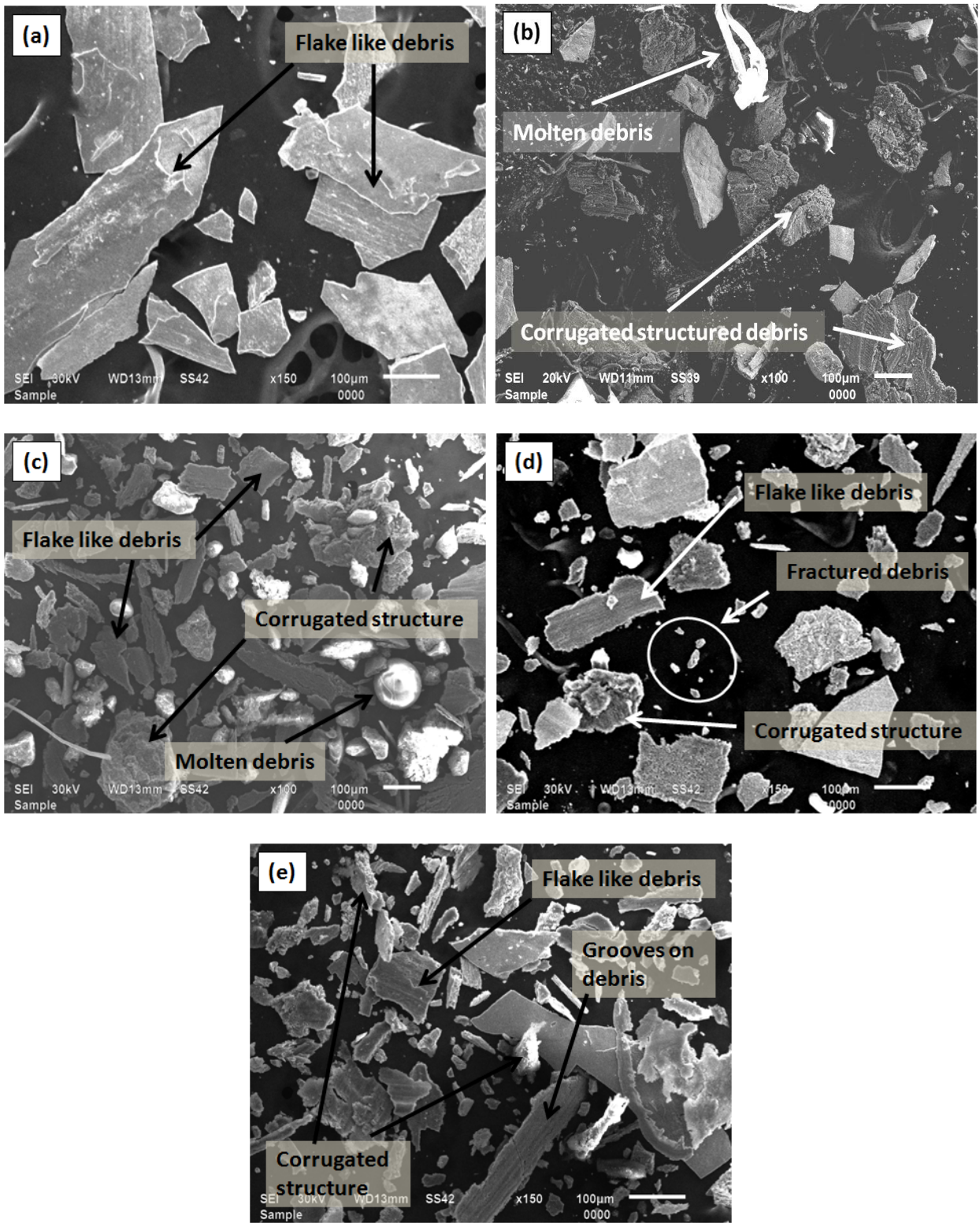

Figure 4.21: SEM images of the wear debris for LM13/15%Zr composite reinforced with coarse size particles tested at (a) 9.8 N, (b) 19.6 N, (c) 29.4 N, (d) 39.2 N and (e) 49 N loads.

The SEM micrographs of wear track of LM13/15%Zr composites reinforced with fine size zircon sand particles tested at different loads of 9.8- 49 N are presented in Fig. 4.22. Figure 4.22 shows the wear track morphology of the tested specimens. However, at higher loads the worn surfaces in some places reveal patches from where the material was removed from the surface during the course of wear [20, 24]. Figure 4.22a shows the SEM micrograph of worn pin of LM13/15%Zr composite reinforced with fine size zircon sand particles at 9.8 N load. The worn surfaces are smooth and ploughing strips are very shallow on the surface. At 19.6 load, the ploughing marks got deeper as shown in Fig. 4.22b and damaged spots in the form of craters can be seen, which grow further in size with increasing load. Particle cracking and microcrack are observed at higher magnification, as shown in Fig. 4.22c. These factors increase the wear rate significantly. This behavior is characterized as severe wear behavior, in which material removal is accelerated. The material of the pin adheres along the flat running surfaces causing adhesive sliding wear as shown in Fig. 4.22d at 29.4 N load. This wear behavior causes the damage to parent material and wear rate increases significantly. The crack running from the removed material is also visible in the matrix.

At 39.2 N load, the material removal increases significantly and the cross section of the craters increases, as shown in Fig. 4.22e. At 49 N load material removal rate is significantly higher. Adhesive wear is dominating at this stage. Microcracks result delamination, which in turn damage the parent material by excessive material loss. The loose wear debris and crushed zircon sand particles are clearly seen in higher magnified image of wear track (Fig. 4.22f).

Wear debris of LM13/15wt.%Zr composite reinforced with fine size zircon sand particles generated at different loads are presented in Fig. 4.23. At low (9.8N) and high (19.6 N) load condition flake type delaminated metallic debris along with some debonded zircon sand particles are generated which indicates that adhesive wear dominates in this condition (Fig. 4.23 a & b).

Figure 4.23c shows wear debris obtained at low (29.4 N) load. Fig.4.23c reveals that wear is governed by delamination which gives plate-like morphology of debris with microcracks. The pull-out of ductile aluminum having thread-type morphology is also seen. Wear debris at 39.6 N load as shown in Fig. 4.23d shows the plate or flakes of alloy matrix and debonded zircon sand particles which get spheroidized as they are trapped in the track during sliding action. The debris particles are likely to act as the third-body abrasive particles and could be responsible for the higher wear rate.

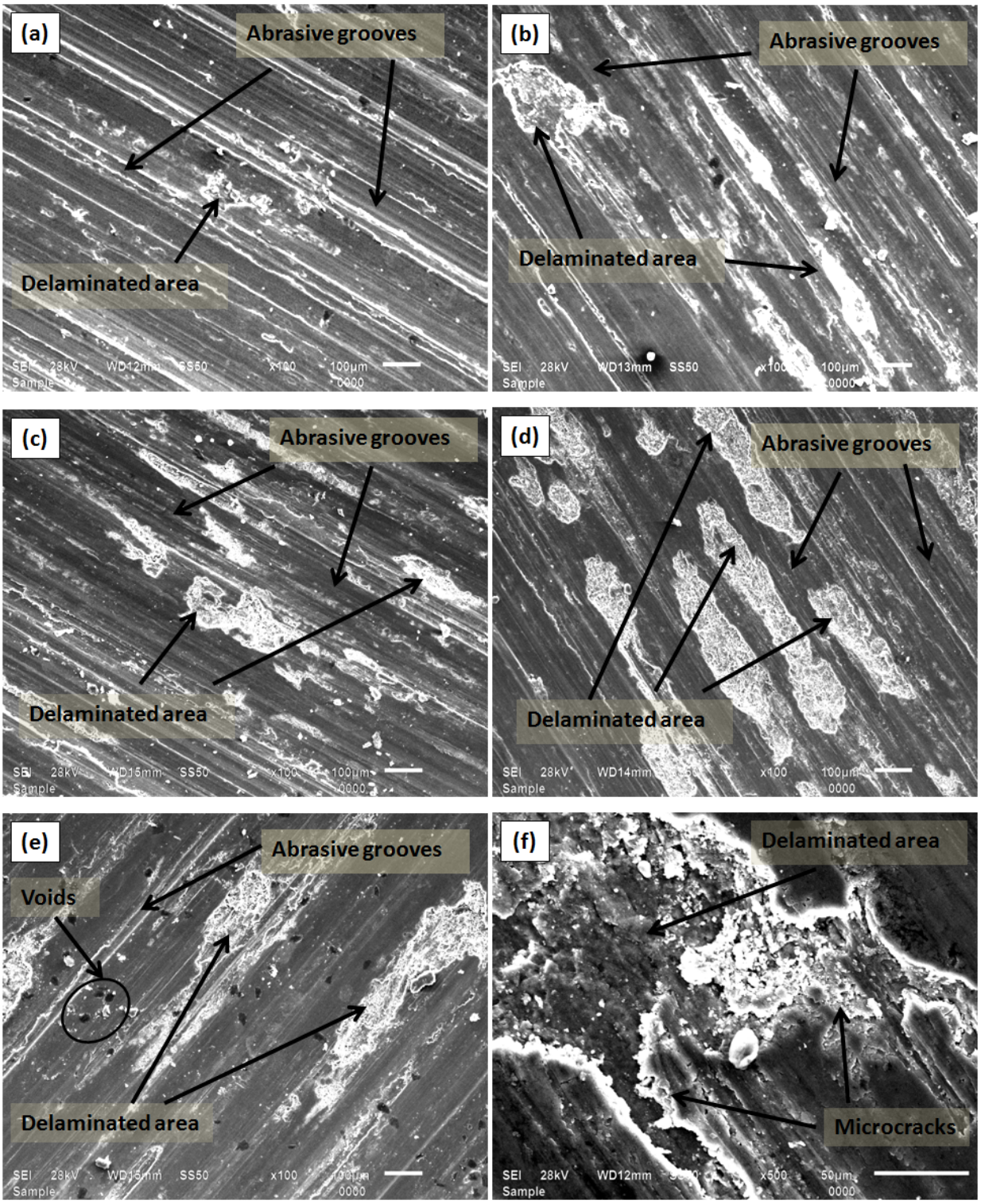

Figure 4.22: SEM images of the wear tracks for LM13/15%Zr composite reinforced with fine size particles tested at (a) 9.8 N, (b) 19.6 N, (c) 29.4 N, (d) 39.2 N, (e) 49 N and (f) higher magnification SEM image of worn track tested at 19.6 N.

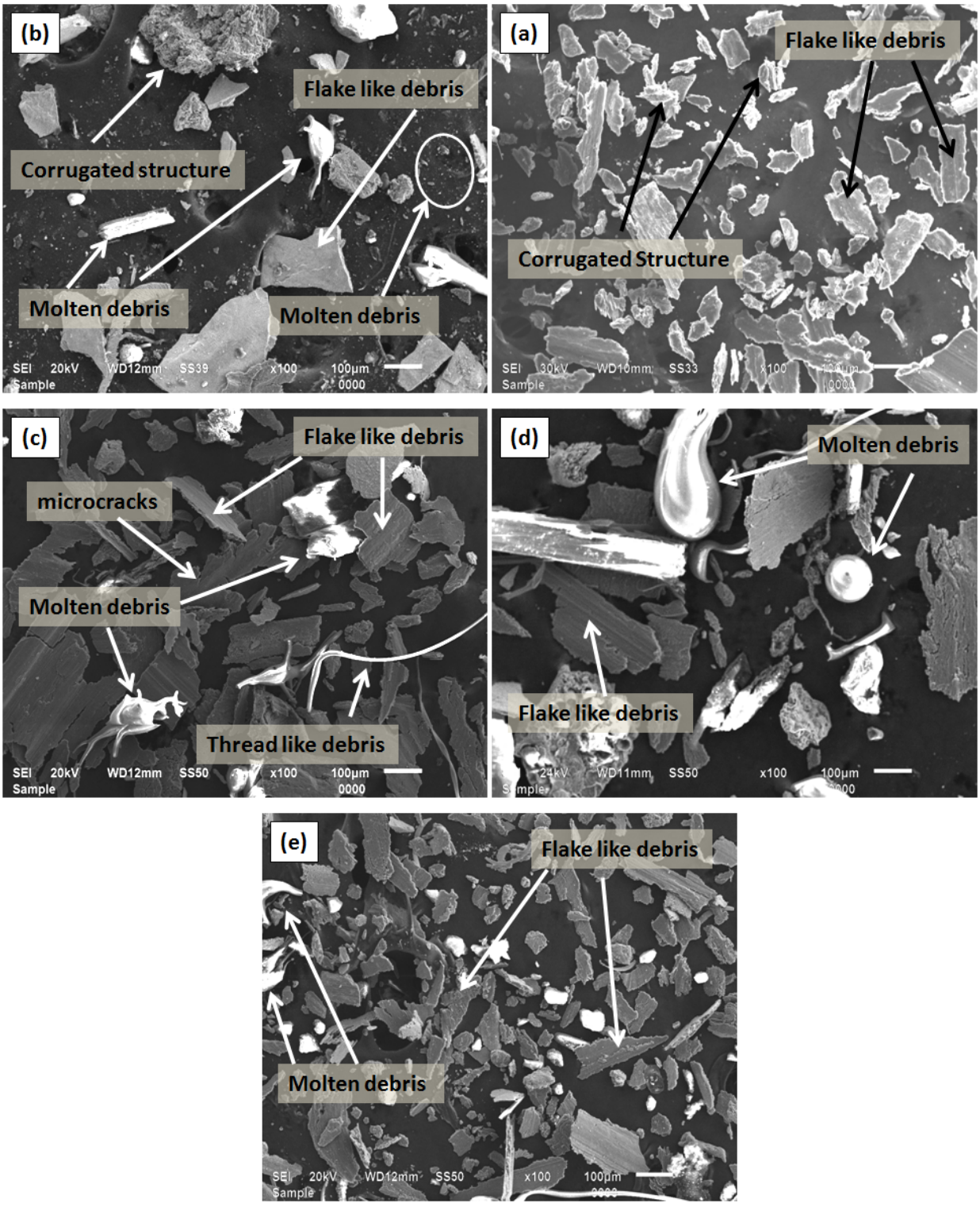

Figure 4.23: SEM images of the wear debris for LM13/15%Zr composite reinforced with fine size particles tested at (a) 9.8 N, (b) 19.6 N, (c) 29.4 N, (d) 39.2 N and (e) 49 N.

4.6.2 Analysis of worn surface and wear debris at different temperature conditions

Loose debris particles trapped between the specimen and the counterface causes a micro-ploughing on the contact surface of the composite. Majority of flakes have number of cracks due to repetitive stress occurred in sliding under high load. When the load is increased, the dominant wear mechanism delaminates and severe plastic deformation occurs. Wear debris generated at 49 N load as shown in Fig. 4.23e is having long flakes along with small flakes generated by delamination. Small flakes are generated by the crushing of the flakes at high load. Debris having long flakes as compared to debris generated at low load depicts the severe wear behavior. Figure 4.24 (a- d) shows the SEM images of the worn pin surface of LM13 alloy at high load (49 N) with variation in temperature. The worn surfaces of the base alloy pins tested at 49 N load were analyzed for specimens tested at 50 to 150 °C, as at higher temperature (above 200 °C) the sample pins were worn out. Figure 4.24a shows the worn surface of LM13 alloy tested at 50 °C, where formation of continuous wear grooves along with some damaged regions can be seen. Flow of materials along the sliding direction, generation of cavities due to delamination of surface material and tearing of surface materials can be seen as shown in Fig. 4.24(a). Figure 4.24b shows the wear track of matrix tested at 100 °C with greater depth of grooves and more delaminated material in comparison to the wear track of matrix tested at 50 °C. This indicates that the matrix shows higher wear rate at higher temperature. The presence of oxide layers can be clearly seen in the SEM micrograph (Fig. 4.24c) of LM13 alloy at 150 °C. Figure 4.24c indicates the simultaneous occurrence of formation and delamination of oxide layers on the worn surface. The onset of transition of mild to severe wear is observed at higher temperature (200 °C), as shown in Fig. 4.24d. High degree of flow of materials along the sliding direction, generation of cavities due to delamination of surface materials and tearing of surface materials are indications of the transition from mild to severe wear at higher temperature. Mondal *et al.* [22] suggested that flow of material in wavy form (serration) and large cavities due to delamination indicate the greater degree of softening of surface materials, partial melting of worn surface and localized adhesion between specimen surface and counter body. The SEM images (Fig. 4.24) also provide evidence that the wear rate of the alloy increases with an increase in temperature. A transition from mild to severe wear is also observed at higher temperature (above 150 °C). Wear products (debris) collected during the wear test yield valuable information about the wear mechanism of the specimen.

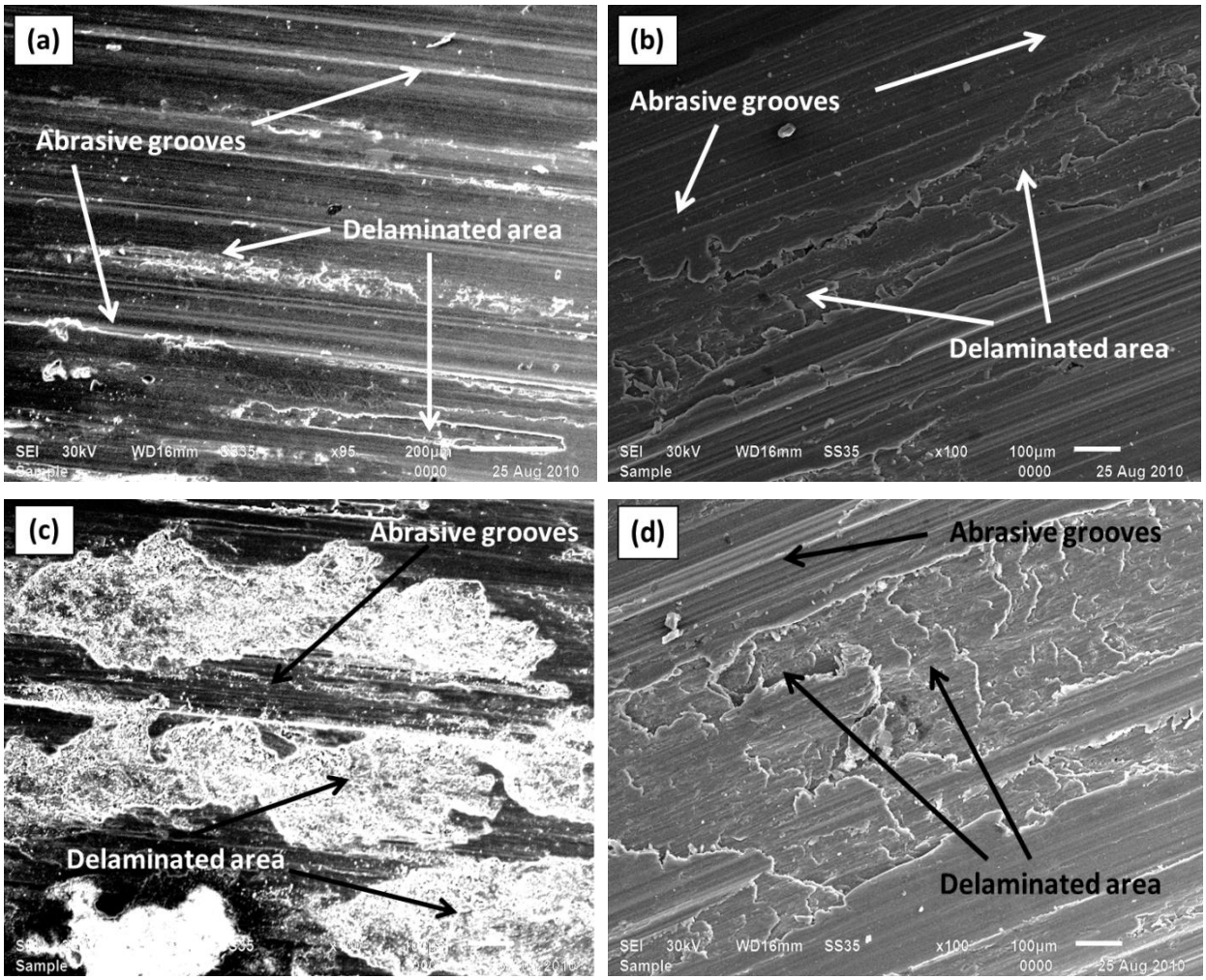

Figure 4.24: SEM images of wear surfaces of LM13 alloy at 49 N load with variation in temperature (a) 50˚C (b) 100˚C (c) 150˚C (d) 200˚C.

SEM images of the collected debris generated from LM13 base alloy at 49 N load and at different temperatures from 50 °C to 300 °C are shown in Fig. 4.25 (a- f). Figure 4.25a represents the SEM micrographs of debris of base alloy at 50 °C for 49 N load. Flake-like debris collected after wear test of the materials are of smaller size. These wear debris (flakes) indicate that adhesive wear dominates in the sliding direction during the test. Due to adhesive nature at high load, metal is removed in the form of flakes as debris. Small flakes are generated by crushing of longer flakes at higher load. Corrugated structure was observed in some debris, which may occur due to constant rubbing between contacting surfaces of sample and counterface. As the temperature is increased to 100 °C, the size of flakes becomes larger (Fig.

4.25b), which indicates that as temperature is increased, matrix becomes soft and wear resistance of the matrix is lowered. An increase in the amount of corrugated structured debris was observed in debris gathered in tests at 100 °C temperature. The elongated delaminated flakes in debris show grooves that indicate that they come out due to shearing of layer in the direction of applied force. At a much higher temperature, around 150 °C or higher, the alloy shows an onset of transition from mild to severe wear. The size and amount of debris collected are much greater than at lower temperature. At higher temperature (Fig. 4.25c–f), thread type morphology is found along with the presence of delaminated plate like debris with microcracks. Thread type debris are created during the pulling out of aluminum matrix in tests at high load and high temperature. The size of debris at high temperature, more than 150 °C (Fig. 4.25d–f), indicates that severe wear dominates for the alloy at this condition (high temperature and high load). In Fig. 4.25d some debris that solidified from the molten state was also observed at higher temperature (200 °C). Its amount and also the amount of delaminated debris was increased at 250 °C and 300 °C temperatures (Fig. 4.25e-f). Some thread like debris corresponding to α Al are trapped in between the grooves and acquire round shape. Due to continuous rubbing action, these get heated and reached the melting point of metal. This can be seen in Fig. 4.25 (e and f). At high temperature, the presence of partially molten state of debris may contribute to an increase in the wear rate of the alloy.

Figure 4.26 (a- d) shows the SEM images of worn surfaces for the composite containing 15 wt.% of coarse size zircon sand particles tested at 9.8 N load with variation in ambient temperature from 150 ºC to 300 ºC respectively.

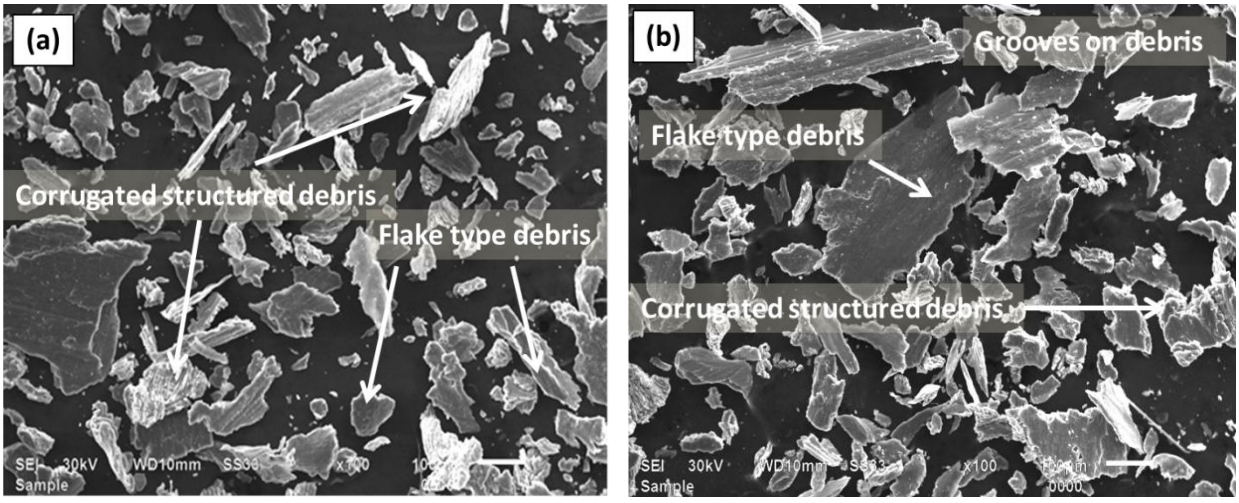

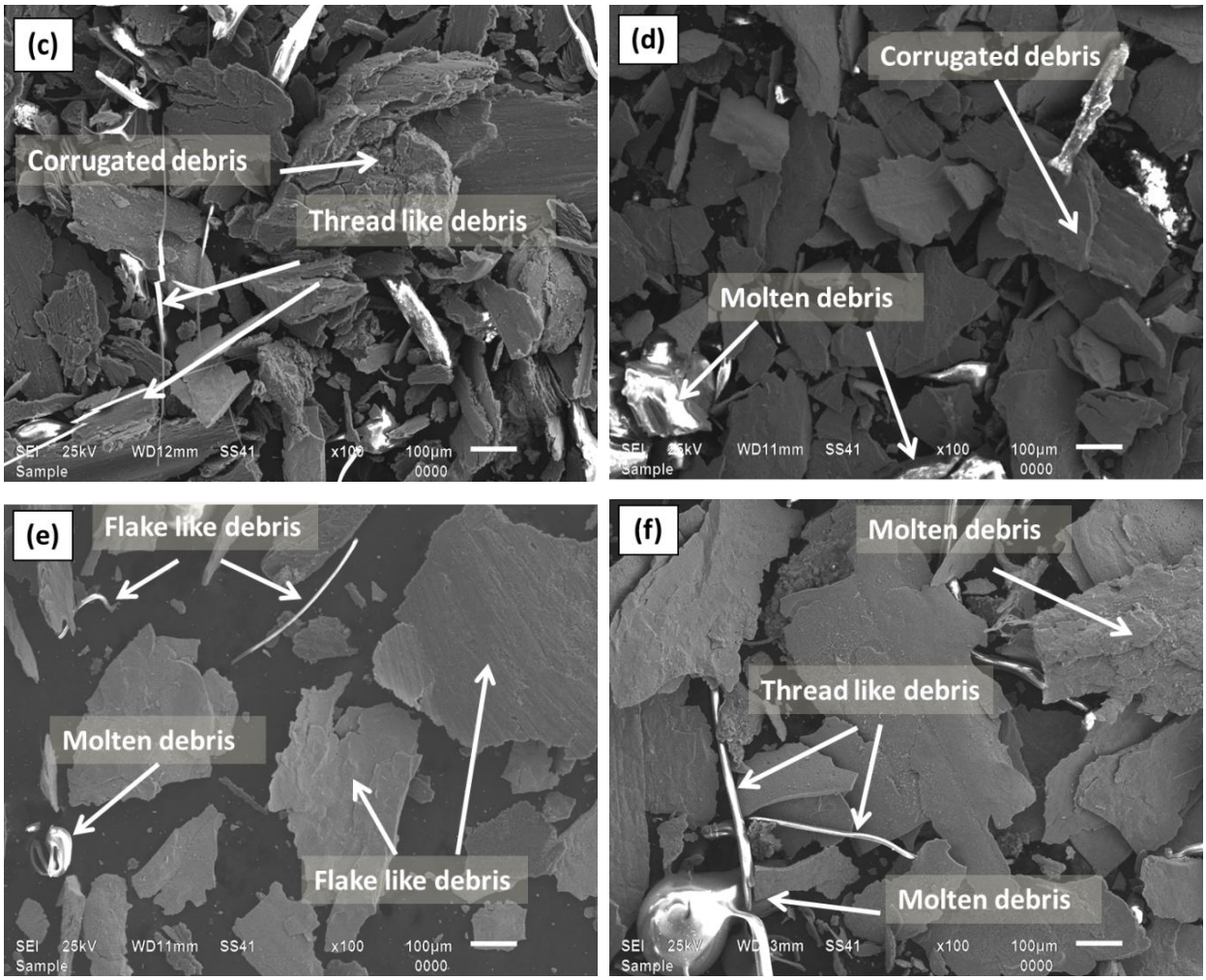

Figure 4.25: SEM micrographs of wear debris of LM13 alloy at high (49 N) load with variation in temperature (a) 50˚C (b) 100˚C (c) 150˚C (d) 200˚C (e) 250˚C and (f) 300˚C.

Figure 4.26a indicates the presence of grooves and voids with the delaminated area which is due to the continuous sliding of trapped zircon sand particles in the matrix during the wear test for the LM13/15wt.%Zr composite tested at 150 °C with 9.8 N load. These trapped particles support the wear resistance by transferring the load during wear test. Lower thermal expansion coefficient of the zircon sand particles in comparison to the matrix also make the composite more wear resistive at higher temperature.

An improved wear resistance in comparison to the base alloy can be observed as depth of grooves and delaminated area is smaller. Figure 4.26b shows SEM micrograph of worn pin surface of the LM13/15%Zr composite at 9.8 N loads, tested at 200 °C. At 200 °C with 9.8 N load, the wear track of LM13/15%Zr composite seems to be smooth, except for a few deep

grooves, as shown in Fig. 4.26b. At 250 °C with 9.8 N load, ruptured oxide layer with more delaminated area can be observed (Fig. 4.26c). At 300 ºC, LM13/15%Zr composite exhibits the worn surface with much more delaminated area and some sign of chipping out of particles during wear test, which is responsible for the higher wear rate as shown in Fig. 4.26d.

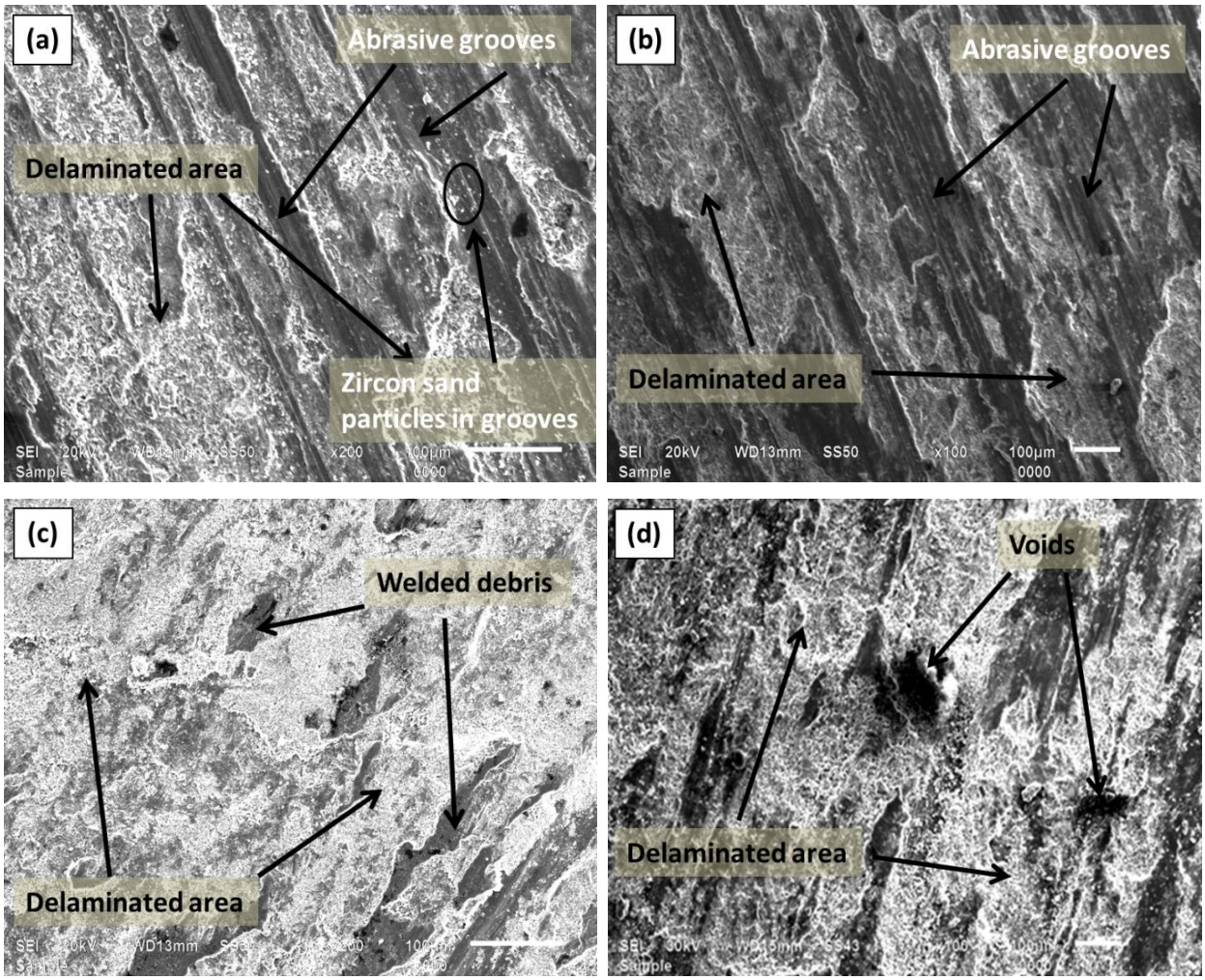

Figure 4.26: Wear track of LM13/15%Zr composite reinforced with coarse size particles tested at 9.8 N load at (a) 150 °C (b) 200 °C (c) 250 °C and (d) 300 °C.

Figure 4.27 shows the collected debris of the LM13/15wt.%Zr composite reinforced with coarse size particles for 9.8 N load at different temperatures. Figure 4.27a shows the wear debris collected for 9.8 N load at 150 ºC. These debris are of flakes type with rough edges which indicates the delamination of material by the propagating crack and microcutting at edges. With increasing the temperature from 150 to 200 ºC, amount and size of debris decreases which

supports the decrement in wear rate in this condition. This is also observed in Fig. 4.16a. At 200 ºC and 9.8 N load, size of debris increases which reveals the increment in wear rate. This is due to softening of matrix at higher temperature. At much higher temperature (300 ºC), large size of flakes is observed, which is due to the chipping out of the soften material. However, presence of grooves and corrugated structure on the debris also indicates about high wear rate.

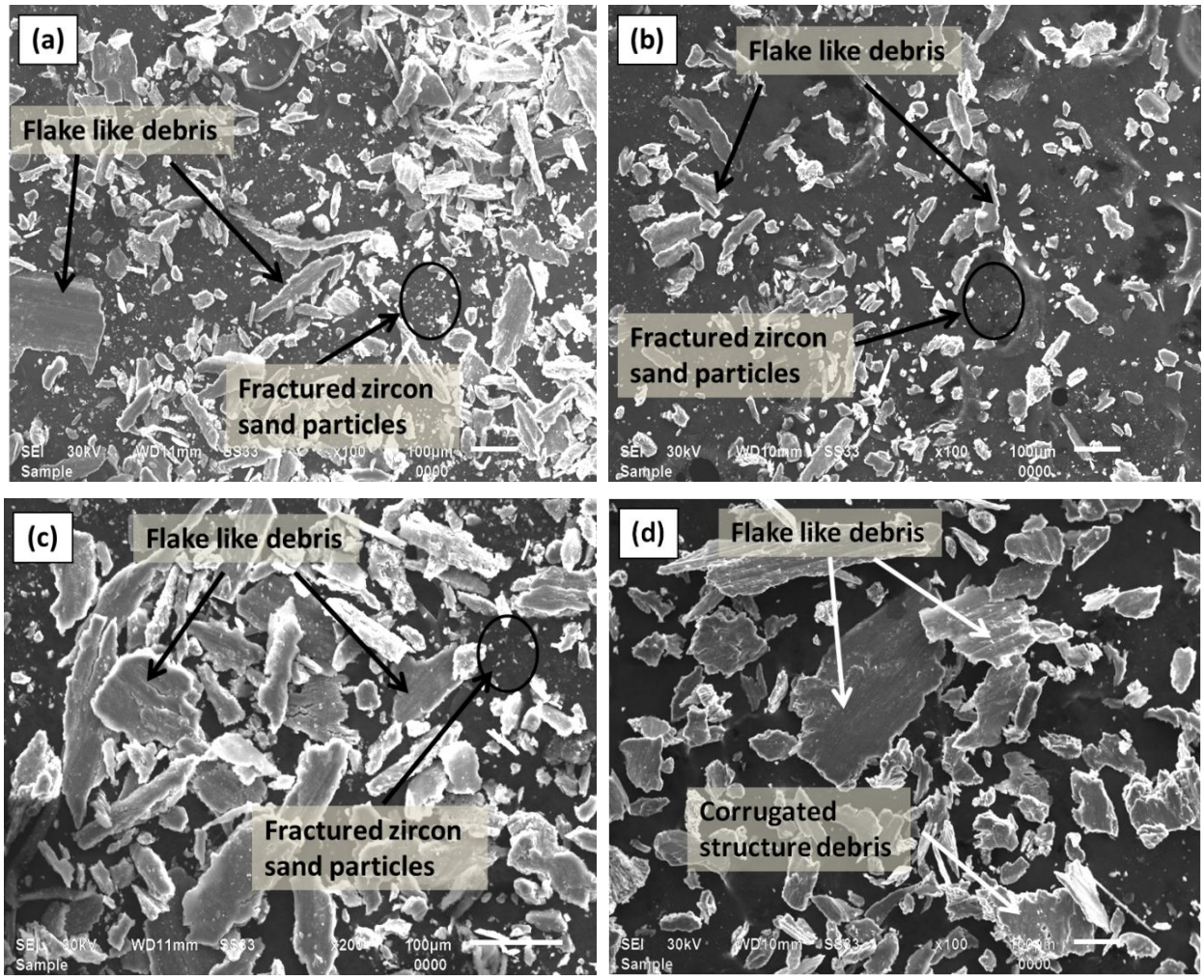

Figure 4.27: Wear debris of LM13/15%Zr composite reinforced with coarse size particles tested at 9.8 N load at (a) 150 °C (b) 200 °C (c) 250 °C and (d) 300 °C.

Figure 4.28 (a-d) shows the SEM images of worn surfaces of LM13/15wt.%Zr composite reinforced with fine size of zircon sand particles tested at 9.8 N load with varying the temperature from 150 ºC to 300 ºC. Figure 4.28a shows the SEM images of wear track taken after the wear test at 9.8 N load and 150 ºC. Grooves with delaminated area are clearly observed

in the micrograph. However, some loosely bonded zircon sand particles are also seen on the worn surface.

Sign of microcraks on the edges of delaminated area indicates the delamination through the crack propagation. Figure 4.28b shows the micrograph of the wear track taken at 9.8 N load and 200 ºC. Lesser delaminated area and grooves with lower depth in comparison to the Fig. 4.28a indicates the low wear rate of the material. At higher temperature (250 ºC) larger delaminated area with bright patches indicates the higher wear rate due to tearing of oxide layers (Fig. 4.28c). With increase in the temperature upto 300 ºC worn surfaces is much rougher as deeper grooves with crates are present on the worn surface, which indicates the higher wear rate (Fig. 4.28d).

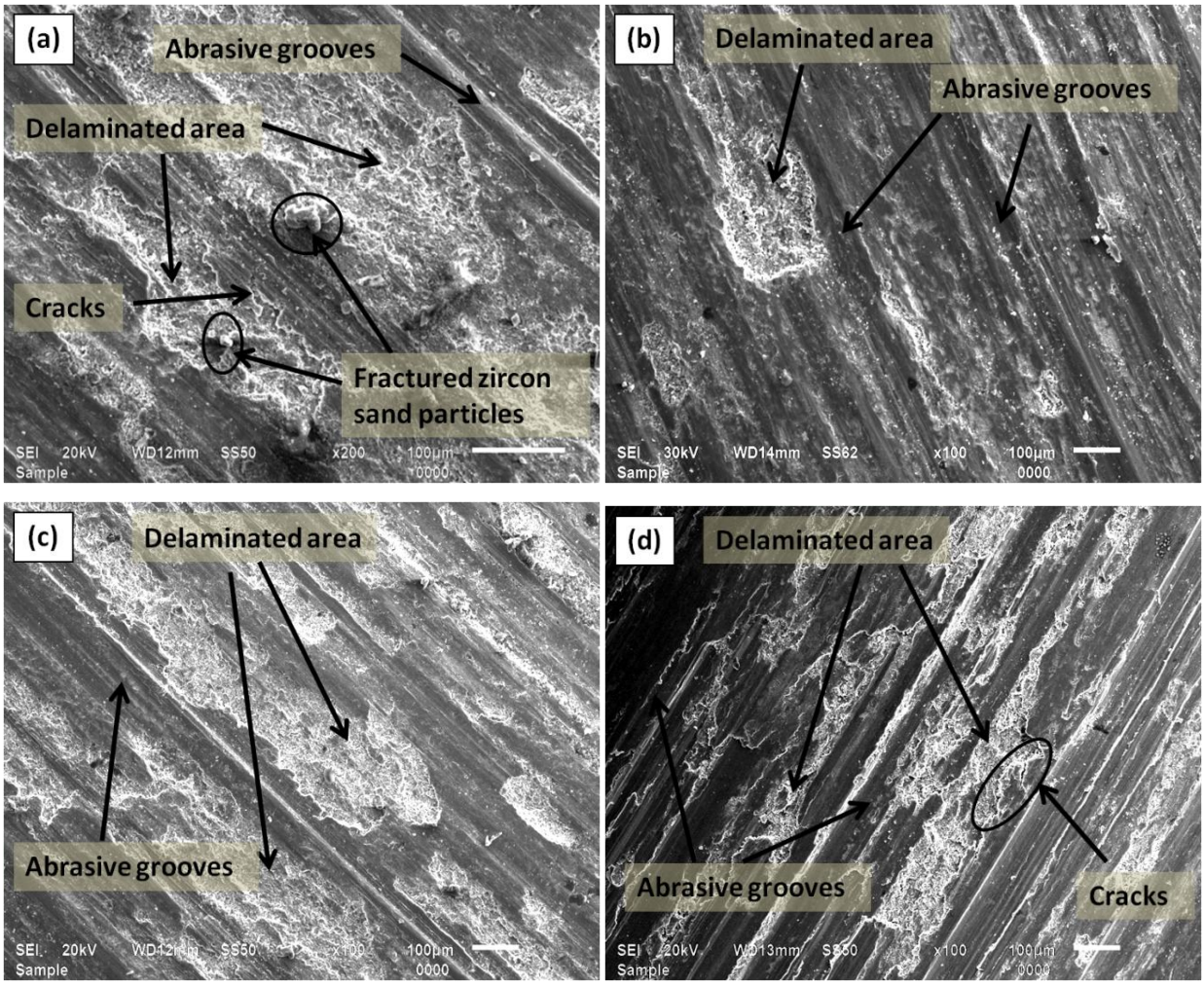

Figure 4.28: Wear track of LM13/15%Zr composite reinforced with fine size particles tested at 9.8 N load and at (a) 150 °C (b) 200 °C (c) 250 °C and (d) 300 °C temperatures.

Figure 4.29 (a- d) shows the wear debris of LM13/15%Zr composite tested at 9.8 N load at different temperatures. Figure 4.29a shows the wear debris of the composite collected at 9.8 N load and 150 °C condition. Flake type debris with corrugated structure and brighten phase indicates the delamination of matrix due to continuous rubbing of material. With increasing the temperature to 200 °C (Fig. 4.29b), size of debris increased but thickness was reduced which indicates the better wear resistance under this condition. The decrement in wear rate is due to formation of oxide layers at 200 °C. At 250 °C and 300 °C with 9.8 N load, collected debris are shown in Fig. 4.29 (c & d) respectively. Larger amount and size of debris with debonded zircon sand particles indicates the higher wear rate. Rough edges with corrugated structure show the removal of materials by continuous rubbing during the wear test.

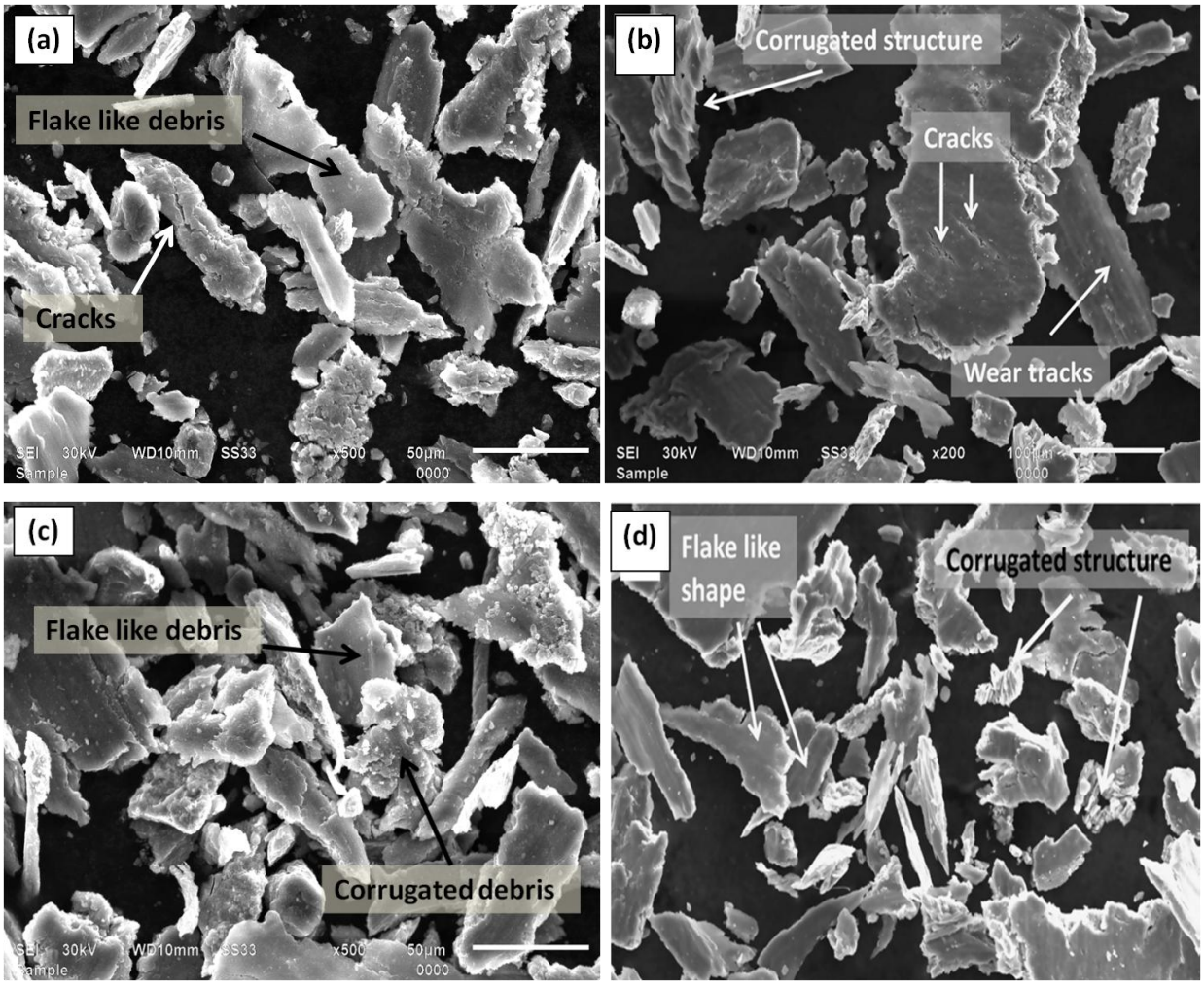

Figure 4.29: Wear debris of LM13/15%Zr composite reinforced with fine size particles tested at 9.8 N load and at (a) 150 °C (b) 200 °C (c) 250 °C and (d) 300 °C temperatures.

Figure 4.30(a- d) represents the worn surface of the LM13/15%Zr composite after tests at high load (49 N) with temperatures ranging from 150 °C to 300 °C. Fig. 4.30(e & f) shows the SEM image of the wear track and the corresponding EDS spectra of the wear track of the composite tested at 49 N load and at 200 °C. Figure 4.30a shows the worn surface of the LM13/15%Zr composite tested at high (49 N) load and at 150 °C temperature. The formation of grooves and small delamination is observed in Fig. 4.30a. Depth of grooves and amount of delamination in the LM13/15%Zr composite are smaller in comparison to the matrix at same temperature and load, which indicates the better wear resistance of the composite with respect to alloy. Fractured zircon sand particles were also observed in the grooves. These trapped particles in grooves help to prevent the delamination of matrix. As the temperature is increased from 150 °C to 300 °C, the composite also shows increment in delaminated area along with presence of oxide layers. However, when compared these SEM images (Fig. 4.30) with those of the matrix (Fig. 4.28), it is observed that there is improvement in wear resistance of the composite in comparison to that of the alloy, particularly at high temperature. This improvement in wear resistance of material is due to presence of reinforced zircon sand particles. Figure 4.30(a-f) reveals that both adhesive and abrasive wear mechanisms contribute to wear of samples. Zahmatkesh *et al.* [23] have also discussed their results based on SEM images which showed metal flow related to the adhesive wear mechanism and plowed grooves that are indicative of abrasive wear mechanisms. The parallel and continuous scratches suggest abrasive wear as characterized by the penetration of the hard zircon sand particles into the softer surface, which is an important contribution to the wear behavior of LM13/zircon composites. The groove on the worn surface indicates the removal of thick oxide layers. SEM image of wear track at higher magnification (Fig. 4.30e) shows the presence of microcracks, which are developed during wear test. These microcracks are the main source of delamination or removal of the material during the wear test. In the area around the cracks where delamination has occurred, a ‘mechanically mixed layer’ containing Fe from the counterface as well as oxides and other elements from the test pin are clearly seen in Fig. 4.30e.
The delaminated area shown in the SEM micrograph in Fig. 4.30f indicates the presence of an oxide layer on the worn surface. This supports the formation of a wear protective oxide layer on the load bearing surfaces at higher temperature. The oxide layer poses a greater resistance to sliding wear and friction, as oxide debris reduces the extent of direct metal to metal contact.

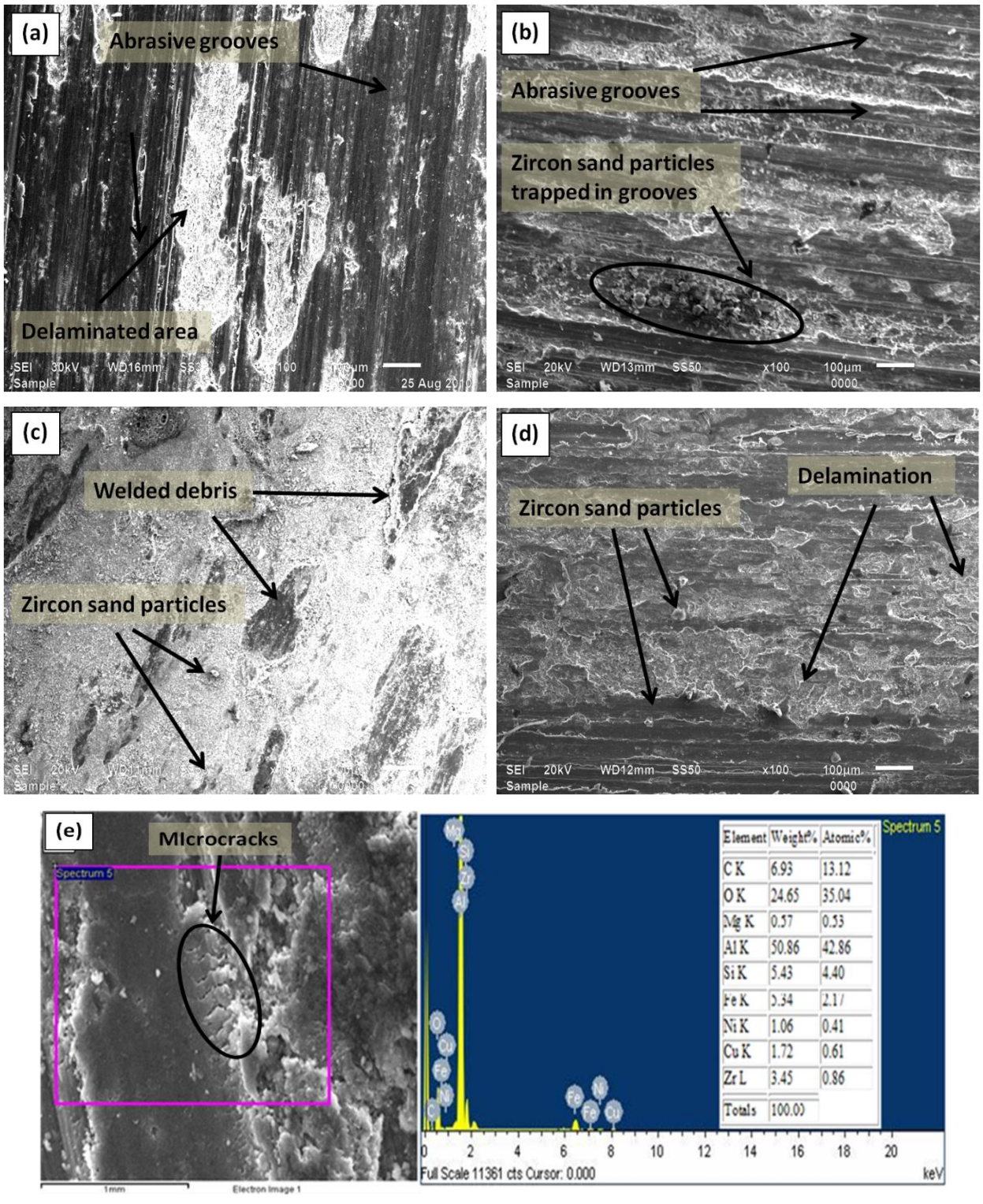
(a)
Abrasive grooves
Delaminated area
(b)
Abrasive grooves
Zircon sand particles trapped in grooves
(c)
Welded debris
Zircon sand particles
(d)
Delamination
Zircon sand particles
(e)
MIcrocracks
Spectrum 5
Element | Weight% | Atomic%
C K | 6.93 | 13.12
O K | 24.65 | 35.04
Mg K | 0.57 | 0.53
Al K | 50.86 | 42.86
Si K | 5.43 | 4.40
Fe K | 5.54 | 2.17
Ni K | 1.06 | 0.41
Cu K | 1.72 | 0.61
Zr L | 3.45 | 0.86
Totals | 100.00
Full Scale 11361 cts Cursor: 0.000
keV

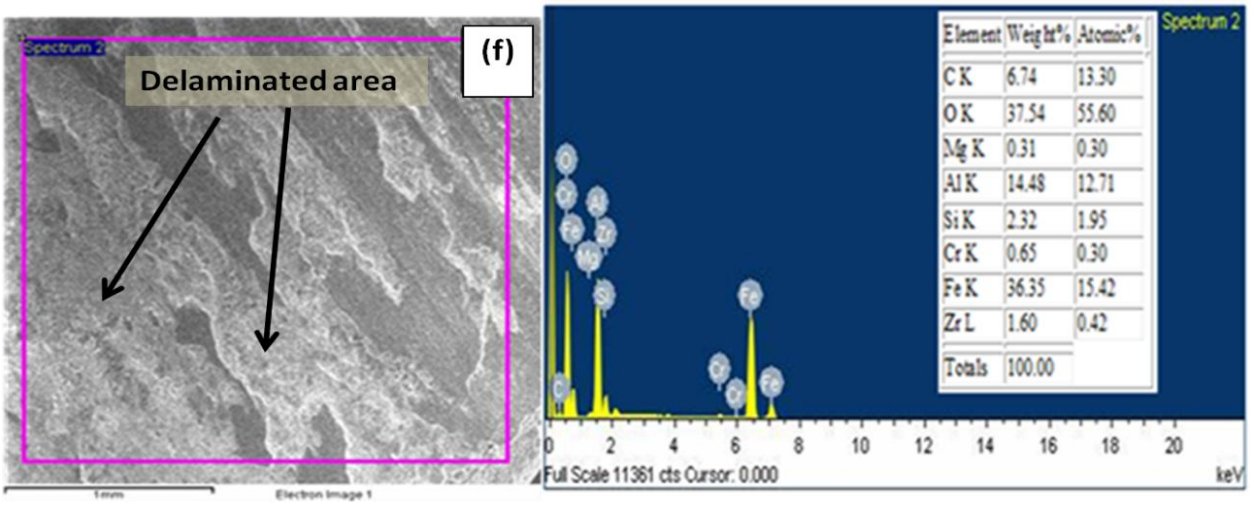

Figure 4.30: SEM images of wear tracks of LM13/15% Zr composite with coarse size particles at 49 N load with variation of temperature (a) 150˚C (b) 200˚C (c) 250˚C and (d) 300˚C (e) SEM images of the wear track at higher magnification (f) EDS of wear track of composite at 200 ºC.

The formation of chemically reacted oxide layer is the result of the oxidation of the exposed metal surface during relative motion. It was also observed that with increasing concentration of zircon sand in LM13 base alloy, grooves become larger with more depth along the direction of sliding. As the concentration of reinforced particles increases, the amount of debris/breaking of sand particles is greater. Banerji *et. al*. [12] have also reported that the zircon sand particles fracture during the wear process at higher load. Fractured particles thereby lose their effectiveness as load-bearing components and the removal of material progresses by the fracture of the particles. However, these fractured particles are trapped in the grooves (Fig. 4.30 b and d). Larsen *et. al.* [24] have also stated that craters are formed on a material's surface under conditions where the grit was trapped (but could still rotate) between the counter face and the specimen. Trapped grit particles that could not rotate resulted in micro grooving of the material's surface. Same type of structural features of microgrooves can be easily seen in SEM micrographs of the composite at higher temperature (Fig. 4.30d).

In order to know the presence of different elements on the worn surface, X-ray dot mapping was also carried out. The presence of different elements on the worn surface is shown in Fig. 4.31. The dot mapping clearly indicates the presence of an oxide layer (Al_2O_3/Fe_2O_3) in the worn out area in which delamination has occurred. Moreover, Si is uniformly distributed throughout the matrix. Presence of Fe confirms the formation of a mechanically mixed layer on the surface. It

also confirms the good bonding of the zircon sand particles with matrix, as these particles are seen inside the mapped area.

Fig. 4.32(a-d) shows the surface morphology of debris collected from LM13/15%Zr composite tested at 49 N load at different temperature from 150 °C to 300 °C. Fig. 4.32 indicates that the amount and size of wear debris of composite is reduced in comparison to that of the matrix specimens (Fig. 4.25) at all temperatures. This is due to the improvement in the wear resistance of the composite after addition of zircon sand as shown in Fig. 4.18. As the zircon sand particles have low coefficient of thermal expansion as compared to LM13 alloy, their presence in matrix improves the overall thermal stability of composite [24]. Hence composites containing a higher amount of zircon sand in the matrix will show better thermal resistance in comparison to base materials. Among the studied composites, LM13/15% Zr composite shows better wear and thermal resistance. SEM image of debris collected after the wear test as shown in Fig. 4.32a gives idea about the wear mechanism of LM13/15%Zr composite at 150 °C at 49 N load. The reduced size of debris of the composite as compared to the base alloy is due to higher hardness of composite, which improves the wear resistance of material. Delamination, multiple ploughing action and shearing features were also observed in Fig. 4.32a. Fragmentation of debris was observed, which may be due to continuous rubbing of delaminated flakes between the contacting surfaces. Debris trapped in wear tracks leads to a corrugated structure. Some fractured zircon sand particles were also observed as shown in Fig. 4.32(a-d).

Dwivedi [25] suggested that a wear particle is detached due to tangential forces acting on surfaces causing nucleation of cracks at surface, which propagate in due course of time causing exposure of fresh surface followed by delamination. Fracture of particulates may arise from either strain transfer to the reinforcement interface from the matrix undergoing plastic deformation in the wear zone or from cracks initiated when the hard particulates are ground against each other and are crushed by striking asperities on the opposing steel counterface. When temperature was increased to 150 °C and 200 °C, the size of debris was increased in comparison to previous ones. Fractured zircon sand particles and corrugated structured debris with delaminated flakes were also observed as shown in Fig. 4.32 (b & c). SEM images of debris collected at higher temperature (Fig. 4.32a- d) indicate smaller size of debris in presence of fractured particles and molten state in same portions of the matrix.

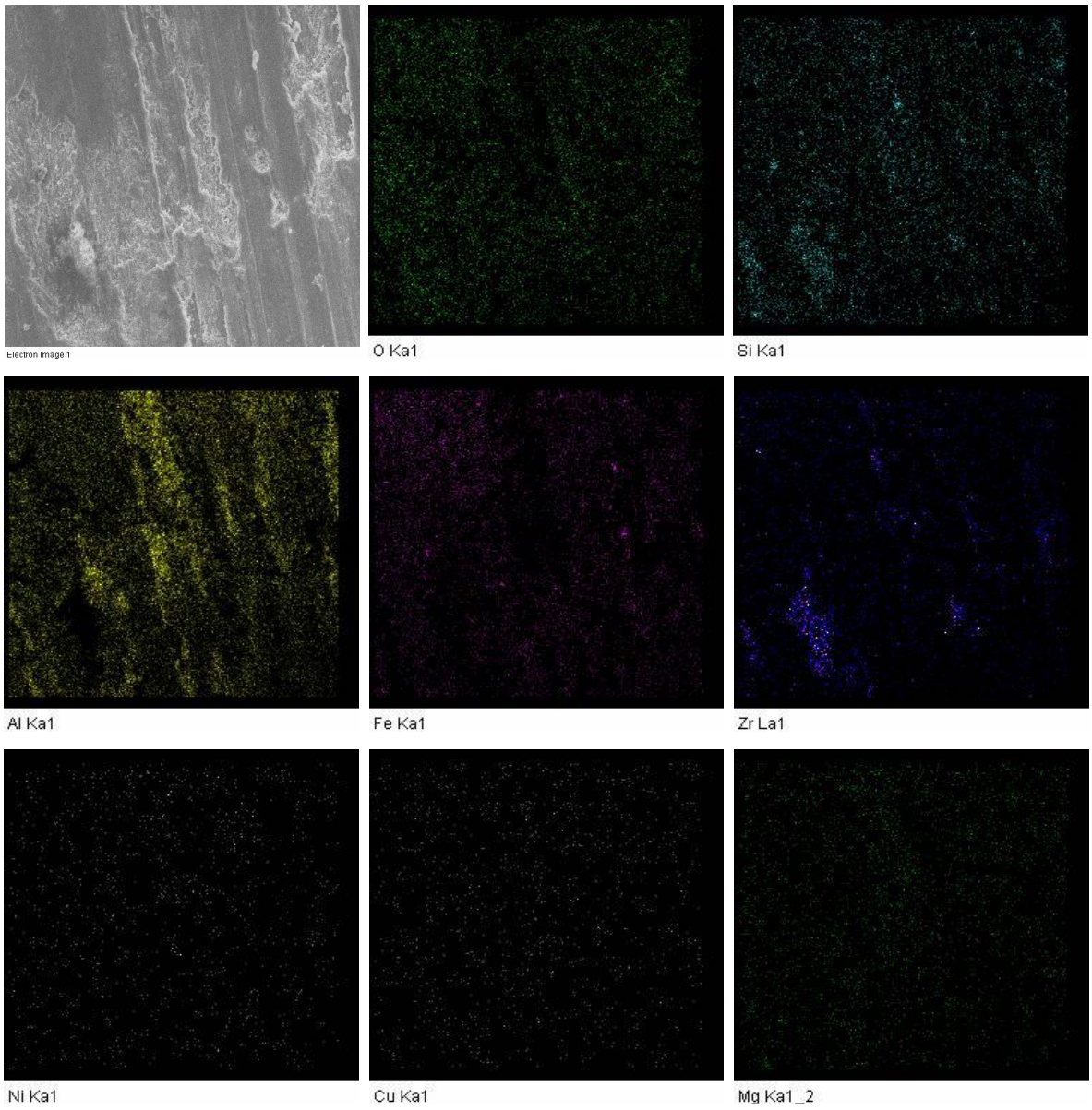

Figure 4.31: X-ray dot mapping from EDS of wear track of the composite.

At elevated temperatures, cavities or voids which are created by particulates fracturing in the subsurface wear zone are liable to be healed by extrusion of the matrix alloy into the region formed between newly fractured particulates [25, 20]. The combined process of particulate fracture and matrix extrusion in the subsurface wear region is responsible for the formation of the characteristic comminuted particulate transfer layers (mechanically mixed layer), which are highly beneficial to matrix composite wear. The X-ray dot mapping confirms such type of

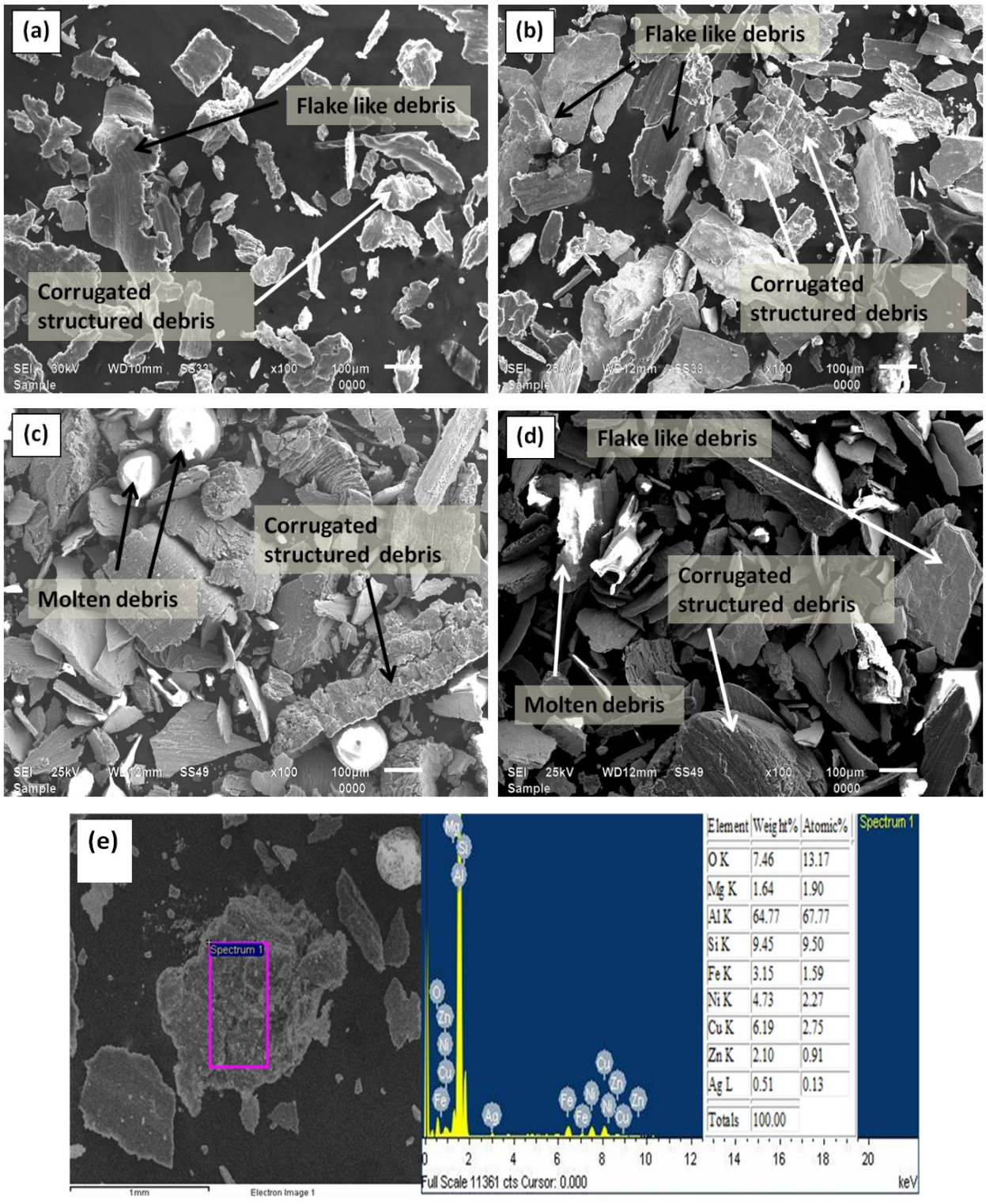
(a)
Flake like debris
Corrugated structured debris
(b)
Flake like debris
Corrugated structured debris
(c)
Corrugated structured debris
Molten debris
(d)
Flake like debris
Corrugated structured debris
Molten debris
(e)
Spectrum 1
Element | Weight% | Atomic%
O K | 7.46 | 13.17
Mg K | 1.64 | 1.90
Al K | 64.77 | 67.77
Si K | 9.45 | 9.50
Fe K | 3.15 | 1.59
Ni K | 4.73 | 2.27
Cu K | 6.19 | 2.75
Zn K | 2.10 | 0.91
Ag L | 0.51 | 0.13
Totals | 100.00
Full Scale 11361 cts Cursor: 0.000
keV

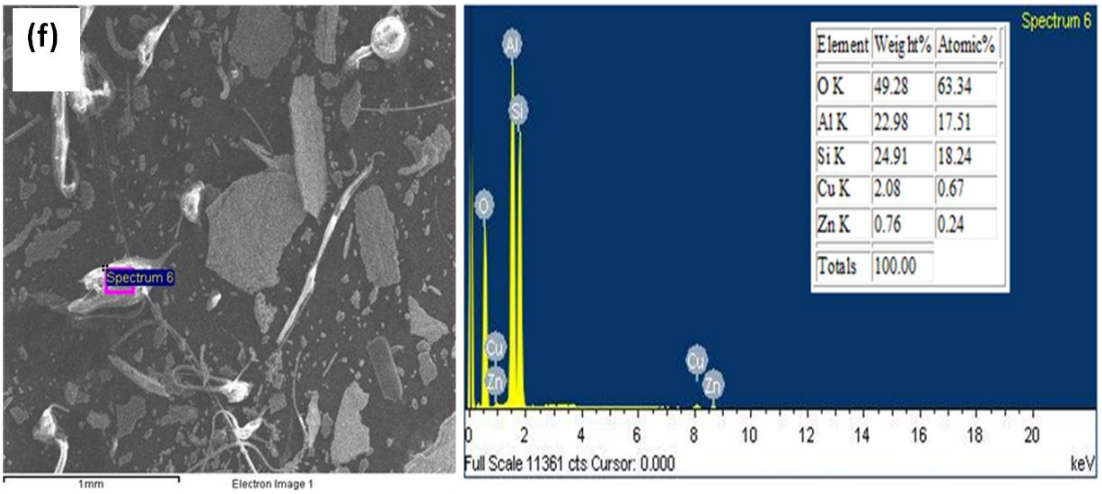

Figure 4.32: SEM images of wear debris of LM13/15% Zr composite with coarse size particles at 49 N load with variation of temperature (a) 150˚C (b) 200˚C (c) 250˚C (d) 300˚C and (e & f) EDS analysis of the wear debris LM13/15%Zr composite at 49 N load.

transition (Fig. 4.31). The step clearly observed in Fig. 4.32 (c & d), may be due to slip to the Al and zircon sand interfaces due to constant rubbing between the wear surfaces. It is also observed that these debris particles undergo multiple ploughing actions, causing cracking in them, which can be seen in delaminated debris marked in Fig. 4.32c. Figure 4.33 (e & f) shows the EDS analysis of debris collected after the wear testing of the LM13/15% Zr composite at 250 °C temperature. EDS analysis of these debris indicate the presence of Al, Si, Fe and O elements. Figure 4.32e shows the EDS spectra of the delaminated debris and Fig. 4.32f shows the EDS spectra of spherical debris which is trapped inside the grooves and got melted due to multiple rubbing action during the wear test. Figure 4.32e also shows the presence of Fe in the debris collected after wear testing. Its presence may be due to the transfer of steel counterface material to the composite surface. The transfer of steel inclusions from counterface surfaces to the composite wear surfaces is another mechanism which contributes to increase in wear resistance of the composites. Here, inclusions may act as additional reinforcement at the wearing surface of the composite [20].

The X-ray diffraction pattern of debris collected after the wear test conducted at 49 N load and 300 °C is shown in Fig. 4.33. Fig. 4.33 also indicates the presence of Al_2SiO_5, Si and $ZrSiO_4$ phase along with Fe. This indicates that apart from base metal, zircon is also coming out from the surface.

Figure 4.34 (a- d) shows the SEM images of wear tracks of LM13/15%Zr composite containing fine size of zircon sand taken at 49 N loads with high temperatures 150, 200, 250 and 300 °C

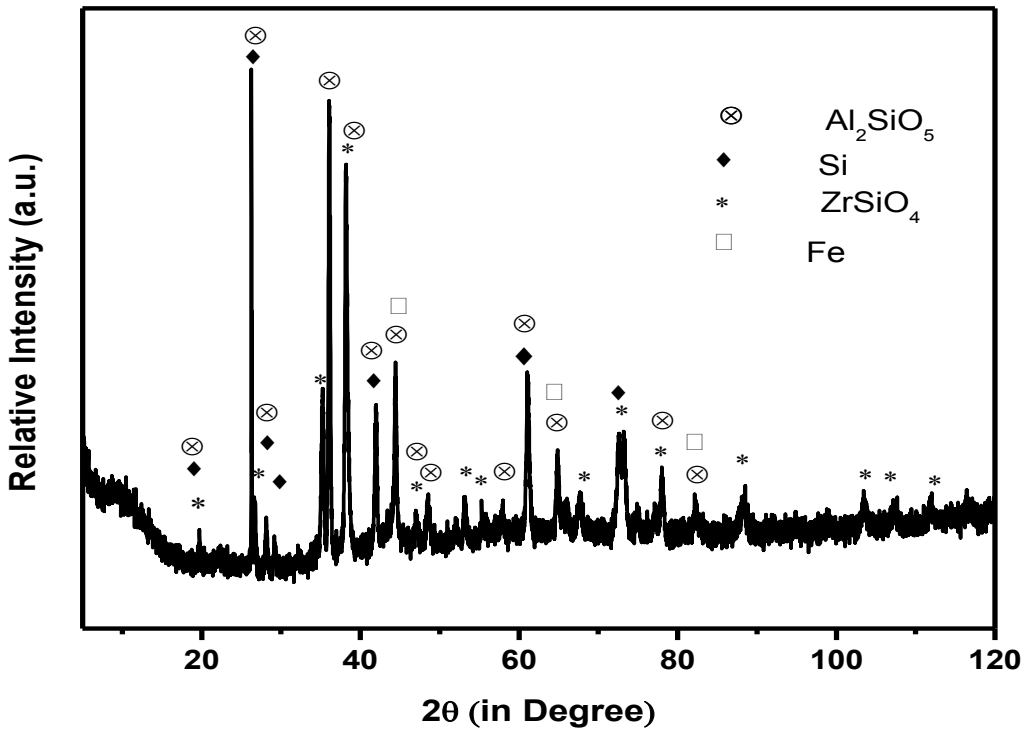

Figure 4.33: XRD pattern of debris of LM13/15%Zr composite at 49 N load and 300˚C.

respectively. Deeper grooves with fractured zircon sand particles along with the delaminated area in the SEM images of the composite indicate the higher wear rate at 150 °C and 49 N load (Fig. 4.34a). However, at much higher temperature (200 °C), due to formation of oxide layer, lower damaged area and low depth of grooves reveals the lower wear rate (Fig. 4.34b) in comparison to the worn surface observed at 150 °C. The wavy pattern of these grooves results from the ploughing action of particles followed by plastic deformation during the wear test. Mondal et al. [22] suggested that the flow of material in wavy form (serration) and large cavity are due to delamination. At higher temperature, the greater degree of softening of surface materials, partial melting of worn surface and localized adhesion between specimen surface and counter body are responsible for the mild to severe wear followed by delamination of the composites as shown in Fig. 4.34 (a- d). With increase in temperature up to 250 °C, the subsurface and surface cracks are visible. The SEM micrograph of composite (Fig. 4.34c) at operating temperature of 250 °C shows large plastic deformation in addition to abrasion action of

zircon sand particles. It shows high degree of flow of materials along the sliding direction, which generates cavities due to tearing and delamination of surface materials causing a transition from mild to severe wear at high temperature. The crack propagation is along the sliding direction and also in perpendicular direction of sliding, which results in material removal by delamination. Sudarshan *et al.* [26] in their work have reported that the void nucleation around the second phase particles in the deformed region and their subsequent growth and linkage parallel to surfaces occurs.

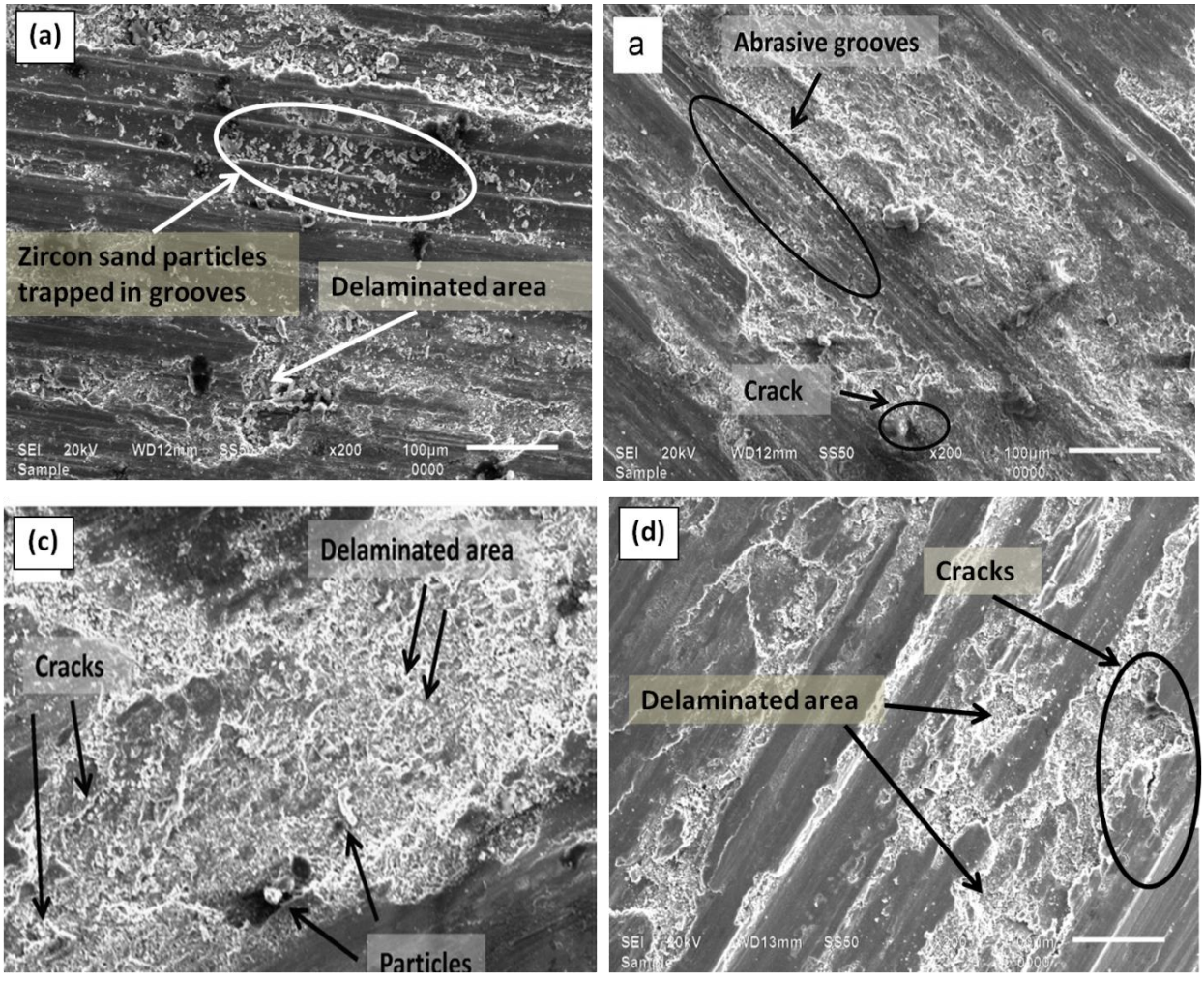

Figure 4.34: SEM images of wear tracks of LM13/15%Zr composite with fine size particles at 49 N load with variation of temperature (a) 150˚C, (b) 200˚C, (c) 250˚C and (d) 300˚C.

This leads to the delamination of subsurface layers and finally to the material loss in the form of plate like debris. At higher temperature (250 °C) the worn surface shows the oxide cover over a

thick area along with fresh surface of aluminum as shown in Fig. 4.34c. The depth of micro-ploughing increased with increasing temperature (300 °C) and new large cavity oxide area is created at this temperature. Presence of cracks also supports the delamination of material due to crack propagation during wear test. However, at 300 °C with 49 N load, composite undergoes for higher wear rate, as deeper grooves with craters are observed in the SEM images of worn surface (Fig. 4.34d).

Figure 4.35 (a- d) shows the SEM images of wear debris for LM13/15%Zr composite containing fine size of zircon sand particles collected at 49 N load at 150, 200, 250 and 300 °C respectively. Flakes generated by cutting action along with delaminated flakes are also observed for the composite at 49 N load. Layered structure of debris in Fig. 4.35a is due to the removal of material in continuous sliding action during the wear test. The flakes having microcracks indicates that the removal of material is also due to crack propagation and delamination. As temperature is increased up to 200 °C, lager size of debris with thinner shape indicates the lower wear rate at higher (49 N) load. Severe wear at higher load and higher temperature is observed in Fig. 4.35b. The smaller debris are agglomerated along with the larger debris due to thermal mechanical welding by repetitive forces during sliding [25]. At higher load and higher temperature, the thread type debris created during the pulling out of aluminum metal is observed in Fig. 4.35b. The oxide debris are created at higher temperature with high load. In Fig. 4.35c at 250 °C temperature, these oxide (Al_2O_3/Fe_2O_3) debris help to reduce the wear rate of composite at higher load as they keep on rotating inside the grooves. In this figure, the small size debris with fine thickness and some corrugated structure are observed. However, some plate like debris with large size are also observed in this micrograph, which indicate the presence of both abrasive and adhesive wear mechanism. The elongated delaminated debris having grooves indicate that these come out due to shearing action of the layer in the direction of applied force. As shown in Fig. 4.35d, these debris undergo multiple ploughing actions causing cracking in it. Moreover, it appears that some of the debris have undergone melting. This is because of generation of high temperature during sliding action in wear test. The sub-surface cracks may be responsible for generating the wear debris. These wear scars are the primary characteristic of abrasive wear. The size of craters and wear debris do not match. In general, wear debris particles are very small than the craters [25].

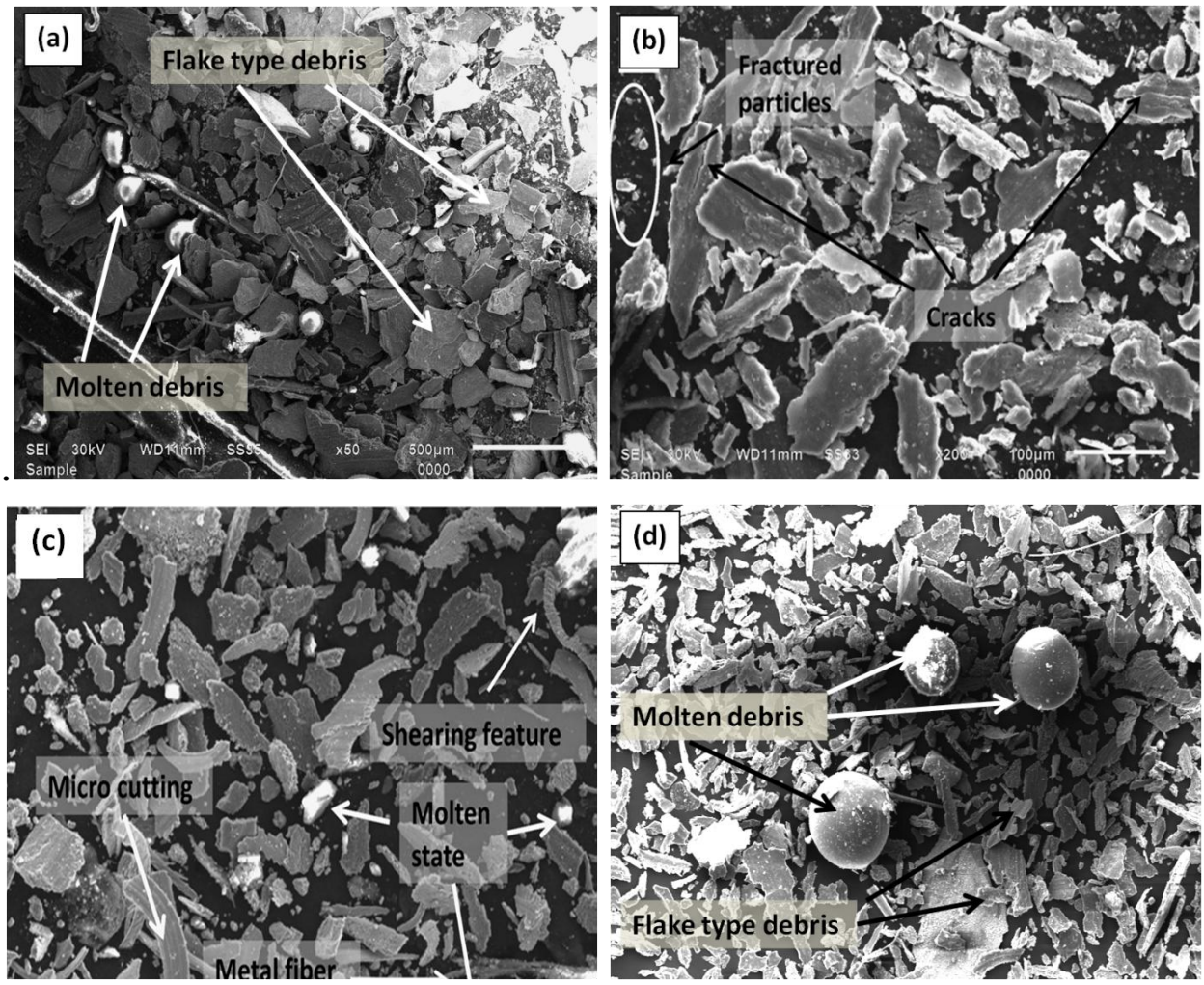

Figure 4.35: SEM images of wear debris of LM13/15%Zr composite with fine size particles at 49 N load with variation of temperature (a) 150˚C (b) 200˚C (c) 250˚C and (d) 300˚C

Under low load and dry wear sliding conditions, wear debris are generally spherical and friable in nature while at high load the wear debris are found to be metallic. Presence of large amount of flake type debris suggests that delamination is the predominating mechanism at high pressure and there is no correlation between size of particles and zircon content. SEM micrographs showing the mechanically mixed layer formed on the contact surface of the composites reveal a bimodal size distribution of fine spherical particles and larger plate-like debris.

REFERENCES:

[1] M Roy, B Venkataraman, VV Bhanuprasad, YR Mahajan and G Sundaraaian; The effect of particulate reinforcement on the sliding wear behaviour of aluminium matrix composites. Metallurgical and Materials Transactions A, 23 (1992) 2833-47.

[2] L Pedersen and L Arnberg; The effect of solution heat treatment and quenching rates on mechanical properties and microstructures in AlSiMg foundry alloys. Metallurgical and Materials Transactions A, 32A (2001) 525-32.

[3] SK Chaudhary, AK Singh, CS Sivaramakrishnan and SC Panigrahi; Wear and friction behavior of spray formed and stir cast Al–2Mg–11TiO_2 composites. Wear, 258 (2005) 759-67.

[4] J Clarke and AD Sarkar; Wear characteristics of as- cast binary aluminum silicon alloys. Wear, 54 (1979) 7–16.

[5] A Mahato, N Verma, V Jayaram and SK Biswas; Severe wear of a near eutectic aluminium-silicon alloy. Acta Materialia, 59(2) (2011) 6069-82.

[6] S Suresh and A Mortensen; Functionally graded metals and metal- ceramic composites part 2: thermomechanical behavior. International Materials Reviews, 42 (1997) 85–116.

[7] S Schicker, DE Garcia, J Bruhn, R Janssen and N Claussen; Reaction synthesized Al_2O_3-based intermetallic composite. Acta Metallurgica et Materialia, 46 (1998) 2485-92.

[8] FM Hosking, FP Folgar, R Wunderlin and R Meharbian; Composites of aluminium alloys: fabrication and wear behavior. Journal of Materials Science, 17 (2) (1982) 477-498.

[9] RL Deuis, C Subramaian and JM Yellup; Dry sliding wear of aluminum composites- a review. Composite Science and Technology, 57 (1997) 415-35.

[10] K Kaur and OP Pandey; Dry sliding behavior of zircon sand reinforced Al–Si alloy. Tribology Letters, 38 (2010), 377- 387.

[11] S Das, V Udarabanu, S Das and K Das; Synthesis and characterization of zircon sand/Al–4.5 wt% Cu composite produced by stir casting route. Journal of Materials Science, 41 (2006) 4668-77.

[12] A Banerji, MK Surappa and PK Rohatgi; Cast aluminum alloys containing dispersions of zircon particles. Metallurgical and Materials Transactions B, 14 (1983) 273- 283.

[13] S Das, S Das and K Das; Abrasive wear of zircon sand and alumina reinforced Al- 4.5 wt% Cu alloy matrix composites- a comparative study. Composite Science and Technology, 67 (2007) 746- 751.

[14] K Kaur and OP Pandey; Wear and microstructural characteristics of spray atomized zircon sand reinforced LM13 alloy. Materialwiss Werkstofftech; 41(7) (2010) 568-74.

[15] D Frey, MB God and WO Peterson, Wear Control Handbook, ASME, New York, 1980, 283–312.

[16] FP Bowden and D Tabor, The Friction and Lubrication of Solids, Part II, Oxford University Press, London, 1964, p 97

[17] J Zhang and AT Alpas; Transition between mild and severe wear in aluminum alloys. Acta Materialia, 45 (1997) 513.

[18] S Wilson and AT Alpas; Effect of temperature on the sliding wear performance of Al alloys and Al matrix composites. Wear, 196 (1996) 270-8.

[19] A Kapoor and KL Johnson: Proceedings of the 19th Leeds-Lyon Symposium on Tribology, Leeds, Sept. 8–11, 1992.

[20] KL Johnson and HR Shercliff; Shakedown of 2-dimensional asperities in sliding contact. International Journal of Mechanical Sciences, 34 (5) (1992) 375–94.

[21] G Rajaram, S Kumaran and RT Srinivasa; High temperature tensile and wear behaviour of aluminum silicon alloy. Material Science and Engineering A 528 (2010) 247- 53.

[22] DP Mondal, S Das, RN Rao and M Singh; Effect of SiC addition and running-in-wear on the sliding wear behavior of Al-Zn-Mg aluminium alloy. Materials Science and Engineering A, 402 (2005) 307- 319.

[23] B Zahmatkesh, MH Enayati and F Karimzadeh; Tribological and microstructural evaluation of friction stir processed Al2024 alloy. Materials Design, 31 (2010) 4891-6.

[24] J Larsen-Basse and B Premaratne; Proc. Wear of materials conf. New York: ASME; 1983. p. 161.

[25] DK Dwivedi; Adhesive wear behavior of cast aluminium–silicon alloys: overview. Materials Design, 31 (2010) 2517- 31.

[26] Sudarshan and MK Surappa; Dry sliding wear of fly ash particle reinforced A356 Al composites. Wear, 265 (2008) 349-360.

CHAPTER 5

RESULTS AND DISCUSSION

(Dual size particles reinforced composites)

Overview:

The results presented in the previous chapter indicate that reinforcement of zircon sand particles exhibit better wear resistance. However, detail study of large size variation of reinforced particles was not done. This chapter describes mainly the wear behavior of the developed composites reinforced with dual size zircon sand particles in the alloy matrix at different conditions. Reinforcement is done up to 20 wt.% coarse (106- 125 µm) and fine (20- 32 µm) size particles in a defined ratios in LM13 alloy matrix. Their distribution inside the matrix was analyzed under the optical microscope. Wear behavior of the composites was studied under different operating conditions (e.g. load and temperatures). Composite containing 15 wt.% zircon sand particles in 1:4 ratio of coarse and fine (DSR-15D composite) shows better wear resistance at all operating conditions in comparison to all other developed composites. The details of these analyses are presented here.

This chapter describes the influences of size variation of reinforced particles on composite properties. Our study presented on previous chapter indicated that 15% reinforcement of fine size zircon sand particles in LM 13 alloy matrix has exhibited better wear resistance as compared to other developed composites. However, fine size particles in higher amount tend to agglomerate, which oppose to good wear resistance of the material. In order to overcome this problem, combination of coarse and fine size particles (dual size reinforcement) was done in the matrix. These dual size reinforced composites were developed by stir casting process. The details of it have been given in the experimental section (table 3.4). However, for the simplicity, all the DSR-composites were given nomenclature on the basis of the amount and ratio of coarse and fine size particles in the matrix as given in table 5.1.

Table 5.1: Nomenclature of the developed dual size reinforced composites.

Composites		
Amount of reinforcement (wt.%)	Ratio of coarse (106- 125 µm) and fine size (20- 32 µm) particles in dual size reinforced (DSR) composite **(coarse : fine)**	Nomenclature
5%	4:1	DSR-5A
	3:2	DSR-5B
	2:3	DSR-5C
	1:4	DSR-5D
10%	4:1	DSR-10A
	3:2	DSR-10B
	2:3	DSR-10C
	1:4	DSR-10D
15%	4:1	DSR-15A
	3:2	DSR-15B
	2:3	DSR-15C
	1:4	DSR-15D
20%	4:1	DSR-20A
	3:2	DSR-20B
	2:3	DSR-20C
	1:4	DSR-20D

5.1 Morphological study:

To observe the effect of dual size zircon sand particles in the matrix, developed DSR-composites were analyzed under optical microscope at different magnifications. Figure 5.1(a-d) shows the optical micrographs of the DSR- 5A, 5B, 5C and 5D composites respectively. A fairly uniform distribution of the particles in the matrix is clearly seen in figure 5.1 (a- d), which is desired for achieving better wear and mechanical properties. Due to the high shear rate during stirring, particles get distributed throughout the melt, which also minimizes the particles settling. Figure 5.1a shows the homogeneous distribution of coarse particles along with the fine size particles in the alloy matrix.

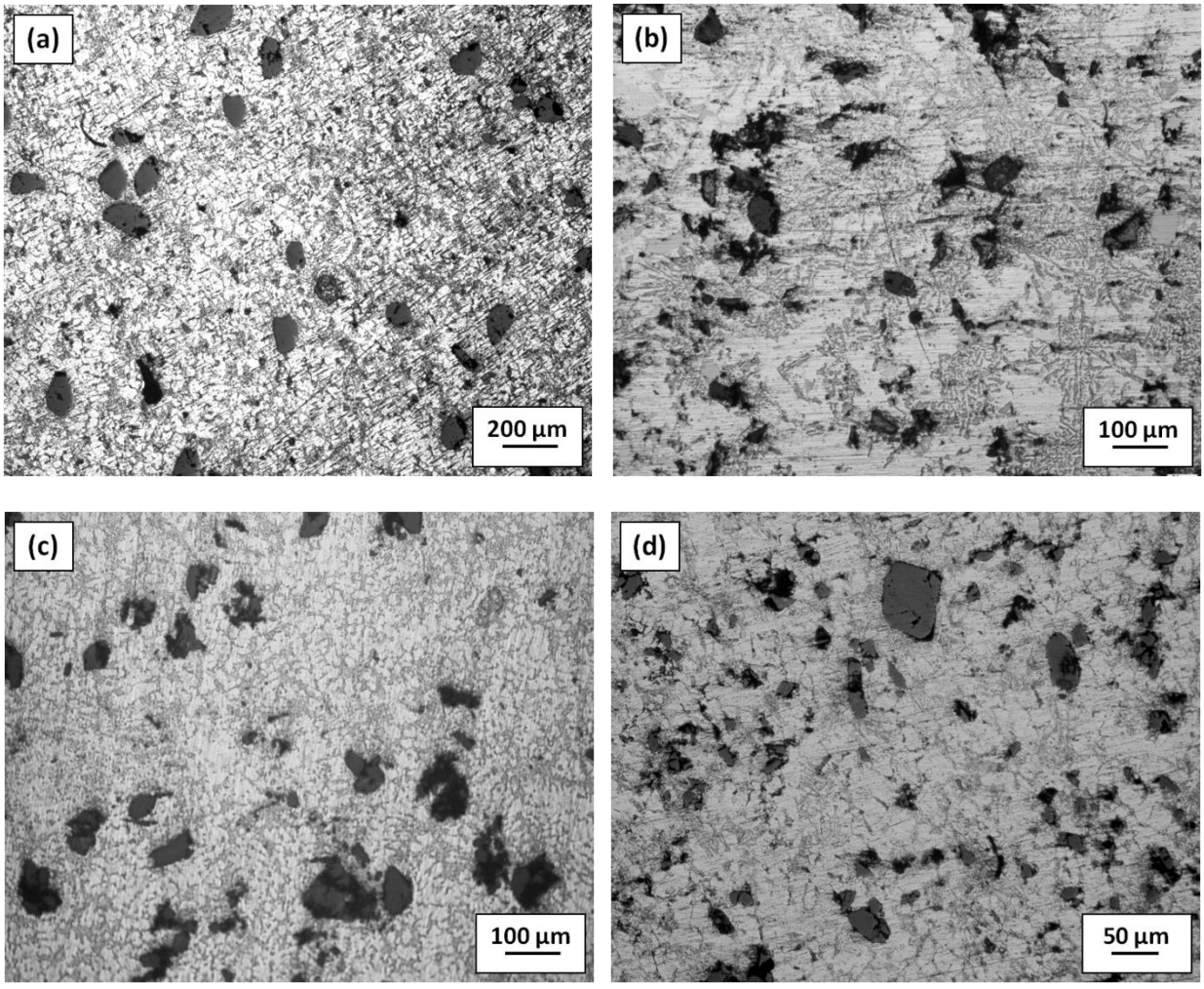

Figure 5.1: Optical micrographs of (a) DSR-5A, (b) DSR-5B, (c) DSR-5C and (d) DSR-5D composites.

The mechanical stirring not only distributes the particles homogeneously but also delays the particle settling prior to solidification [1]. With increasing the amount of fine size particles and decreasing the amount of coarse size particles in the matrix, agglomeration of fine particles is observed at certain places (Fig. 5.1 b- d). The smooth interface provides better mechanical and tribological properties as transfer of load occurs through the interface. Figure 5.1(a & c) shows the micrograph of the composite where fragmented dendrites in the alloy matrix can be seen, though limited dendritic growth in the particle depleted region is also visible. This growth has occurred because of clustering of zircon sand particles. Fine size zircon sand particles are pushed or engulfed by advancing solid–liquid interface creating sufficient space inside the matrix which leads to growth of dendrite [2]. Dendritic fragmentation can be attributed to the shearing of initial dendritic arms by the stirring action. During particle addition, local solidification of the melt occurs which is induced by the particles as there is a temperature difference between the particle and the melt. It was also found that the perturbation in the solute field due to the presence of particles can change the dendrite tip radius and the dendrite tip temperature. Also, the length of the dendrite is reduced in the presence of the particles [2]. At some places particle clustering and porosity due to entrapment of air during pouring are also observed (fig. 5.1 c & d). Figure 5.2 (a- d) shows the optical micrographs of DSR-10A, 10B, 10C and 10D composites respectively. Figure 5.2 (a & b) shows the homogeneous distribution of the coarse and fine size particles in the alloy matrix. Fig 5.2 (a & c) shows the presence of long dendrite in areas where particle is not present. The second phase (hard particles) restricts the growth of dendrite and modifies the matrix with more refined structure leading to improvement in strength [3- 7]. It also contributes for refinement of silicon phase. The silicon possessing acicular morphology in the matrix acquires globular form in vicinity to the particles. Similar modification in silicon morphology was reported in earlier work by Kaur *et al.* [1] and attributed this morphological transformation to the localized rapid cooling effect produced by zircon sand particle due to large temperature difference in the melt around its vicinity. In figure 5.2d, optical micrographs of DSR-10D composite shows agglomeration of fine particles as amount of fine size particles in the matrix is higher than the DSR-10A, 10B and 10C composites.

Figure 5.3(a- d) shows the optical micrographs of the DSR-15A, 15B, 15C and 15D composites respectively. A fair distribution of coarse and fine size particles in the matrix can be seen in figure 5.3(a- d). Dendritic structure got modified during casting, which is influenced by many

factors such as dendritic fragmentation, restriction of dendritic growth by the particles and thermal conductivity mismatch between the particles and melt. Ceramic particles also act as a barrier for the dendritic growth and this phenomenon is more pronounced if the cooling rate is high [8].

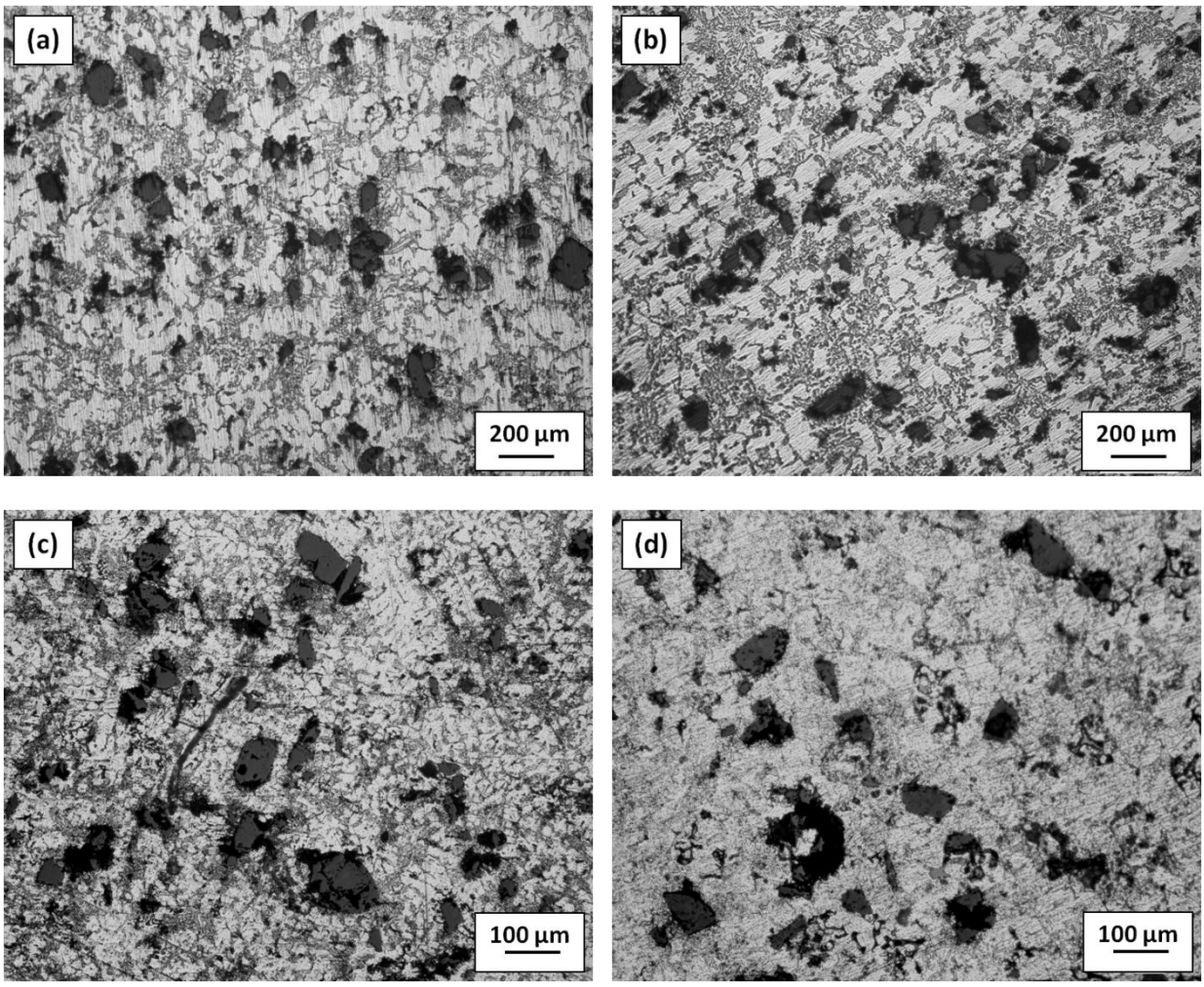

Figure 5.2: Optical micrographs of (a) DSR-10A, (b) DSR-10B, (c) DSR-10C and (d) DSR-10D composites.

During stirring process the fine particles are pushed at faster rate which gets agglomerated around the area away from stirrer which is visible at certain places in the microstructure. During stirring, shearing force is applied on the molten mass. As nucleation starts the dendrites get fragmented due to shearing action and solidify as cellular structure. As the solid–liquid interface moves, the dendrite acquires cellular type of features on small under cooling which always exits

ahead of solid–liquid interface. Second phase particles present in the melt also provide nucleation center. Since the system is continuously in the agitated state, where second phase particles are fairly distributed throughout the melt, it hinders the growth of long dendrites. This results in cellular growth because of interference offered by these particles, as shown in fig. 5.3(a–c).

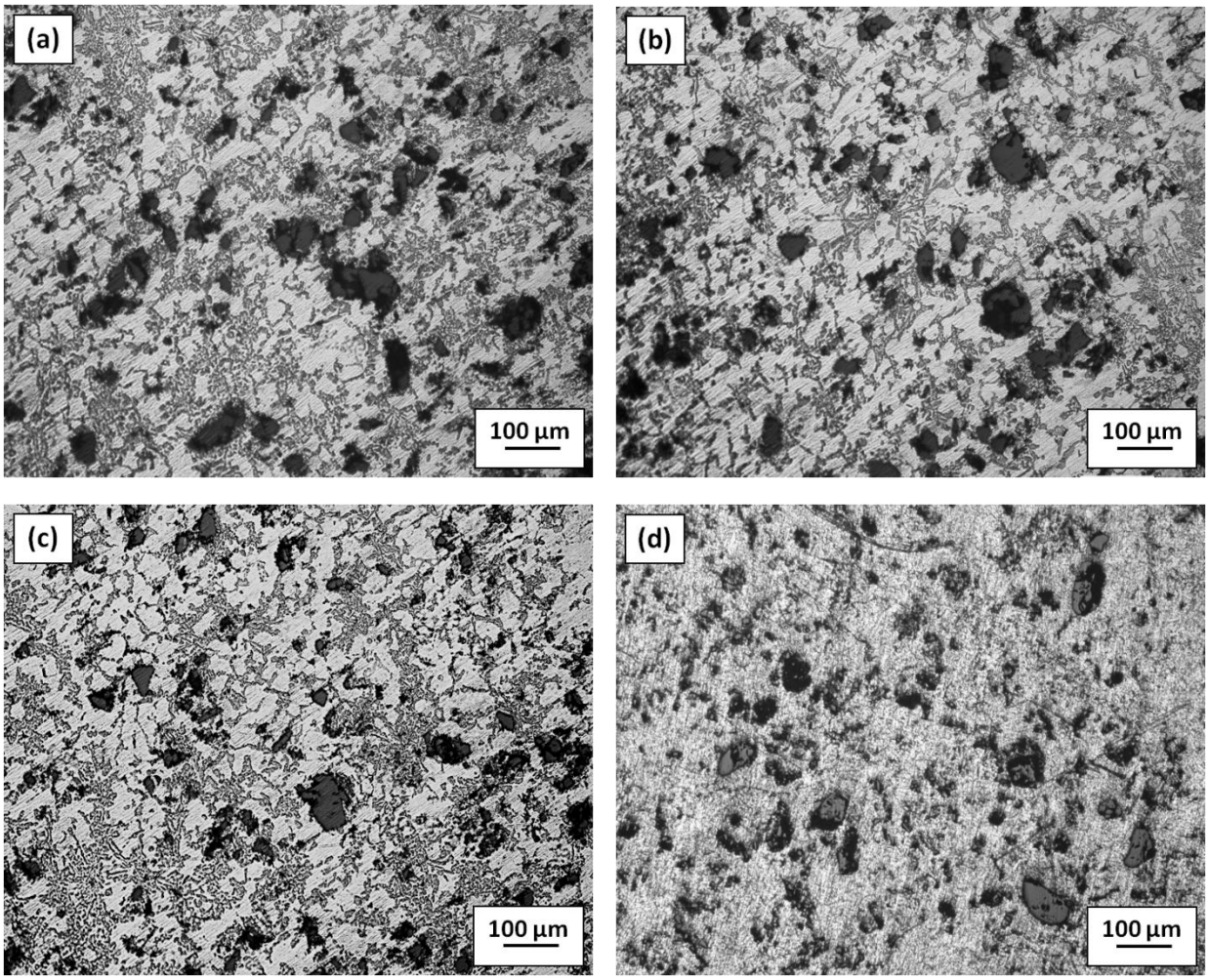

Figure 5.3: Optical micrographs of (a) DSR-15A, (b) DSR-15B, (c) DSR-15C and (d) DSR-15D composites.

Figure 5.4 (a- d) shows the optical micrographs of the DSR- 20A, 20B, 20C and 20D composites respectively. Fine distribution of the coarse and fine size particles in matrix can be seen easily in figure 5.4 (a- d). In the micrograph of the DSR- 20A composite (fig 5.4a), fragmented dendrites in the matrix can also be seen, though limited dendritic growth in the particle depleted region is

also visible in this figure. Larger amount of reinforcement leads to agglomeration of both coarse and fine size particles in the matrix (fig. 5.4 a, b & d). The structure depicts the presence of voids and porosity. Overall analysis of the structure indicates that fine particles have a tendency to cluster in the composite, because they are pushed to a greater extent by the solidification front as compared to coarse particles. Fine particles are observed to form a network structure, and some fine particles are engulfed within the grains (fig. 5d) [9]. However, agglomeration of the fine particles in larger extent supports to chipping out of the particles during grinding and polishing due to loose bonding, which can be easily seen in figure 5.4d.

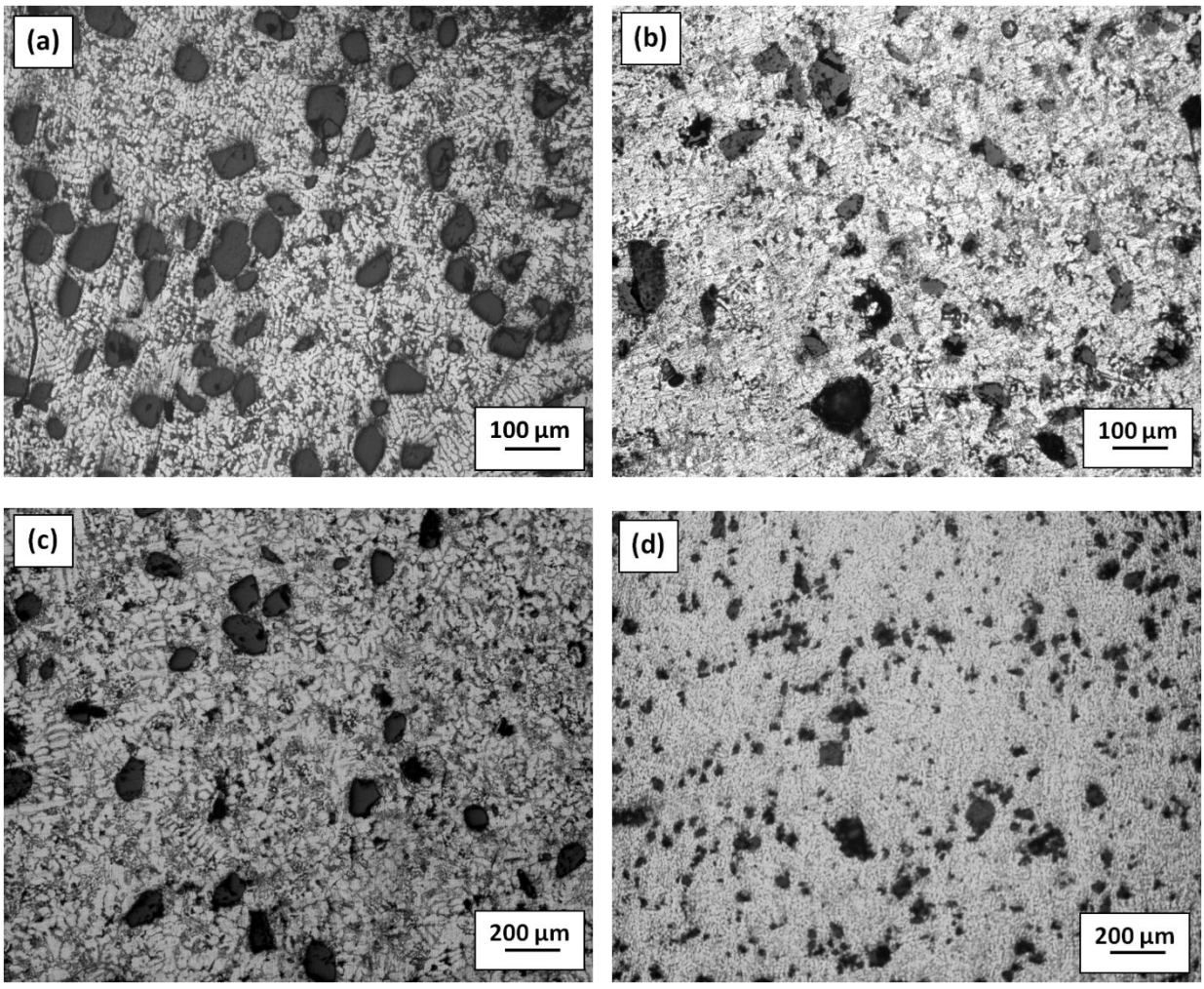

Figure 5.4: Optical micrographs of (a) DSR-20A, (b) DSR-20B, (c) DSR-20C and (d) DSR-20D composites.

5.2 Hardness:

Change in hardness of developed DSR- composites with the varying amount and ratio of coarse and fine size particles in the matrix was measured by Rockwell hardness testing machine. Figure 5.5 shows the change in bulk hardness for different DSR- composites. An average of ten hardness tests of each sample was carried out to get significant values. It was observed that hardness of the composites increases with increasing the total amount of dual size (coarse and fine) zircon sand particles as well with increasing the ratio of fine size particle in comparison to the coarser size particle as reinforcement for DSR- composites. As discussed earlier, presence of a new harder phase (Al_2SiO_5) at particle and matrix interface is responsible for the improvement in overall hardness of the composites. Hence larger surface area of fine size particles is key factor to enhance the hardness of the composites containing more ratio of fine size particles in comparison to coarser size particles significantly.

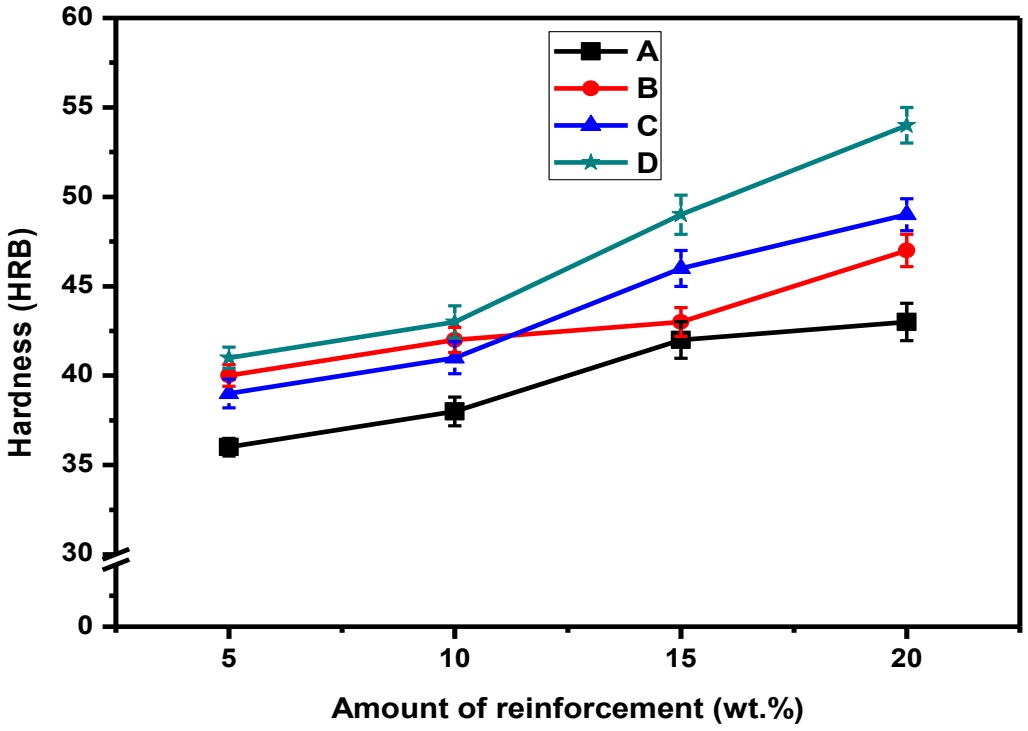

Figure 5.5: Bulk hardness of the DSR- composites.

5.3 Wear Behavior:

5.3.1 Effect of applied load on the wear behavior

Wear has been recognized as the phenomenon of material removal from a surface due to interaction with a mating surface. Almost all machines lose their durability and reliability due to wear, hence ceramic particles are incorporated to improve the wear resistance of the material. Figure 5.6 (a- d) shows the change in wear rate of the DSR-5A, 5B, 5C and 5D composites against the sliding distance at 9.8 N, 19.6 N, 29.4 N, 39.2 N and 49 N loads tested at a constant sliding velocity of 1.6 m/s respectively. Figure 5.6 (a- d) shows two types of changes in wear rate of the DSR- 5 composites. In the initial stage of wear test, wear rate increases abruptly known as run in wear, while second stage indicate a steady state of wear rate. Adhesive wear during the initial stage of wear test at applied load is mainly responsible for the run in wear condition which removes more material, hence wear rate increases [10]. However, after running more distance wear rate decreases and tends towards constant wear rate due to acquirement of a critical temperature between the specimen and countersurface at particular load. For practical applications, the wear rate of a material is taken as average of wear rate during steady state. It was observed that wear rate for the DSR-5(A- D) decreases with the increasing amount of fine size particles. However, wear rate of all the DSR-5 composites increases with increasing applied load form 9.8 N to 49 N loads. Increment in wear rate with increasing applied load is due to higher pressure at actual contact area between the specimen and countersurface. Presence of fine particles improves the hardness of the material significantly as well as enhances the wear resistance of the material. However, coarse particles helps to transfer the load during wear test hence a combination of coarse and fine size particles provides good wear resistance to the materials. Figure 5.6e shows that DSR-5D composite exhibits better wear resistance in comparison to DSR-5A, 5B and 5C composites at all applied loads.

Figure 5.7 (a- d) shows the wear behavior against sliding distance of DSR-10A, 10B, 10C and 10D composites at different loads respectively. Improvement in wear resistance with increasing the amount of zircon sand particles (coarse and fine) from 5 wt.% to 10 wt.% was observed at all applied loads (fig. 5.6 & 5.7). High wear rate of the material during run in wear stage was observed for the DSR-10 (A- D) composites.

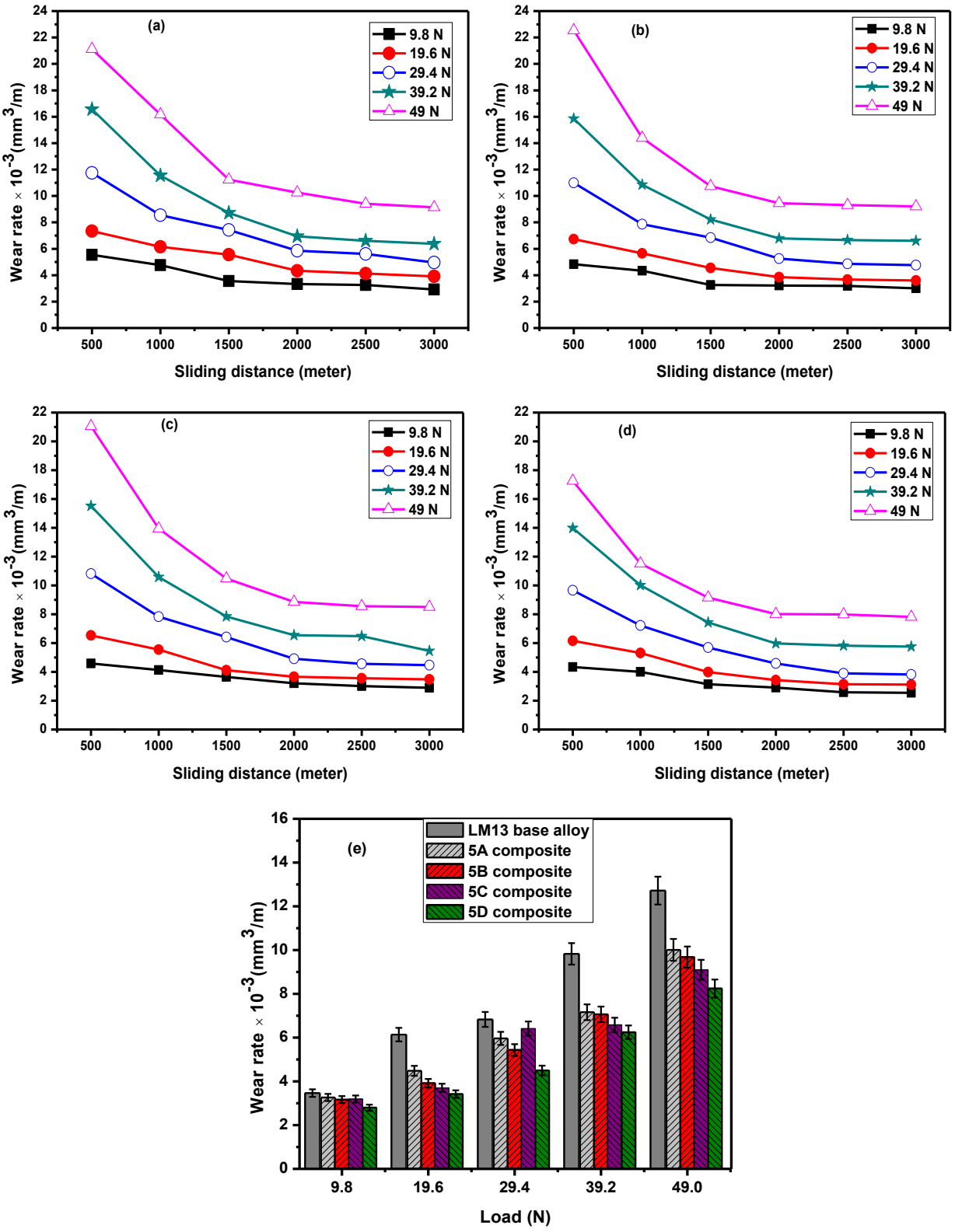

Figure 5.6: Wear rate against the sliding distance at different loads for (a) DSR-5A (b) DSR-5B (c) DSR-5C (d) DSR-5D and (e) Comparison of wear rate at all loads.

However, wear rate of DSR-10(A- D) composites (fig. 5.7) during the run in wear condition is having lesser slope than that for DSR-5(A- D) composites (Fig. 5.6), which indicates the improvement in wear resistance of composites with increasing the amount of zircon sand particles in matrix. This improvement in wear rate was also observed during the steady state wear test. However, with increasing the applied load from 9.8 N to 49 N, wear rate of the composites increases significantly. A transition from mild to severe wear was observed at high load (49 N) condition. However, for the total (coarse and fine size) 10 wt.% amount of zircon sand, wear rate of the composite decreases with increasing the amount of fine size particles, which is minimum for DSR-10D composite (Fig 5.7d). This decrement in the wear rate is due to improvement in the hardness of the composites with increasing the ratio of fine size particles. Presence of fine size particles in the matrix improves the hardness significantly in comparison to the coarse size particles due to large surface area. Figure 5.7e shows the comparison in wear rate of DSR-10A, 10B, 10C and 10D composites at different loading conditions. It indicates that wear rate increases with increase in applied loads for DSR-10 composites. However, different ratio of coarse and fine size particles affects the wear rate significantly. Composite with coarse and fine size particles in composition of 1:4 (DSR-10D composite) shows better wear resistance in comparison to DSR-10A, 10B and 10C composites for all loading conditions.

Figure 5.8 (a- d) shows the change in wear rate against the sliding distance at different applied loads for the DSR-15A, 15B, 15C and 15D composites respectively. Figure 5.8a shows the wear behavior of the DSR-15A composite with variation in applied load from 9.8 N to 49 N load. Increment in the wear rate was observed with increasing applied load as actual pressure on the real contact area is responsible for the high wear rate. However, mild to severe change in wear behavior of composite was observed at higher (49 N) load condition. Figure 5.8 (a- d) also indicates that decrement in wear rate occurs with increased sliding distance. After running a particular sliding distance (around 1500 meters) at constant load wear rate tends to achieve the steady state. Higher amount of fine size particles in ratio of coarse and fine size particles in DSR-15 composites enhances the wear resistance significantly. With increasing content of fine size particles in DSR-15C & 15D composites, the wear rate at high load approaches constant value which indicates the good wear resistance of the materials at high (49 N) load (Fig. 5.8 c & d). Figure 5.8e shows that wear rate decreases significantly with increasing the amount of fine size particles in the matrix at all loading conditions.

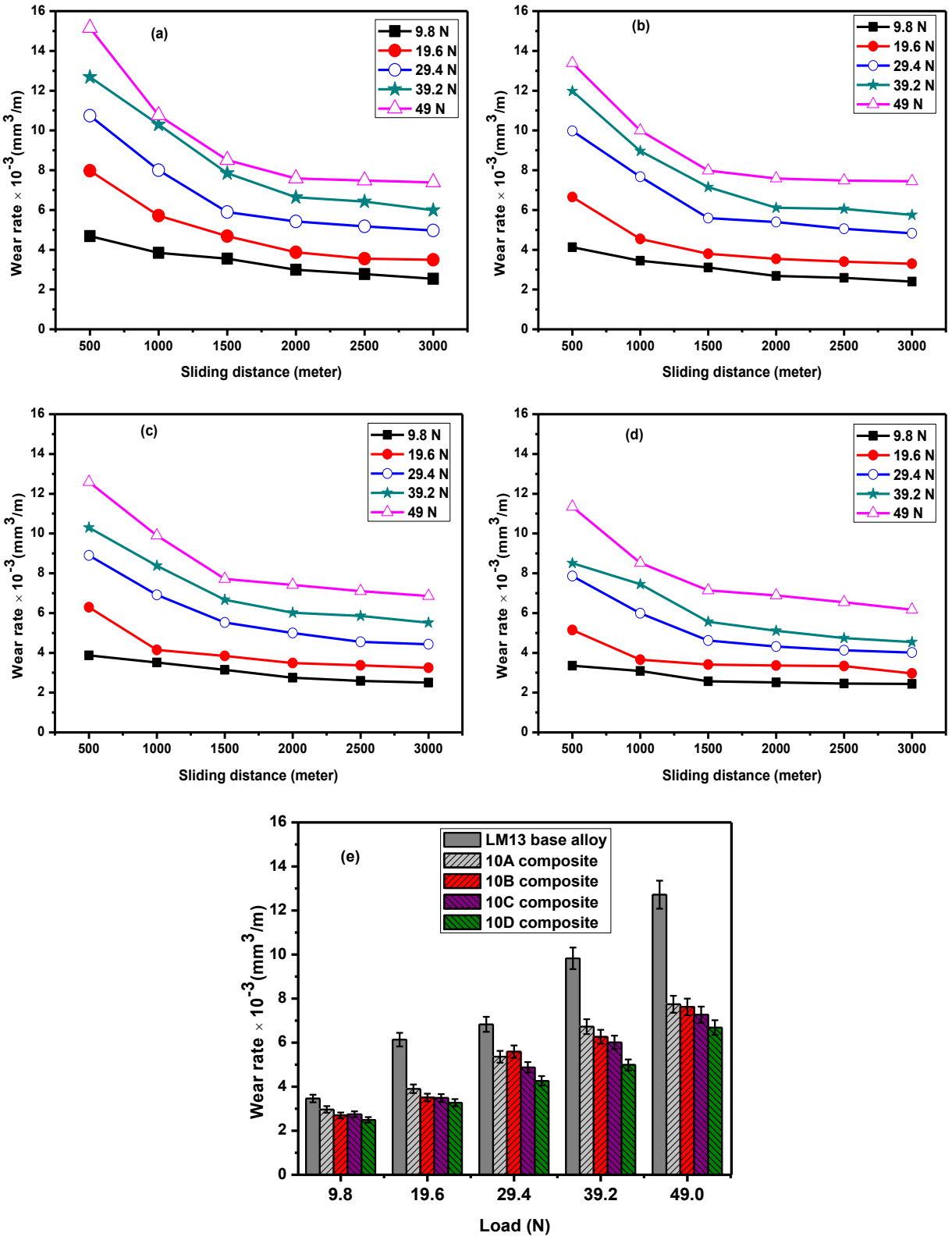

Figure 5.7: Wear rate against the sliding distance at different loads for (a) DSR-10A (b) DSR-10B (c) DSR-10C (d) DSR-10D and (e) Comparison of wear rate at all loads.

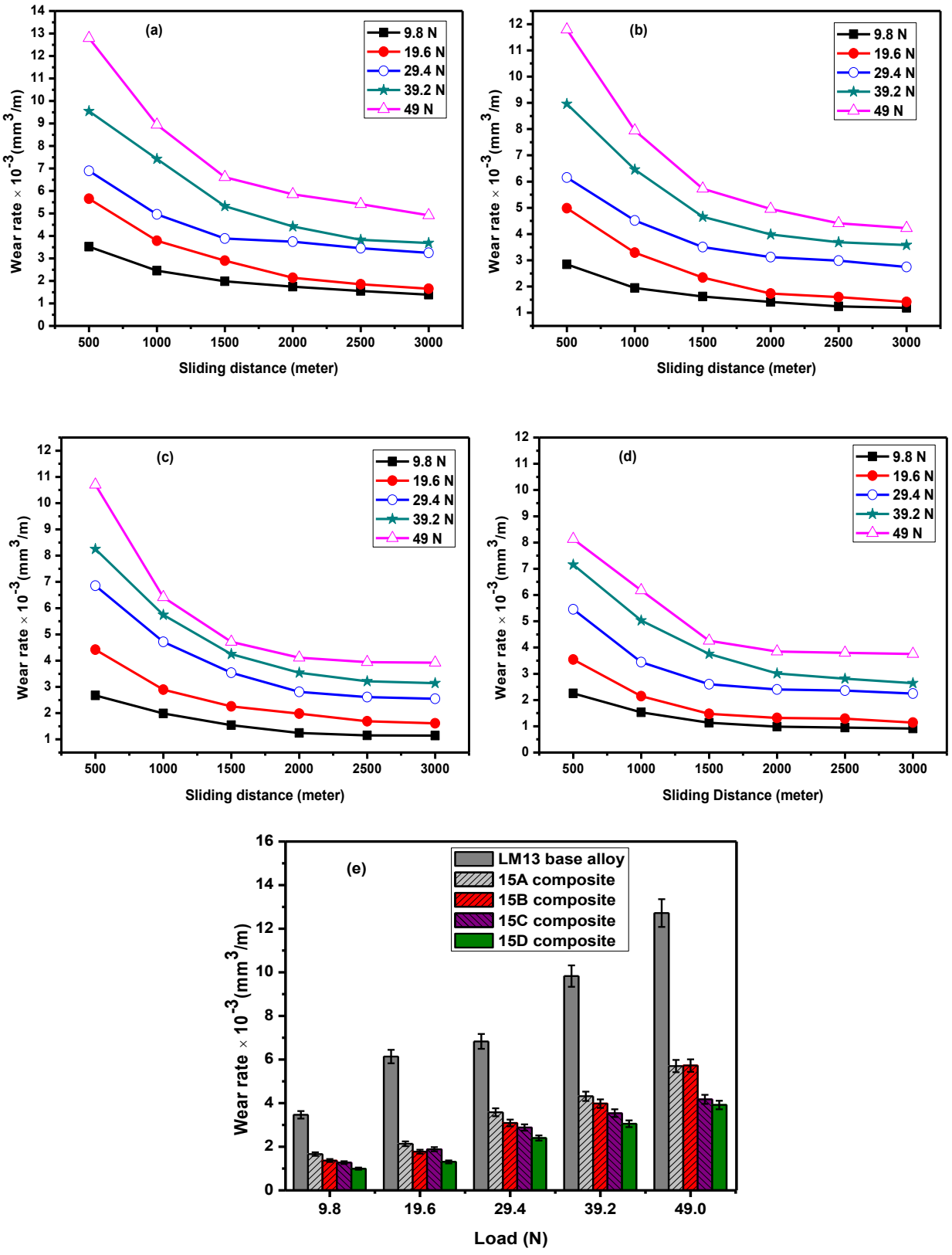

Figure 5.8: Wear rate against the sliding distance at different loads for (a) DSR-15A (b) DSR-15B (c) DSR-15C (d) DSR-15D and (e) Comparison of wear rate at all loads.

This improvement in the wear resistance is due to increment in the hardness in presence of fine size reinforced particles (Fig. 5.5). However, mild to severe transition in wear mode is also observed at high load (49 N) for DSR-15A, 15B, 15C and 15D composites.

Figure 5.9 (a- d) shows the change in wear rate against the sliding distance at different loading conditions for the DSR-20A, 20B, 20C and 20D composites respectively. Figure 5.9a shows the wear behavior of the DSR-20A composites with varying the load from 9.8 N to 49 N. High wear rate in run in wear condition for DSR- 20 (Fig. 5.9) was observed which is similar to other DSR- composites (Fig. 5.6, 5.7 and 5.8). However, lower wear rate in run in wear condition indicates the improvement in wear resistance of DSR- 20A, 20B, 20C and 20D composites in comparison to other DSR- composites (Fig 5.6 – Fig 5.9). As the amount of fine particles in ratio of coarse and fine size particles (DSR-20D) increases, the wear rate changes sharply. Figure 5.9e shows the comparison of wear rate for the all DSR-20 composites (DSR-20A, 20B, 20C and 20D) at different loads. Figure 5.9e indicates that wear rate of all DSR-20 composites increases with increasing the applied loads. However, wear rate changes with changing the ratio of coarse and fine size particles in the composites. Wear rate decreases with increasing the amount of fine size particles. However, mild to severe wear was observed for all DSR-20 composites at high (49 N) load.

Figure 5.6 – 5.9 show the wear behavior of DSR- composites with different amount of dual size reinforced particles in the LM13 alloy matrix. It was observed that overall wear rate of DSR composites decreases with increasing the total amount of dual size reinforced particles in matrix. However, wear rate increases significantly with increasing the applied load for all DSR composites and mild to severe wear was observed at high (49 N) load. Wear rate of each DSR composite tends to get steady state after running some particular sliding distance. This steady state was also improved with increasing the total amount of dual size particles as well as fine size particles in the ratio of coarse and fine size particles in LM13 alloy matrix.

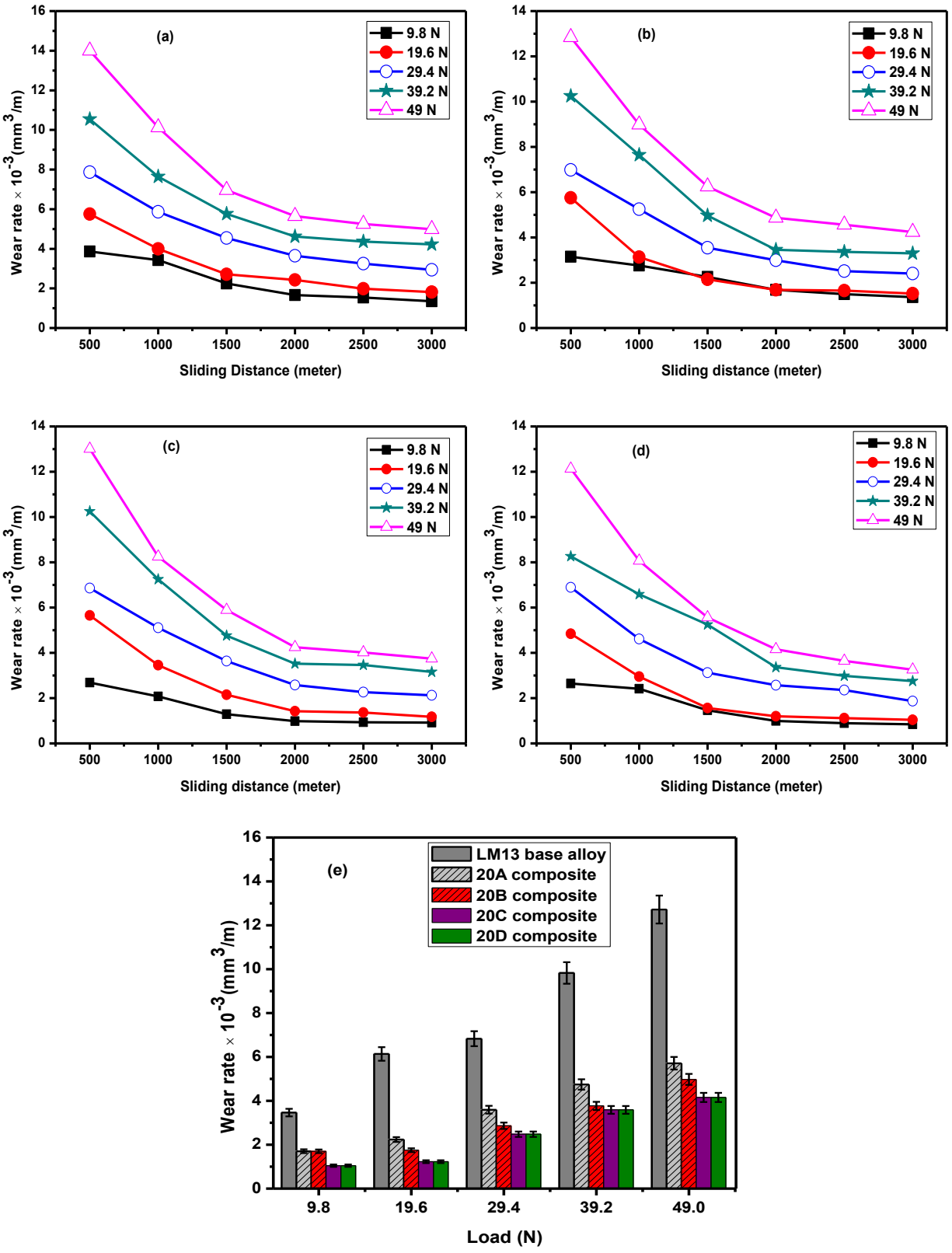

Figure 5.9: Wear rate against the sliding distance at different loads for (a) DSR-20A (b) DSR-20B (c) DSR-20C (d) DSR-20D and (e) Comparison of wear rate at all loads.

5.3.2 Effect of temperature on wear behavior at low (9.8 N) and high (49 N) load:

Figure 5.10 (a & b) shows the wear behavior of composites reinforced with 5 wt.% of dual size particles incorporated with different ratio of coarse and fine size particles (DSR-5A, 5B, 5C and 5D) tested at different temperatures with low (9.8 N) and high (49 N) load conditions. Figure 5.10a shows the change in wear rate of the DSR-5A, 5B, 5C and 5D composites at 9.8 N load with temperature variation from 50 °C to 300 °C. It was observed that wear rate of all the composites decreases slightly with the increase in ambient temperatures from 50 °C- 150 °C at low (9.8 N) load. At low load (9.8 N) particles stick in the soften matrix, these particles support to improve the wear resistance at low load conditions. At 200 °C, wear rate of the composites decreases significantly due to formation of oxide layer between the surfaces of specimen and steel disc [11]. This oxide layer avoids the metal to metal contact of specimen and steel disc during wear test, which is responsible for the lower wear rate of the composites. At much higher temperature (250 °C and 300 °C), due to tearing of oxide layer at low load, wear rate increases significantly. At higher temperature, tearing of oxide layers exposes new area for the wear, which supports to higher wear rate.

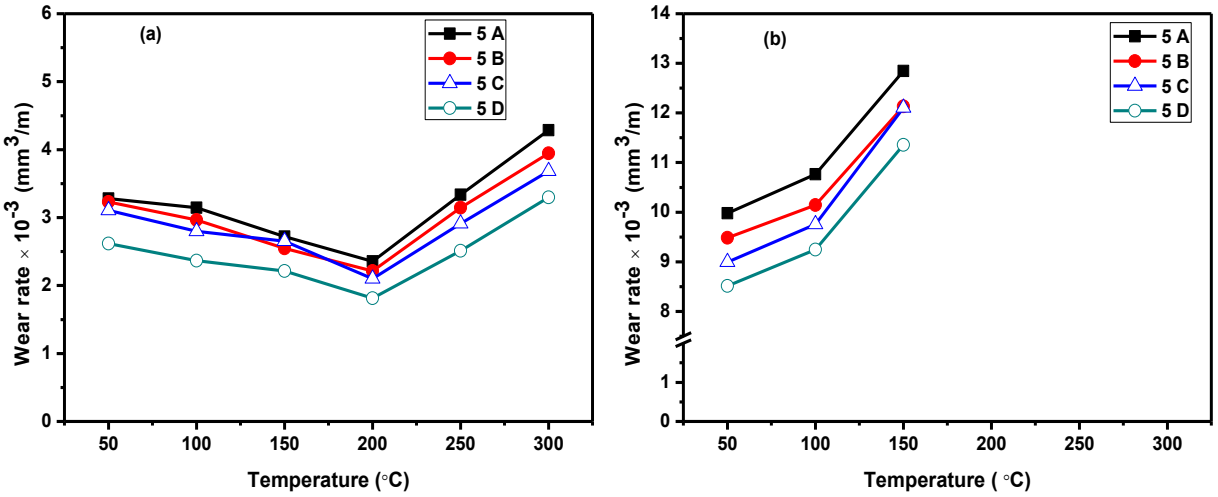

Figure 5.10: Wear rate against the temperature for DSR-5 at (a) 9.8 N and (b) 49 N load.

Figure 5.10b shows the change in wear rate of DSR- 5A, 5B, 5C and 5D composites at high (49 N) load with variation in the ambient temperature from 50- 300 °C. Figure 5.10b shows that at high (49 N) load, wear rate of the DSR- 5 (A, B, C and D) composites increases sharply with

increasing the temperature from 50- 150 °C. This is due to the fact that under high load condition composite materials undergo the adhesive as well as abrasive wear mechanism which increases with increasing the temperature. However, above 150 °C composite becomes soft and a severe wear occurs at high load condition. At 200 °C, 250 °C and 300 °C temperature during wear test, composite has undergone for worn out condition. In this worn out condition, material removal (change in length of sample pin) is more than 2 mm, which is limit for the instrument. Composite was worn out after running a sliding distance of 1475 m, 1350 m and 1100 meter at 200 °C, 250 °C and 300 °C respectively.

Figure 5.11 (a & b) shows the wear behavior of DSR-10A, 10B, 10C and 10D composites tested at different ambient temperatures from 50- 300 °C with low (9.8 N) and high (49 N) loads respectively. Figure 5.11a shows wear behavior of the DSR-10 (A, B, C and D) composites at low (9.8 N) load condition with variation in the temperature from 50- 300 °C. It was observed that wear of DSR composites containing 10 wt.% of dual size zircon sand particles in different ratio decreases with increasing the temperature from 50- 150 °C. This decrement in wear rate is due to the good bonding of particles with matrix. At low load condition, these particles get further inserted in the soften matrix and avoid the abrasive wear. Hence, wear rate decreases slightly. However, DSR-10D composite shows improved wear resistance in comparison to other DSR-10 composites (DSR-10A, 10B & 10C). This improvement in wear resistance is due to presence of higher amount of fine size particles in the matrix, which enhances the hardness and wear resistance of composites significantly [11].

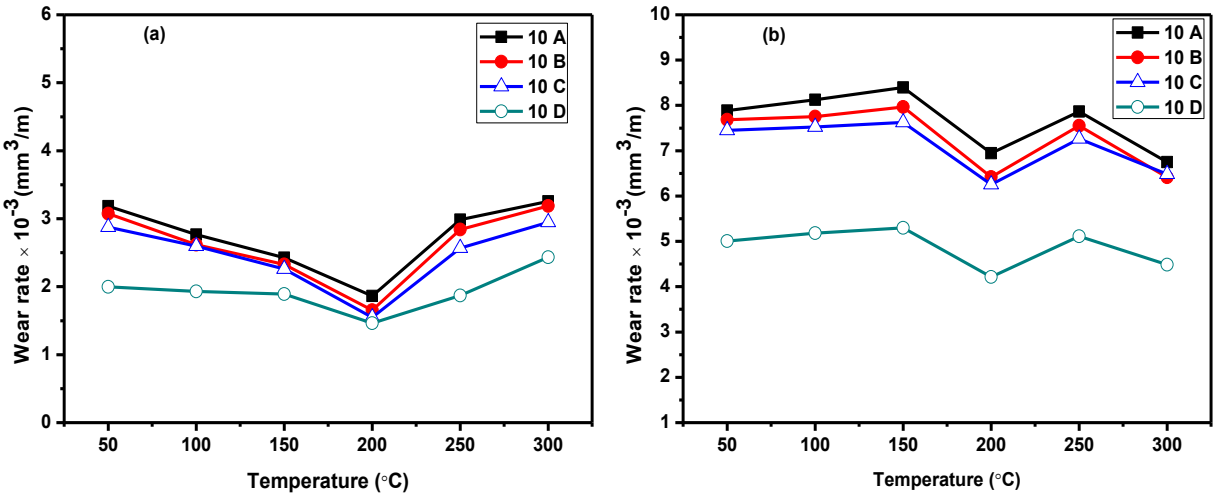

Figure 5.11: Wear rate against the temperature for DSR-10 at (a) 9.8 N and (b) 49 N load.

At much higher temperature (200 °C), wear for all DSR- 10 composites decreases significantly due to the formation of oxide layer between the contact surfaces at this temperature, which avoids the direct metal to metal contact and supports to lower wear rate. However, at 250 °C and 300 °C wear rate again increases sharply due to tearing of oxide layers at higher temperature which provide new area for delamination. Hence wear rate increases sharply.

Figure 5.11b shows the wear behavior of DSR- 10A, 10B, 10C and 10D composites at high (49 N) load with varying the ambient temperature from 50- 300 °C. It was observed that at high load, wear rate of the DSR- 10 composites increases slightly with increasing the temperature from 50-150 °C. This may be due to the removal of material at high applied pressure. However, at 200 °C, again due to formation of oxide layer at this temperature wear rate decreases and increases with increasing the operating temperature up to 250 °C as oxide layers tear off exposing new area for delamination. However, at high (300 °C) temperature, wear rate decreases as at this temperature and high load condition some Fe particles from countersurface of steel disc also get involved in wear and decrease the wear rate significantly. Here inclusions may act as additional reinforcement at the wearing surface of the composite [12].

Figure 5.12 (a & b) shows the change in wear rate of the DSR-15A, 15B, 15C and15D composites with varying the ambient temperature from 50- 300 °C at low (9.8 N) and high (49 N) loads respectively. Figure 5.12a shows that wear rate of the DSR-15 composite decreases slightly at low load condition for 50- 150 °C temperature and wear rate is minimum at 200 °C due to presence of oxide layer between the contact surfaces. However, at much higher temperature (250 °C and 300 °C), wear rate of the DSR-15 (A, B, C & D) composites increases. Moreover, for DSR-15D composite wear rate is nearly constant with increasing temperature from 50- 250 °C which indicates a better wear resistance property of material at low load condition. More amounts of fine particles in DSR-15D composite is responsible for good wear resistance as finer particles provide better hardness.

Figure 5.12b shows the change in wear rate for DSR-15 (A, B, C & D) composites at high load with varying the temperature from 50- 300 °C. It was observed that at high loading condition wear rate decreases when amount of coarse size particles is more than fine size particle in dual size reinforcement (DSR-15A, 15B) and increases with increasing the amount of fine size particles in dual size reinforcement (DSR-15C, 15D) composites. It shows that coarse size particles transfer the load easily to matrix in comparison to the fine size particles, which is

responsible for the better wear resistance at high load conditions. However, at 200 °C wear rate decreases and at 250 °C it increases due to formation and tearing of oxide layers at high loading conditions respectively. At 300 °C, wear rate decreases due to involvement of Fe particles from steel disc which supports lower wear rate of material.

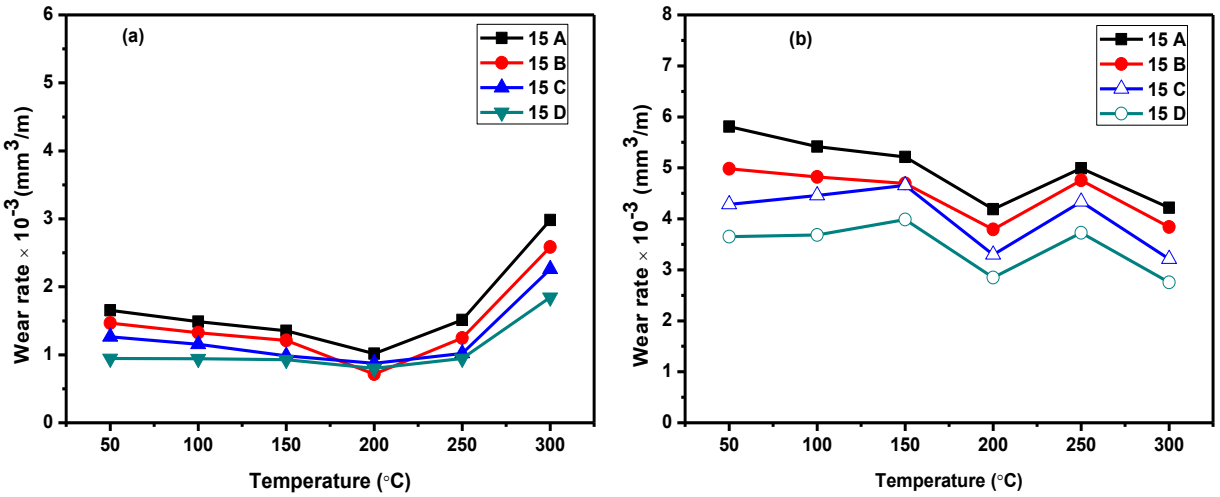

Figure 5.12: Wear rate against the temperature for DSR-15 at (a) 9.8 N and (b) 49 N load.

Figure 5.13 (a & b) shows the wear behavior of DSR- 20A, 20B, 20C and 20D composites tested with varying the temperature from 50- 300 °C at low (9.8 N) and high (49 N) loads respectively. Figure 5.13a shows the change in wear rate of DSR- 20 (A, B, C & D) composites at different ambient temperature condition of 9.8 N load. Wear rate decreases with increasing the temperature from 50- 150 °C and is minimum at 200 °C for low load condition. However, wear rate increases at higher temperature (250 °C & 300 °C). It was observed that higher amount of fine size particles in dual size reinforced composites (DSR- 20D) shows better wear resistance at all temperatures (50- 300 °C) with low load condition.

Figure 5.13b shows the wear behavior of DSR-20A, 20B, 20C and 20D composites tested at 49 N load with variation in temperature from 50 to 300 ºC. Wear rate of the DSR-20 (A, B, C &D) composites increases slightly with increasing temperature from 50 ºC to 150 ºC at high load conditions. However, at 200 ºC, due to formation of oxide layer wear rate decreases sharply. At higher temperature (250 ºC) wear rate again increases. This increment may be due to tearing of oxide layer at higher temperature and high load condition, which exposes new area for wear. At

much higher temperature (300 ºC), wear rate of all DSR- 20 composites decreases which is due to entrapment of the Fe particles from steel disc to soft composites, which helps to lower the wear rate of the composites [10].

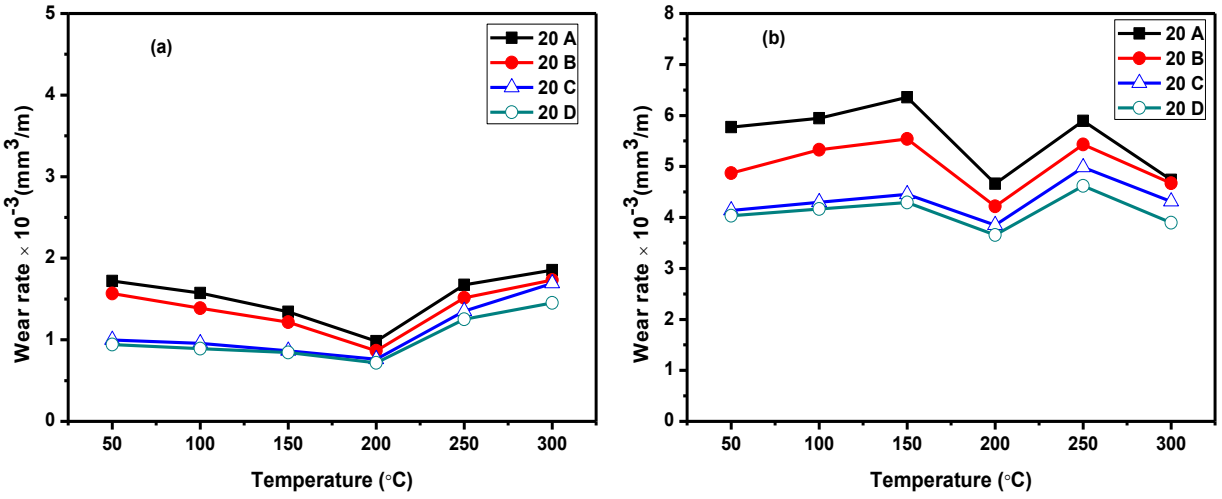

Figure 5.13: Wear rate against the temperature for DSR-20 at (a) 9.8 N and (b) 49 N load.

Figure 5.10- 5.13 indicates that wear rate of the all DSR composites (DSR-5, 10, 15 and 20) increases with increasing the applied load. Decrement in wear rate of DRS composites was observed with increasing the total amount of reinforcement from 5- 20 wt.% in matrix. However, for each DSR composite, ratio of coarse and fine size particles affects the wear rate significantly. Higher amount of fine size particles in coarse and fine size ratio of reinforced particles decreases the wear rate of DSR composites at all loading condition. Ambient temperature is also a key factor which affects the wear rate of composites at different loading conditions. At critical temperature 0.4- 0.5 T_m, wear rate decreases with addition of zircon sand particles in matrix. More than 10 wt.% reinforcement of zircon sand particles enhances the thermal stability of composites. However, DSR- composites show different type of wear behavior at low and high load condition with variation in the ambient temperature. Among all DSR composites (fig. 5.10- 5.13), DSR-15 composite shows better wear resistance at all testing conditions (different loads and temperatures), as DSR-20 composite leads to agglomeration of reinforced particles.

5.4 Topographical Analysis of the Worn Surfaces and Wear Debris

Topographical analysis of the specimen surface after wear test depicts the wear mechanism involved during the wear test at different testing conditions. For this purpose worn surfaces of the pin as well as debris (removed material) collected after wear test for each specimen were examined under SEM. However, the SEM images of worn surface and wear debris of only DSR-15 composites is presented here as it shows better wear resistance in comparison to other composites.

5.4.1 Analysis of the worn surfaces and wear debris under different loading condition

Figure 5.14 (a- e) shows the SEM images of the worn surfaces of DSR-15A composite tested at 9.8 N, 19.6 N, 29.4 N, 39.2 N and 49 N loads respectively. Figure 5.14a shows the delaminated area along with the abrasive grooves on the worn surface of DSR-15A composites. Due to presence of ceramic particles in the matrix, abrasive grooves are created on the surfaces during the continuous sliding of the materials. Surface presents the delaminated area as observed in the micrograph (Fig. 5.14a). Figure 5.14b shows the worn surface of DSR-15A composites tested at 19.6 N. Larger delaminated area with deeper grooves indicates the higher wear rate in comparison to fig. 5.14a. Figure 5.14 (c- e) shows the SEM images of the worn surfaces collected after the wear test conducted at 29.4 N, 93.2 N and 49 N loads. One of the common features observed at different loading condition is the formation of grooves and ridges running parallel to the sliding direction in composites. However, with increasing the applied load, more delaminated area along with deeper grooves are seen which also indicates the transition from mild to severe wear for the DSR-15A composite.

Figure 5.15 (a- e) shows the SEM micrographs of the collected debris of DSR-15A composite tested at 9.8 N, 19.6 N, 29.4N, 39.2 N and 49 N loads respectively. Flake type debris observed in micrographs indicate the adhesive delamination of the materials during sliding wear test at different loads. Figure 5.15a shows wear debris obtained at 9.8 N load in which plate-like debris of matrix alloy and thread type debris are observed. Wear is governed by delamination which gives plate-like morphology of debris with microcracks [13, 14]. Thread type morphology is due to pull-out of ductile aluminum matrix under applied load during sliding wear. Fractured debris observed in the SEM micrographs (fig. 5.15 a- e) are due to trapment of debris between the specimen and the counterface during wear test.

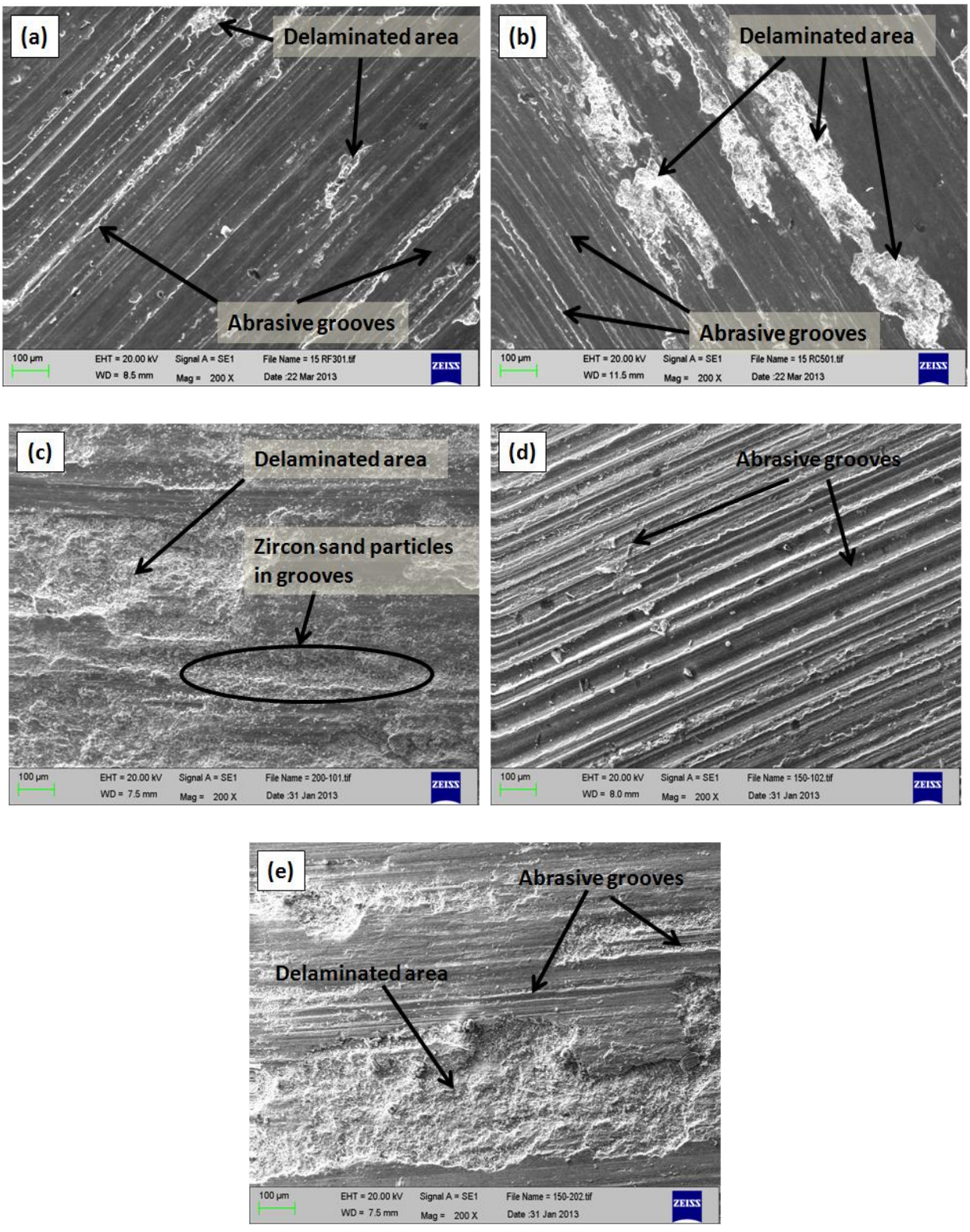

Figure 5.14: SEM micrographs of wear tracks for the DSR-15A composite at (a) 9.8 N, (b) 19.6 N, (c) 29.4 N, (d) 39.2 N and (e) 49 N loads.

Majority of flakes have number of cracks due to repetitive stress occurred in sliding under high load. When the load is increased severe plastic deformation occurs and delamination is dominant wear mechanism. The corrugated structure observed is due to rubbing caused by constant sliding between the pin material and the counterface where each of the steps observed is caused by the deforming force subjected in one rotation. Similar morphology of wear debris is earlier reported by Bakshi *et al.* [15] for aluminum–silicon composite coatings prepared by cold spraying. At higher loading (fig. 5.15d & e), fractures zircon sand particles along with molten debris are observed. Molten debris observed in SEM micrographs are due to generation of frictional heat between the specimen and counter surface at higher loads causing melting of trapped debris.

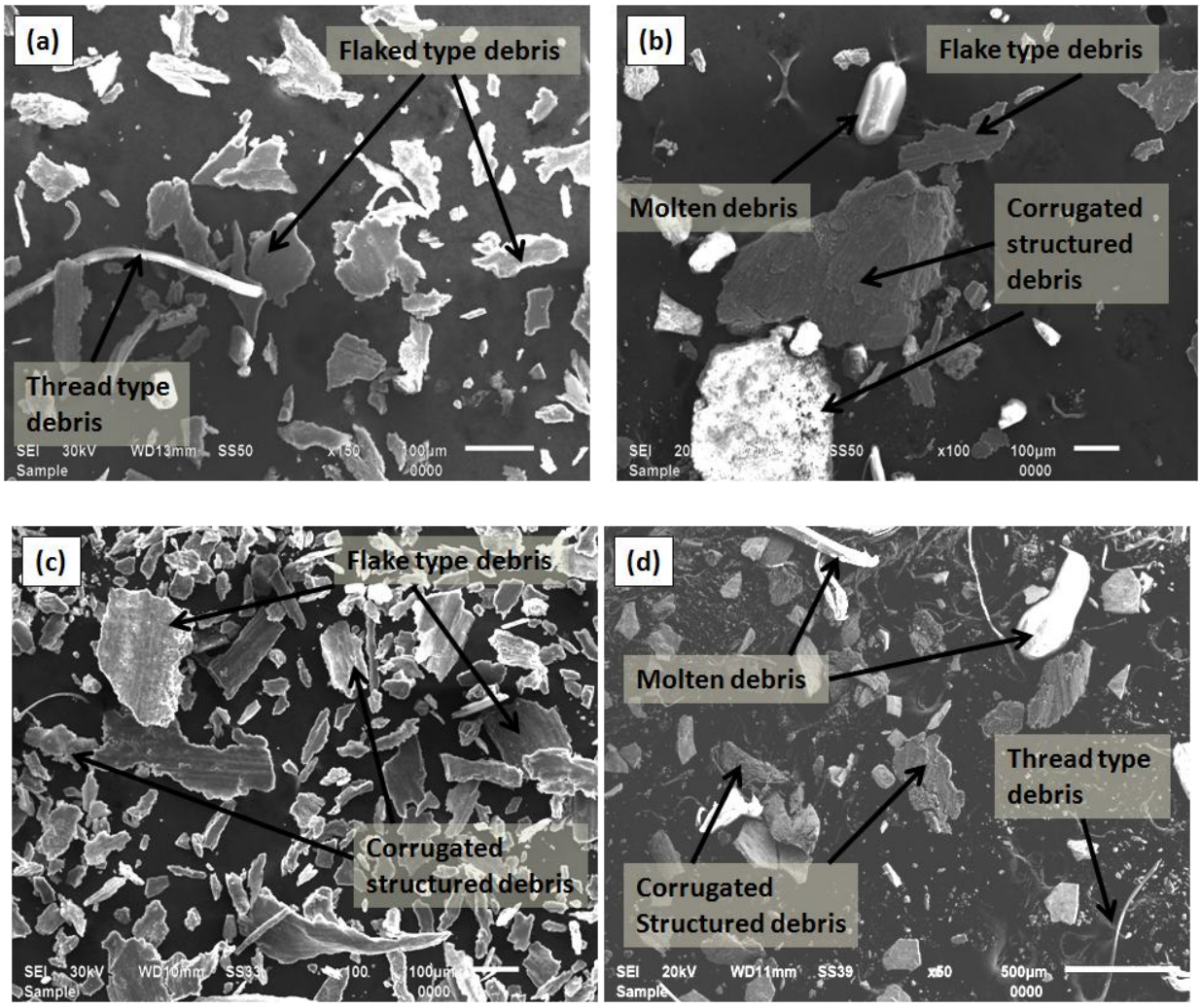

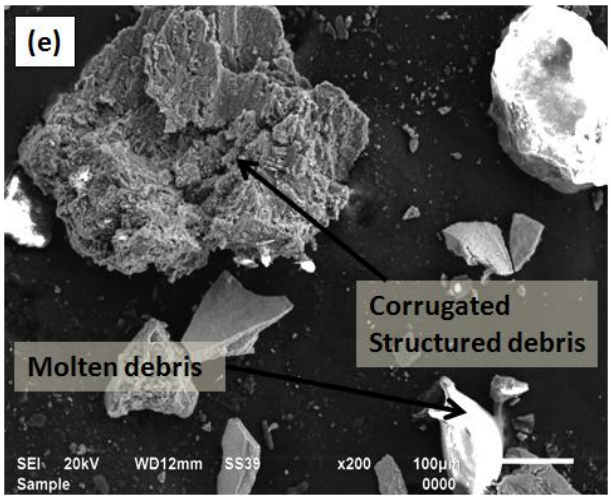

Figure 5.15: SEM micrographs of wear debris for the DSR-15A composite at (a) 9.8 N, (b) 19.6 N, (c) 29.4 N, (d) 39.2 N and (e) 49 N loads.

Figure 5.16 (a- e) shows the SEM images of the wear track DSR-15B composite tested at 9.8 N, 19.6 N, 29.4 N, 39.2 N and 49 N loads respectively. Figure 5.16a shows the SEM image of composite tested at 9.8 N load. Delamination along with grooves is observed in the SEM images of the composites at low load (9.8 N) condition. Some zircon sand particles chipped out from the surface are also observed in the SEM image (Fig. 5.15a). With increasing the applied load larger delaminated area (fig. 5.15b) is observed which supports to higher wear rate at higher load. At higher load (fig. 5.15 c, d & e) lager delamination area along with deeper grooves indicates higher wear rate of the composites. However, in comparison to the DSR-15A composite, SEM images of DSR-15B composite is relatively smooth which shows better wear resistance of the DSR-15B composite. Groove depth and delaminated area also indicates the lower wear rate of DSR-15 B composites. This improvement in wear is due to higher amount of fine size zircon sand particles in matrix. Increment in load initiates the formation of crater and crack, as shown in fig. 5.15 (c, d & e). The rupture of mechanically mixed layer initiates the adhesive wear mechanism and crater grows in size at higher load. At higher load (49 N) the cracks propagate and removal of material occurs by delamination, as shown in fig 5.15e.

Figure 5.17 (a- e) shows the SEM micrographs of DSR- 15B composite collected after the wear test at 9.8 N, 19.6 N, 29.4 N, 39.2 N and 49 N respectively. The long flakes with microcracks along with abrasive grooves are observed in the collected debris as shown in fig. 5.17 (a- e). At higher load, i.e., 49 N load, the flakes having number of microcracks along the edges reveals that cracks are responsible for their delamination from the parent material [13].

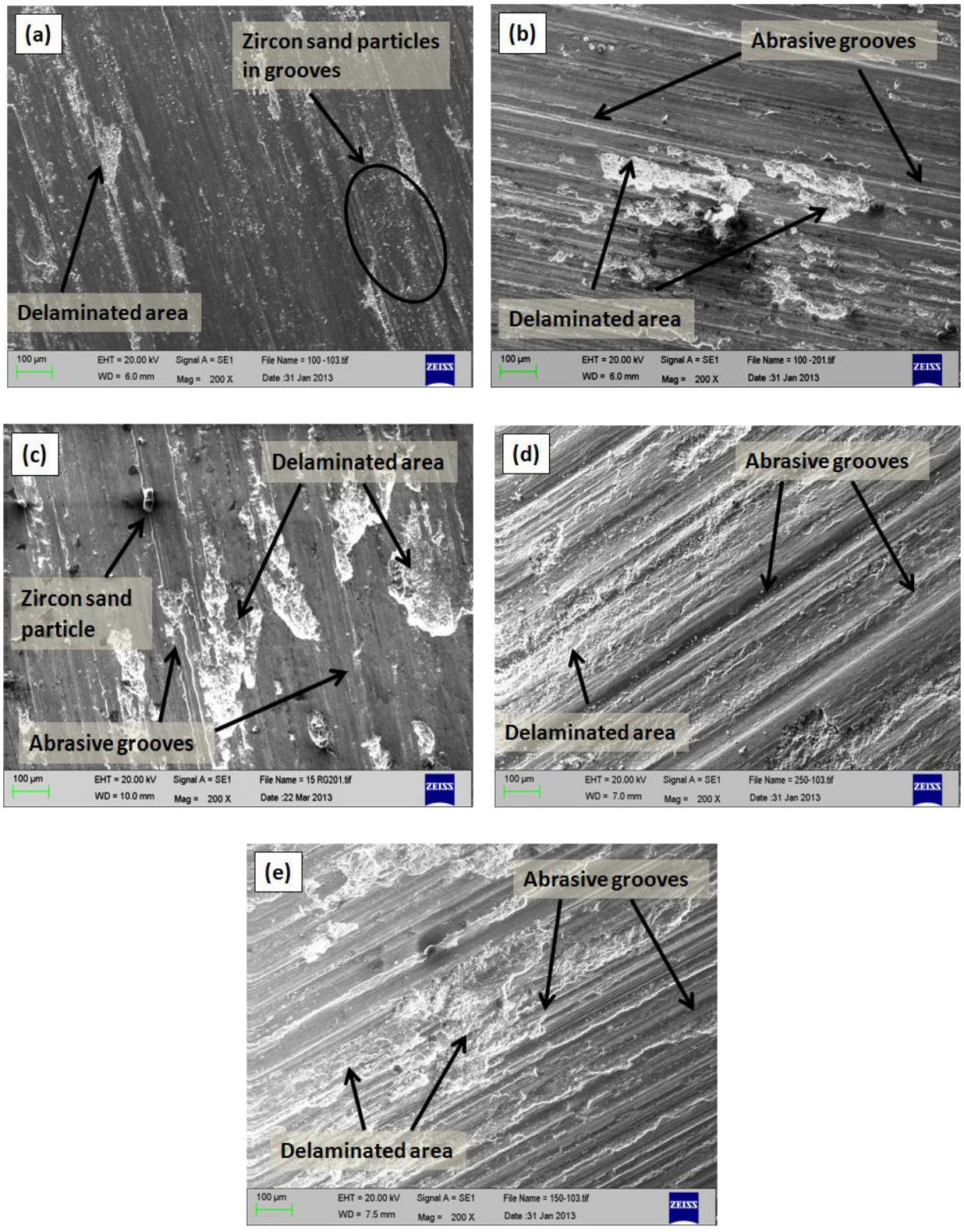

Figure 5.16: SEM micrographs of wear tracks for the DSR-15B composite at (a) 9.8 N, (b) 19.6 N, (c) 29.4 N, (d) 39.2 N and (e) 49 N loads.

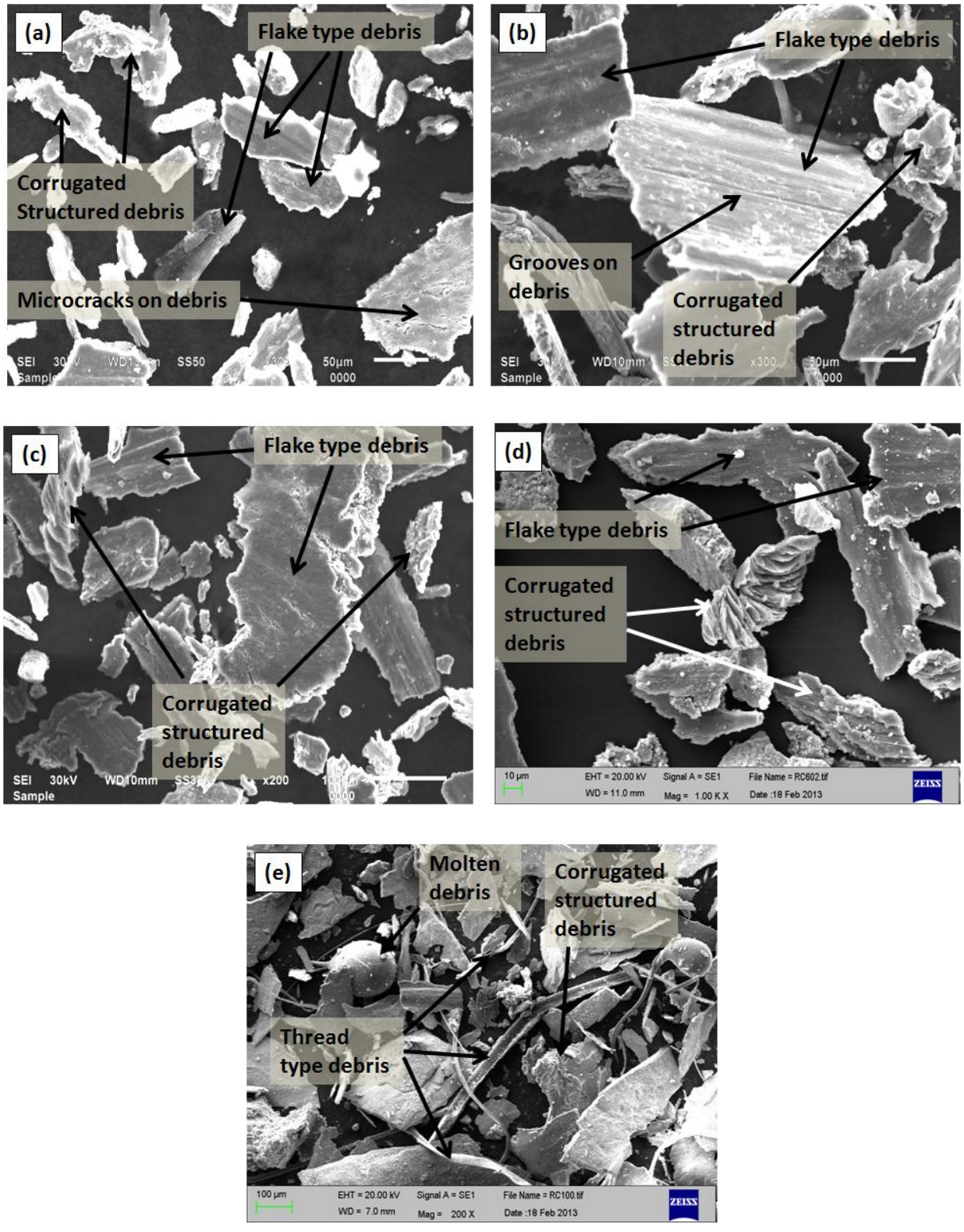

Figure 5.17: SEM micrographs of wear debris for the DSR-15B composite at (a) 9.8 N, (b) 19.6 N, (c) 29.4 N, (d) 39.2 N and (e) 49 N loads.

Some flakes having embedded particles which are pulled out with the parent material due to excessive plastic deformation as shown in figure 5.17(b & c) are observed. Wear debris generated at higher load show corrugated and layered structure (fig. 5.17c, d & e) which reveals the microlevel delamination on a flake itself and occurs due to number of microcracks [16]. The long flakes with microcracks and flakes with embedded zircon sand particle are observed in wear debris generated at 39.2 N, as shown in fig. 5.17d. At much higher load (Fig. 5.17e), presence of large size debris along with thread type morphology and molten debris indicates the mild to severe wear transition at this condition. Figure 5.18 (a- e) show the SEM images of the worn surfaces of DSR-15Ccompsoites testes at 9.8 N, 19.6 N, 29.4 N, 39.2 N and 49 N loads respectively. At low load (9.8 N), detachment of zircon sand particles which are trapped in the grooves during wear test are observed (Fig. 5.18a). With increasing the applied load larger delaminated area is observed which indicates the higher wear rate. However, depth of grooves is also increased due to higher pressure applied during wear test. Moreover, chipout of the zircon sand particles creates grooves during continious sliding (Fig. 5.18 c & d). Figure 5.18d shows the presence of the partially detached material along with the microcracks which indicates the initiation of the material removal due to microcracking. At high (49 N) load worn surface of the composite shows the much larger delaminated area with deeper grooves indicating the severe wear at this condition.

Figure 5.19 (a- e) shows the SEM images of the wear debris collected for DSR-15C composites which have been tested at 9.8 N, 19.6 N, 29.4 N, 39.2 N and 49 N loads respectively. At low (9.8 N) load, collected wear debris of flake shape shows the delamination of the material due to adhesive wear meachanism. However, debris with corrugated/layered sturcture indicate the formation of delaminated layer due to continuous rubbing of debris during wear test. At 19.6 N load, larger size of debris (fig. 5.19b) indicates more wear loss of material at higher load. Rough edges of debris support the delamination by mircocracking [13]. Thick debris in large amount at higher load condition indicate the higher wear rate. The molten debris are genrated due to the more frictinal heat generated between the acting sufaces at higher load (figure 5.19 c, d & e). Thread type morphology of debris is due to the result of pulling off the plastically deformed matrix under higher loading conditions. Figure 5.19e shows the thick corrugated stucture of collected derbis which is broken due to the severe wear during sliding wear test at higher (49 N) load.

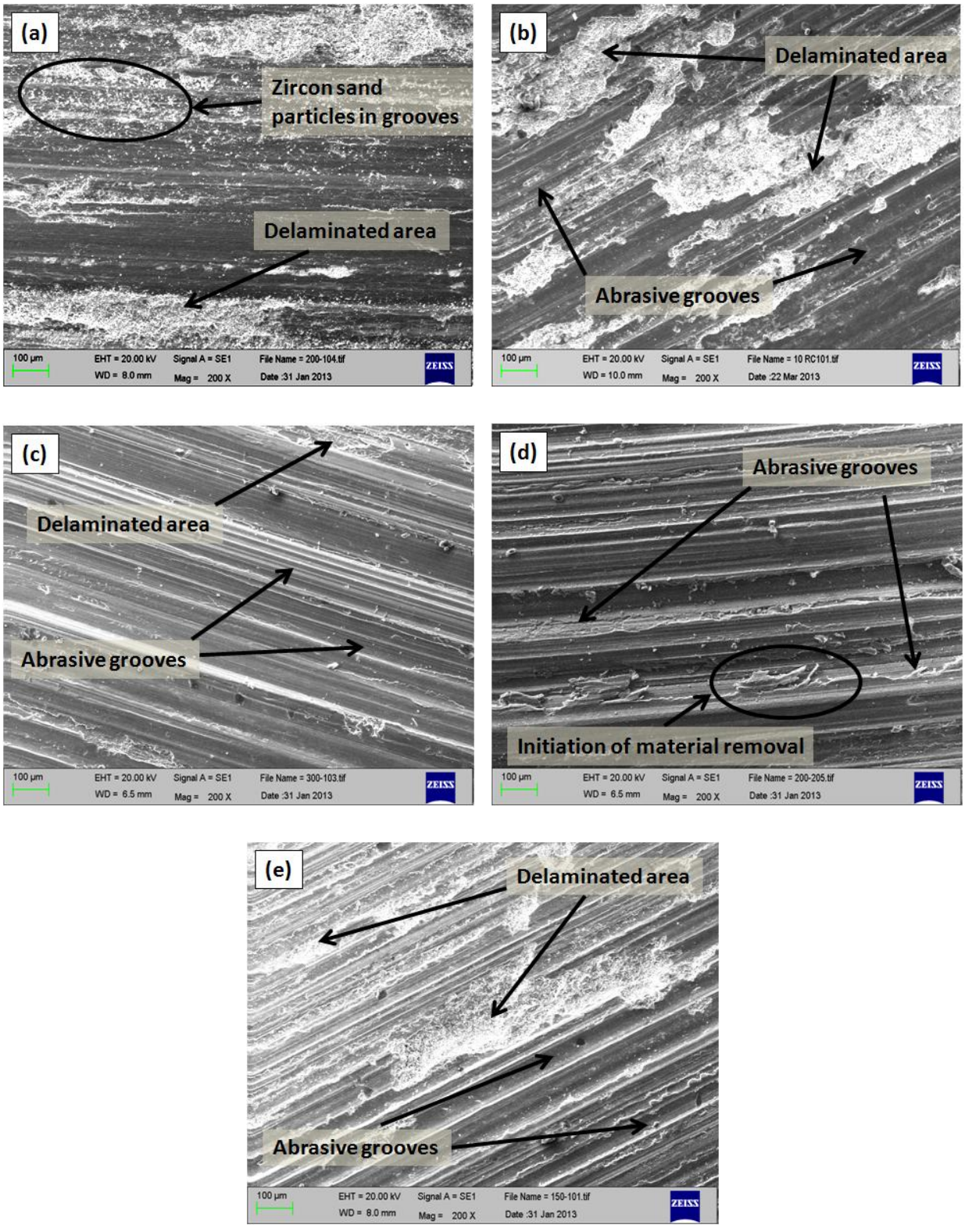

Figure 5.18: SEM micrographs of wear tracks for the DSR-15C composite at (a) 9.8 N, (b) 19.6 N, (c) 29.4 N, (d) 39.2 N and (e) 49 N loads.

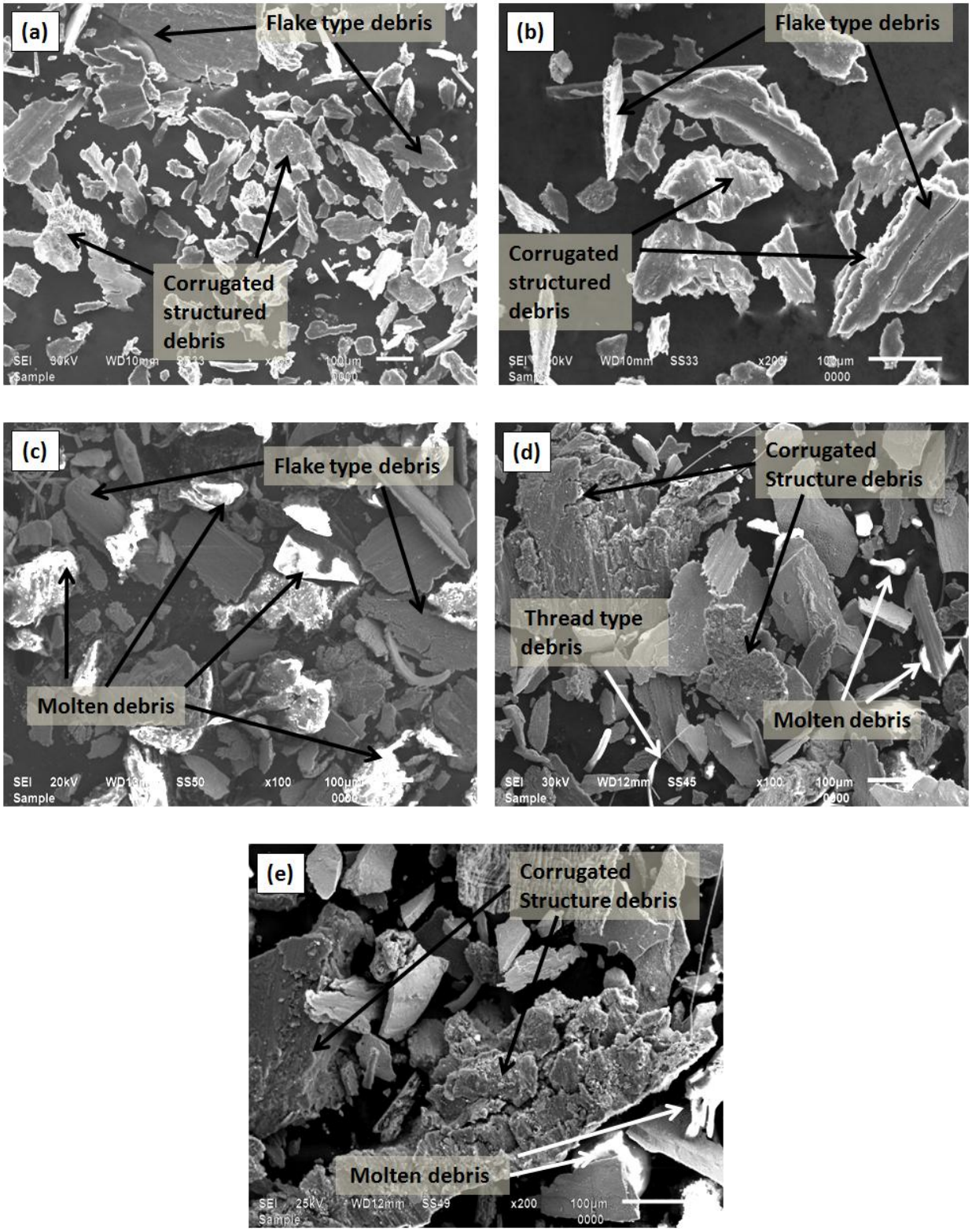

Figure 5.19: SEM micrographs of wear debris for the DSR-15C composite at (a) 9.8 N, (b) 19.6 N, (c) 29.4 N, (d) 39.2 N and (e) 49 N loads.

Figure 5.20(a- e) shows SEM micrographs of wear tracks for DSR-15D composite tested at 9.8 N, 19.6 N, 29.4 N, 39.2 N and 49 N loads respectively. Figure 5.20a shows the worn surface of sample pin tested at 9.8 N load. Smaller delaminated area with smoother grooves indicates the lower wear rate. However, as discussed earlier with increasing the load wear rate increases, figure 5.20 (a- e) supports this phenomenon. Figure 5.20 (a- d) shows the SEM images of the worn surface for DSR-15D composite samples tested at 9.8 N, 19.6 N, 29.4 N, 39.2 N and 49 N loads respectively. Smaller delaminated areas with much smoother grooves (fig. 5.20a) indicate the lower wear rate as discussed earlier (figure 5.8). However, with increase in applied load, delaminated area with deeper grooves increases as shown in figure 5.20 (b- e). Wavy pattern observed on the wear tracks (fig. 5.20c) is due to plastic deformation during continuous rubbing of the surface. With increasing the applied load (39.2 N), grooves become more deeper. Moreover, the edges of the grooves indicate the delamination of material due to microcracking. Presence of welded zircon sand particles in the grooves is due to the attachment of particles to the matrix due to frictional heat generated between the surfaces (fig. 5.20d). At higher (49 N) load, more damaged area with voids and abrasive grooves indicate the severe wear at this condition (fig. 5.20e). Craters like damage on the worn surface and voids are due to agglomeration of the particles, as 15wt.% of dual size particles with more ratio of fine size particles tends to agglomerate, which is responsible for the higher wear rate.

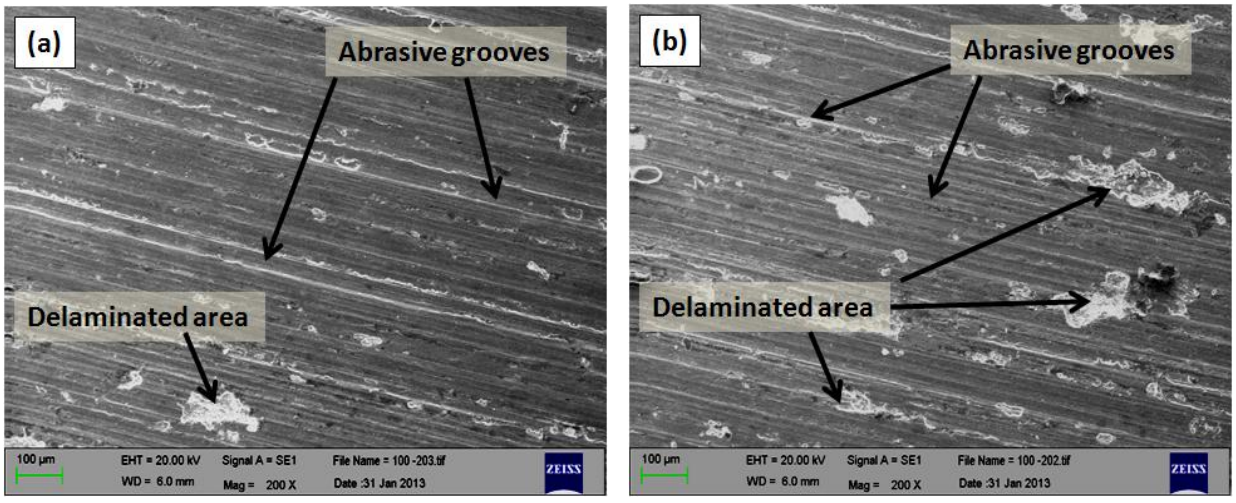

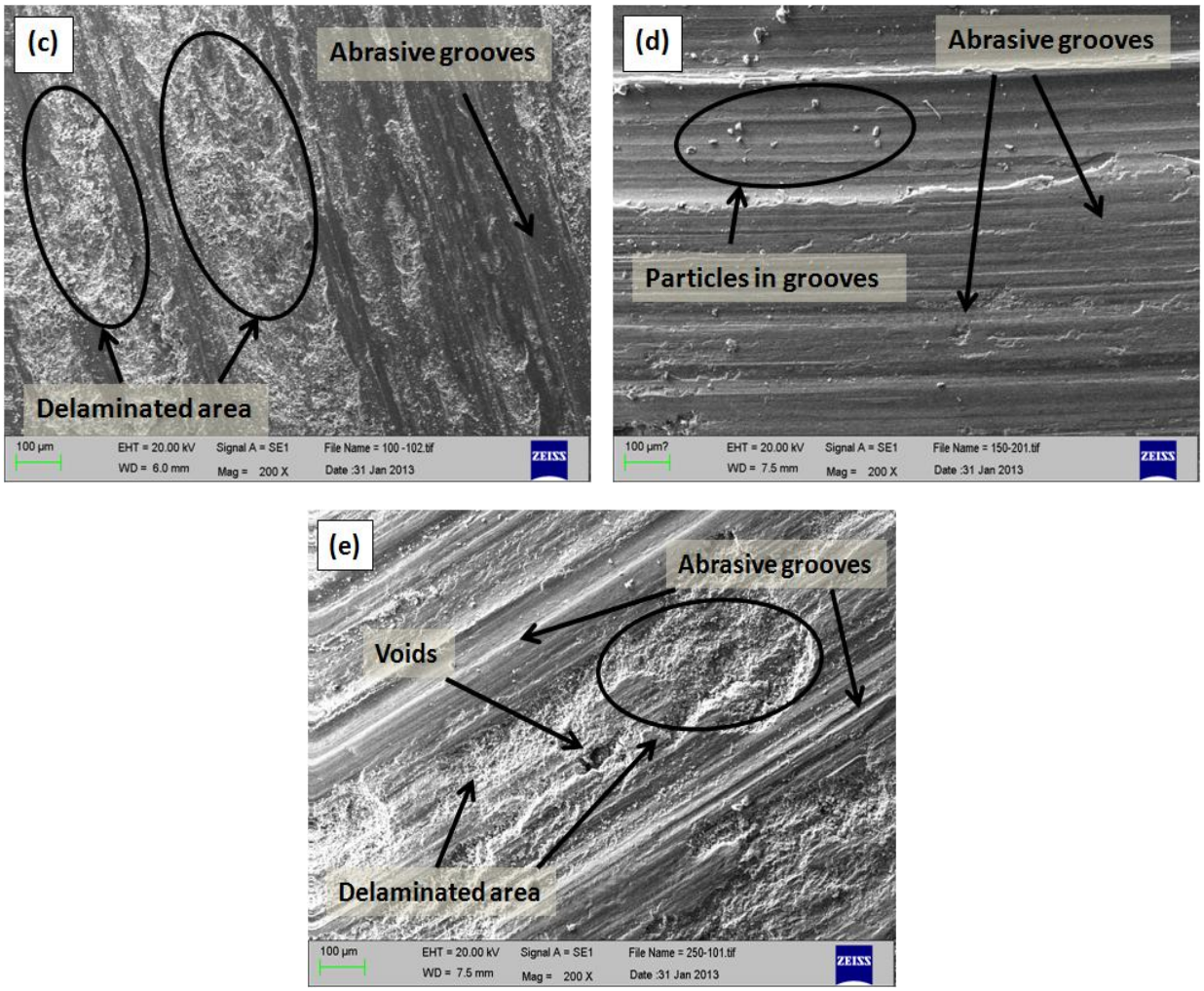

Figure 5.20: SEM micrographs of wear tracks for the DSR-15D composite at (a) 9.8 N, (b) 19.6 N, (c) 29.4 N, (d) 39.2 N and (e) 49 N loads.

Figure 5.21 (a- e) shows the SEM images of the collected debris for DSR-15D composites tested at 9.8 N, 19.6 N, 29.4 N, 39.2 N and 49 N loads respectively. Figure 5.21a shows the flake type debris mostly with sharp edges which represent the delamination of the material with fine size particles. However, some debris with soft edges are also seen which indicates the adhesive mechanism involved at low (9.8 N) load condition. At higher load, as shown in figure 5.21 (b- e), flakes debris with corrugated structure becomes larger, which indicate the higher wear rate of the composites at this condition. Edges of the debris clearly indicate the delamination of the material by initiation of microcrakes during wear tests. At 49 N load, thick corrugated structure of debris is indication of removal of material in large amount as shown in figure 5.21e. Thread type morphology is due to the pull out of the soften matrix from grooves at high load.

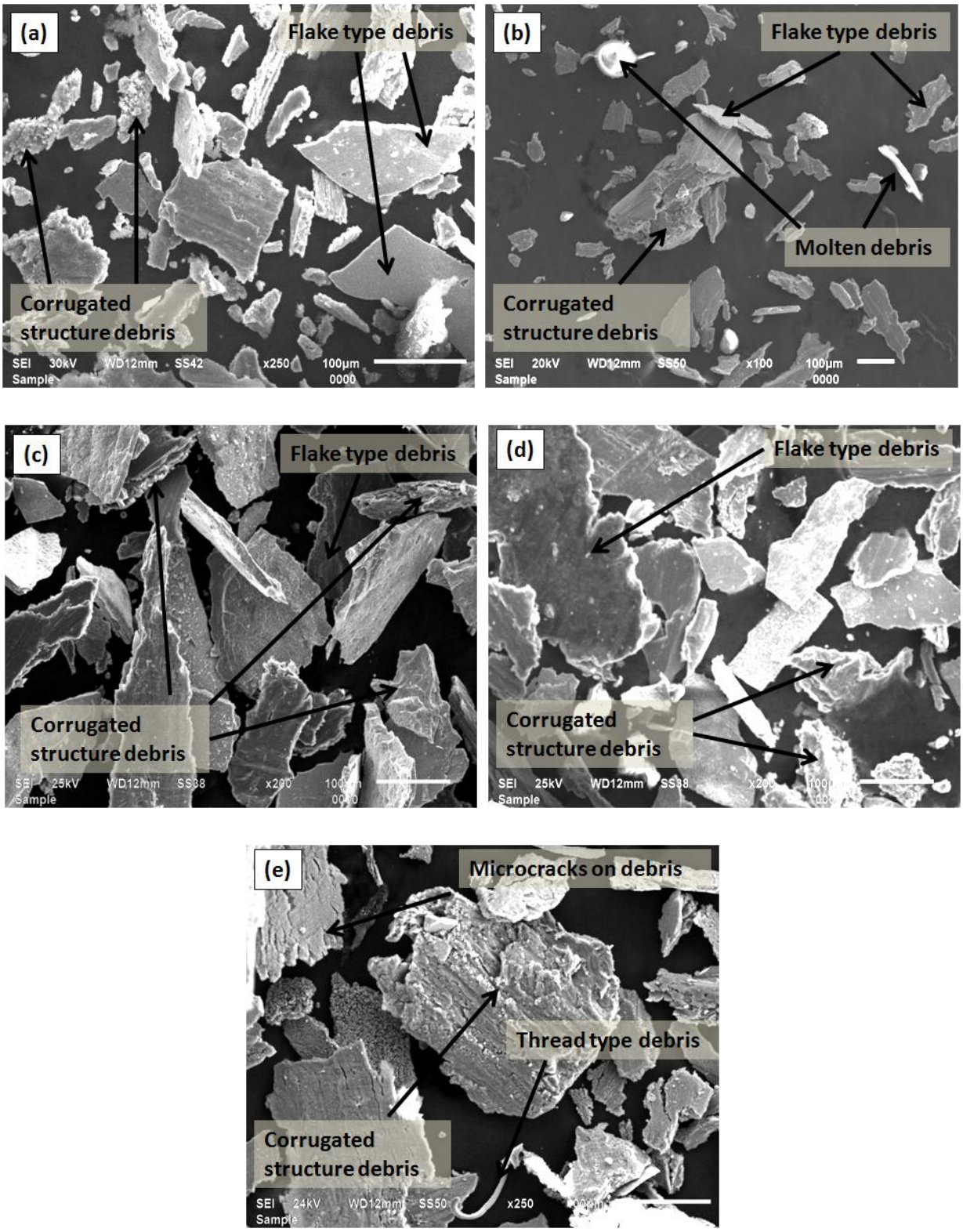

Figure 5.21: SEM micrographs of wear debris for the DSR-15D composite at (a) 9.8 N, (b) 19.6 N, (c) 29.4 N, (d) 39.2 N and (e) 49 N loads.

5.4.2 Analysis of the worn surfaces and wear debris under different ambient temperature and loading condition

Figure 5.10- 5.13 reveal that wear behavior of the DSR- composites is affected by ambient temperature significantly at different loading conditions. In this section, we have discussed about the SEM of worn surfaces and wear debris collected after the wear test of DSR-15A, 15B, 15C and 15D composites only at high (49 N) load condition with variation of ambient temperature. Here, the SEM micrographs of the worn surfaces and wear debris of DSR-15 (A, B, C & D) composites tested at 150 ºC, 200 ºC, 250 ºC and 300 ºC at high (49 N) load only are presented for simplicity. Figure 5.22 (a- d) shows the SEM images of the worn surface of the DSR-15A composite tested at 49 N load with 150 ºC, 200 ºC, 250 ºC and 300 ºC respectively. Figure 5.22a shows the SEM images of the DSR-15A composites tested at 150 ºC and 49 N load. With increase in temperature, delamination of the surface was observed due to plastic deformation of soften matrix at high load condition. Presence of microcracks on the edges of delaminated area indicates the removal of material by propagation of cracks at higher stress. At 200 ºC and 49 N load, brighten phase observed in SEM micrograph of the worn surface of DSR-15A composites (fig. 5.22b) is the evidence of presence of oxide layers. These oxide layers are responsible for the lower wear rate as they are avoid of the metal to metal contact. However, at much higher temperature, larger delaminated area along with zircon sand particles in the grooves indicates the higher wear rate. Tearing of oxide layers on the edges of the delaminated area can be seen (fig. 5.22c). It causes higher wear rate, which is enhanced further as new area for the delamination is exposed out. Figure 5.22d shows the particles on the worn surface, these hard particles on the surface act as barrier to the metal- metal contact and help to reduce the wear rate at such high temperature (300 °C) and high load (49 N) condition.

Figure 5.23 (a- d) shows the SEM images of wear debris collected for the DSR-15A composite tested at 49 N load for 150 °C, 200 °C, 250 °C and 300 °C temperatures respectively. Larger debris with corrugated structure epitomize the higher wear rate. These corrugated structures on debris are due to the continuous rubbing of materials during wear test [16]. However, grooves on the debris shown in fig. 5.23a are due to trapped zircon sand particles between the contact surfaces during wear tests. Smaller amount of the debris in presence of fractured debris shown in figure 5.23b, indicates the lower wear rate at this condition. With increasing the temperature up to 250 °C, shape and size of the debris shown in figure 5.23c indicates the higher wear rate at

high loading condition. In fig. 5.23d some debris that solidified from the molten state were also observed at higher temperature (300 °C). Due to continuous rubbing action, these get heated and reach the melting point of metal. However, presence of free particles along with the flake shape debris indicates the lower wear rate of the composite in this condition.

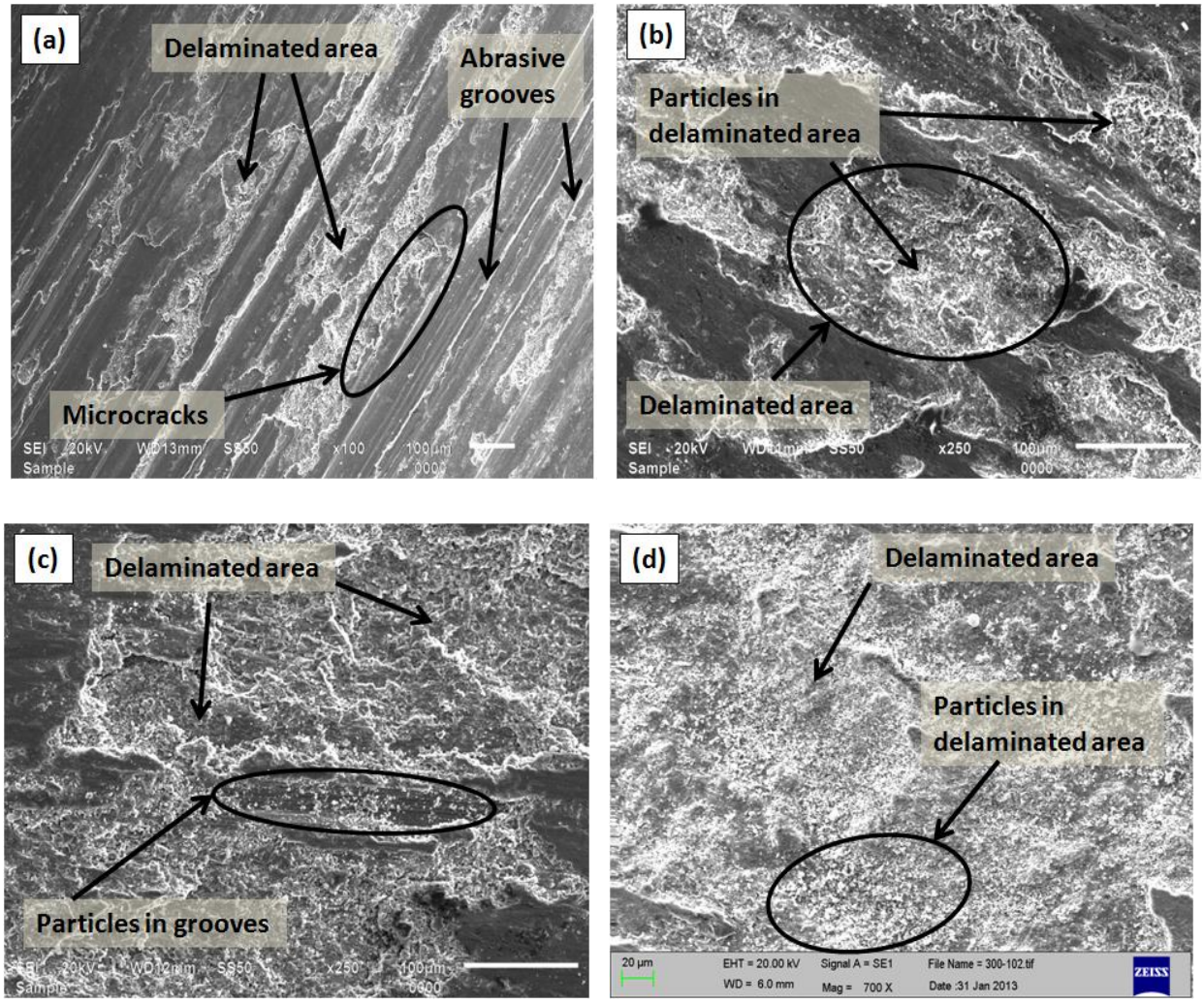

Figure 5.22: SEM images of the wear tracks for the DSR-15A composite at 49 N loads for (a) 150 °C, (b) 200 °C, (c) 250 °C and (d) 300 °C.

Figure 5.24 (a- d) shows the SEM images of wear tracks for the DSR-15B composite tested at 49 N loads at 150 °C, 200 °C, 250 °C and 300 °C temperatures respectively. Figure 5.24a shows the SEM micrograph for the DSR-15B composites tested at 150 °C with 49 N load.

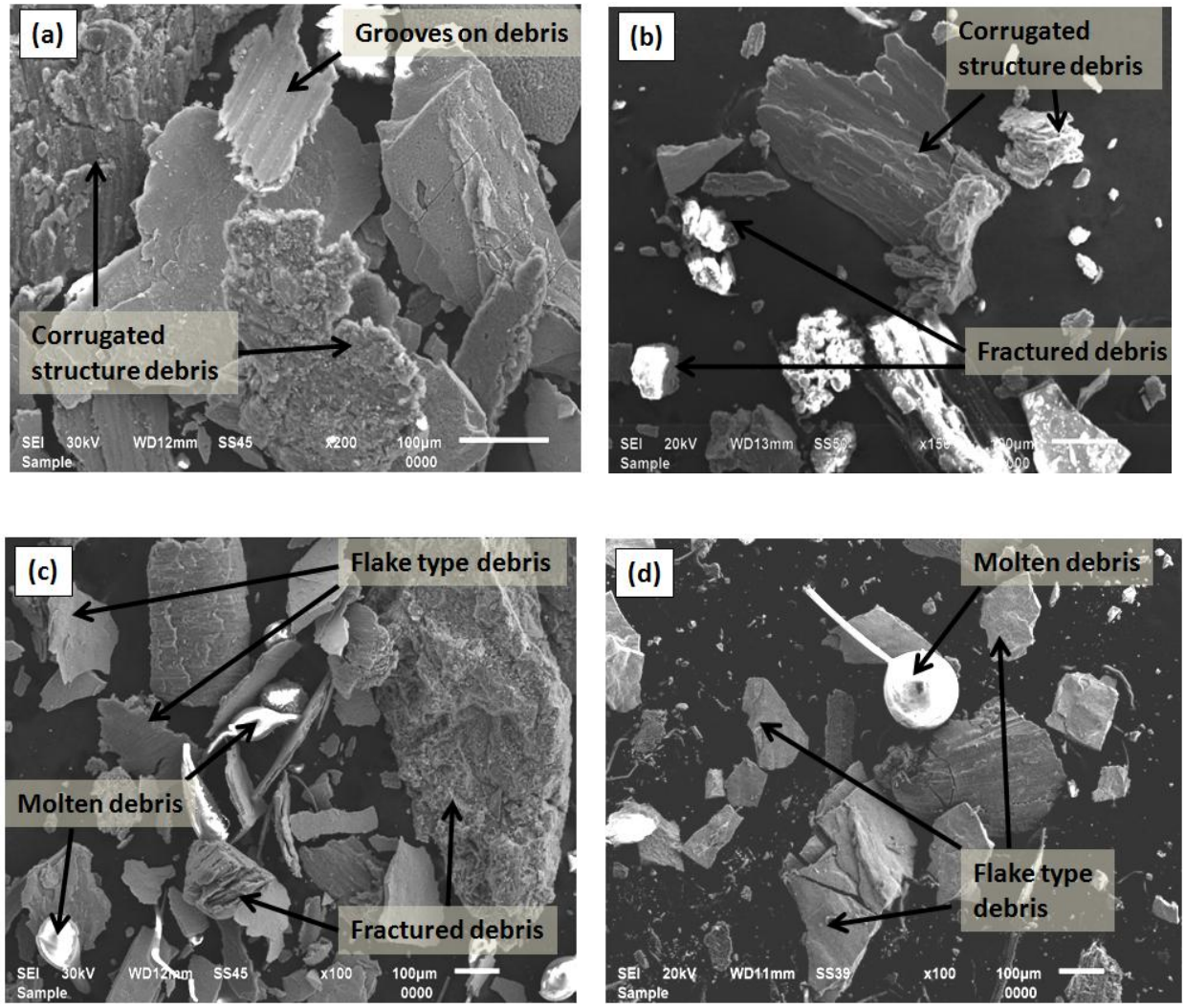

Figure 5.23: SEM images of the wear debris for the DSR-15A composite at 49 N loads for (a) 150 °C, (b) 200 °C, (c) 250 °C and (d) 300 °C.

Presence of deep grooves along with the delaminated area in sliding direction indicates the higher wear rate of the composite at this condition. A high degree of flow of materials along the sliding direction, the generation of cavities due to delamination of surface materials, and the tearing of surface materials indicate the transition from mild to severe wear at high temperature. Mondal *et al*.[17] suggested that the flow of material in wavy form (serration) and large cavity due to delamination indicates the greater degree of softening of surface materials, partial melting of the worn surface, and localized adhesion between the specimen surface and counter body. Figure 5.24b shows the SEM image of the worn surface for DSR-15B composite tested at 200 °C with 49 N load. Smaller delaminated debris along with abrasive grooves in direction of sliding

indicates the delamination of the materials due to abrasive mechanism. However, wavy pattern and rough edges along the delaminated area indicate the removal of materials due to propagation of microcracks during continuous rubbing of material. Presence of grooves indicates the materials removal due to peel out of the matrix caused by trapped zircon sand particles. However, at higher temperature (250 °C) more delaminated area observed in figure 5.24c indicates the severe wear during the test at high load. At much higher temperature (300 °C), SEM image of DSR-15B composite (Fig. 5.24d) shows that delaminated area is smaller and grooves are flatter in comparison to the worn surface observed at 250 °C (fig. 5.24c).

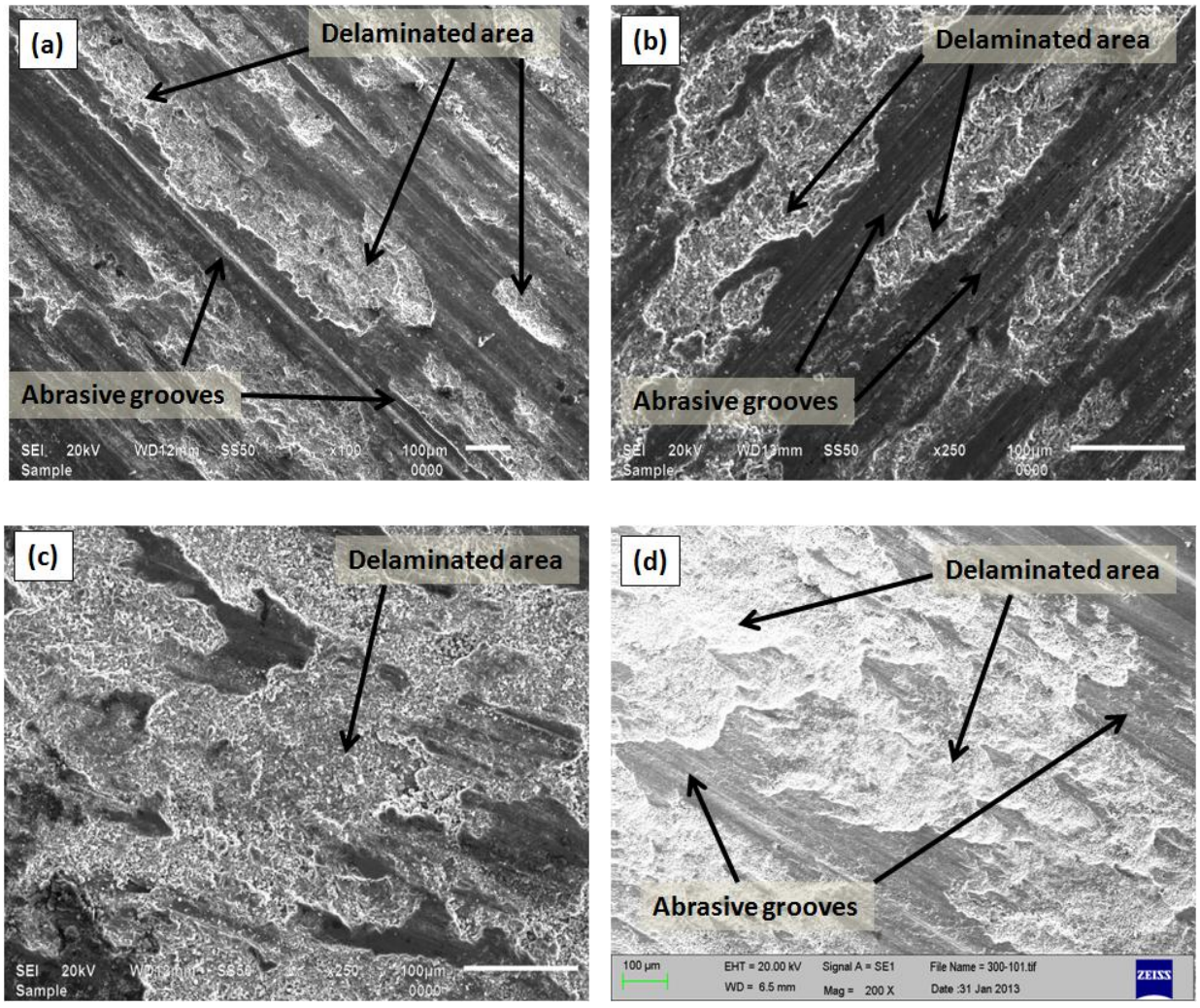

Figure 5.24: SEM images of the wear tracks for the DSR-15B composite at 49 N loads for (a) 150 °C, (b) 200 °C, (c) 250 °C and (d) 300 °C.

Figure 5.25 (a- d) shows the SEM micrographs of wear debris collected for DSR-15B composite tested at 49 N loads with 150 °C, 200 °C, 250 °C and 300 °C temperatures respectively. Figure 5.25a shows the SEM images of wear debris collected for the composite tested at 49 N load and 150 °C temperature. Presence of soft looking debris indicates the delamination of material due to softening of matrix at 150 °C.

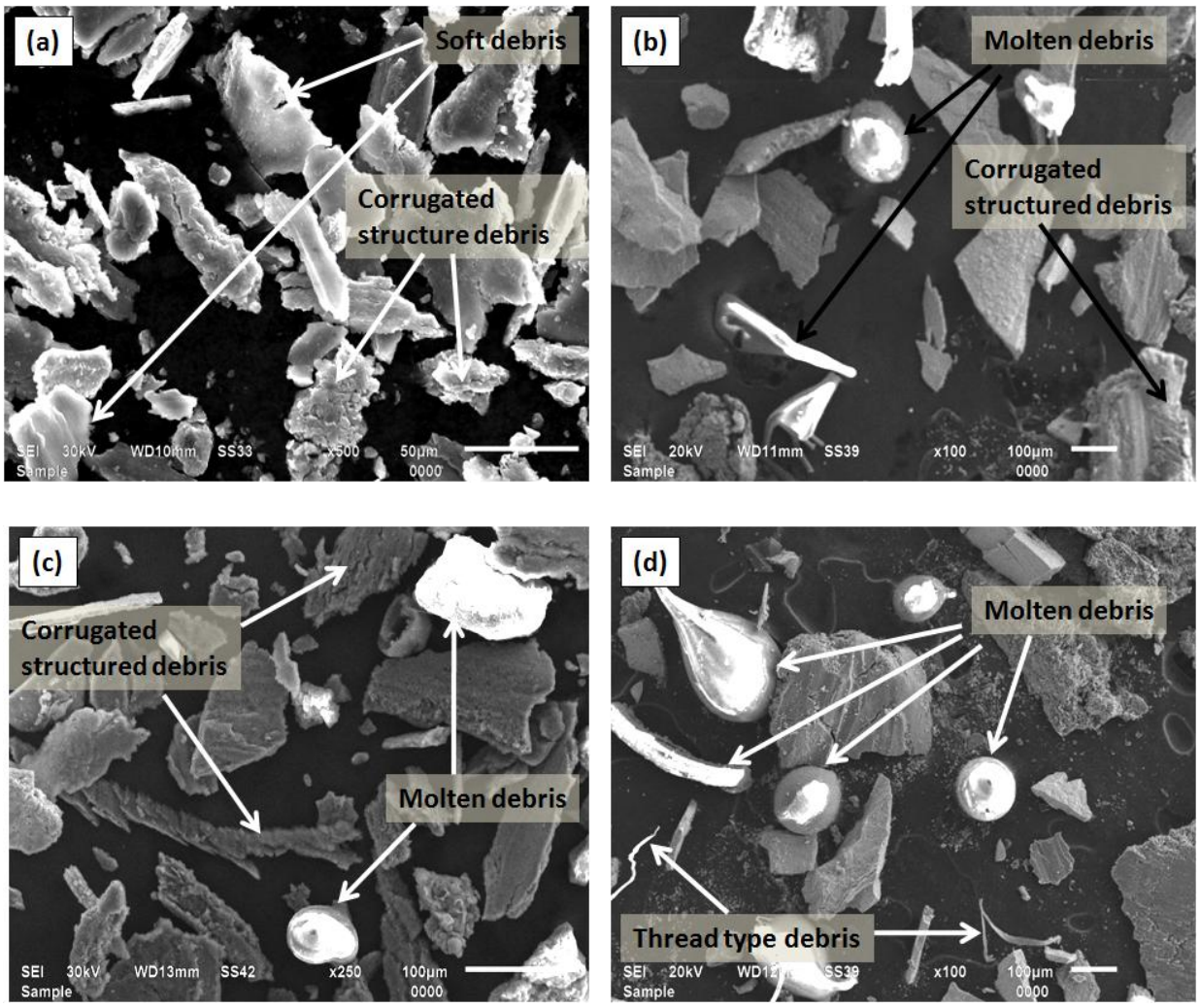

Figure 5.25: SEM images of the wear debris for the DSR-15B composite at 49 N loads for (a) 150 °C, (b) 200 °C, (c) 250 °C and (d) 300 °C.

Flake type debris along with corrugated structure shows the more wear at high load condition. At higher temperature (200 °C), smaller amount of debris along with spherical shape molten debris clearly indicate the decrement in wear at high load conditions (fig. 4.25b). However, at 250 °C

temperature with 49 N load, debris collected (fig. 5.25c) after the wear test point out the higher removal of material in comparison to the fig. 5.25b, as collected debris are thicker in shape and larger in amount. Figure 5.25d shows the SEM images of wear debris of DSR- 15B composite tested at 300°C with 49 N load. Presence of free zircon sand particles along with round shape molten debris supports less material removal during wear test.

Figure 5.26 (a- d) shows the SEM images of the worn surface of DSR15C composite tested at 49 N load with 150 °C, 200 °C, 250 °C and 300 °C temperature respectively. Figure 5.26a shows the worn surface of DSR- 15C composite tested at 150 °C and 49 N load. Deeper grooves shown in fig. 5.26a indicate the higher removal of material. Welded zircon sand particles on the worn surfaces are also observed. At higher temperature (200 °C), decrement in delaminated area and depth of grooves indicates the improvement in wear resistance due to presence of oxide layers (brighten phase) on the worn surface of composite. However, at much higher temperature (250 °C) increment in the delaminated area along with deeper grooves and zircon sand particles depicts the higher wear rate. This increment in wear rate is due to the fracture of oxide layer during wear test at high load, which provide new area for wear. Figure 5.26d indicates the smaller delaminated area with flattened grooves which demonstrate the lower wear rate. Presence of crater on the worn surface indicates the chipping out of loosely bound agglomerated particles during wear test.

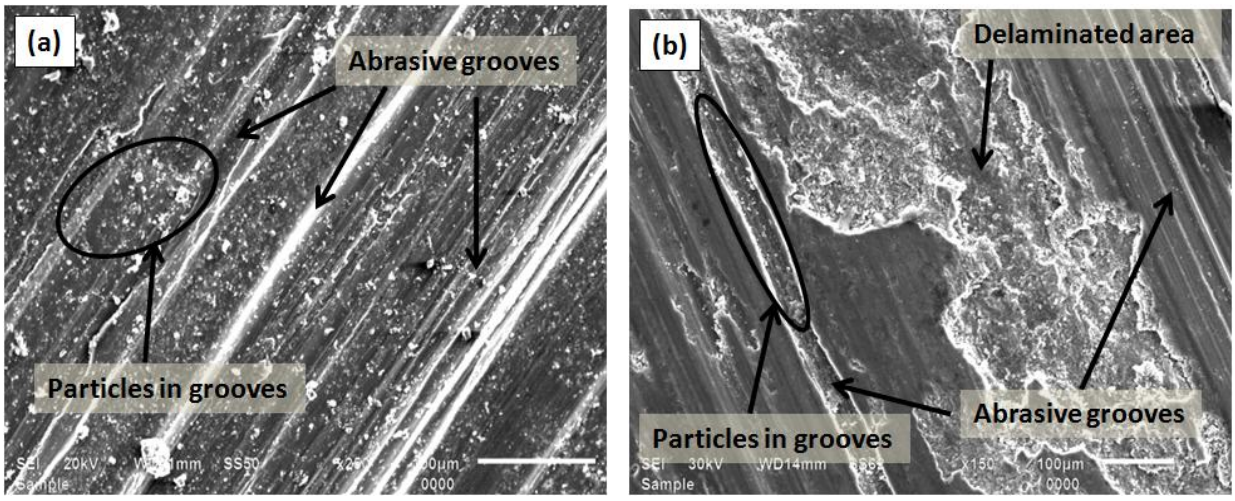

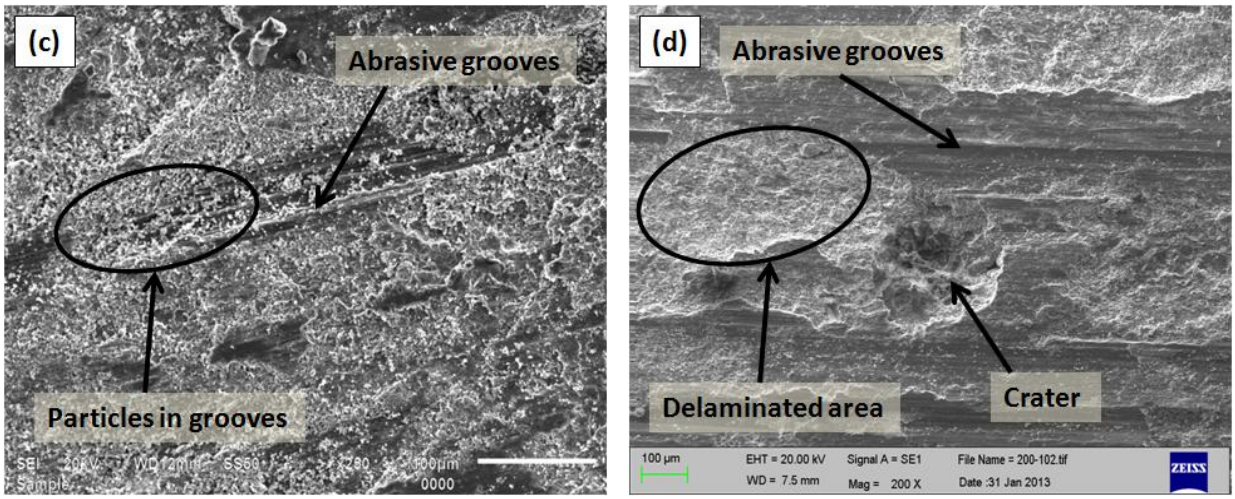

Figure 5.26: SEM images of the wear tracks for the DSR-15C composite at 49 N loads for (a) 150 °C, (b) 200 °C, (c) 250 °C and (d) 300 °C.

Figure 5.27 (a- d) shows the SEM images of the wear debris collected for the DSR-15C composite tested at 49 N load and 150 °C, 200 °C, 250 °C and 300 °C temperatures respectively. Figure 5.27a shows the debris with soft edges along with corrugated structure, this corrugated/ layered structure is due to continuous rubbing of composites during wear test at high load [16]. Debris with rough edges shows the detachment of the material due to initiation of microcracking. Lager amount of debris depicts the higher removal of material. At 200 °C and 49 N load, wear debris are less in amount (Fig. 5.27b), indicating the lower wear rate in comparison to the wear test done at 150 °C and 49 N load.

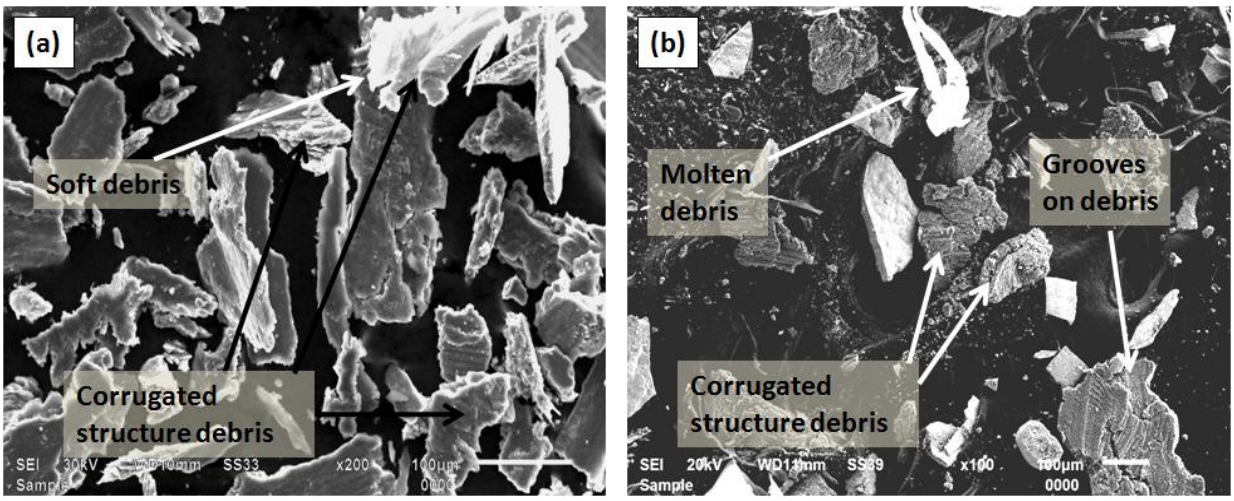

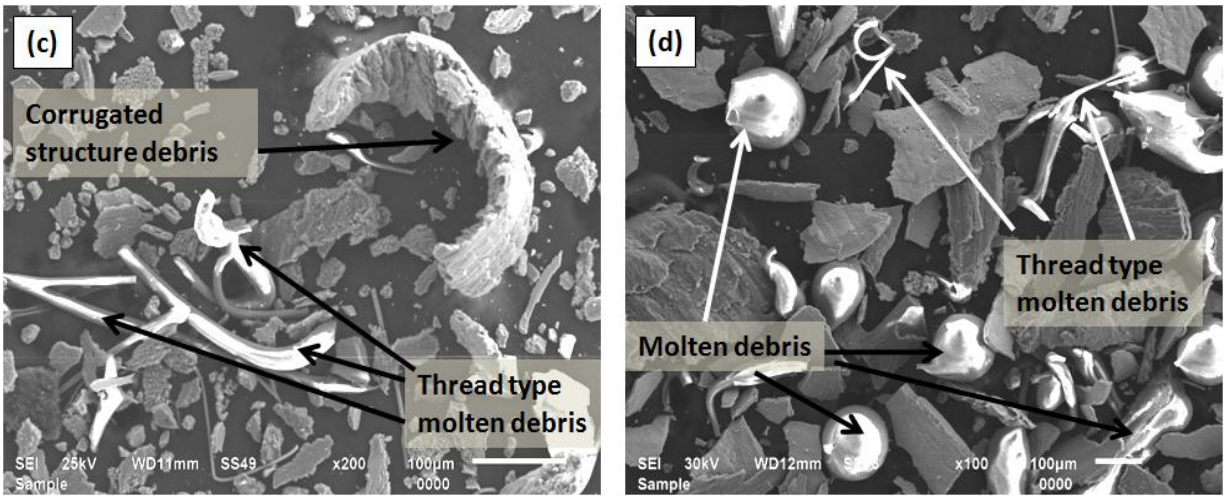

Figure 5.27: SEM images of the wear debris for the DSR-15C composite at 49 N loads for (a) 150 °C, (b) 200 °C, (c) 250 °C and (d) 300 °C.

However, at much higher temperature (250 °C) collected debris are thicker and thread type morphology is also observed (Fig. 5.27c), which is an indication of higher wear rate. Figure 5.27d indicates the large amount of round shape molten debris and thread type morphology of debris. Flake shape debris indicates plastic deformation during the wear test. However, due to continuous rubbing of removed material, wavy pattern is clearly seen on the debris (Fig. 5.27d). Figure 5.28 (a- d) shows the SEM images of the worn surfaces for the DSR-15D composite tested at 49 N load with 150 °C, 200 °C, 250 °C and 300 °C temperatures respectively. DSR-15D composite contains more ratio of fine size particles in dual size reinforcement in matrix. SEM images (5.28 a- d) of wear tracks clearly indicate that zircon sand particles chipout easily at higher temperature, because the surrounding matrix becomes soft and there is a lack of support for loosely bound agglomerated particles. Moreover, the thick oxide covers that prevent the surface also come out due to sliding of surface at higher temperature. Figure 5.28c depicts the higher removal of material as larger delaminated area with crater and deeper grooves is clearly observed [16]. However, due to involvement of particles, wear rate decreases at higher temperature (300 °C) and high (49 N) load. Figure 5.28d shows that plastic deformation has occurred and debris are sliding along the edges of the ploughing marks causing negative wear.

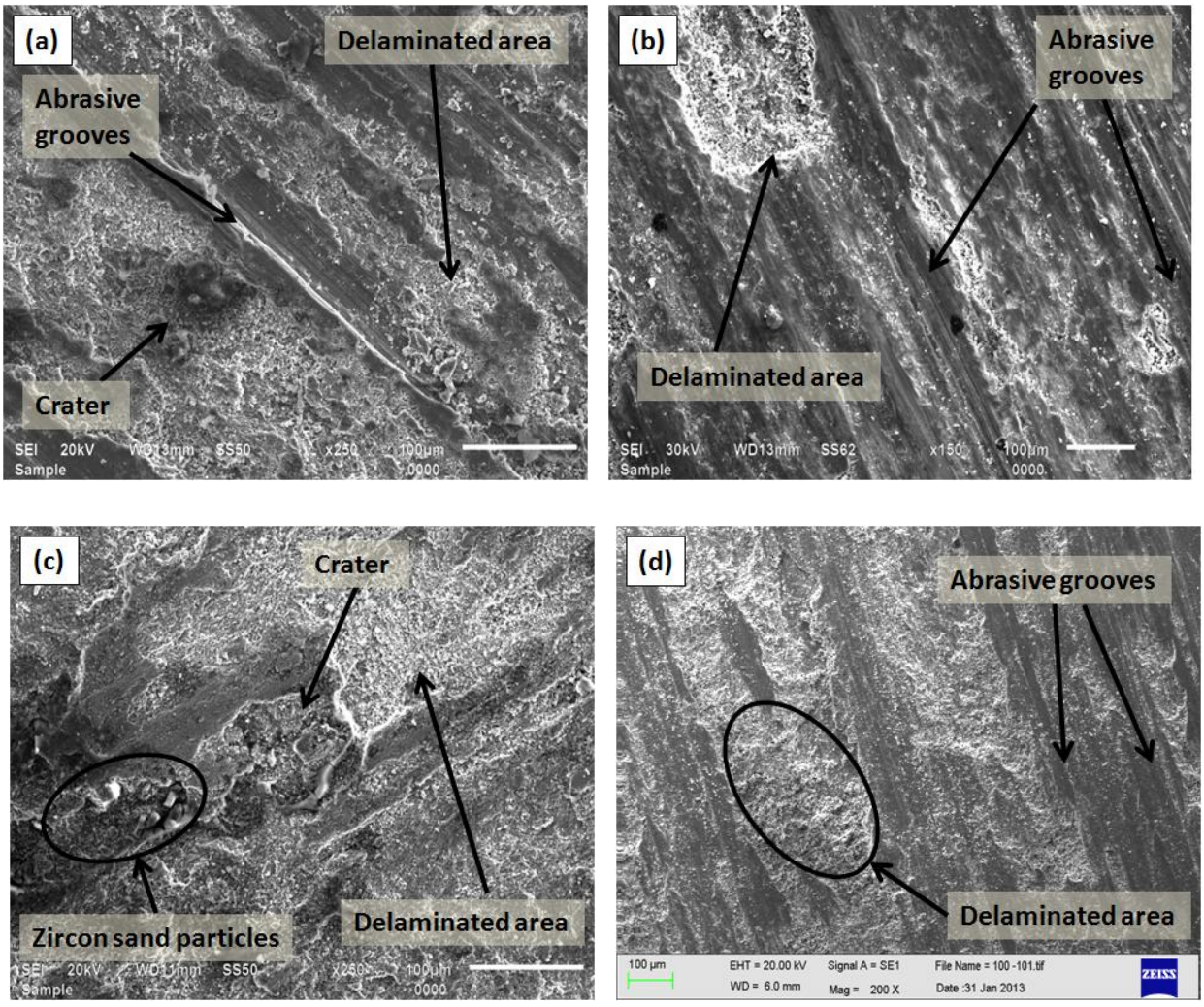

Figure 5.28: SEM images of the wear tracks for the DSR-15D composite at 49 N loads for (a) 150 °C, (b) 200 °C, (c) 250 °C and (d) 300 °C.

Figure 5.29 (a- d) shows the SEM images of the wear debris collected for the DSR-15D composite tested at 49 N load with 150 °C, 200 °C, 250 °C and 300 °C respectively. Presence of more amount of fine size particles in the composite also reflects the nature of collected debris. Due to presence of fine particles flake type debris with shallower grooves are observed in the micrograph. Due to high (49 N) loading condition, fractured debris are also seen in figure 5.29a. However, with increasing the temperature, size of debris decreased along with the presence of thread like molten debris, as shown in figure 5.29 (b- d). Amount of molten debris was increased with the increase in the ambient temperature during wear test.

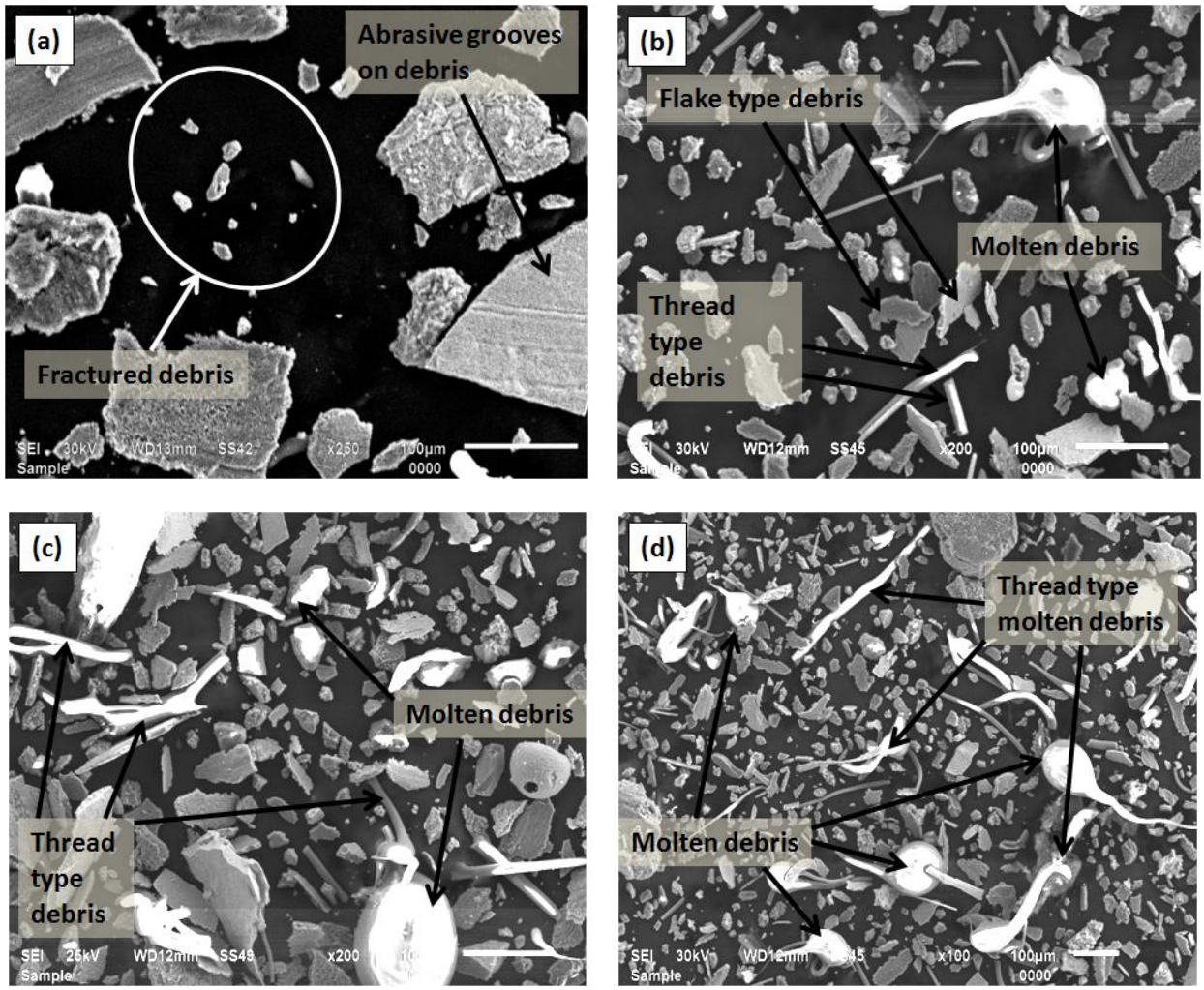

Figure 5.29: SEM images of the wear Debris for the DSR-15D composite at 49 N loads for (a) 150 °C, (b) 200 °C, (c) 250 °C and (d) 300 °C.

REFERENCES:

[1] K Kaur and OP Pandey; Dry sliding wear behavior of zircon sand reinforced Al–Si alloy. Tribology Letters, 38 (2010) 377- 387.

[2] J Hashim, L Looney and MSJ Hashmi; Particle distribution in cast metal matrix composites- part I. Journal of Materials Processing Technology, 123, (2002) 251- 257.

[3] J Hashim, L Looney and MSJ Hashmi; Particle distribution in cast metal matrix composites- part II. Journal of Materials Processing Technology, 12 (2002) 258–263.

[4] YM Youssef, RJ Dashwood and PD Lee; Effect of clustering on particle pushing and solidification behavior in TiB_2 reinforced aluminium PMMCs. Composite A, 36 (2005) 747- 763

[5] H Nakae and S Wu; Engulfment of Al_2O_3 particles during solidification of aluminum matrix composites. Materials Science and Engineering A, 252 (1998) 232–238.

[6] J Segurado, C Gonzalez and JL Lorca; A numerical investigation of the effect of particle clustering on the mechanical properties of composites. Acta Materialia, 51(2003) 2355-2369.

[7] KS Cruz, ES Meza, FAP Fernandes, JMV Quaresma, LC Casteletti and A Garcia; Dendritic arm spacing affecting mechanical properties and wear behavior of Al- Sn and Al-Si alloys directionally solidified under unsteady state conditions. Metallurgical and Materials Transactions A, 41 (2010), 972- 984.

[8] S Das, S Das and K Das; Abrasive wear of zircon sand and alumina reinforced Al- 4.5 wt% Cu alloy matrix composites- a comparative study. Composite Science and Technology, 67 (2007) 746- 751.

[9] TFJ Quinn, JL Sullivan and DM Rowson; Origins and development of oxidational wear at low ambient-temperatures. Wear, 94 (1984) 175–91.

[10] K Kaur and OP Pandey; Wear and microstructural characteristics of spray atomized zircon sand reinforced LM13 alloy. Materialwiss Werkstofftech; 41(7) (2010) 568-74.

[11] MA Martinez, A Martin and J Llorca; Wear of SiC-reinforced Al-matrix composites in the temperature range 20-200℃. Wear, 193 (1996) 169–79.

[12] S Wilson and AT Alpas; Effect of temperature on the sliding wear performance of Al alloys and Al matrix composites. Wear, 196 (1996) 270-78.

[13] KL Johnson and HR Shercliff; Shakedown of 2-dimensional asperities in sliding contact. International Journal of Mechanical Sciences, 34(5) (1992) 375–94.

[14] J Larsen-Basse and B Premaratne; Proc. Wear of materials conf. New York: ASME; 1983. p. 161.

[15] SR Bakshi, D Wang, T Price, D Zhang, AK Keshri, Y Chen, P McCartney, D Graham, H Shipway and A Agarwal; Microstructure and wear properties of aluminum/aluminum-silicon composite coatings prepared by cold spraying. Surface Coating and technology, 204 (2009) 503–551.

[16] J Zhang and AT Alpas; Transition between mild and severe wear in aluminum alloys. Acta Materialia, 45 (1997) 513.

[17] DP Mondal, S Das, RN Rao and M Singh; Effect of SiC addition and running-in-wear on the sliding wear behavior of Al-Zn-Mg aluminium alloy. Materials Science and Engineering A, 402 (2005) 307- 319.

CHAPTER 6

CONCLUSIONS AND FUTURE SCOPE

Overview:

The present chapter concludes the results obtained from various experiments discussed in previous chapters. Effect of applied load as well as temperature on the wear behavior of base alloy (LM13 alloy) and particle reinforced composites has been summarized. The role of reinforced amount as well as particle size of the reinforced zircon sand composites on the morphology, hardness and wear behavior of composites is also concluded in this chapter.

6.1 Conclusions:

Wear is related to interaction between surfaces and more specifically the removal and deformation of material from the surface as a result of mechanical action of the opposite surface. The ability of a material to resist the gradual removal of material caused by abrasion and friction is known as wear resistance of the material. In order to improve the wear resistance of metal, we incorporate the hard ceramic particles to the metal matrix. During this work, an alloy of aluminum (LM13 alloy) as matrix and zircon sand particles as reinforcement was taken to study the change in wear resistance of the metal by reinforcing ceramic particles. Aluminum alloy was chosen as matrix due to low density, good corrosion resistance, high damping capacity and high thermal and electrical conductivity. However, high modulus, high hardness, excellent thermal stability and easy availability of zircon sand ($ZrSiO_4$) particle make them a good choice for reinforcement.

In the present study, particle reinforced metal matrix composite was developed by stir casting process. During this process, LM13 alloy was melted at 800 °C in a resistance furnace and mechanically stirred with a graphite stirrer. During the stirring, after creating the vortex in the melt, zircon sand particles of defined size range and in particular amount were incorporated. After the stirring, molten mass was poured in the mold and samples were cut down for their further characterization and testing. To investigate the effect of particles on the microstructure and wear behavior of the composites, zircon sand particles of different size ranges as coarse (106- 125 µm), medium (50-75 µm) and fine (20- 32 µm) were incorporated in different amounts (5, 10, 15, 20 wt.%). Apart from this, zircon sand particles in dual size (a combination of coarse and fine size particles) were also reinforced to study the wear behavior of dual size reinforced composites.

Different characterization techniques such as X- ray diffraction (XRD), Optical microscopy, Scanning electron microscopy (SEM), Energy dispersive spectroscopy (EDS), Rockwell hardness testing, Vickers hardness testing and wear testing with pin-on-disc machine were used to see the effect of zircon sand particles on the microstructural, mechanical as well as tribological properties of LM13 alloy.

Distribution and interaction of particles in the matrix was observed under optical microscope. A fair distribution of particles in the matrix was observed with good interfacial bonding of the

zircon sand particles with matrix. However, agglomeration of the particles was also observed with higher amount (>15wt.%) of reinforcement in matrix. It was also observed that fine size particles show more agglomeration in comparison to the coarser size particles in the matrix at higher amount of reinforcement.

Both bulk and micro hardness of composites were measured using Rockwell and Vicker's hardness testing machines. Improvement in the hardness was observed with addition of zircon sand particles in the matrix. However, hardness of the composites increases with increasing the amount and with decreasing the size of zircon sand particles. Zircon sand particles interact with LM13 alloy causing the formation of new harder phase (Al_2SiO_5) at the particle/matrix interface, which is responsible for the improvement in hardness of the composites. Due to larger surface area, fine size particles increases the hardness of the composites significantly.

Wear behavior of the developed composites was studied by testing the samples with pin- on- disc machine at different operating parameters. A cylindrical shape of samples with 8 mm diameter having flat ends was used for wear testing. Each developed composite was tested at constant sliding velocity (1.6 m/s). Wear behavior of the base alloy and composites was tested at different loads (9.8 N to 49 N) and also at different temperatures (50- 300 °C). Change in wear rate of the material was assessed by measuring the change in height of material during wear test at different testing conditions. Developed composites were characterized into two main categories;

(a) Composites with single size reinforced particles (coarse, medium and fine size particles)

(b) Composites with dual size (combination of coarse and fine size) reinforced particles (DSR-composites).

Change in wear behavior of the single size particle reinforced composites was monitored with sliding distance at different loading conditions. It was observed that wear rate of the all composites increases with increasing the applied load. A mild to severe transition in wear was observed at higher loading conditions (49 N). Wear rate of the composites was decreased with increasing the amount of zircon sand particles in the matrix. However, 20 wt.% zircon sand particles shows increased wear behavior in comparison to the composites with 15 wt.% amount. This increment in the wear rate was due to agglomeration of particles at higher amount. Decrement in wear rate of composites was observed with decreasing the size of the reinforced particles at different loads. Wear rate of the single size reinforced composites change at different temperature condition at different loads. Wear rate of the composites decreases with increasing

the temperature from 50- 200 °C at low (9.8 N) load. Wear rate of all composites is minimum at 200 °C, which is due to the formation of oxide layers between the contact surfaces which avoids the direct metal to metal contact. However, wear rate increases with increasing the temperature during the wear test for all developed composites at low load. At higher loading condition, wear behavior of the composites is different from the wear behavior at low (49 N) load. Wear rate increases with the increase in temperature from 50- 150 °C at high load and is minimum at 200 °C due to formation of oxide layer at this critical temperature. At much higher temperature (250 °C), wear rate increases again and decreases at 300 °C with 49 N load. Involvement of Fe particles from the steel disc at high temperature and high load condition decreases the wear rate of the composites. After analyzing all the data for single size reinforced composites, it was concluded that composite with 15 wt.% of fine size particles shows better wear resistance at different loads and temperature conditions in comparison to other developed composites.

After analyzing wear rate, it was observed that wear resistance is optimum for the composite containing 15 wt.% of fine size zircon sand particles. However, finer size particles tend to agglomerate during casting at higher amount of reinforcement. Hence, the dual size (combination of coarse and fine size particles) particles reinforced composites were developed to avoid the agglomeration as well as to improve the wear resistance of the composite. Dual size reinforced composites (DSR- composites) with different amount of dual size reinforcement (5- 20 wt.%) and different ratio of coarse and fine size particles in the matrix were developed by stir casting process. Wear resistance of the DSR- composites was improved in comparison to the single size reinforced composites with similar amount of zircon sand particles. However, DSR- composites with different ratios of coarse and fine size particles also shows different wear rate at particular operating condition. It was observed that DSR- composites with composition 1:4 of coarse and fine size particles (DSR- 15D composite) show better wear resistance in comparison to other composition for particular amount of reinforcement.

After the dry sliding wear test, to get the better idea about the wear mechanism, worn surfaces and wear debris were analyzed under SEM. SEM micrographs indicate that both adhesive and abrasive wear mechanism are involved during the wear test. Presence of flake shape debris along with thread like debris are symptoms of adhesive wear mechanism. Marks of grooves on wear debris indicate the involvement of abrasive wear mechanism. Corrugated structured debris point out the continuous rubbing of the delaminated material during wear test. Shape and amount of

debris increases with increasing the applied load during wear test. Worn surfaces and wear debris collected at higher temperature condition show presence of molten state of matrix generated due to frictional heat between the contact surfaces.

All the data presented in this thesis can be further summarized as follows:

- Aluminum matrix composites reinforced with zircon sand particles were developed by stir casting process.
- From microstructural analysis, it has been found that there is good bonding between the LM13 alloy and zircon sand particles. However, clustering of reinforced particles is also observed at higher amount (20 wt.%) of fine size reinforcement.
- Hardness of the composite material increased with an increase in amount as well as decreasing the size of reinforced zircon sand particles.
- Wear rate of the both matrix and composites increased with an increase in applied load.
- Wear resistance of the composite materials increases with an increase in reinforcement of zircon sand, although an increase in zircon sand content from 15 wt.% to 20 wt.% does not result in an appreciable change in wear rate.
- The effect of temperature on wear was also studied at different loads. Composites with higher concentration (15 wt.%) of dual size zircon sand particles in 1:4 ratio (DSR- 15D composite) shows better wear resistance in comparison to other composites.
- The microstructural study of specimen after wear test concludes that both adhesive and abrasive wear mechanisms contribute for wear of composites.

6.2 Future scope

The work done in present investigation has led to some conclusions which have been described in this chapter. However, the possibilities of further investigations of these developed composites based on above work can be explored. These are as below:

- The developed composites can be further investigated for their tensile strength, corrosion resistance along with some electrical and thermal measurement. It will help to widen their area of application in different engineering designs and applications.
- The wear behavior of the composites can be further analyzed at different environmental

conditions like under lubricating condition and corrosive environment where temperature variation can be done.

- Effect of heat treatment on wear properties of the composites can also be examined to have their wider applications.
- Apart from this, a new composite of sandwich nature like LM13-Zr-Cu can be fabricated for different military applications.

RESEARCH PUBLICATIONS

JMEPEG (2013) 22:1765–1775
DOI: 10.1007/s11665-012-0383-0

1059-9495/$19.00

Study of Wear Behavior of Zircon Sand-Reinforced LM13 Alloy Composites at Elevated Temperatures

Ranvir Singh Panwar and O.P. Pandey

(Submitted April 28, 2012; in revised form August 21, 2012; published online December 11, 2012)

The present article describes in detail the wear behavior of zircon sand-reinforced LM13 alloy composite at elevated temperatures with variation in load. Zircon sand particles in different amounts were reinforced into LM13 alloy by stir casting route. Dispersion of reinforced particle was examined under optical and scanning electron microscope. The hardness values of the composites were observed to increase with the increasing amount of reinforcement. The coefficients of thermal expansion of LM13 alloy and zircon sand-reinforced composites were recorded in different temperature ranges. Wear behaviors of base alloy and composites have been studied with variation in applied load. Effect of temperature (from 50 to 300 °C) on wear behaviors of both alloy and composites were determined at low (1 kg) and high (5 kg) loads. The improvement in the wear resistance was noticed with the higher amount of reinforcement. A transition from mild-to-severe wear with variations in temperature and load was observed. The results are discussed in light of operative wear mechanisms. Wear track and wear debris of composite materials were also analyzed under SEM to understand the operative wear mechanism under different conditions.

Keywords casting, metal matrix composite, thermal properties, wear

1. Introduction

The conventional monolithic metals and alloys have a limitation of specific strength, which cannot be enhanced beyond certain value. This has led to the development of hybrid materials in the form of composites, which show the combination of properties like specific strength, stiffness, and wear resistance over conventional materials. Lightweight, high-strength aluminum metal matrix composites (Al-MMCs) are such a class of materials used for a number of applications in modern engineering field (Ref 1-5). The composites reinforced with ceramic particles (TiC, TiN, Al_2O_3, SiC, etc.) are gradually being implemented in electronic, automotive, or aircraft industries for components like fan exit guide vane (FEGV) in the gas turbine engine, as ventral fins and fuel access cover doors in military aircraft. Particle-reinforced aluminum matrix composites (PAMCs) are also used as rotating blade sleeves in helicopters and in the braking systems of trains and cars (Ref 6-9).

Aluminum matrix composites (AMCs) are conventionally fabricated by different techniques. Among these, stir casting process is well accepted because of its simplicity and lower production cost. The reinforcement of hard ceramic particles like alumina (Ref 10-12), silicon carbide (Ref 13), or zirconia (Ref 14, 15) into aluminum alloys enhances the wear properties, which are widely studied composites. However, zircon sand-reinforced composites have not been studied in detail. Studies reporting on the abrasive wear behavior of aluminum composite reinforced with zircon sand are limited (Ref 16, 17). Das et al. (Ref 16) have also reported that zircon sand-reinforced composite shows better wear resistance than alumina-reinforced composite because of the former's superior particle–matrix bonding.

The requirement for the high-temperature wear-resistant material with good thermal stability in different components of automobile and aircraft industries motivates to develop new ceramic-reinforced AMCs. The presence of ceramic particle in the matrix also improves the thermal stability as well as durability of the materials. In automotive applications, PAMCs are used as high-speed rotating or reciprocating mass items such as pistons, connecting rods, valves, crankshafts, gear parts, and suspension arms (Ref 9). These components often operate near the critical temperature ($0.4T_m$, where T_m is melting temperature of the Al) of the material (Ref 18). Few studies are available on the high-temperature wear test of PAMCs (Ref 18-20). However, till date, no data are available on the wear behavior of the LM13/Zr composite at high temperature (300 °C). In the present study, LM13 alloys reinforced with zircon sand are developed via stir casting route, and their wear properties from room to elevated temperatures are investigated at different loads.

2. Materials and Experimental Details

2.1 Materials

Commercial grade piston alloy LM13 containing 12 wt.% Si was chosen as the matrix and zircon sand ($ZrSiO_4$) with a particle size in the range of 106-125 μm containing 67% ZrO_2(+HfO_2) and 33% SiO_2 as reinforcement. The chemical composition of aluminum alloy is given in Table 1.

Ranvir Singh Panwar and **O.P. Pandey**, School of Physics and Materials Science, Thapar University, Patiala 147004 Punjab, India. Contact e-mail: oppandey123@rediffmail.com; oppandey@thapar.edu.

Available online at www.sciencedirect.com

SciVerse ScienceDirect

www.elsevier.com/locate/matchar

Analysis of wear track and debris of stir cast LM13/Zr composite at elevated temperatures

*Ranvir Singh Panwar, O.P. Pandey**

School of Physics and Materials Science, Thapar University, Patiala, 147004, India

ARTICLE DATA

Article history:
Received 24 April 2012
Received in revised form
3 November 2012
Accepted 6 November 2012

Keywords:
Metal matrix composite
Stir casting
Sliding wear
Scanning electron microscope
Debris

ABSTRACT

Particulate reinforced aluminum metal matrix composite is in high demand in automobile industry where the operational conditions vary from low to high temperature. In order to understand the wear mode at elevated temperature, this study was planned. For this purpose we developed a metal matrix composite containing aluminum alloy (LM13) as matrix and zircon sand as particulate reinforcement by stir casting process. Different amounts of zircon sand (5, 10, 15 and 20 wt.%) were incorporated in the matrix to study the effect of reinforcement on the wear resistance. Dispersion of zircon sand particles in the matrix was confirmed by using optical microscopy. Sliding wear tests were done to study the durability of the composite with respect to the base alloy. The effects of load and temperature on wear behavior from room temperature to 300 °C were studied to understand the wear mechanism deeply. Surface morphology of the worn surfaces after the wear tests as well as wear debris was observed under scanning electron microscope. Mild to severe wear transition was noticed in tests at high temperature and high load. However, there is interesting change in wear behavior of the composite near the critical temperature of the composite. All the observed behavior has been explained with reference to the observed microstructure of the wear track and debris.

1. Introduction

At the present time, durability of materials, especially those of tribological importance, is of great interest for motor vehicles and other engineering applications. Utility of Al–Si alloys in automobile industry has received considerable attention due to lightweight, good machinability and easy casting characteristics [1–3]. Clarke and Sarkar [4] suggested that presence of Si in Al–Si alloy of near eutectic composition improves the wear resistance of alloy. In similar investigations it was also found that particulate reinforced aluminum matrix composite (PAMCs) shows great improvement in wear resistance [5–9]. However, for better tribological and mechanical properties of the composites, selection and volume fractions of particulates, their size, shape and distribution in matrix are still being studied. Present work is an effort in this direction.

Among the available techniques to develop the PAMCs, the stir casting process is widely accepted in industries due to the lower production cost, simplicity, flexibility and applicability to large quantity production [10,11]. High hardness, high modulus of elasticity and good thermal stability of zircon sand particles attracted the researchers to use these particles as reinforcement in AMCs. Das et al. [12] have also reported that zircon sand reinforced composite shows better wear resistance than alumina reinforced composite due to its superior particle–matrix bonding. However, until now wear behavior and particularly the surface analysis of worn surfaces of Al–Si/Zr composites at elevated temperatures is not available.

Considering this fact, in the present work we studied about the surface morphology of worn pins of Al–Si/Zr PAMCs at different loads and temperatures. Different amount of zircon sand was also added to the metal matrix to study the effect of

* *Corresponding author*. Tel.: +91 175 2393116; fax: +91 175 2393020.
E-mail addresses: ranvir.panwar@thapar.edu (R.S. Panwar), oppandey@thapar.edu (O.P. Pandey).

1044-5803/$ – see front matter © 2012 Elsevier Inc. All rights reserved.
http://dx.doi.org/10.1016/j.matchar.2012.11.003

Study of Wear Mechanism for LM13/Zr Composite Under Dry Sliding Conditions at Different Loads

Ranvir Singh Panwar, Suresh Kumar, O. P. Pandey

School of Physics and Materials Science, Thapar University, Patiala, Punjab (INDIA)

Email: ranvir.panwar@thapar.edu

Abstract. In the present paper, well known piston alloy (LM13) reinforced with $ZrSiO_4$ particles was developed and studied as wear resistant material. The particle reinforced aluminum metal matrix (PAMC) was developed by stir casting route. Composite was developed by reinforcing 10 wt. % of $ZrSiO_4$ particles into LM13 alloy. Wear behavior of LM13 alloy reinforced with $ZrSiO_4$ particles have been carried out with different applied load. Micrographs of worn surfaces after wear test were examined by scanning electron microscope. These micrographs indicate the presence of the adhesive and abrasive wear mechanism, and transition from mild to severe wear at higher load.

Keywords: Metal matrix composite, wear, SEM.
PACS: 81.05.Mh, cermets, ceramics and refractory composites

INTRODUCTION

Metal matrix composite materials show the combination of properties like specific strength, stiffness and wear resistance over conventional metals and alloys. Light weight, excellent mechanical properties and relatively low production cost make aluminum metal matrix composites (Al MMCs) attractive for the number of applications in modern engineering field [1-5]. The composites reinforced with ceramic particles are gradually being implemented in electronic, automotive or aircraft industries [6-8].

In the present work LM13 alloy reinforced with zircon sand is developed via stir casting route. Advantages of stir cast lie in its simplicity, flexibility and applicability to large quantity production. Due to high hardness and high modulus of elasticity along with good thermal stability, zircon particles are used as reinforcement in AMCs. Wear behavior of LM13/Zircon sand particles is studied with varying loads from 1 kg to 5 kg. This LM13/zircon sand composite may be useful in automotive and defence areas due to the improved property like high hardness, good wear resistance as compared to aluminum alloys [9].

EXPERIMENTAL

Commercial grade piston alloy (LM13) containing 12% Si was chosen as the matrix and zircon sand ($ZrSiO_4$) (with a particle size in range of 106-125 μm) as reinforcements. For stir casting, a resistance furnace was used. A graphite coated fire clay crucible of capacity around 2 kg was used for melting the aluminum alloy. About 1500 grams of aluminum alloy (LM13) was melted at 800°C then it was held at 750ºC. The molten metal was stirred with graphite stirrer at a speed in the range of 620-630 rpm. Preheated zircon sand was added inside the vortex created during stirring of molten metal. Melt LM13 alloy reinforced with zircon sand was stirred mechanically for 5 minutes in order to get homogeneous composition. Form this stir cast composite material, specimen were prepared for the characterization and testing. Wear tests of the samples were carried out with pin-on-disc method. EN32 grade steel disc was used as counterface. A constant sliding velocity of 1.6 m/s was maintained during the wear rate. Wear test was conducted for 3000 meters as a total sliding distance. Worn surfaces of the samples were examined under SEM for better understanding of the wear mechanism during the wear test.

RESULTS & DISCUSSION

To study the effect of applied load on wear behavior of LM13 alloy and composites, wear test of was done at room temperature with variation of load from 1 kg to 5 kg. From figure 1 it can be noted that wear rate of the investigated materials increase with increment in the applied load. In the entire study the graphs show two type of wear behavior under the applied load. In the initial stage of wear testing, there is a rise in wear corresponding to the run in wear. This may be due to adhesive nature of sample to the

Proceeding of International Conference on Recent Trends in Applied Physics and Material Science
AIP Conf. Proc. 1536, 1143-1144 (2013); doi: 10.1063/1.4810641

Tribol Lett (2012) 47:231–251
DOI 10.1007/s11249-012-9983-y

ORIGINAL PAPER

Wear Behavior of Dual Particle Size (DPS) Zircon Sand Reinforced Aluminum Alloy

Suresh Kumar · Vipin Sharma · Ranvir Singh Panwar · O. P. Pandey

Received: 1 July 2011 / Accepted: 11 May 2012 / Published online: 26 May 2012

Abstract The present investigation aims to find the combined effect of coarse and fine size particle reinforcement of zircon sand in aluminum alloy LM13 on the wear behavior. The composites are fabricated by varying the reinforcement of fine and coarse size zircon sand particles and compared with the single size reinforcement. Coarse and fine particle zircon sand of 106–125 and 20–32-μm size, respectively, are used in this study. The wear test was carried out on pin-on-disc machine. Microhardness measurement was done for developed composites. Wear track and debris are analyzed by SEM to study the wear mechanism. Line profile and EDS analysis is also done to validate the microstructural results. Study reveals that a combination of 3 % fine and 12 % coarse particle reinforced composite exhibits better wear resistance while 3 % coarse and 12 % fine particle reinforcement decreases the wear resistance. It is also observed that zircon sand particles provide effective nucleation site for the eutectic silicon. Microstructural examination shows globular and finely distributed eutectic silicon in the vicinity of the reinforced particles.

Keywords Composite · Stir casting · Dual particle size · AMCs · Zircon sand

1 Introduction

Aluminum–silicon alloys find their application in different engineering components because of their good castability, high corrosion resistance, and low density. Wear resistance of these alloys can be enhanced by incorporation of ceramic phase in the soft aluminum matrix [1]. Reinforcement of hard ceramic particulates imparts a combination of properties not achievable in either of the constituents individually. In recent years, many processing techniques have been developed to prepare particulate reinforced aluminum matrix composites (AMCs). These techniques are stir casting, liquid metal infiltration, squeeze casting, spray co-deposition, powder metallurgy, etc. Among the variety of processing techniques available for particulate or discontinuous reinforced metal matrix composites, stir casting is one of the methods accepted for the production of large quantity composites. It is attractive because of simplicity, flexibility, and is most economical for large size components to be fabricated [1–5]. In recent years, numerous research works have been reported on production of AMCs by stir casting technique, but very limited research work has been done on reinforcement of dual size particles [6, 7]. Moreover, to the best of our knowledge no work is reported on wear behavior of aluminum composites reinforced with dual size zircon sand particles.

Prabhakar and co-workers [6] studied tribological behavior of dual particle size (DPS) SiC particles reinforced composite and compared with single particle size (SPS) reinforced composite. They found that the DPS composite exhibited better wear resistance compared to same volume fraction of SPS composite. Zhang et al. [7] studied thermal conductivity of Al–12Si matrix composite reinforced with 70 vol % SiC particles of two different sizes and analyzed the effect of dual-sized particles on structural and thermal conduction properties. The composites fabricated with finer reinforcement particulates exhibit greater strength as compared to coarser with the same quantity of reinforcement. Ahmad et al. [8] studied

S. Kumar · V. Sharma · R. S. Panwar · O. P. Pandey (✉)
School of Physics and Material Science, Thapar University, Patiala 147004, Punjab, India
e-mail: oppandey@thapar.edu

Advanced Materials Research Vol. 585 (2012) pp 574-578
Online available since 2012/Nov/12 at www.scientific.net

doi:10.4028/www.scientific.net/AMR.585.574

Tribological characteristics of Aluminium tri-reinforced particles (Al-TRP) composites developed by liquid metallurgy route

Suresh Kumar[1, a], Ranvir Singh Panwar [1,b] and O.P. Pandey[1, c]

[1]School of Physics and Materials Science,Thapar University, Patiala, INDIA-147004

[a]skumartom@gmail.com, [b]ranvir.panwar@thapar.edu, [c]oppandey@thapar.edu

Keywords: Metal matrix composite**,** wear rate, debris, SEM

Abstract :

Discontinuous reinforced aluminum matrix composites (DAMCs) are widely used in automobiles, military and many other engineering areas due to their attractive properties. DAMCs are used in automobile industries for manufacturing bogies, cars and other structural components. Apart from this it is also used in components which are subjected to high temperatures. In the present work we have studied the tribological characteristics of DAMCs containing zircon sand, SiC and Zirfloor as reinforced ceramic particles in Al alloy. These three types of ceramic particles (particle size 5-32 μm) are reinforced in the Al-12Si alloy (LM13) by liquid metallurgy route (stir casting technique). Total 15 wt% of the tri reinforced particles (TRP) are added in LM13 alloy to fabricate Al–TRP composite for tribological application. Wear characteristics of Al–TRP composites have been investigated under dry sliding conditions. Dry sliding wear tests have been carried out using a pin-on-disc method at 1Kg and 5Kg loads. Sliding distance during the wear test was about 3000 meters with a constant sliding velocity of 1.6 ms^{-1}. In the study it was observed that wear rate of the composite increases with increase in amount of load. Microhardness measurement was done for the developed Al-TRP composite. SEM images of wear track on composite gives better idea of the wear mechanism. Wear debris collected after the wear test was also examined for deeper understanding of wear behavior. Study reveals that about equal amount of $ZrSiO_4$, SiC and Zirfloor reinforced particle in Al-TRP composite exhibits better wear resistance compared to aluminum base alloy.

Introduction:

The high demand of weight reduction in automobile and aircraft industries requires the optimum design of products employing low weight materials [1]. Aluminum and its alloys including LM13 are used extensively in aerospace and automotive industries because of its low density and high strength to weight ratio [2]. For many applications, the useful life of components often depends on their surface properties such as wear resistance. Recently, much attention has been paid to stir casting technique, which is known as a surface modification technique [3, 4]. AMCs reinforced with SiC particulates are known for higher modulus, strength and wear resistance compared to conventional alloys. Garcia et al. [5] have observed that the specific wear behavior of AA6061–SiC composites decreases with increase in volume fraction and size of reinforcement. Kumar et al. [6] have studied the dry sliding wear behavior of Al-matrix composites reinforced with $ZrSiO_4$ and SiC particulate up to 15%. Study shows that dual reinforcement particle (DRP) composite exhibites better wear resistance as compared to single particle reinforcement if mixed in a definite proportion [6,7].

The present study is aimed to analyze the combined effect of the hard particles reinforcement in aluminum alloy composite fabricated by modified two step stir casting [6,7]. Our study is mainly focused on investigating the microstructural features and wear properties of tri-reinforced particles (TRP) consisting of $ZrSiO_4$, SiC and Zirfloor, which has not been studied so far. The effect of tri-reinforced particle on the mechanical properties, microstructures and wear resistance of the particulate reinforced composite at room temperature is reported in this work.

Wear Behavior at High Temperature of Dual-Particle Size Zircon-Sand-Reinforced Aluminum Alloy Composite

SURESH KUMAR, RANVIR SINGH PANWAR, and O.P. PANDEY

The basic aim of the present investigation is to study the role of particle size for high-temperature application of $ZrSiO_4$-reinforced aluminum-based LM13 alloy composite as a bearing material. Composites containing 15 wt pct $ZrSiO_4$ particles of two different size ranges (20 to 32 and 106 to 125 μm) in different proportion were prepared by the stir casting route. The microhardness measured at different areas indicates good interfacial bonding. Transition in the wear mode for all composites occurs after temperature 423 K (150 °C). The overall wear properties of DPS-2 composite containing 12 pct fine and 3 pct coarse particles are better at all temperatures for both low and high loads.

DOI: 10.1007/s11661-012-1504-y

I. INTRODUCTION

THE high-temperature wear-resistant material for high-performance tribological applications is one of the major requirements of industry. The lightweight ceramic-reinforced aluminum alloys are a major class of composites that are being worked out to serve the preceding purpose. Various categories of ceramic particles are currently used as abrasives, and their performance varies per the morphological features. Theoretical approaches and experimental evidence of the relationships between the particle morphology, wear rate, hardness, and fracture toughness have been well studied and reported in the literature.[1–7] The abrasive wear resistance of Al-Si alloys is strongly dependent on the type of reinforcement and its composition, applied load, and sliding speed.[8,9] Among the variety of processing techniques available for particulate- or discontinuous-reinforced metal matrix composites, stir casting is one of the methods adopted for the production of large quantity composites. Stir casting is also attractive because of its simplicity and flexibility, and it is most economical in the fabrication of large size components.[10–14] In recent years, much research work has been reported on the production of Aluminum metal matrix composites (AMCs) by the stir casting technique, but very limited research work has been done on reinforcement of dual-size particles.[15–17] Moreover, to the best of our knowledge, no work is reported on high-temperature wear behavior of aluminum composites reinforced with dual-size zircon sand particles.

Bindumadhavan *etal*.[15] studied the wear and mechanical properties of dual particle size (DPS) reinforced particulate metal matrix composites, and they found that for the same total volume fraction of SiC reinforcement, DPS composites containing both small (47 μm) and large (120 μm) SiC particles showed higher wear resistance than composites having only small size particles. The DPS composites were found to have higher impact energy than SPS composites containing only small (47 μm) SiC-reinforced particles. Martin *etal*.[18] reported the lower wear resistance of Al-Si alloy than Al-Si alloy reinforced with large Si or SiC particulates in the temperature range of 293 K to 473 K (20 °C to 200 °C). The oxidation of metallic materials and the role of oxide scale in establishing the wear mechanism are also reported.[7,19] The tensile properties of aluminum casting alloys are strongly dependent on secondary dendrite arm spacing, porosity level, and the modifications that occur during heat treatment of the alloys.[20–22] The mechanical properties were minimally affected by temperatures below 473 K (200 °C).[23] During high-temperature tensile tests, the voids were formed at the boundaries of inclusions or the second-phase particles, which leads to local necking. The tensile properties of pure aluminum are strongly affected by thermal recovery due to the annihilation of crystal lattice dislocations into grain boundaries.[24] Rajaram *et al*.[25] studied the wear resistance of the Al-Si alloy, which increased linearly with increasing the operating temperature. This effect is due to the oxide film and formation of the glazing layer on sliding components, which is more rapid at higher operating temperatures. These layers prevent the direct metal-to-metal contact of sliding surfaces.

From the preceding analysis, it can be concluded that at high temperature, the main governing factor for strength and wear properties is particle interface bonding, which provides a site for growth of cracks. Considering this fact, we planned to investigate the high-temperature wear behavior of composites containing 15 wt pct zircon sand particles in LM13 alloy produced by the stir casting technique. The wear properties of MMCs depend on the reinforced particle amount, type, size, shape, temperature, *etc*. In the present work, we focused on a comparative study of the

SURESH KUMAR and RANVIR SINGH PANWAR, Ph.D. Scholars, and O.P. PANDEY, Senior Professor, are with the School of Physics and Materials Science, Thapar University, Patiala, Punjab, India 147004. Contact e-mail: oppandey@thapar.edu
Manuscript submitted January 6, 2012.

Published online: 27 November 2012

JMEPEG
DOI: 10.1007/s11665-013-0642-8

1059-9495/$19.00

Effect of Particle Size on Wear of Particulate Reinforced Aluminum Alloy Composites at Elevated Temperatures

Suresh Kumar, Ratandeep Pandey, Ranvir Singh Panwar, and O.P. Pandey

(Submitted March 18, 2013; in revised form June 22, 2013)

The present paper describes the effect of particle size on operative wear mechanism in particle reinforced aluminum alloy composites at elevated temperatures. Two composites containing zircon sand particles of 20-32 μm and 106-125 μm were fabricated by stir casting process. The dry sliding wear tests of the developed composites were performed at low and high loads with variation in temperatures from 50 to 300 °C. The transition in wear mode from mild-to-severe was observed with variation in temperature and load. The wear at 200 °C presented entirely different wear behavior from the one at 250 °C. The wear rate of fine size reinforced composite at 200 °C at higher load was substantially lower than that of coarse size reinforced composite. Examination of wear tracks and debris revealed that delamination occurs after run in wear mode followed by formation of smaller size wear debris, transfer of materials from the counter surfaces and mixing of these materials on the contact surfaces. The volume loss was observed to increase with increase in load and temperature. Composite containing bigger size particles exhibit higher loss under similar conditions.

Keywords metal matrix composite, SEM, wear debris, wear mechanism

1. Introduction

The mechanism of wear encountered in a sliding system and parameters affecting the wear provides a better understanding for fabricating materials with enhanced wear resistance. Aluminum alloy matrix composites (AMCs) are widely used in engineering applications due to high specific strength, high corrosion resistance, ease of fabrication, and low cost (Ref 1-5). AMCs with ceramic particles reinforcement are suitable candidate for materials used in tribological applications. The particle size and nature of reinforced ceramics have pronounced effect on microstructural and tribological properties of AMCs. The wear characteristics greatly depend on reinforcement volume and size of the reinforced particles. The dry sliding un-lubricated wear of the composites is a complex process involving not only mechanical but also thermal and chemical interactions between the surfaces in contact. In sliding system the drastic change in wear rate occurs by delamination. Though, it is not the only reason but mostly observed under severe wear conditions. The study of wear surface indicates that parameters accelerating delamination wear are of great importance for sliding systems to check the severe wear of the materials.

Studies on the tribological characteristics of AMCs containing varying percentage and various reinforcements such as Al_2O_3, SiC, TiO_2, TiC, B_4C, TiB_2, and fly ash of various sizes are available in the literature (Ref 4-6). Apart from these the number of work discussing the wear performance of fine and coarse particle reinforced composites also exists (Ref 1, 5-12). However, report on the wear behavior of fine and coarse size reinforced composites with variation in temperature is limited (Ref 13). Moreover, study of wear behavior of fine and coarse particles reinforced composites in the light of delamination mechanism is not reported. In this work, emphasis is made to understand the effect of reinforced particle size on type of wear, particularly delamination wear in discontinuous particle reinforced aluminum alloy composites. Apart from this other operative mechanism is also discussed to correlate the entire wear behavior with variation in load and temperature.

The mechanism of delamination wear was proposed by Suh (Ref 14), on the basis of series of experiments. Suh and Jahanmir (Ref 15) have explained various factors affecting the delamination wear of materials. They have given the reasons for delamination where the removal of large wear particles occur by the process of plastic deformation of the surface layer which occurs by subsurface crack nucleation followed by crack propagation. Kanchanomai et al. (Ref 16) investigated the role of porosity on delamination wear of metal injection molded 316L stainless steel and reported that at low sliding speed effect of porosity on delamination wear is not pronounced as compared to high sliding speed. Similarly delamination wear is correlated with porosity by Simchi and Danninger (Ref 17) in sintered plain iron. Huang et al. (Ref 9) investigated the size effect of SiC particles on the tribological behavior of SiC reinforced magnesium AMCs prepared by melt-stirring technique. Their results show variable wear rate at different particle size. However, hardness is observed to increase with increasing particle size. Mondal et al. (Ref 10) conducted abrasive wear test of SiC particles reinforced aluminum alloy composites as a function of applied load, reinforcement size, and volume fraction. They found that the wear resistance of composite

Suresh Kumar, Ranvir Singh Panwar, and **O.P.Pandey**, School of Physics and Materials Science, Thapar University, Patiala 147004 Punjab, India; and **Ratandeep Pandey**, Department of Mechanical Engineering, BBSBEC, Fatehgarh Sahib, Patiala 140407, India. Contact e-mail: oppandey@thapar.edu.

Published online: 09 July 2013

J Mater Sci (2012) 47:6633–6646
DOI 10.1007/s10853-012-6599-4

Microstructural and wear behavior of dual reinforced particle (DRP) aluminum alloy composite

Vipin Sharma · Suresh Kumar · Ranvir Singh Panwar · O. P. Pandey

Received: 28 November 2011 / Accepted: 21 May 2012 / Published online: 6 June 2012

Abstract The present investigations are a comparative study of single and dual reinforcement particles on microstructural features and wear behavior in LM-13 aluminum–silicon alloy. Silicon carbide and zircon sand particles of 20–32 μm are reinforced in the alloy by two-step stir casting method. Wear study reveals that the dual particle reinforcement enhances the wear resistance as compared to single particle reinforcement if mixed in a definite proportion. Study also indicate that a combination of 15 % reinforcement of zircon sand and silicon carbide particles in the ratio of 1:3 into the composite exhibits better wear resistance as compared to other combination.

Introduction

Aluminum alloy matrix composites (AMCs) with multiple reinforcements or hybrid AMCs are finding increased applications in various sectors because of improved mechanical and tribological properties and hence are better substitutes for single reinforced composites [1, 2]. Aluminum and its alloys when reinforced with hard ceramic particulates impart a combination of properties not achievable in either of the constituents individually. Aluminum alloys provide a good matrix for the development of particulate reinforced composites owing to their low density, high specific strength, high corrosion resistance, ease of fabrication, and low cost [3].

In recent years many processing techniques have been developed to prepare particulate reinforced aluminum matrix composites (AMCs). Among the variety of processing techniques available for particulate or discontinuous reinforced metal matrix composites, stir casting is one of the methods accepted for the production of large quantity composites. It is attractive because of simplicity, near net shaping, flexibility and is most economical for large size components to be fabricated. However, it suffers from poor incorporation and distribution of the reinforcement particles in the matrix. These problems become especially significant as the reinforcement size decreases due to greater agglomeration tendency and reduced wettability of the particles with the melt [4–6]. The dendritic growth and porosity also exists in stir cast composites. Therefore, innovations in processing method of stir casting are of great importance. Stir casting process is modified by various researchers to achieve the desired properties in the composite [7–11].

Two-step stir casting have an advantage in terms of promoting wettability, reduction of porosity, and homogeneous distribution of particles. Moreover, the microstructure is also refined which provide better mechanical properties [9, 10]. In earlier reported two-step stir casting method the mixing of particle is done in semisolid melt by manually stirring with steel rod, which is cumbersome process and also the agglomeration of fine particles occurs. Moreover, mixing is not efficient in reinforcement of fine particle as total volume occupied is increased and semisolid melt solidifies before mixing is completed. In the present study the conventional stir cast processing is bifurcated. In first step the melting and mixing is done properly as is being followed in stir casting and melt is solidified in crucible. In the second step the solidified mass is re-melted for stirring process followed by casting.

In recent years numerous research works have been reported on production of multiparticle reinforced or

V. Sharma · S. Kumar · R. S. Panwar · O. P. Pandey (✉)
School of Physics and Materials Science, Thapar University, Patiala 147004, Punjab, India
e-mail: oppandey@thapar.edu

Available online at www.sciencedirect.com

SciVerse ScienceDirect

Ceramics International 39 (2013) 6333–6342

CERAMICS INTERNATIONAL

www.elsevier.com/locate/ceramint

Effect of dual reinforced ceramic particles on high temperature tribological properties of aluminum composites

Suresh Kumar, Ranvir Singh Panwar, O.P. Pandey*

School of Physics and Materials Science, Thapar University, Patiala-147004, Punjab, India

Received 7 November 2012; received in revised form 18 January 2013; accepted 19 January 2013
Available online 1 February 2013

Abstract

The nature and distribution of hard ceramic particles in composite materials influences the properties to greater extent. In the present work, the role of hard ceramic reinforced particles on the tribological behaviour of aluminum metal matrix composites consisting of single (SRP) and dual reinforced particles (DRP) is studied at different temperatures. Zircon sand and silicon carbide particles of size 20–32 μm were used as reinforcement in commercial grade LM13 piston alloy. Composites of dual reinforced particles in aluminum matrix (DRP-AMCs) were developed by mixing 15 wt% reinforced particles by two step stir casting technique. The wear behaviour of DRP-AMCs and SRP-AMCs (single reinforced particles aluminum matrix composite) was investigated using a pin-on-disc method at high temperatures under dry sliding condition. The microstructural examination of developed composites shows globular and finely distributed eutectic silicon in the vicinity of the reinforced particles. Metallographic investigation revealed that the wear zone of the SRP composite consisted of a hardened layer, which is responsible for high wear loss observed in the SRP composite. The results further indicate a transition in the wear mode that occurs after 150 °C for all composites. Study reveals that the dual reinforcement of particles enhances the wear resistance as compared to single reinforced particles if mixed in a definite ratio. A combination of 3% zircon sand and 12% silicon carbide particle reinforced composite exhibits better wear resistance as compared to other combinations at all the temperatures for low and high loads both.

Keywords: Aluminum matrix composite; Wear; Debris; SEM

1. Introduction

Aluminum matrix composites (AMCs), particularly hybrid AMCs are finding increased applications in various sectors of transportation industries such as brake drums, engine pistons and other components because of the high strength, low density, corrosion resistance, wear resistance and easy workability.

In recent years, few attempts have been made to develop hybrid AMCs reinforced with SiC, Al_2O_3 and graphite or in combination of the above [1–3]. The room temperature sliding wear behavior of Al_2O_3 and SiCp reinforced aluminum matrix hybrid composites under both, the dry and lubricant conditions have been investigated by Wang et al. [4] and reported the improvement in tribological properties of hybrid composites. The dry sliding wear behavior of Al based composites reinforced with Gr and SiC particulate up to 10 wt% was studied at room temperature by Suresha et al. [5]. They have reported that Al–SiC–Gr hybrid composite exhibits better wear resistance. The role of magnesium addition along with SiC and Al_2O_3 particles on dry sliding wear behavior of the aluminium matrix hybrid composites at room temperature indicate that wear resistance of the composites increased with increasing Mg addition [6].

Das et al. [7] have compared the wear properties of alumina and zircon sand reinforced AMCs and reported that decrease in particle size improves wear resistance at room temperature. Ahmad et al. [8] studied the effect of particle size for Al_2O_3 reinforced AMCs and reported that the fine particle reinforced composites have higher hardness as compared to coarse particles. This is because composites reinforced with the finer particle size offer

*Corresponding author. Tel.: +91 1752393130; fax: +91 1752393005.
E-mail address: oppandey@thapar.edu (O.P. Pandey).

0272-8842/$ - see front matter © 2013 Elsevier Ltd and Techna Group S.r.l. All rights reserved.
http://dx.doi.org/10.1016/j.ceramint.2013.01.059

Tribological Properties of Zircon Sand and Zirfloor Reinforced LM13 Alloy Matrix Composite-A Comparative Study

Suresh Kumar*, Ranvir Singh Panwar, O.P. Pandey

School of Physics and Materials Science, Thapar University, Patiala-147004, Punjab, India.
Email: skumartom@gmail.com

Abstract. The tribological behaviour of samples of LM13 alloy matrix reinforced with 15 wt. % Zircon sand also 15wt.% and Zirfloor particles in low and high range of loads (1kg and 5kg) was determined using a pin-on-disc wear and friction monitor at a constant velocity of 1.6 m/s. Zircon sand and Zirfloor sand (particles size 5-32μm) are reinforced in the LM13 alloy by stir casting method. Optical microscopy show uniform distribution of particles and reveal better bonding in the case of zircon particles reinforced composite compared to that in zirfloor particles reinforced composite. It is observed that the zircon particle reinforced composite shows relatively better wear resistance property compared to zirfloor-reinforced composite.

Keywords: Aluminum matrix composite, Wear, Debris.
PACS: 81.05.Mh , Cermets, ceramic and refractory composites

INTRODUCTION

The mechanism of wear encountered in a sliding system and parameters affecting the mechanism provides a better understanding for tailoring material with enhanced wear resistance. Aluminum alloy matrix composites (AMCs) are widely used in engineering applications due to high specific strength, high corrosion resistance, ease of fabrication and low cost [1-3]. Stir casting is also attractive because of simplicity, flexibility and is most economical for large size components to be fabricated [4]. AMCs with ceramic particles reinforcement are suitable candidate for material used in tribological applications. Numerous research works have been reported on dry sliding wear behavior of AMCs reinforced with various particulates such as SiC, TiC, glass beads, B_4N and Al_2O_3 [5–6]. However, limited work has been reported on abrasive wear behavior of aluminum composites reinforced with zircon particles and zirfloor sand. In the present work, the tribological properties of zircon sand and zirfloor reinforced LM13 alloy matrix composite have been reported. Influence of reinforcement type on abrasive wear of composites has been studied and correlated. Microstructural characterization has been carried out to investigate the particle–matrix bonding of composites.

EXPERIMENTAL

In the present study, well known piston alloy (LM13) is used as matrix material and zircon sand and zirfloor as reinforcement. Particles of fine grade (5-32μm) were used for investigating role of particle's nature. The 15 wt.% reinforcement in matrix was taken for the present study of both composites. The composites were developed by stir casting route. The detailed description of the casting process is given in our earlier work [2, 4]. Dry sliding wear tests of the composites were done by using pin-on-disc method. The wear tests of specimen from each set of composites have been conducted up to 3000 m of sliding distance at a constant sliding velocity of 1.6 m/s with 1kg and 5kg loads. Wear rate for the samples are calculated from the volume loss of material during the test. The microstructural analysis has been done with the help of optical microscope (Eclipse MA-100, Nikon).

RESULTS & DISCUSSION

Microstructural analysis

The optical micrograph of composite reinforced with zircon sand particles is shown in Fig. 1(a). Eutectic silicon observed in figure 1b is arranged in colonies around the zircon sand particle. However, the eutectic silicon is having smaller and less acicular morphology. This type of morphological features enhances wear resistance at low load as an additional hard phase of eutectic silicon supports the particle [2]. The optical micrograph of composite reinforced with zirfloor (Fig. 1b) shows the refinement of eutectic silicon in the vicinity of the particle. It is observed that

Proceeding of International Conference on Recent Trends in Applied Physics and Material Science
AIP Conf. Proc. 1536, 1286-1287 (2013); doi: 10.1063/1.4810712